

GRAHAM COOP

# POPULATION AND QUANTITATIVE GENETICS

**Author:** Graham Coop

Author address: Department of Evolution and Ecology & Center for Population Biology,  
University of California, Davis.

To whom correspondence should be addressed: [gmccoop@ucdavis.edu](mailto:gmccoop@ucdavis.edu)

This work is licensed under a Creative Commons Attribution 3.0 Unported License.

<http://creativecommons.org/licenses/by/3.0/>

i.e. you are free to reuse and remix this work, but please include an attribution to the original.

Typeset using L<sup>A</sup>T<sub>E</sub>X and the TUFTE-LATEX book style.

The L<sup>A</sup>T<sub>E</sub>X code and R code for this book are kept here <https://github.com/cooplab/popgen-notes/> and again are  
under a Creative Commons Attribution 3.0 Unported License.

*Updated on February 2019*

This book was developed from my set of notes for the Population Biology graduate group core class (PBGG) and Undergraduate Population and Quantitative Genetics class (EVE102) at UC Davis. Thanks to the many students who've read these notes and suggested improvements. Thanks to Simon Aeschbacher, Vince Buffalo, and Erin Calfee who read and edited earlier drafts of these notes. To illustrate these notes I've used old scientific and natural history illustrations, in part because they are out of copyright but mainly because they bring me joy. Many of the old images come from Biodiversity Heritage Library a consortium of natural history institutions that are digitizing their collections and make them freely available online. If you enjoy the images consider donating to the BHL. Many of the data and simulation graphics in the book were prepared in R (2018), the code for each is linked to from the caption of each figure. In many cases data was extracted from old figures using the WebPlotDigitizer tool, as such I advise re-extracting the data if you wish to use it for research purposes.



## *Contents*

|   |  |     |
|---|--|-----|
| 1 | <i>Introduction</i>  | 7   |
| 2 | <i>Allele and Genotype Frequencies</i>                             | 11  |
| 3 | <i>Genetic Drift and Neutral Diversity</i>                         | 45  |
| 4 | <i>Phenotypic Variation and the Resemblance Between Relatives.</i> | 89  |
| 5 | <i>The Response to Phenotypic Selection</i>                        | 109 |
| 6 | <i>One-Locus Models of Selection</i>                               | 123 |
| 7 | <i>The Impact of Genetic Drift on Selected Alleles</i>             | 159 |
| 8 | <i>The Effects of Linked Selection.</i>                            | 171 |
| 9 | <i>Bibliography</i>  | 187 |



# 1

## *Introduction*

BIOLOGICAL EVOLUTION IS THE CHANGE OVER TIME IN THE GENETIC COMPOSITION OF A POPULATION.<sup>1</sup> Our population is made up of a set of interbreeding individuals, the genetic composition of which is made up of the genomes that each individual carries. The genetic composition of the population alters due to the death of individuals or the migration of individuals in or out of the population. If our individuals vary in the number of children they have, this also alters the genetic composition of the population in the next generation. Every new individual born into the population subtly changes the genetic composition of the population. Their genome is a unique combination of their parents' genomes, having been shuffled by segregation and recombination during meioses, and possibly changed by mutation. These individual events seem minor at the level of the population, but it is the accumulation of small changes in aggregate across individuals and generations that is the stuff of evolution. It is the compounding of these small changes over tens, hundreds, and millions of generations that drives the amazing diversity of life that has emerged on this earth.

Population genetics is the study of the genetic composition of natural populations and its evolutionary causes and consequences. Quantitative genetics is the study of the genetic basis of phenotypic variation and how phenotypic changes evolve over time. Both fields are closely conceptually aligned as we'll see throughout these notes. They seek to describe how the genetic and phenotypic composition of populations can be changed over time by the forces of mutation, recombination, selection, migration, and genetic drift. To understand how these forces interact, it is helpful to develop simple theoretical models to help our intuition. In these notes we will work through these models and summarize the major areas of population- and quantitative-genetic theory.

While the models we will develop will seem naïve, and indeed they are, they are nonetheless incredibly useful and powerful. Throughout

<sup>1</sup> DOBZHANSKY, T., 1951 *Genetics and the Origin of Species* (3rd Ed. ed.), pp. 16

"All models are wrong but some are useful" - Box (1979).

the course we will see that these simple models often yield accurate predictions, such that much of our understanding of the process of evolution is built on these models. We will also see how these models are incredibly useful for understanding real patterns we see in the evolution of phenotypes and genomes, such that much of our analysis of evolution, in a range of areas from human medical genetics to conservation, is based on these models. Therefore, population and quantitative genetics are key to understanding various applied questions, from how medical genetics identifies the genes involved in disease to how we preserve species from extinction.

Population genetics emerged from early efforts to reconcile Mendelian genetics with Darwinian thought. Part of the power of population genetics comes from the fact that the basic rules of transmission genetics are simple and nearly universal. One of the truly remarkable things about population genetics is that many of the important ideas and mathematical models emerged before the 1940s, long before the mechanistic-basis of inheritance (DNA) was discovered, and yet the usefulness of these models has not diminished. This is a testament to the fact that the models are established on a very solid foundation, building from the basic rules of genetic transmission combined with simple mathematical and statistical models.

Much of this early work traces to the ideas of R.A. Fisher, Sewall Wright, and J.B.S. Haldane, who, along with many others, described the early principals and mathematical models underlying our understanding of the evolution of populations. Building on this conceptual fusion of genetics and evolution, there followed a flourishing of evolutionary thought, the modern evolutionary synthesis, combining these ideas with those from the study of speciation, biodiversity, and paleontology. In total this work showed that both short-term evolutionary change and the long-term evolution of biodiversity could be well understood through the gradual accumulation of evolutionary change within and among populations. This evolutionary synthesis continues to this day, combining new insights from genomics, phylogenetics, ecology, and developmental biology.

Population and quantitative genetics are a necessary but not a sufficient description of evolution; it is only by combining the insights of many fields that a rich and comprehensive picture of evolution emerges. We certainly do not need to know the genes underlying the displays of the birds of paradise to study how the divergence of these displays, due to sexual selection, may drive speciation. Indeed, as we'll see in our discussion of quantitative genetics, we can predict how populations respond to selection, including sexual selection and assortative mating, without any knowledge of the loci involved. Nor do we need to know the precise selection pressures and the ordering of genetic

See PROVINE (2001) for a history of early population genetics.

PROVINE, W. B., 2001 *The origins of theoretical population genetics: with a new afterword.* University of Chicago Press

“DOBZHANSKY (1951)  
once defined evolution as ‘a  
change in the genetic com-  
position of the populations’  
an epigram that should not  
be mistaken for the claim  
that everything worth saying  
about evolution is contained  
in statements about genes”

— LEWONTIN

changes to study the emergence of the tetrapod body plan. We do not necessarily need to know all the genetic details to appreciate the beauty of these, and many other, evolutionary case-studies. However, every student of biology gains from understanding the basics of population and quantitative genetics, allowing them to base their studies and speculations on a solid bedrock of understanding of the processes that underpin all evolutionary change.



# 2

## Allele and Genotype Frequencies

In this chapter we will work through how the basics of Mendelian genetics play out at the population level in sexually reproducing organisms.

Loci and alleles are the basic currency of population genetics—and indeed of genetics. If all individuals in the population carry the same allele, we say that the locus is *monomorphic*; at this locus there is no genetic variability in the population. If there are multiple alleles in the population at a locus, we say that this locus is *polymorphic* (this is sometimes referred to as a segregating site).

Table 2.1 show a small stretch orthologous sequence for the ADH locus from samples from *Drosophila melanogaster*, *D. simulans*, and *D. yakuba*. *D. melanogaster* and *D. simulans* are sister species and *D. yakuba* is a close outgroup to the two. Each column represents a single haplotype from an individual (the individuals are diploid but were inbred so they're homozygous for their haplotype). Only sites that differ among individuals of the three species are shown. Site 834 is an example of a polymorphism; some *D. simulans* individuals carry a *C* allele while others have a *T*. Fixed differences are sites that differ between the species but are monomorphic within the species. Site 781 is an example of a fixed difference between *D. melanogaster* and the other two species.

We can also annotate the alleles and loci in various ways. For example, position 781 is a non-synonymous fixed difference. We call the less common allele at a polymorphism the *minor allele* and the common allele the *major allele*, e.g. at site 1068 the *T* allele is the minor allele in *D. melanogaster*. We call the more evolutionarily recent of the two alleles the *derived allele* and the older of the two the *ancestral allele*. The *T* allele at site 1068 is the derived allele as the *C* is found in both the other species, suggesting that the *T* allele arose via a *C* → *T* mutation.

**Question 1. A)** How many segregating sites does the sample

A *locus* (plural: *loci*) is a specific spot in the genome. A locus may be an entire gene, or a single nucleotide base pair such as A-T. At each locus, there may be multiple genetic variants segregating in the population—these different genetic variants are known as *alleles*.

| pos. | con. | a | b | c | d | e | f | g | h | i | j | k | l | a | b | c | d | e | f | g | h | i | j | k | l | NS/S |
|------|------|---|---|---|---|---|---|---|---|---|---|---|---|---|---|---|---|---|---|---|---|---|---|---|---|------|
| 781  | G    | T | T | T | T | T | T | T | T | T | - | - | - | - | - | - | - | - | - | - | - | - | - | - | - | NS   |
| 789  | T    | - | - | - | - | - | - | - | - | - | - | - | - | C | C | C | C | C | C | C | C | C | C | C | C | S    |
| 808  | A    | - | - | - | - | - | - | - | - | - | T | T | T | T | T | T | G | G | G | G | G | G | G | G | G | NS   |
| 816  | G    | T | T | T | T | - | - | - | - | - | - | - | - | C | C | - | - | - | - | - | - | - | - | - | - | S    |
| 834  | T    | - | - | - | - | - | - | - | - | - | - | - | - | C | - | - | - | - | - | - | - | - | - | - | - | S    |
| 859  | C    | - | - | - | - | - | - | - | - | - | - | - | - | G | G | G | G | G | G | G | G | G | G | G | G | NS   |
| 867  | C    | - | - | - | - | - | - | - | - | - | - | - | - | G | G | G | G | G | A | G | G | G | G | G | G | S    |
| 870  | C    | T | T | T | T | T | T | T | T | T | - | - | - | - | - | - | - | - | - | - | - | - | - | - | S |      |
| 950  | G    | - | - | - | - | - | - | - | - | - | - | - | - | A | - | - | - | - | - | - | - | - | - | - | - | S    |
| 974  | G    | - | - | - | - | - | - | - | - | - | T | - | T | T | T | T | - | - | - | - | - | - | - | - | S |      |
| 983  | T    | - | - | - | - | - | - | - | - | - | - | - | - | C | C | C | C | C | C | C | C | C | C | C | C | S    |
| 1019 | C    | - | - | - | - | - | - | - | - | - | - | - | - | - | - | - | - | - | - | - | - | - | - | - | S |      |
| 1031 | C    | - | - | - | - | - | - | - | - | - | - | - | - | - | - | - | - | - | - | - | - | - | - | - | S |      |
| 1034 | T    | - | - | - | - | - | - | - | - | - | - | - | - | C | C | C | C | C | - | - | A | - | - | - | - | S    |
| 1043 | C    | - | - | - | - | - | - | - | - | - | - | - | - | - | - | - | - | - | - | - | - | - | - | - | S |      |
| 1068 | C    | T | T | - | - | - | - | - | - | - | - | - | - | A | A | A | A | A | A | - | - | - | - | - | - | NS   |
| 1089 | C    | - | - | - | - | - | - | - | - | - | - | - | - | A | A | A | A | A | A | A | A | A | A | A | A | NS   |
| 1101 | G    | - | - | - | - | - | - | - | - | - | - | - | - | A | A | A | A | A | A | A | A | A | A | A | A | S    |
| 1127 | T    | - | - | - | - | - | - | - | - | - | - | - | - | C | C | C | C | C | C | C | C | C | C | C | C | S    |
| 1131 | C    | - | - | - | - | - | - | - | - | - | - | - | - | T | - | - | - | - | - | - | - | - | - | - | - | S    |
| 1160 | T    | - | - | - | - | - | - | - | - | - | - | - | - | C | C | C | C | C | C | C | C | C | C | C | C | S    |

from *D. simulans* have in the ADH gene?

**B)** How many fixed differences are there between *D. melanogaster* and *D. yakuba*?

## 2.1 Allele frequencies

Allele frequencies are a central unit of population genetics analysis, but from diploid individuals we only get to observe genotype counts. Our first task then is to calculate allele frequencies from genotype counts. Consider a diploid autosomal locus segregating for two alleles ( $A_1$  and  $A_2$ ). We'll use these arbitrary labels for our alleles, merely to keep this general. Let  $N_{11}$  and  $N_{12}$  be the number of  $A_1A_1$  homozygotes and  $A_1A_2$  heterozygotes, respectively. Moreover, let  $N$  be the total number of diploid individuals in the population. We can then define the relative frequencies of  $A_1A_1$  and  $A_1A_2$  genotypes as  $f_{11} = N_{11}/N$  and  $f_{12} = N_{12}/N$ , respectively. The frequency of allele  $A_1$  in the population is then given by

$$p = \frac{2N_{11} + N_{12}}{2N} = f_{11} + \frac{1}{2}f_{12}. \quad (2.1)$$

Note that this follows directly from how we count alleles given individuals' genotypes, and holds independently of Hardy–Weinberg proportions and equilibrium (discussed below). The frequency of the alternate allele ( $A_2$ ) is then just  $q = 1 - p$ .

### 2.1.1 Measures of genetic variability

**Nucleotide diversity ( $\pi$ )** One common measure of genetic diversity is the average number of single nucleotide differences between haplotypes chosen at random from a sample. This is called nucleotide diversity and is often denoted by  $\pi$ . For example, we can calculate  $\pi$  for our ADH locus from Table 2.1 above: we have 6 sequences from *D. simulans* (a-f), there's a total of 15 ways of pairing these sequences, and

Table 2.1: Variable sites in exons 2 and 3 of the ADH gene in *Drosophila* McDONALD and KREITMAN (1991). The first column (pos.) gives the position in the gene; exon 2 begins at position 778 and we've truncated the dataset at site 1175. The second column gives the consensus nucleotide (con.), i.e. the most common base at that position; individuals with nucleotides that match the consensus are marked with a dash. The first columns of sequence (a-l) are from *D. melanogaster*; the next columns (a-f) give sequences from *D. simulans*, and the final set of columns (a-l) from *D. yakuba*. The last column shows whether the difference is a non-synonymous (N) or synonymous (S) change.

$$\pi = \frac{1}{15} ((2+1+1+1+0)+(3+3+3+2)+(0+0+1)+(0+1)+(1)) = 1.2\bar{6} \quad (2.2)$$

where the first bracketed term gives the pairwise differences between a and b-f, the second bracketed term the differences between b and c-f and so on.

Our  $\pi$  measure will depend on the length of sequence it is calculated for. Therefore,  $\pi$  is usually normalized by the length of sequence, to be a per site (or per base) measure. For example, our ADH sequence covers 397bp of DNA and so  $\pi = 1.2\bar{6}/397 = 0.0032$  per site in *D. simulans* for this region. Note that we could also calculate  $\pi$  per synonymous site (or non-synonymous). For synonymous site  $\pi$ , we would count up number of synonymous differences between our pairs of sequences, and then divide by the total number of sites where a synonymous change could have occurred.<sup>1</sup>

*Number of segregating sites.* Another measure of genetic variability is the total number of sites that are polymorphic (segregating) in our sample. One issue is that the number of segregating sites will grow as we sequence more individuals (unlike  $\pi$ ). Later in the course, we'll talk about how to standardize the number of segregating sites for the number of individuals sequenced (see eqn (3.39)).

*The frequency spectrum.* We also often want to compile information about the frequency of alleles across sites. We call alleles that are found once in a sample *singletons*, alleles that are found twice in a sample *doubletons*, and so on. We count up the number of loci where an allele is found  $i$  times out of  $n$ , e.g. how many singletons are there in the sample, and this is called the *frequency spectrum*. We'll want to do this in some consistent manner, so we often calculate the minor allele frequency spectrum, or the frequency spectrum of derived alleles.

**Question 2.** How many minor-allele singletons are there in *D. simulans* in the ADH region?

*Levels of genetic variability across species.* Two observations have puzzled population geneticists since the inception of molecular population genetics. The first is the relatively high level of genetic variation observed in most obligately sexual species. This first observation, in part, drove the development of the Neutral theory of molecular evolution, the idea that much of this molecular polymorphism may simply reflect a balance between genetic drift and mutation. The second observation is the relatively narrow range of polymorphism across species

<sup>1</sup> Technically we would need to divide by the total number of possible point mutations that would result in a synonymous change; this is because some mutational changes at a particular nucleotide will result in a non-synonymous or synonymous change depending on the base-pair change.

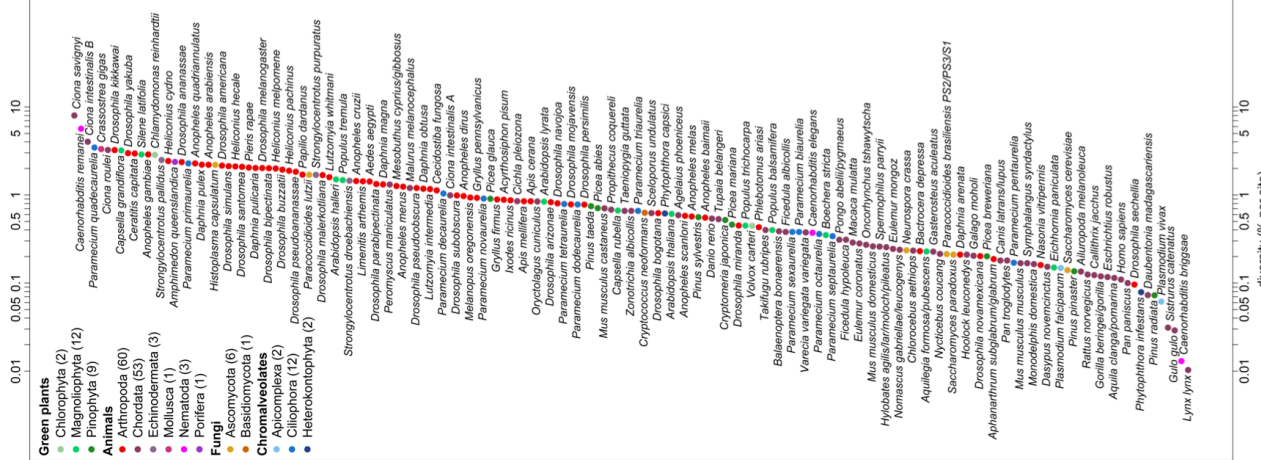
with vastly different census sizes. This observation represented a puzzle as Neutral theory predicts that levels of genetic diversity should scale population size. Much effort in theoretical and empirical population genetics has been devoted to trying to reconcile models with these various observations. We'll return to discuss these ideas throughout our course.

The first observations of molecular genetic diversity within natural populations were made from surveys of allozyme data, but we can revisit these general patterns with modern data.



Figure 2.1: Sea Squirt (*Ciona intestinalis*).

Einleitung in die vergleichende gehirnphysiologie und Vergleichende psychologie. Loeb, J. 1899. Image from the Biodiversity Heritage Library. Contributed by MBLWHOI Library. No known copyright restrictions.



For example, LEFFLER *et al.* (2012) compiled data on levels of within-population, autosomal nucleotide diversity ( $\pi$ ) for 167 species across 14 phyla from non-coding and synonymous sites (Figure 2.2). The species with the lowest levels of  $\pi$  in their survey was Lynx, with  $\pi = 0.01\%$ , i.e. only 1/10000 bases differed between two sequences. In contrast, some of the highest levels of diversity were found in *Ciona savignyi*, Sea Squirts, where a remarkable 1/12 bases differ between pairs of sequences. This 800-fold range of diversity seems impressive, but census population sizes have a much larger range.

### 2.1.2 Hardy–Weinberg proportions

Imagine a population mating at random with respect to genotypes, i.e. no inbreeding, no assortative mating, no population structure, and no sex differences in allele frequencies. The frequency of allele  $A_1$  in the population at the time of reproduction is  $p$ . An  $A_1A_1$  genotype is made by reaching out into our population and independently drawing two  $A_1$  allele gametes to form a zygote. Therefore, the probability that an individual is an  $A_1A_1$  homozygote is  $p^2$ . This probability is also the expected frequencies of the  $A_1A_1$  homozygote in the popula-

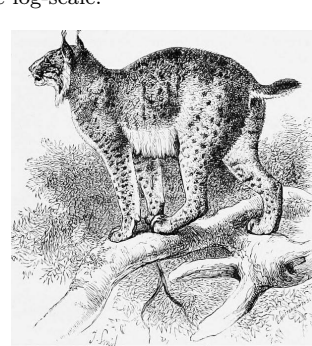


Figure 2.3: Eurasian Lynx (*Lynx lynx*).

An introduction to the study of mammals living and extinct. Flower, W.H. and Lydekker, R. 1891. Image from the Biodiversity Heritage Library. Contributed by Cornell University Library. No known copyright restrictions.

tion. The expected frequency of the three possible genotypes are

$$\begin{array}{ccc} f_{11} & f_{12} & f_{22} \\ \hline p^2 & 2pq & q^2 \end{array}$$

Note that we only need to assume random mating with respect to our focal allele in order for these expected frequencies to hold in the zygotes forming the next generation. Evolutionary forces, such as selection, change allele frequencies within generations, but do not change this expectation for new zygotes, as long as  $p$  is the frequency of the  $A_1$  allele in the population at the time when gametes fuse.

**Question 3.** On the coastal islands of British Columbia there is a subspecies of black bear (*Ursus americanus kermodei*, Kermode's bear). Many members of this black bear subspecies are white; they're sometimes called spirit bears. These bears aren't hybrids with polar bears, nor are they albinos. They are homozygotes for a recessive change at the MC1R gene. Individuals who are *GG* at this SNP are white while *AA* and *AG* individuals are black.

Below are the genotype counts for the MC1R polymorphism in a sample of bears from British Columbia's island populations from RITLAND *et al.*

| <i>AA</i> | <i>AG</i> | <i>GG</i> |
|-----------|-----------|-----------|
| 42        | 24        | 21        |

What are the expected frequencies of the three genotypes under HWE?

See Figure 2.5 for a nice empirical demonstration of Hardy-Weinberg proportions. The mean frequency of each genotype closely match their HW expectations, and much of the scatter of the dots around the expected line is due to our small sample size ( $\sim 60$  individuals). While HW often seems like a silly model, it often holds remarkably well within populations. This is because individuals don't mate at random, but they do mate at random with respect to their genotype at most of the loci in the genome.

**Question 4.** You are investigating a locus with three alleles, A, B, and C, with allele frequencies  $p_A$ ,  $p_B$ , and  $p_C$ . What fraction of the population is expected to be homozygotes under Hardy-Weinberg?

Microsatellites are regions of the genome where individuals vary for the number of copies of some short DNA repeat that they carry. These regions are often highly variable across individuals, making them a suitable way to identify individuals from a DNA sample. This so-called DNA-fingerprinting has a range of applications from establishing paternity, identifying human remains, to matching individuals to DNA samples from a crime scene. The FBI make use of the CODIS



**Figure 2.4:** Kermode's bear.  
Extinct and vanishing mammals of the western hemisphere. 1942. Glover A. Image from the Biodiversity Heritage Library. Contributed by Prelinger Library. Not in copyright.

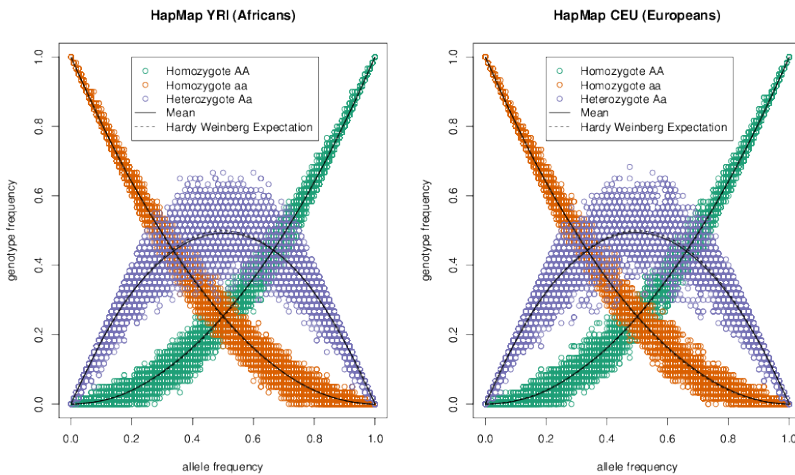


Figure 2.5: Demonstrating Hardy–Weinberg proportions using 10,000 SNPs from the HapMap European (CEU) and African (YRI) populations. Within each of these populations the allele frequency against the frequency of the 3 genotypes; each SNP is represented by 3 different coloured points. The solid lines show the mean genotype frequency. The dashed lines show the predicted genotype frequency from Hardy–Weinberg equilibrium. [Code here](#). [Blog post on figure here](#).

database<sup>2</sup>. The CODIS database contains the genotypes of over 13 million people, most of whom have been convicted of a crime. Most of the profiles record genotypes at 13 microsatellite loci that are tetranucleotide repeats (since 2017, 20 sites have been genotyped).

The allele counts for two loci (D16S539 and TH01) are shown in table 2.2 and 2.3 for a sample of 155 people of European ancestry. You can assume these two loci are on different chromosomes.

| allele name  | 80 | 90 | 100 | 110 | 120 | 121 | 130 | 140 | 150 |
|--------------|----|----|-----|-----|-----|-----|-----|-----|-----|
| allele count | 3  | 34 | 13  | 102 | 97  | 1   | 44  | 13  | 3   |

| allele name   | 60 | 70 | 80 | 90 | 93 | 100 | 110 |
|---------------|----|----|----|----|----|-----|-----|
| allele counts | 84 | 42 | 37 | 67 | 77 | 1   | 2   |

**Question 5.** You extract a DNA sample from a crime scene. The genotype is 100/80 at the D16S539 locus and 70/93 at TH01.

**A)** You have a suspect in custody. Assuming this suspect is innocent and of European ancestry, what is the probability that their genotype would match this profile by chance (a false-match probability)?

**B)** The FBI uses  $\geq 13$  markers. Why is this higher number necessary to make the match statement convincing evidence in court?

**C)** An early case that triggered debate among forensic geneticists was a crime among the Abenaki, a Native American community in Vermont (see LEWONTIN, 1994, for discussion). There was a DNA sample from the crime scene, and the perpetrator was thought likely

<sup>2</sup> CODIS: Combined DNA Index System

Table 2.2: Data for 155 Europeans at the D16S539 microsatellite from CODIS from ALGEE-HEWITT *et al.*. The top row gives the number of tetranucleotide repeats for each allele, the bottom row gives the sample counts.

Table 2.3: Same as 2.2 but for the TH01 microsatellite.

to be a member of the Abenaki community. Given that allele frequencies vary among populations, why would people be concerned about using data from a non-Abenaki population to compute a false match probability?

## 2.2 Allele sharing among related individuals and Identity by Descent

All of the individuals in a population are related to each other by a giant pedigree (family tree). For most pairs of individuals in a population these relationships are very distant (e.g. distant cousins), while some individuals will be more closely related (e.g. sibling/first cousins). All individuals are related to one another by varying levels of relatedness, or *kinship*. Related individuals can share alleles that have both descended from the shared common ancestor. To be shared, these alleles must be inherited through all meioses connecting the two individuals (e.g. surviving the  $1/2$  probability of segregation each meiosis). As closer relatives are separated by fewer meioses, closer relatives share more alleles. In Figure 2.6 we show the sharing of chromosomal regions between two cousins. As we'll see, many population and quantitative genetic concepts rely on how closely related individuals are, and thus we need some way to quantify the degree of kinship among individuals.



Figure 2.6: First cousins sharing a stretch of chromosome identical by descent. The different grandparental diploid chromosomes are coloured so we can track them and recombinations between them across the generations. Notice that the identity by descent between the cousins persists for a long stretch of chromosome due to the limited number of generations for recombination.

We will define two alleles to be identical by descent (IBD) if they are identical due to transmission from a common ancestor in the past few generations<sup>3</sup>. For the moment, we ignore mutation, and we will be more precise about what we mean by ‘past few generations’ later on. For example, parent and child share exactly one allele identical by descent at a locus, assuming that the two parents of the child are randomly mated individuals from the population. In Figure 2.12, I show a pedigree demonstrating some configurations of IBD.

<sup>3</sup> COTTERMAN, C. W., 1940 A calculus for statistico-genetics. Ph. D. thesis, The Ohio State University; and MALÉCOT, G., 1948 Les mathématiques de l'hérédité

One summary of how related two individuals are is the probability that our pair of individuals share 0, 1, or 2 alleles identical by descent (see Figure 2.7). We denote these probabilities by  $r_0$ ,  $r_1$ , and  $r_2$  respectively. See Table 2.4 for some examples. We can also interpret these probabilities as genome-wide averages. For example, on average, at a quarter of all their autosomal loci full-sibs share zero alleles identical by descent.

One summary of relatedness that will be important is the probability that two alleles picked at random, one from each of the two different individuals  $i$  and  $j$ , are identical by descent. We call this quantity the *coefficient of kinship* of individuals  $i$  and  $j$ , and denote it by  $F_{ij}$ . It is calculated as

$$F_{ij} = 0 \times r_0 + \frac{1}{4}r_1 + \frac{1}{2}r_2. \quad (2.3)$$

The coefficient of kinship will appear multiple times, in both our discussion of inbreeding and in the context of phenotypic resemblance between relatives.

| Relationship (i,j)*     | $r_0$ | $r_1$ | $r_2$ | $F_{ij}$ |
|-------------------------|-------|-------|-------|----------|
| parent-child            | 0     | 1     | 0     | $1/4$    |
| full siblings           | $1/4$ | $1/2$ | $1/4$ | $1/4$    |
| Monzygotic twins        | 0     | 0     | 1     | $1/2$    |
| 1 <sup>st</sup> cousins | $3/4$ | $1/4$ | 0     | $1/16$   |

**Question 6.** What are  $r_0$ ,  $r_1$ , and  $r_2$  for  $1/2$  sibs? ( $1/2$  sibs share one parent but not the other).

Our  $r$  coefficients are going to have various uses. For example, they allow us to calculate the probability of the genotypes of a pair of relatives. Consider a biallelic locus where allele 1 is at frequency  $p$ , and two individuals who have IBD allele sharing probabilities  $r_0$ ,  $r_1$ ,  $r_2$ . What is the overall probability that these two individuals are both homozygous for allele 1? Well that's

$$\begin{aligned} P(A_1A_1) &= P(A_1A_1|0 \text{ alleles IBD})P(0 \text{ alleles IBD}) \\ &\quad + P(A_1A_1|1 \text{ allele IBD})P(1 \text{ allele IBD}) \\ &\quad + P(A_1A_1|2 \text{ alleles IBD})P(2 \text{ alleles IBD}) \end{aligned} \quad (2.4)$$

Or, in our  $r_0$ ,  $r_1$ ,  $r_2$  notation:

$$\begin{aligned} P(A_1A_1) &= P(A_1A_1|0 \text{ alleles IBD})r_0 \\ &\quad + P(A_1A_1|1 \text{ allele IBD})r_1 \\ &\quad + P(A_1A_1|2 \text{ alleles IBD})r_2 \end{aligned} \quad (2.5)$$



Figure 2.7: A pair of diploid individuals (X and Y) sharing 0, 1, or 2 alleles IBD where lines show the sharing of alleles by descent (e.g. from a shared ancestor).

Table 2.4: Probability that two individuals of a given relationship share 0, 1, or 2 alleles identical by descent on the autosomes. \*Assuming this is the only close relationship the pair shares.

If our pair of relatives share 0 alleles IBD, then the probability that they are both homozygous is  $P(A_1A_1|0 \text{ alleles IBD}) = p^2 \times p^2$ , as all four alleles represent independent draws from the population. If they share 1 allele IBD, then the shared allele is of type  $A_1$  with probability  $p$ , and then the other non-IBD allele, in both relatives, also needs to be  $A_1$  which happens with probability  $p^2$ , so  $P(A_1A_1|1 \text{ alleles IBD}) = p \times p^2$ . Finally, our pair of relatives can share two alleles IBD, in which case  $P(A_1A_1|2 \text{ alleles IBD}) = p^2$ , because if one of our individuals is homozygous for the  $A_1$  allele, both individuals will be. Putting this all together our equation (2.5) becomes

$$P(A_1A_2) = p^4r_0 + p^3r_1 + p^2r_2 \quad (2.6)$$

Note that for specific cases we could also calculate this by summing over all the possible genotypes their shared ancestor(s) had; however, that would be much more involved and not as general as the form we have derived here.

We can write out terms like eq (2.6) for all of the possible configurations of genotype sharing/non-sharing between a pair of individuals. Based on this we can write down the expected number of polymorphic sites where our individuals are observed to share 0, 1, or 2 alleles.

**Question 7.** The genotype of our suspect in Question 5 turns out to be 100/80 for D16S539 and 70/80 at TH01. The suspect is not a match to the DNA from the crime scene; however, they could be a sibling.

Calculate the joint probability of observing the genotype from the crime and our suspect:

- A) Assuming that they share no close relationship.
- B) Assuming that they are full sibs.
- C) Briefly explain your findings.

There's a variety of ways to estimate the relationships among individuals using genetic data. An example of using allele sharing to identify relatives is offered by the work of Nancy Chen (in collaboration with Stepfanie Aguillon, see CHEN *et al.*, 2016; AGUILLON *et al.*, 2017). CHEN *et al.* has collected genotyping data from thousands of Florida Scrub Jays at over ten thousand loci. These Jays live at the Archbold field site, and have been carefully monitored for many decades allowing the pedigree of many of the birds to be known. Using these data she estimates allele frequencies at each locus. Then by equating the observed number of times that a pair of individuals share 0, 1, or 2 alleles to the theoretical expectation, she estimates the probability of  $r_0$ ,  $r_1$ , and  $r_2$  for each pair of birds. A plot of these are shown in Figure 2.9, showing how well the estimates match those known from the pedigree.



Figure 2.8: Florida Scrub-Jays (*Aphelocoma coerulescens*).

The birds of America : from drawings made in the United States and their territories. 1880. Audubon J.J. Image from the Biodiversity Heritage Library. Contributed by Smithsonian Libraries. Licensed under CC BY-2.0.

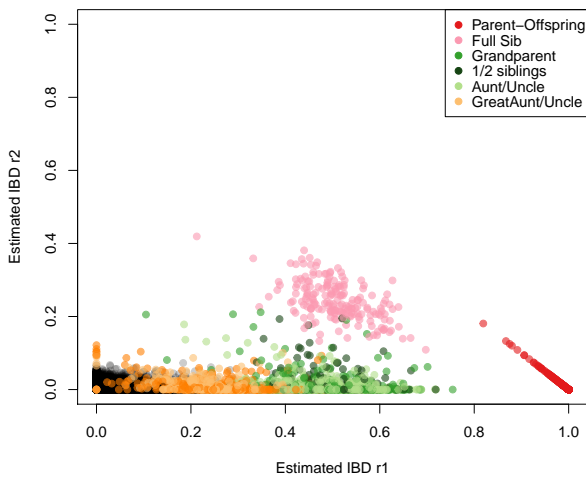


Figure 2.9: Estimated coefficient of kinship from Florida Scrub Jays. Each point is a pair of individuals, plotted by their estimated IBD ( $r_1$  and  $r_2$ ) from their genetic data. The points are coloured by their known pedigree relationships. Note that most pairs have low kinship, and no recent genealogical relationship, and so appear as black points in the lower left corner. Thanks to Nancy Chen for supplying the data. Code here.

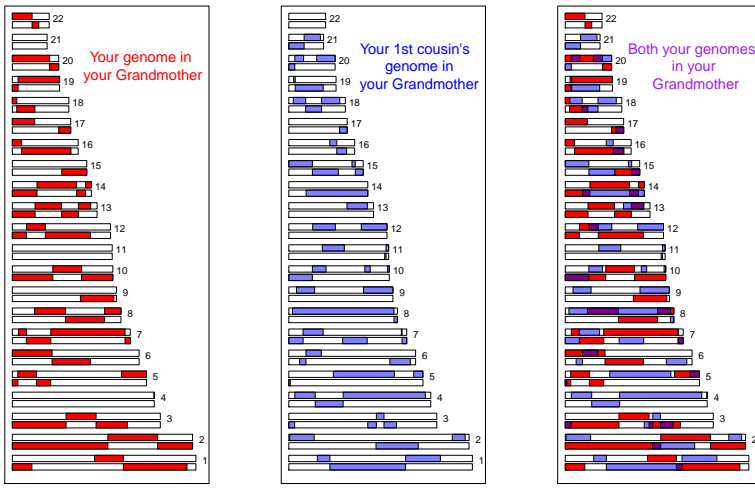


Figure 2.10: A simulation of sharing between first cousins. The regions of your grandmother's 22 autosomes that you inherited are coloured red, those that your cousins inherited are coloured blue. In the third panel we show the overlapping genomic regions in purple, these regions will be IBD in you and your cousin. If you are full first cousins, you will also have shared genomic regions from your shared grandfather, not shown here. Details about how we made these simulations here.

*Sharing of genomic blocks among relatives.* We can more directly see the sharing of the genome among close relatives using high-density SNP genotyping arrays. Below we show a simulation of you and your first cousin's genomic material that you both inherited from your shared grandmother. Colored purple are regions where you and your cousin will have matching genomic material, due to having inherited it IBD from your shared grandmother.

You and your first cousin will share at least one allele of your genotype at all of the polymorphic loci in these purple regions. There's a

range of methods to detect such sharing. One way is to look for unusually long stretches of the genome where two individuals are never homozygous for different alleles. By identifying pairs of individuals who share an unusually large number of such putative IBD blocks, we can hope to identify unknown relatives in genotyping datasets. In fact, companies like 23&me and Ancestry.com use signals of IBD to help identify family ties.

As another example, consider the case of third cousins. You share one of eight sets of great-great grandparents with each of your (likely many) third cousins. On average, you and each of your third cousins each inherit one-sixteenth of your genome from each of those two great-great grandparents. This turns out to imply that on average, a little less than one percent of your and your third cousin's genomes ( $2 \times (1/16)^2 = 0.78\%$ ) will be identical by virtue of descent from those shared ancestors. A simulated example where third cousins share blocks of their genome (on chromosome 16 and 2) due to their great, great grandmother is shown in Figure 2.11.



Figure 2.11: A simulation of sharing between third cousins, the details are the same as in Figure 2.10.

Note how if you compare Figure 2.11 and Figure 2.10, individuals inherit less IBD from a shared great, great grandmother than from a shared grandmother, as they inherit from more total ancestors further back. Also notice how the sharing occurs in shorter genomic blocks, as it has passed through more generations of recombination during meiosis. These blocks are still detectable, and so third cousins can be detected using high-density genotyping chips, allowing more distant relatives to be identified than single marker methods alone.<sup>4</sup> More distant relations than third cousins, e.g. fourth cousins, start to have

<sup>4</sup> Indeed the suspect in case of the Golden State Killer was identified through identifying third cousins that genetically matched a DNA sample from an old crime scene (see a [here](#) for more details).

a significant probability of sharing none of their genome IBD. But you have many fourth cousins, so you will share some of your genome IBD with some of them; however, it gets increasingly hard to identify the degree of relatedness from genetic data the deeper in the family tree this sharing goes.

### 2.2.1 Inbreeding

We can define an inbred individual as an individual whose parents are more closely related to each other than two random individuals drawn from some reference population.

When two related individuals produce an offspring, that individual can receive two alleles that are identical by descent, i.e. they can be homozygous by descent (sometimes termed autozygous), due to the fact that they have two copies of an allele through different paths through the pedigree. This increased likelihood of being homozygous relative to an outbred individual is the most obvious effect of inbreeding. It is also the one that will be of most interest to us, as it underlies a lot of our ideas about inbreeding depression and population structure. For example, in Figure 2.12 our offspring of first cousins is homozygous by descent having received the same IBD allele via two different routes around an inbreeding loop.

As the offspring receives a random allele from each parent ( $i$  and  $j$ ), the probability that those two alleles are identical by descent is equal to the kinship coefficient  $F_{ij}$  of the two parents (Eqn. 2.3). This follows from the fact that the genotype of the offspring is made by sampling an allele at random from each of our parents.

| $f_{11}$          | $f_{12}$     | $f_{22}$          |
|-------------------|--------------|-------------------|
| $(1 - F)p^2 + Fp$ | $(1 - F)2pq$ | $(1 - F)q^2 + Fq$ |

The only way the offspring can be heterozygous ( $A_1A_2$ ) is if their two alleles at a locus are not IBD (otherwise they would necessarily be homozygous). Therefore, the probability that they are heterozygous is

$$(1 - F)2pq, \quad (2.7)$$

where we have dropped the indices  $i$  and  $j$  for simplicity. The offspring can be homozygous for the  $A_1$  allele in two different ways. They can have two non-IBD alleles that are not IBD but happen to be of the allelic type  $A_1$ , or their two alleles can be IBD, such that they inherited allele  $A_1$  by two different routes from the same ancestor. Thus, the probability that an offspring is homozygous for  $A_1$  is

$$(1 - F)p^2 + Fp. \quad (2.8)$$



Figure 2.12: Alleles being transmitted through an inbred pedigree. The two sisters (mum and aunt) share two alleles identical by descent (IBD). The cousins share one allele IBD. The offspring of first cousins is homozygous by descent at this locus.

Table 2.5: Generalized Hardy–Weinberg

Therefore, the frequencies of the three possible genotypes can be written as given in Table 2.5, which provides a generalization of the Hardy–Weinberg proportions.

Note that the generalized Hardy–Weinberg proportions completely specify the genotype probabilities, as there are two parameters ( $p$  and  $F$ ) and two degrees of freedom (as  $p$  and  $q$  have to sum to one). Therefore, any combination of genotype frequencies at a biallelic site can be specified by a combination of  $p$  and  $F$ .

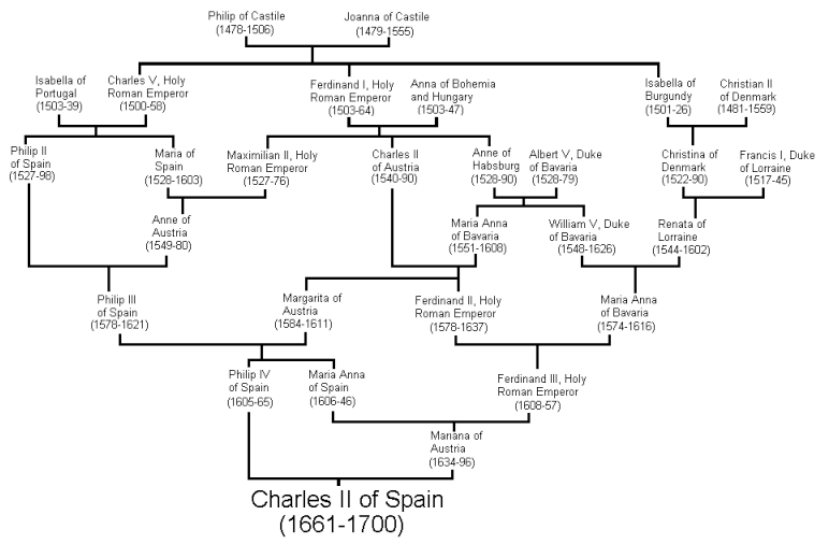
**Question 8.** The frequency of the  $A_1$  allele is  $p$  at a biallelic locus. Assume that our population is randomly mating and that the genotype frequencies in the population follow from HW. We select two individuals at random to mate from this population. We then mate the children from this cross. What is the probability that the child from this full sib-mating is homozygous?

*Multiple inbreeding loops in a pedigree.* Up to this point we have assumed that there is at most one inbreeding loop in the recent family history of our individuals, i.e. the parents of our inbred individual have at most one recent genealogical connection. However, an individual who has multiple inbreeding loops in their pedigree can be homozygous by descent thanks to receiving IBD alleles via multiple different different loops. To calculate inbreeding in pedigrees of arbitrary complexity, we can extend beyond our original relatedness coefficients  $r_0$ ,  $r_1$ , and  $r_2$  to account for higher order sharing of alleles IBD among relatives. For example, we can ask, what is the probability that *both* of the alleles in the first individual are shared IBD with one allele in the second individual? There are nine possible relatedness coefficients in total to completely describe kinship between two diploid individuals, and we won't go in to them here as it's a lot to keep track of. However, we will show how we can calculate the inbreeding coefficient of an individual with multiple inbreeding loops more directly.

Let's say the parents of our inbred individual (B and C) have  $K$  shared ancestors, i.e. individuals who appear in both B and C's recent family trees. We denote these shared ancestors by  $A_1, \dots, A_K$ , and we denote by  $n$  the total number of individuals in the chain from B to C via ancestor  $A_i$ , including B, C, and  $A_i$ . For example, if B is C's aunt, then B and C share two ancestors, which are B's parents and, equivalently, C's grandparents. In this case, there are  $n=4$  individuals from B to C through each of these two shared ancestor. In the general case, the kinship coefficient of B and C, i.e. the inbreeding coefficient of their child, is

$$F = \sum_{i=1}^K \frac{1}{2^{n_i}} (1 + f_{A_i}) \quad (2.9)$$

where  $f_{A_i}$  is the inbreeding coefficient of the ancestor  $A_i$ . What's happening here is that we sum over all the mutually-exclusive paths in the pedigree through which B and C can share an allele IBD. With probability  $1/2^{n_i}$ , a pair of alleles picked at random from B and C is descended from the same ancestral allele in individual  $A_i$ , in which case the alleles are IBD.<sup>5</sup> However, even if B inherits the maternal allele and C inherits the paternal allele of shared ancestor  $A_i$ , if  $A_i$  was themselves inbred, with probability  $f_{A_i}$  those two alleles are themselves IBD. Thus a shared *inbred* ancestor further increases the kinship of B and C.



Multiple inbreeding loops increase the probability that a child is homozygous by descent at a locus, which can be calculated simply by plugging in  $F$ , the child's inbreeding coefficient, into our generalized HW equation.

As one extreme example of the impact of multiple inbreeding loops in an individual's pedigree, let's consider king Charles II of Spain, the last of the Spanish Habsburgs. Charles was the son of Philip IV of Spain and Mariana of Austria, who were uncle and niece. If this were the only inbreeding loop, then Charles would have had an inbreeding coefficient of  $1/8$ . Unfortunately for Charles, the Spanish Habsburgs had long kept wealth and power within their family by arranging marriages between close kin. The pedigree of Charles II is shown in Figure 2.13, and multiple inbreeding loops are apparent. For example, Phillip III, Charles II's grandfather and great-grandfather, was himself

<sup>5</sup> For example, in the case of our aunt-nephew case, assuming that the aunt's two parents are their only recent shared ancestors, then  $F = 1/2^4 + 1/2^4 = 1/8$ , in agreement with the answer we would obtain from eqn (2.3).

Figure 2.13: The pedigree of King Charles II of Spain. Pedigree from wikimedia drawn by Lec CRP1, public domain.



Figure 2.14: Charles the second of Spain (by Juan Carreño de Miranda, 1685). Public Domain.

a child of an uncle-niece marriage.

ALVAREZ *et al.* (2009) calculated that Charles II had an inbreeding coefficient of 0.254, equivalent to a full-sib mating, thanks to all of the inbreeding loops in his pedigree. Therefore, he is expected to have been homozygous by descent for a full quarter of his genome. As we'll talk about later in these notes, this means that Charles may have been homozygous for a number of recessive disease alleles, and indeed he was a very sickly man who left no descendants due to his infertility.<sup>6</sup> Thus plausibly the end of one of the great European dynasties came about through inbreeding.

### 2.2.2 Calculating inbreeding coefficients from genetic data

If the observed heterozygosity in a population is  $H_O$ , and we assume that the generalized Hardy–Weinberg proportions hold, we can set  $H_O$  equal to  $f_{12}$ , and solve Eq. (2.7) for  $F$  to obtain an estimate of the inbreeding coefficient as

$$\hat{F} = 1 - \frac{f_{12}}{2pq} = \frac{2pq - f_{12}}{2pq}. \quad (2.10)$$

As before,  $p$  is the frequency of allele  $A_1$  in the population. This can be rewritten in terms of the observed heterozygosity ( $H_O$ ) and the heterozygosity expected in the absence of inbreeding,  $H_E = 2pq$ , as

$$\hat{F} = \frac{H_E - H_O}{H_E} = 1 - \frac{H_O}{H_E}. \quad (2.11)$$

Hence,  $\hat{F}$  quantifies the deviation due to inbreeding of the observed heterozygosity from the one expected under random mating, relative to the latter.

**Question 9.** Suppose the following genotype frequencies were observed for an esterase locus in a population of *Drosophila* (A denotes the “fast” allele and B denotes the “slow” allele):

| AA  | AB  | BB  |
|-----|-----|-----|
| 0.6 | 0.2 | 0.2 |

What is the estimate of the inbreeding coefficient at the esterase locus?

If we have multiple loci, we can replace  $H_O$  and  $H_E$  by their means over loci,  $\bar{H}_O$  and  $\bar{H}_E$ , respectively. Note that, in principle, we could also calculate  $F$  for each individual locus first, and then take the average across loci. However, this procedure is more prone to introducing a bias if sample sizes vary across loci, which is not unlikely when we are dealing with real data.

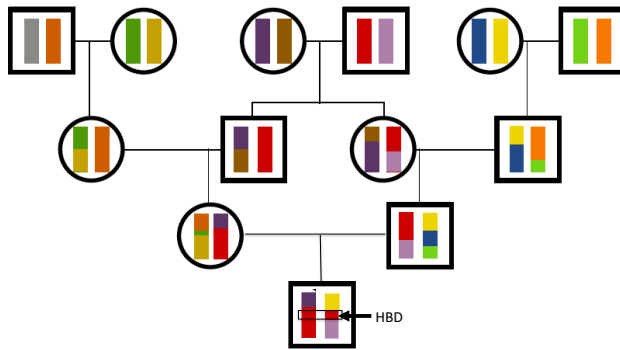
Genetic markers are commonly used to estimate inbreeding for wild and/or captive populations of conservation concern. As an example of

<sup>6</sup> Pedro Gargantilla, who performed Charles' autopsy, stated that his body "did not contain a single drop of blood; his heart was the size of a peppercorn; his lungs corroded; his intestines rotten and gangrenous; he had a single testicle, black as coal, and his head was full of water." While some of this description may refer to actual medical conditions, some of these details seem a little unlikely. See here.

this, consider the case of the Mexican wolf (*Canis lupus baileyi*), also known as the lobo, a sub-species of gray wolf.

They were extirpated in the wild during the mid-1900s due to hunting, and the remaining five lobos in the wild were captured to start a breeding program. vonHOLDT *et al.* (2011) estimated the current-day, average expected heterozygosity to be 0.18, based on allele frequencies at over forty thousand SNPs. However, the average lobo individual was only observed to be heterozygous at 12% of these SNPs. Therefore, the average inbreeding coefficient for the lobo is  $F = 1 - 0.12/0.18$ , i.e.  $\sim 33\%$  of a lobo's genome is homozygous due to recent inbreeding in their pedigree.

*Genomic blocks of homozygosity due to inbreeding.* As we saw above, close relatives are expected to share alleles IBD in large genomic blocks. Thus, when related individuals mate and transmit alleles to an inbred offspring, they transmit these alleles in big blocks through meiosis. An example, lets return to the case of our hypothetical first cousins from Figure 2.6. If this pair of individuals had a child, one possible pattern of genetic transmission is shown in Figure 2.16. The child has inherited the red stretch of chromosome via two different routes through their pedigree from the grandparents. This is an example of an autozygous segment, where the child is homozygous by descent at all of the loci in this red region. The inbreeding coefficient



of the child sets the proportion of their genome that will be in these autozygous segments. For example, a child of first full cousins is expected to have 1/16 of their genome in these segments. The more distant the loop in the pedigree, the more meioses that chromosomes have been through and the shorter individual blocks will be. A child of first cousins will have longer blocks than a child of second cousins, for example.

Individuals with multiple inbreeding loops in their family tree can have a high inbreeding coefficient due to the combined effect of many



Figure 2.15: Grey wolf (*Canis lupus*). Dogs, jackals, wolves, and foxes: a monograph of the Canidae. 1890. y J.G. Keulemans. Image from the Biodiversity Heritage Library. Contributed by University of Toronto - Gerstein Science Information Centre. Not in copyright.

Figure 2.16: .

small blocks of autozygosity. For example, Carlos the second had an inbreeding coefficient that is equivalent to that of the child of full-sibs, with a quarter of his genome expected to homozygous by descent, but this would be made up of many shorter blocks.

We can hope to detect these blocks by looking for unusually long genomic runs of homozygosity (ROH) sites in an individual's genome. One way to estimate an individual's inbreeding coefficient is then to total up the proportion of an individual's genome that falls in such ROH regions. This estimate is called  $F_{ROH}$ .

An example of using  $F_{ROH}$  to study inbreeding comes from the work of SAMS and BOYKO (2018b), who identified runs of homozygosity in 2,500 dogs, ranging from 500kb up to many megabases. Fig-



Figure 2.17: English bulldog. The dogs of Boytown. 1918. Dyer, W. A.

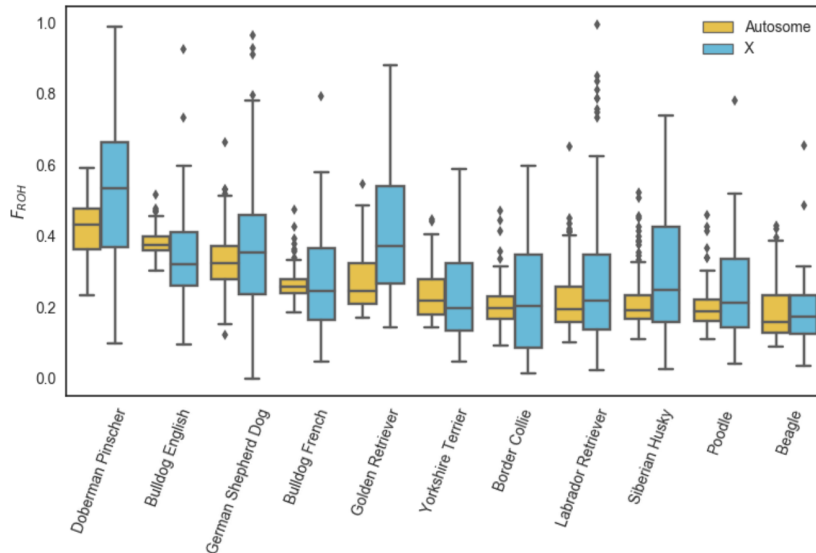


Figure 2.18: The distribution of  $F_{ROH}$  of individuals from various dog breeds from SAMS and BOYKO (2018a), licensed under CC BY 4.0.

ure 2.18 shows the distribution of  $F_{ROH}$  of individuals in each dog breed for the X and autosome. In Figure 2.19 this is broken down by the length of ROH segments.

Dog breeds have been subject to intense breeding that has resulted in high levels of inbreeding. Of the population samples examined, Doberman Pinschers have the highest levels of their genome in runs of homozygosity ( $F_{ROH}$ ), somewhat higher than English bulldogs. In 2.19 we can see that English bulldogs have more short ROH than Doberman Pinschers, but that Doberman Pinschers have more of their genome in very large ROH ( $> 16\text{ Mb}$ ). This suggests that English bulldogs have had long history of inbreeding but that Doberman Pinschers have a lot of recent inbreeding in their history.



Figure 2.19: Cumulative density of length of ROH length, measured in megabases (Mb) from SAMS and BOYKO (2018a) for various dog breeds (licensed under CC BY 4.0). Note that longer lengths of ROH are on the left of the plot.

## 2.3 Summarizing population structure

INDIVIDUALS RARELY MATE COMPLETELY AT RANDOM; your parents weren't two Bilateria plucked at random from the tree of life. Even within species, there's often geographically-restricted mating among individuals. Individuals tend to mate with individuals from the same, or closely related sets of populations. This form of non-random mating is called population structure and can have profound effects on the distribution of genetic variation within and among natural populations.

### 2.3.1 Inbreeding as a summary of population structure.

It turns out that statements about inbreeding represent one natural way to summarize population structure. We defined inbreeding as having parents that are more closely related to each other than two individuals drawn at random from some reference population. The question that naturally arises is: Which reference population should we use? While I might not look inbred in comparison to allele frequencies in the United Kingdom (UK), where I am from, my parents certainly are not two individuals drawn at random from the world-wide population. If we estimated my inbreeding coefficient  $F$  using allele frequencies within the UK, it would be close to zero, but would likely be larger if we used world-wide frequencies. This is because there is a somewhat lower level of expected heterozygosity within the UK than in the human population across the world as a whole.

WRIGHT<sup>7</sup> developed a set of ‘F-statistics’ (also called ‘fixation indices’) that formalize the idea of inbreeding with respect to different levels of population structure. See Figure 2.20 for a schematic diagram. Wright defined  $F_{XY}$  as the correlation between random gametes, drawn from the same level  $X$ , relative to level  $Y$ . We will return to why  $F$ -statistics are statements about correlations between alleles in just a moment. One commonly used  $F$ -statistic is  $F_{IS}$ , which is the inbreeding coefficient between an individual ( $I$ ) and the subpopulation ( $S$ ). Consider a single locus, where in a subpopulation ( $S$ ) a fraction  $H_I = f_{12}$  of individuals are heterozygous. In this subpopulation, let the frequency of allele  $A_1$  be  $p_S$ , such that the expected heterozygosity under random mating is  $H_S = 2p_S(1 - p_S)$ . We will write  $F_{IS}$  as

$$F_{IS} = 1 - \frac{H_I}{H_S} = 1 - \frac{f_{12}}{2p_S q_S}, \quad (2.12)$$

a direct analog of eqn. 2.10. Hence,  $F_{IS}$  is the relative difference between observed and expected heterozygosity due to a deviation from random mating within the subpopulation. We could also compare the observed heterozygosity in individuals ( $H_I$ ) to that expected in the total population,  $H_T$ . If the frequency of allele  $A_1$  in the total population is  $p_T$ , then we can write  $F_{IT}$  as

$$F_{IT} = 1 - \frac{H_I}{H_T} = 1 - \frac{f_{12}}{2p_T q_T}, \quad (2.13)$$

which compares heterozygosity in individuals to that expected in the total population. As a simple extension of this, we could imagine comparing the expected heterozygosity in the subpopulation ( $H_S$ ) to that expected in the total population  $H_T$ , via  $F_{ST}$ :

$$F_{ST} = 1 - \frac{H_S}{H_T} = 1 - \frac{2p_S q_S}{2p_T q_T}. \quad (2.14)$$

We can relate the three  $F$ -statistics to each other as

$$(1 - F_{IT}) = \frac{H_I}{H_S} \frac{H_S}{H_T} = (1 - F_{IS})(1 - F_{ST}). \quad (2.15)$$

Hence, the reduction in heterozygosity within individuals compared to that expected in the total population can be decomposed to the reduction in heterozygosity of individuals compared to the subpopulation, and the reduction in heterozygosity from the total population to that in the subpopulation.

If we want a summary of population structure across multiple subpopulations, we can average  $H_I$  and/or  $H_S$  across populations, and use a  $p_T$  calculated by averaging  $p_S$  across subpopulations (or our samples from sub-populations). For example, the average  $F_{ST}$  across

<sup>7</sup> WRIGHT, S., 1943 Isolation by Distance. *Genetics* 28(2): 114–138; and WRIGHT, S., 1949 The Genetical Structure of Populations. *Annals of Eugenics* 15(1): 323–354

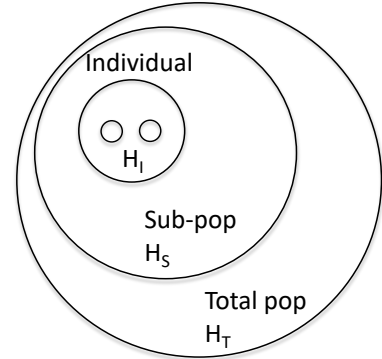


Figure 2.20: The hierarchical nature of F-statistics. The two dots within an individual represent the two alleles at a locus for an individual  $I$ . We can compare the heterozygosity on individuals ( $H_I$ ), to that found by randomly drawing alleles from the sub-population (S), to that found in the total population (T).

$K$  subpopulations (sampled with equal effort) is

$$F_{ST} = 1 - \frac{\bar{H}_S}{H_T}, \quad (2.16)$$

where  $\bar{H}_S = 1/K \sum_{i=1}^K H_S^{(i)}$ , and  $H_S^{(i)} = 2p_i q_i$  is the expected heterozygosity in subpopulation  $i$ . If the total population contains the subpopulation then  $2psqs \leq 2ptqt$ , and so  $F_{IS} \leq F_{IT}$  and  $F_{ST} \geq 0$ . Furthermore, if we have multiple sites, we can replace  $H_I$ ,  $H_S$ , and  $H_T$  with their averages across loci (as above).<sup>8</sup>

As an example of comparing a genome-wide estimate of  $F_{ST}$  to that at individual loci we can look at some data from blue- and golden-winged warblers (*Vermivora cyanoptera* and *V. chrysoptera* 1-2 & 5-6 o, Figure 2.21).

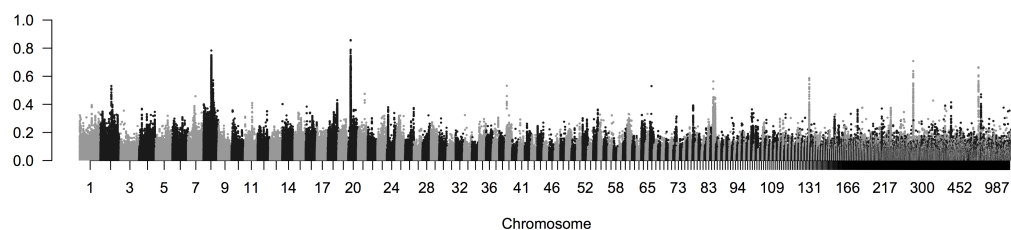
These two species are spread across eastern Northern America, with the golden-winged warbler having a smaller, more northerly range. They're quite different in terms of plumage, but have long been known to have similar songs and ecologies. The two species hybridize readily in the wild; in fact two other previously-recognized species, Brewster's and Lawrence's warbler (4 & 3 in 2.21), are actually found to just be hybrids between these two species. The golden-winged warbler is listed as 'threatened' under the Canadian endangered species act. The golden-winged warbler's habitat is under pressure from human activity and increased hybridization with the blue warbler, which is moving north into its range, also poses a significant issue. TOEWS *et al.* investigated the population genomics of these warblers, sequencing ten golden- and ten blue-winged warblers. They found very low divergence among these species, with a genome-wide  $F_{ST} = 0.0045$ .

In Figure 2.22, per SNP  $F_{ST}$  is averaged in 2000bp windows moving along the genome. The average is very low, but some regions of very

<sup>8</sup> Averaging heterozygosity across loci first, then calculating  $F_{ST}$ , rather than calculating  $F_{ST}$  for each locus individually and then taking the average, has better statistical properties as statistical noise in the denominator is averaged out.



Figure 2.21: Blue-, golden-winged, and Lawrence's warblers (*Vermivora*). The warblers of North America. Chapman, F.M. 1907. Image from the Biodiversity Heritage Library. Contributed by American Museum of Natural History Library. Not in copyright.



high  $F_{ST}$  stand out. Nearly all of these regions correspond to large allele frequency difference at loci in, or close, to genes known to be involved in plumage colouration difference in other birds. To illustrate these frequency differences TOEWS *et al.* genotyped a SNP in each of these high- $F_{ST}$  regions. Here's their genotyping counts from the SNP, segregating for an allele 1 and 2, in the *Wnt* region, a key regulatory

Figure 2.22:  $F_{ST}$  between blue- and golden-winged warbler population samples at SNPs across the genome. Each dot is a SNP, and SNPs are coloured alternating by scaffold. Thanks to David Toews for the figure.

gene involved in feather development:

| Species       | 11 | 12 | 22 |
|---------------|----|----|----|
| Blue-winged   | 2  | 21 | 31 |
| Golden-winged | 48 | 12 | 1  |

**Question 10.** With reference to the table of *Wnt*-allele counts:

- A) Calculate  $F_{IS}$  in blue-winged warblers.
- B) Calculate  $F_{ST}$  for the sub-population of blue-winged warblers compared to the combined sample.
- C) Calculate mean  $F_{ST}$  across both sub-populations.

*Interpretations of F-statistics* Let us now return to Wright's definition of the  $F$ -statistics as correlations between random gametes, drawn from the same level  $X$ , relative to level  $Y$ . Without loss of generality, we may think about  $X$  as individuals and  $S$  as the subpopulation.

Rewriting  $F_{IS}$  in terms of the observed homozygote frequencies ( $f_{11}$ ,  $f_{22}$ ) and expected homozygosities ( $p_S^2$ ,  $q_S^2$ ) we find

$$F_{IS} = \frac{2psqs - f_{12}}{2psqs} = \frac{f_{11} + f_{22} - p_S^2 - q_S^2}{2psqs}, \quad (2.17)$$

using the fact that  $p^2 + 2pq + q^2 = 1$ , and  $f_{12} = 1 - f_{11} - f_{22}$ . The form of eqn. (2.17) reveals that  $F_{IS}$  is the covariance between pairs of alleles found in an individual, divided by the expected variance under binomial sampling. Thus,  $F$ -statistics can be understood as the correlation between alleles drawn from a population (or an individual) above that expected by chance (i.e. drawing alleles sampled at random from some broader population).

We can also interpret  $F$ -statistics as proportions of variance explained by different levels of population structure. To see this, let us think about  $F_{ST}$  averaged over  $K$  subpopulations, whose frequencies are  $p_1, \dots, p_K$ . The frequency in the total population is  $p_T = \bar{p} = 1/K \sum_{i=1}^K p_i$ . Then, we can write

$$F_{ST} = \frac{2\bar{p}\bar{q} - \frac{1}{K} \sum_{i=1}^K 2p_i q_i}{2\bar{p}\bar{q}} = \frac{\left(\frac{1}{K} \sum_{i=1}^K p_i^2 + \frac{1}{K} \sum_{i=1}^K q_i^2\right) - \bar{p}^2 - \bar{q}^2}{2\bar{p}\bar{q}} = \frac{\text{Var}(p_1, \dots, p_K)}{\text{Var}(\bar{p})}, \quad (2.18)$$

which shows that  $F_{ST}$  is the proportion of the variance explained by the subpopulation labels.

### 2.3.2 Other approaches to population structure

There is a broad spectrum of methods to describe patterns of population structure in population genetic datasets. We'll briefly discuss two broad-classes of methods that appear often in the literature: assignment methods and principal components analysis.

### 2.3.3 Assignment Methods

Here we'll describe a simple probabilistic assignment to find the probability that an individual of unknown population comes from one of  $K$  predefined populations. For example, there are three broad populations of common chimpanzee (*Pan troglodytes*) in Africa: western, central, and eastern. Imagine that we have a chimpanzee, whose population of origin is unknown (e.g. it's from an illegal private collection). If we have genotyped a set of unlinked markers from a panel of individuals representative of these populations, we can calculate the probability that our chimp comes from each of these populations.

We'll then briefly explain how to extend this idea to cluster a set of individuals into  $K$  initially unknown populations. This method is a simplified version of what population genetics clustering algorithms such as STRUCTURE and ADMIXTURE do.<sup>9</sup>

*A simple assignment method* We have genotype data from unlinked  $S$  biallelic loci for  $K$  populations. The allele frequency of allele  $A_1$  at locus  $l$  in population  $k$  is denoted by  $p_{k,l}$ , so that the allele frequencies in population 1 are  $p_{1,1}, \dots, p_{1,L}$  and population 2 are  $p_{2,1}, \dots, p_{2,L}$  and so on.

You genotype a new individual from an unknown population at these  $L$  loci. This individual's genotype at locus  $l$  is  $g_l$ , where  $g_l$  denotes the number of copies of allele  $A_1$  this individual carries at this locus ( $g_l = 0, 1, 2$ ).

The probability of this individual's genotype at locus  $l$  conditional on coming from population  $k$ , i.e. their alleles being a random HW draw from population  $k$ , is

$$P(g_l | \text{pop } k) = \begin{cases} (1 - p_{k,l})^2 & g_l = 0 \\ 2p_{k,l}(1 - p_{k,l}) & g_l = 1 \\ p_{k,l}^2 & g_l = 2 \end{cases} \quad (2.19)$$

Assuming that the loci are independent, the probability of the individual's genotype across all  $S$  loci, conditional on the individual coming from population  $k$ , is

$$P(\text{ind.} | \text{pop } k) = \prod_{l=1}^S P(g_l | \text{pop } k) \quad (2.20)$$

We wish to know the probability that this new individual comes from population  $k$ , i.e.  $P(\text{pop } k | \text{ind.})$ . We can obtain this through Bayes' rule

$$P(\text{pop } k | \text{ind.}) = \frac{P(\text{ind.} | \text{pop } k)P(\text{pop } k)}{P(\text{ind.})} \quad (2.21)$$

<sup>9</sup> PRITCHARD, J. K., M. STEPHENS, and P. DONNELLY, 2000 Inference of population structure using multilocus genotype data. *Genetics* 155(2): 945–959; and ALEXANDER, D. H., J. NOVEMBRE, and K. LANGE, 2009 Fast model-based estimation of ancestry in unrelated individuals. *Genome research* 19(9): 1655–1664

where

$$P(\text{ind.}) = \sum_{k=1}^K P(\text{ind.}|\text{pop } k)P(\text{pop } k) \quad (2.22)$$

is the normalizing constant. We interpret  $P(\text{pop } k)$  as the prior probability of the individual coming from population  $k$ , and unless we have some other prior knowledge we will assume that the new individual has an equal probability of coming from each population  $P(\text{pop } k) = 1/K$ .

We interpret

$$P(\text{pop } k|\text{ind.}) \quad (2.23)$$

as the posterior probability that our new individual comes from each of our  $1, \dots, K$  populations.

More sophisticated versions of this are now used to allow for hybrids, e.g., we can have a proportion  $q_k$  of our individual's genome come from population  $k$  and estimate the set of  $q_k$ 's.

### Question 11.

Returning to our chimp example, imagine that we have genotyped a set of individuals from the Western and Eastern populations at two SNPs (we'll ignore the central population to keep things simpler). The frequency of the capital allele at two SNPs ( $A/a$  and  $B/b$ ) is given by

| Population | locus A | locus B |
|------------|---------|---------|
| Western    | 0.1     | 0.85    |
| Eastern    | 0.95    | 0.2     |

**A)** Our individual, whose origin is unknown, has the genotype  $AA$  at the first locus and  $bb$  at the second. What is the posterior probability that our individual comes from the Western population versus Eastern chimp population?

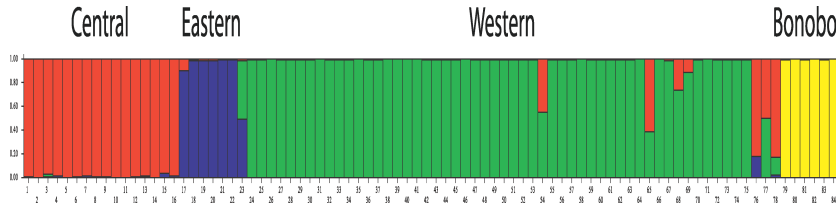
**B)** Let's assume that our individual is a hybrid. At each locus, with probability  $q_W$  our individual draws an allele from the Western population and with probability  $q_C = 1 - q_W$  they draw an allele from the Eastern population. What is the probability of our individual's genotype given  $q_C$ ?

**Optional** You could plot this probability as a function of  $q_W$ . How does your plot change if our individual is heterozygous at both loci?

*Clustering based on assignment methods* While it is great to be able to assign our individuals to a particular population, these ideas can be pushed to learn about how best to describe our genotype data in terms of discrete populations without assigning any of our individuals to populations *a priori*. We wish to cluster our individuals into  $K$  unknown populations. We begin by assigning our individuals at random to these  $K$  populations.

1. Given these assignments we estimate the allele frequencies at all of our loci in each population.
2. Given these allele frequencies we chose to reassign each individual to a population  $k$  with a probability given by eqn. (2.20).

We iterate steps 1 and 2 for many iterations (technically, this approach is known as *Gibbs Sampling*). If the data is sufficiently informative, the assignments and allele frequencies will quickly converge on a set of likely population assignments and allele frequencies for these populations.



To do this in a full Bayesian scheme we need to place priors on the allele frequencies (for example, one could use a beta distribution prior). Technically we are using the joint posterior of our allele frequencies and assignments. Programs like STRUCTURE, use this type of algorithm to cluster the individuals in an “unsupervised” manner (i.e. they work out how to assign individuals to an unknown set of populations). See Figure 2.23 for an example of Becquet *et al* using STRUCTURE to determine the population structure of chimpanzees.

STRUCTURE-like methods have proven incredible popular and useful in examining population structure within species. However, the results of these methods are open to misinterpretation, see LAWSON *et al.* (2018) for a recent discussion. Two common mistakes are 1) taking the results of STRUCTURE-like approaches for some particular value of  $K$  and taking this to represent the best way to describe population-genetic variation. 2) Thinking that these clusters represent ‘pure’ ancestral populations.

There is no right choice of  $K$ , the number of clusters to partition into. There are methods of judging the ‘best’  $K$  by some statistical measure given some particular dataset, but that is not the same as saying this is the most meaningful level on which to summarize population structure in data. For example, running STRUCTURE on world-wide human populations for low value of  $K$  will result in population clusters that roughly align with continental populations (ROSENBERG *et al.*, 2002). However, that does not tell us that assigning ancestral at the level of continents is a particularly meaningful way of partitioning individuals. Running the same data for higher value of  $K$ ,

Figure 2.23: BECQUET *et al.* (2007) genotyped 78 common chimpanzee and 6 bonobo at over 300 polymorphic markers (in this case microsatellites). They ran STRUCTURE to cluster the individuals using these data into  $K = 4$  populations. In BECQUET *et al.* (2007) above figure they show each individual as a vertical bar divided into four colours depicting the estimate of the fraction of ancestry that each individual draws from each of the four estimated populations (licensed under CC BY 4.0). We can see that these four colours/populations correspond to: Red, central; blue, eastern; green, western; yellow, bonobo.

or within continental regions, will result in much finer-scale partitioning of continental groups (ROSENBERG *et al.*, 2002; LI *et al.*, 2008). No one of these layers of population structure identified is privileged as being more meaningful than another.

It is tempting to think of these clusters as representing ancestral populations, which themselves are not the result of admixture. However, that is not the case, for example, running STRUCTURE on world-wide human data identifies a cluster that contains many European individuals, however, on the basis of ancient DNA we know that modern Europeans are a mixture of distinct ancestral groups.

### 2.3.4 Principal components analysis

Principal component analysis (PCA) is a common statistical approach to visualize high dimensional data, and used by many fields. The idea of PCA is to give a location to each individual data-point on each of a small number principal component axes. These PC axes are chosen to reflect major axes of variation in the data, with the first PC being that which explains largest variance, the second the second most, and so on. The use of PCA in population genetics was pioneered by Cavalli-Sforza and colleagues and now with large genotyping datasets, PCA has made come back.<sup>10</sup>

Consider a dataset consisting of  $N$  individuals at  $S$  biallelic SNPs. The  $i^{th}$  individual's genotype data at locus  $\ell$  takes a value  $g_{i,\ell} = 0, 1$ , or  $2$  (corresponding to the number of copies of allele  $A_1$  an individual carries at this SNP). We can think of this as a  $N \times S$  matrix (where usually  $N \ll S$ ).

Denoting the sample mean allele frequency at SNP  $\ell$  by  $p_\ell$ , it's common to standardize the genotype in the following way

$$\frac{g_{i,\ell} - 2p_\ell}{\sqrt{2p_\ell(1 - p_\ell)}} \quad (2.24)$$

i.e. at each SNP we center the genotypes by subtracting the mean genotype ( $2p_\ell$ ) and divide through by the square root of the expected variance assuming that alleles are sampled binomially from the mean frequency ( $\sqrt{2p_\ell(1 - p_\ell)}$ ). Doing this to all of our genotypes, we form a data matrix (of dimension  $N \times S$ ). We can then perform principal components analysis of this data matrix to uncover the major axes of genotype variance in our sample. Figure 2.24 shows a PCA from BECQUET *et al.* (2007) using the same chimpanzee data as in Figure 2.23.

It is worth taking a moment to delve further into what we are doing here. There's a number of equivalent ways of thinking about what PCA is doing. One of these ways is to think that when we do PCA we are building the individual by individual covariance matrix and per-

<sup>10</sup> MENOZZI, P., A. PIAZZA, and L. CAVALLI-SFORZA, 1978 Synthetic maps of human gene frequencies in Europeans. *Science* 201(4358): 786–792; and PATTERSON, N., A. L. PRICE, and D. REICH, 2006 Population structure and eigenanalysis. *PLoS genetics* 2(12): e190



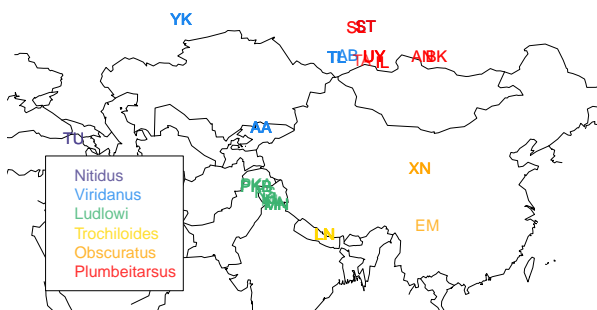
forming an eigenvalue decomposition of this matrix (with the eigenvectors being the PCs). This individual by individual covariance matrix has entries the  $[i, j]$  given by

$$\frac{1}{S-1} \sum_{\ell=1}^S \frac{(g_{i,\ell} - 2p_\ell)(g_{j,\ell} - 2p_\ell)}{2p_\ell(1-p_\ell)} \quad (2.25)$$

Note that this is the covariance, and is very similar to those we encountered in discussing  $F$ -statistics as correlations (equation (2.17)), except now we are asking about the covariance between two individuals above that expected if they were both drawn from the total sample at random (rather than the covariance of alleles within a single individual). So by performing PCA on the data we are learning about the major (orthogonal) axes of the kinship matrix.

As an example of the application of PCA, let's consider the case of the putative ring species in the Greenish warbler (*Phylloscopus trochiloides*) species complex. This set of subspecies exists in a ring around the edge of the Himalayan plateau. ALCAIDE *et al.* (2014) collected 95 greenish warbler samples from 22 sites around the ring, and the sampling locations are shown in figure 2.25.

Figure 2.24: Principal Component Analysis by BECQUET *et al.* (2007) using the same chimpanzee data as in Figure 2.23. Here BECQUET *et al.* (2007) plot the location of each individual on the first two principal components (called eigenvectors) in the left panel, and on the second and third principal components (eigenvectors) in the right panel (licensed under CC BY 4.0). PCA, The individuals identified as all of one ancestry by STRUCTURE cluster together by population (solid circles). While the nine individuals identified by STRUCTURE as hybrids (open circles) are for the most part fall at intermediate locations in the PCA. There are two individuals (red open circles) reported as being of a particular population but that but appear to be hybrids.



It is thought that these warblers spread from the south, northward in two different directions around the inhospitable Himalayan plateau, establishing populations along the western edge (green and blue populations) and the eastern edge (yellow and red populations). When they came into secondary contact in Siberia, they were reproductive isolated from one another, having evolved different songs and accumulated other reproductive barriers from each other as they spread independently north around the plateau, such that *P. t. viridanus* (blue) and *P. t. plumbeitarsus* (red) populations presently form a stable hybrid zone.

ALCAIDE *et al.* (2014) obtained sequence data for their samples at 2,334 snps. In Figure 2.27 you can see the matrix of kinship coefficients, using (2.25), between all pairs of samples. You can already see a lot about population structure in this matrix. Note how the red and yellow samples, thought to be derived from the Eastern route around the Himalayas, have higher kinship with each other, and blue and the (majority) of the green samples, from the Western route, form a similarly close group in terms of their higher kinship.

We can then perform PCA on this kinship matrix to identify the major axes of variation in the dataset. Figure 2.28 shows the samples plotted on the first two PCs. The two major routes of expansion clearly occupy different parts of PC space. The first principal component distinguishes populations running North to South along the western route of expansion, while the second principal component distinguishes among populations running North to South along the Eastern route of expansion. Thus genetic data supports the hypothesis that the Greenish warblers speciated as they moved around the Himalayan plateau. However, as noted by ALCAIDE *et al.* (2014), it also suggests additional complications to the traditional view of these

Figure 2.25: The sampling locations of 22 populations of Greenish warblers from ALCAIDE *et al.* (2014). The samples are coloured by the subspecies. Code here.



Figure 2.26: Greenish warbler, subsp. *viridanus* (*Phylloscopus trochiloides viridanus*). Coloured figures of the birds of the British Islands. 1885. Lilford T. L. P.. Image from the Biodiversity Heritage Library. Contributed by American Museum of Natural History Library. Not in copyright. (Greenish warblers are rare visitors to the UK.)



Figure 2.27: The matrix of kinship coefficients calculated for the 95 samples of Greenish warblers. Each cell in the matrix gives the pairwise kinship coefficient calculated for a particular pair. Hotter colours indicating higher kinship. The x and y labels of individuals are the population labels from Figure 2.25, and coloured by subspecies label as in that figure. The rows and columns have been organized to cluster individuals with high kinship. [Code here.](#)

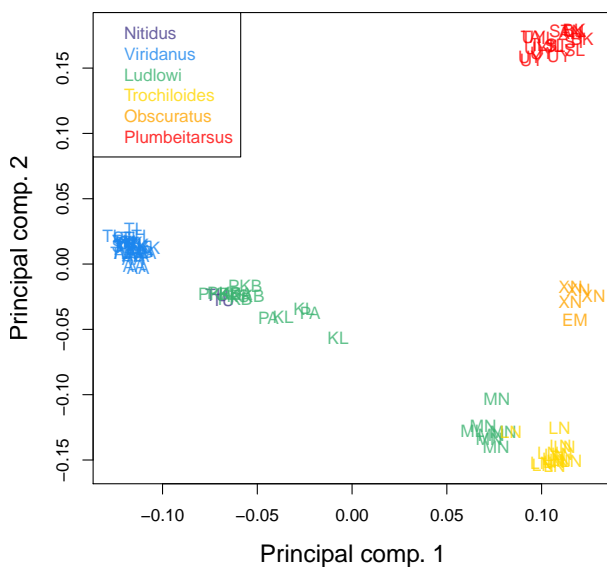


Figure 2.28: The 95 greenish warbler samples plotted on their locations on the first two principal components. The labels of individuals are the population labels from Figure 2.25, and coloured by subspecies label as in that figure. [Code here.](#)

warblers as an unbroken ring species, a case of speciation by continuous geographic isolation. The *Ludlowi* subspecies shows a significant genetic break, with the southern most MN samples clustering with the *Trochiloides* subspecies, in both the PCA and kinship matrix (Figures 2.28 and 2.27), despite being much more geographically close to the other *Ludlowi* samples. This suggests that genetic isolation is not just a result of geographic distance, and other biogeographic barriers must be considered in the case of this broken ring species.

Finally, while PCA is a wonderful tool for visualizing genetic data, care must be taken in its interpretation. The U-like shape in the case of the Greenish warbler PC might be consistent with some low level of gene flow between the red and the blue populations, pulling them genetically closer together and helping to form a genetic ring as well as a geographic ring. However, U-like shapes are expected to appear in PCAs even if our populations are just arrayed along a line, and more complex geometric arrangements of populations in PC space can result under simple geographic models (NOVEMBRE and STEPHENS, 2008). Inferring the geographical and population-genetic history of species requires the application of a range of tools; see ALCAIDE *et al.* (2014) and BRADBURD *et al.* (2016) for more discussion of the Greenish warblers.

### 2.3.5 Correlations between loci, linkage disequilibrium, and recombination

Up to now we have been interested in correlations between alleles at the same locus, e.g. correlations within individuals (inbreeding) or between individuals (relatedness). We have seen how relatedness between parents affects the extent to which their offspring is inbred. We now turn to correlations between alleles at different loci.

*Recombination* To understand correlations between loci we need to understand recombination a bit more carefully. Let us consider a heterozygous individual, containing  $AB$  and  $ab$  haplotypes. If no recombination occurs between our two loci in this individual, then these two haplotypes will be transmitted intact to the next generation. While if a recombination (i.e. an odd number of crossing over events) occurs between the two parental haplotypes, then  $1/2$  the time the child receives an  $Ab$  haplotype and  $1/2$  the time the child receives an  $aB$  haplotype. Effectively, recombination breaks up the association between loci. We'll define the recombination fraction ( $r$ ) to be the probability of an odd number of crossing over events between our loci in a single meiosis. In practice we'll often be interested in relatively short regions such that recombination is relatively rare, and so we might think that  $r = r_{BP}L \ll \frac{1}{2}$ , where  $r_{BP}$  is the average recombination rate (in Morgans) per base pair (typically  $\sim 10^{-8}$ ) and  $L$  is the number of base pairs separating our two loci.

*Linkage disequilibrium* The (horrible) phrase linkage disequilibrium (LD) refers to the statistical non-independence (i.e. a correlation) of alleles in a population at different loci. It's an awful name for a fantastically useful concept; LD is key to our understanding of diverse topics, from sexual selection and speciation to the limits of genome-wide association studies.

Our two biallelic loci, which segregate alleles  $A/a$  and  $B/b$ , have allele frequencies of  $p_A$  and  $p_B$  respectively. The frequency of the two locus haplotype  $AB$  is  $p_{AB}$ , and likewise for our other three combinations. If our loci were statistically independent then  $p_{AB} = p_A p_B$ , otherwise  $p_{AB} \neq p_A p_B$ . We can define a covariance between the  $A$  and  $B$  alleles at our two loci as

$$D_{AB} = p_{AB} - p_A p_B \quad (2.26)$$

and likewise for our other combinations at our two loci ( $D_{Ab}$ ,  $D_{aB}$ ,  $D_{ab}$ ). Gametes with two similar case alleles (e.g. A and B, or a and b) are known as *coupling* gametes, and those with different case alleles are known as *repulsion* gametes (e.g. a and B, or A and b). Then,

we can think of  $D$  as measuring the *excess* of coupling to repulsion gametes. These  $D$  statistics are all closely related to each other as  $D_{AB} = -D_{Ab}$  and so on. Thus we only need to specify one  $D_{AB}$  to know them all, so we'll drop the subscript and just refer to  $D$ . Also a handy result is that we can rewrite our haplotype frequency  $p_{AB}$  as

$$p_{AB} = p_A p_B + D. \quad (2.27)$$

If  $D = 0$  we'll say the two loci are in linkage equilibrium, while if  $D > 0$  or  $D < 0$  we'll say that the loci are in linkage disequilibrium (we'll perhaps want to test whether  $D$  is statistically different from 0 before making this choice). You should be careful to keep the concepts of linkage and linkage disequilibrium separate in your mind. Genetic linkage refers to the linkage of multiple loci due to the fact that they are transmitted through meiosis together (most often because the loci are on the same chromosome). Linkage disequilibrium merely refers to the covariance between the alleles at different loci; this may in part be due to the genetic linkage of these loci but does not necessarily imply this (e.g. genetically unlinked loci can be in LD due to population structure).

**Question 12.** You genotype 2 bi-allelic loci (A & B) segregating in two mouse subspecies (1 & 2) which mate randomly among themselves, but have not historically interbreed since they speciated. On the basis of previous work you estimate that the two loci are separated by a recombination fraction of 0.1. The frequencies of haplotypes in each population are:

| Pop | $p_{AB}$ | $p_{Ab}$ | $p_{aB}$ | $p_{ab}$ |
|-----|----------|----------|----------|----------|
| 1   | .02      | .18      | .08      | .72      |
| 2   | .72      | .18      | .08      | .02      |

- A) How much LD is there within species? (i.e. estimate  $D$ )  
 B) If we mixed individuals from the two species together in equal proportions, we could form a new population with  $p_{AB}$  equal to the average frequency of  $p_{AB}$  across species 1 and 2. What value would  $D$  take in this new population before any mating has had the chance to occur?

Our linkage disequilibrium statistic  $D$  depends strongly on the allele frequencies of the two loci involved. One common way to partially remove this dependence, and make it more comparable across loci, is to divide  $D$  through by its the maximum possible value given the frequency of the loci. This normalized statistic is called  $D'$  and varies between +1 and -1. In Figure 2.29 there's an example of LD across the TAP2 region in human and chimp. Notice how physically close SNPs, i.e. those close to the diagonal, have higher absolute values of  $D'$  as

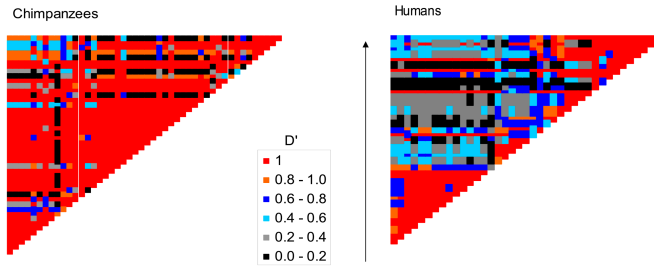


Figure 2.29: LD across the TAP2 gene region in a sample of Humans and Chimps, from PTAK *et al.* (2004), licensed under CC BY 4.0. The rows and columns are consecutive SNPs, with each cell giving the absolute  $D'$  value between a pair of SNPs. Note that these are different sets of SNPs in the two species, as shared polymorphisms are very rare.

closely linked alleles are separated by recombination less often allowing high levels of LD to accumulate. Over large physical distances, away from the diagonal, there is lower  $D'$ . This is especially notable in humans as there is an intense, human-specific recombination hotspot in this region, which is breaking down LD between opposite sides of this region.

Another common statistic for summarizing LD is  $r^2$  which we write as

$$r^2 = \frac{D^2}{p_A(1-p_A)p_B(1-p_B)} \quad (2.28)$$

As  $D$  is a covariance, and  $p_A(1-p_A)$  is the variance of an allele drawn at random from locus  $A$ ,  $r^2$  is the squared correlation coefficient. Note that this  $r$  in  $r^2$  is NOT the recombination fraction.

Figure 2.31 shows  $r^2$  for pairs of SNPs at various physical distances in two population samples of *Mus musculus domesticus*. Again LD is highest between physically close markers as LD is being generated faster than it can decay via recombination; more distant markers have much lower LD as here recombination is winning out. Note the decay of LD is much slower in the advanced-generation cross population than in the natural wild-caught population. This persistence of LD across megabases is due to the limited number of generations for recombination since the cross was created.

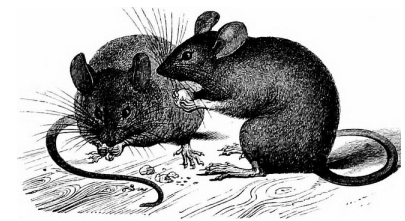
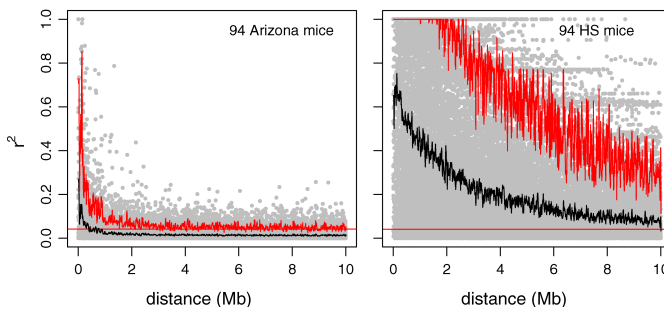


Figure 2.30: *Mus musculus*. A history of British quadrupeds, including the Cetacea. 1874. Bell T., Tomes, R. F. m Alston E. R. Image from the Biodiversity Heritage Library. Contributed by Cornell University Library. No known copyright restrictions.

Figure 2.31: The decay of LD for autosomal SNP in *Mus musculus domesticus*, as measured by  $r^2$ , in a wild-caught mouse population from Arizona and a set of advanced-generation crosses between inbred lines of lab mice. Each dot gives the  $r^2$  for a pair of SNPs a given physical distance apart, for a total of  $\sim 3000$  SNPs. The solid black line gives the mean, the jagged the 95<sup>th</sup> percentile, and the flat red line a cutoff for significant LD. From LAURIE *et al.* (2007), licensed under CC BY 4.0.

*The generation of LD.* Various population genetic forces can generate LD. Selection can generate LD by favouring particular combinations of alleles. Genetic drift will also generate LD, not because particular combinations of alleles are favoured, but simply because at random particular haplotypes can by chance drift up in frequency. Mixing between divergent populations can also generate LD, as we saw in the mouse question above.

*The decay of LD due to recombination* We will now examine what happens to LD over the generations if we only allow recombination to occur in a very large population (i.e. no genetic drift, i.e. the frequencies of our loci follow their expectations). To do so, consider the frequency of our  $AB$  haplotype in the next generation,  $p'_{AB}$ . We lose a fraction  $r$  of our  $AB$  haplotypes to recombination ripping our alleles apart but gain a fraction  $rp_{APB}$  per generation from other haplotypes recombining together to form  $AB$  haplotypes. Thus in the next generation

$$p'_{AB} = (1 - r)p_{AB} + rp_{APB} \quad (2.29)$$

The last term above, in eqn 2.29, is  $r(p_{AB} + p_{Ab})(p_{AB} + p_{aB})$  simplified, which is the probability of recombination in the different diploid genotypes that could generate a  $p_{AB}$  haplotype.

We can then write the change in the frequency of the  $p_{AB}$  haplotype as

$$\Delta p_{AB} = p'_{AB} - p_{AB} = -rp_{AB} + rp_{APB} = -rD \quad (2.30)$$

So recombination will cause a decrease in the frequency of  $p_{AB}$  if there is an excess of  $AB$  haplotypes within the population ( $D > 0$ ), and an increase if there is a deficit of  $AB$  haplotypes within the population ( $D < 0$ ). Our LD in the next generation is

$$\begin{aligned} D' &= p'_{AB} - p'_{APB} \\ &= (p_{AB} + \Delta p_{AB}) - (p_A + \Delta p_A)(p_B + \Delta p_B) \\ &= p_{AB} + \Delta p_{AB} - p_{APB} \\ &= (1 - r)D \end{aligned} \quad (2.31)$$

where we can cancel out  $\Delta p_A$  and  $\Delta p_B$  above because recombination only changes haplotype, not allele, frequencies. So if the level of LD in generation 0 is  $D_0$ , the level  $t$  generations later ( $D_t$ ) is

$$D_t = (1 - r)^t D_0 \quad (2.32)$$

Recombination is acting to decrease LD, and it does so geometrically at a rate given by  $(1 - r)$ . If  $r \ll 1$  then we can approximate this by an exponential and say that

$$D_t \approx D_0 e^{-rt} \quad (2.33)$$

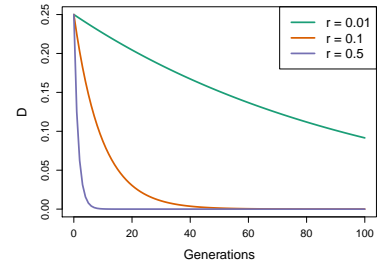


Figure 2.32: The decay of LD from an initial value of  $D_0 = 0.25$  over time (Generations) for a pair of loci a recombination fraction  $r$  apart. Code here.

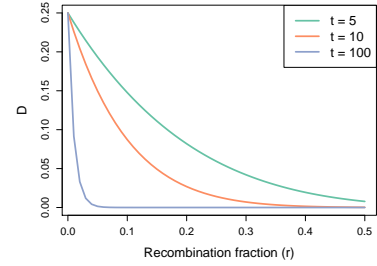
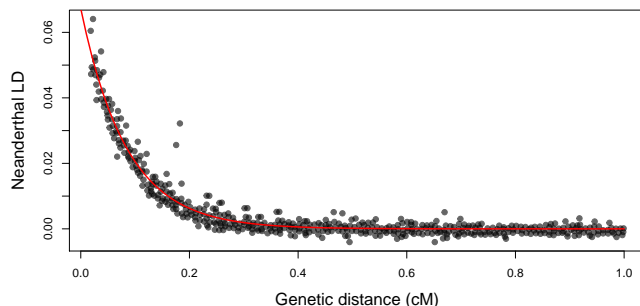


Figure 2.33: The decay of LD from an initial value of  $D_0 = 0.25$  due to recombination over  $t$  generations, plotted across possible recombination fractions ( $r$ ) between our pair of loci. Code here.

**Question 13.** You find a hybrid population between the two mouse subspecies described in the question above, which appears to be comprised of equal proportions of ancestry from the two subspecies. You estimate LD between the two markers to be 0.0723. Assuming that this hybrid population is large and was formed by a single mixture event, can you estimate how long ago this population formed?

A particularly striking example of the decay of LD generated by the mixing of populations is offered by the LD created by the interbreeding between humans and Neanderthals. Neanderthals and modern Humans diverged from each other likely over half a million years ago, allowing time for allele frequency differences to accumulate between the Neanderthal and modern human populations. The two populations spread back into secondary contact when humans moved out of Africa over the past hundred thousand years or so. One of the most exciting findings from the sequencing of the Neanderthal genome was that modern-day people with Eurasian ancestry carry a few percent of their genome derived from the Neanderthal genome, via interbreeding during this secondary contact. To date the timing of this interbreeding, SANKARARAMAN *et al.* (2012) looked at the LD in modern humans between pairs of alleles found to be derived from the Neanderthal genome (and nearly absent from African populations). In Figure 2.35 we show the average LD between these loci as a function of the genetic distance ( $r$ ) between them, from the work of SANKARARAMAN *et al.*.



Assuming a recombination rate  $r$ , we can fit the exponential decay of LD predicted by eqn. (2.33) to the data points in this figure; the fit is shown as a red line. Doing this we estimate  $t = 1200$  generations, or about 35 thousand years (using a human generation time of 29 years). Thus the LD in modern Eurasians, between alleles derived from the interbreeding with Neanderthals, represents over thirty thousand years of recombination slowly breaking down these old associations.

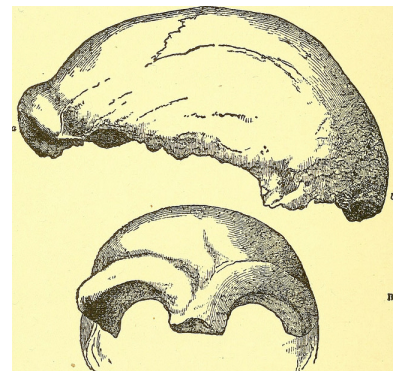


Figure 2.34: The earliest discovered fossil of a Neanderthal, fragments of skull found in a cave in the Neander Valley in Germany.  
Man's place in nature. 1890. Huxley, T. H.  
Image from the Internet Archive. Contributed by The Library of Congress. No known copyright restrictions.

Figure 2.35: The LD between putative-Neanderthal alleles in a modern European population (the CEU sample from the 1000 Genomes Project). Each point represents the average D statistic between a pair of alleles at a given genetic distance apart (as given on the x-axis and measured in centiMorgans (cM)). The putative Neanderthal alleles are alleles where the Neanderthal genome has a derived allele that is at very low frequency in a modern-human West African population sample (thought to have little admixture from Neanderthals). The red line is the fit of an exponential decay of LD, using non-linear least squared (nls in R).

The calculation done by SANKARARAMAN *et al.* (2012) is actually a bit more involved as they account for inhomogeneity in recombination rates and arrive at a date of 47,334 – 63,146 years.

# 3

## *Genetic Drift and Neutral Diversity*

RANDOMNESS IS INHERENT TO EVOLUTION, from the lucky birds blown of course to colonize some new oceanic island, to which mutations arise first in the HIV strain infecting an individual taking anti-retroviral drugs. One major source of stochasticity in evolutionary biology is genetic drift. Genetic drift occurs because more or less copies of an allele by chance can be transmitted to the next generation. This can occur because, by chance, the individuals carrying a particular allele can leave more or less offspring in the next generation. In a sexual population, genetic drift also occurs because Mendelian transmission means that only one of the two alleles in an individual, chosen at random at a locus, is transmitted to the offspring.

Genetic drift can play a role in the dynamics of all alleles in all populations, but it will play the biggest role for neutral alleles. A neutral polymorphism occurs when the segregating alleles at a polymorphic site have no discernible differences in their effect on fitness. We'll make clear what we mean by "discernible" later, but for the moment think of this as "no effect" on fitness.

*The neutral theory of molecular evolution.* The role of genetic drift in molecular evolution has been hotly debated since the 60s when the Neutral theory of molecular evolution was proposed (see OHTA and GILLESPIE, 1996, for a history).<sup>1</sup> The central premise of Neutral theory is that patterns of molecular polymorphism within species and substitution between species can be well understood by supposing that the vast majority of these molecular polymorphisms and substitutions were neutral alleles, whose dynamics were just subject to the vagaries of genetic drift and mutation. Early proponents of this view suggested that the vast majority of new mutations are either neutral or highly deleterious (e.g. mutations that disrupt important protein functions). This latter class of mutations are too deleterious to contribute much to common polymorphisms or substitutions be-

<sup>1</sup> KIMURA, M., 1968 Evolutionary rate at the molecular level. *Nature* *217*(5129): 624–626; KING, J. L. and T. H. JUKES, 1969 Non-darwinian evolution. *Science* *164*(3881): 788–798; and KIMURA, M., 1983 *The neutral theory of molecular evolution*. Cambridge University Press

tween species, because they are quickly weeded out of the population by selection.

Neutral theory can sound strange given that much of the time our first brush with evolution often focuses of adaptation and phenotypic evolution. However, proponents of this world-view didn't deny the existence of advantageous mutations, they simply thought that beneficial mutations are rare enough that their contribution to the bulk of polymorphism or divergence can be largely ignored. They also often thought that much of phenotypic evolution may well be adaptive, but again the loci responsible for these phenotypes are a small fraction of all the molecular change that occur. The original neutral theory of molecular evolution was original proposed to explain protein polymorphism. However, we can apply it more broadly to think about neutral evolution genome-wide. With that in mind, what types of molecular changes could be neutral? Perhaps:

1. Changes in non-coding DNA that don't disrupt regulatory sequences. For example, in the human genome only about 2% of the genome codes for proteins. The rest is mostly made up of old transposable element and retrovirus insertions, repeats, pseudo-genes, and general genomic clutter. Current estimates suggesting that, even counting conserved, functional, non-coding regions that < 10% of our genome is subject to evolutionary constraint (RANDS *et al.*, 2014).
2. Synonymous changes in coding regions, i.e. those that don't change the amino-acid encoded by a codon.
3. Non-synonymous changes that don't have a strong effect on the functional properties of the amino acid encoded, e.g. changes that don't change the size, charge, or hydrophobic properties of the amino acid too much.
4. An amino-acid change with phenotypic consequences, but little relevance to fitness, e.g. a mutation that causes your ears to be a slightly different shape, or that prevents an organism from living past 50 in a species where most individuals reproduce and die by their 20s.

There are counter examples to all of these ideas, e.g. synonymous changes can affect the translation speed and accuracy of proteins and so are subject to selection. However, the list above hopefully convinces you that the general thinking that some portion of molecular change may not be subject to selection isn't as daft as it may have initially sounded.

Various features of molecular polymorphism and divergence have been viewed as consistent with the neutral theory of molecular evo-

lution. The two we'll focus on in this chapter are the high level of molecular polymorphism in many species, see for example Figure 2.2, and the molecular clock. We'll see that various aspects of the original neutral theory have merit in describing some features and types of molecular change, but we'll also see that it is demonstrably wrong in some cases. We'll also see the primary utility of the neutral theory isn't whether it is right or wrong, but that it serves as a simple null model that can be tested and in some cases rejected, and subsequently built on. The broader debate currently in the field of molecular evolution is the balance of neutral, adaptive, and deleterious changes that drive different types of evolutionary change.

### 3.1 Loss of heterozygosity due to drift.

Genetic drift will, in the absence of new mutations, slowly purge our population of neutral genetic diversity, as alleles slowly drift to high or low frequencies and are lost or fixed over time.

Imagine a randomly mating population of a constant size  $N$  diploid individuals, and that we are examining a locus segregating for two alleles that are neutral with respect to each other. This population is randomly mating with respect to the alleles at this locus. See Figures 3.1 and 3.2 to see how genetic drift proceeds, by tracking alleles within a small population.

In generation  $t$  our current level of heterozygosity is  $H_t$ , i.e. the probability that two randomly sampled alleles in generation  $t$  are non-identical is  $H_t$ . Assuming that the mutation rate is zero (or vanishing small), what is our level of heterozygosity in generation  $t + 1$ ?



Figure 3.1: Loss of heterozygosity over time, in the absence of new mutations. A diploid population of 5 individuals over the generations, with lines showing transmission. In the first generation every individual is a heterozygote. Code here.

In the next generation ( $t + 1$ ) we are looking at the alleles in the offspring of generation  $t$ . If we randomly sample two alleles in generation  $t + 1$  which had different parental alleles in generation  $t$ , that is just like drawing two random alleles from generation  $t$ . So the probability that these two alleles in generation  $t + 1$ , that have different parental



Figure 3.2: Loss of heterozygosity over time, in the absence of new mutations. A diploid population of 5 individuals. In the first generation I colour every allele a different colour so we can track their descendants. Code here.

alleles in generation  $t$ , are non-identical is  $H_t$ .

Conversely, if the two alleles in our pair had the same parental allele in the proceeding generation (i.e. the alleles are identical by descent one generation back) then these two alleles must be identical (as we are not allowing for any mutation).

In a diploid population of size  $N$  individuals there are  $2N$  alleles. The probability that our two alleles have the same parental allele in the proceeding generation is  $1/(2N)$  and the probability that they have different parental alleles is  $1 - 1/(2N)$ . So by the above argument, the expected heterozygosity in generation  $t + 1$  is

$$H_{t+1} = \frac{1}{2N} \times 0 + \left(1 - \frac{1}{2N}\right) H_t \quad (3.1)$$

Thus, if the heterozygosity in generation 0 is  $H_0$ , our expected heterozygosity in generation  $t$  is

$$H_t = \left(1 - \frac{1}{2N}\right)^t H_0 \quad (3.2)$$

i.e. the expected heterozygosity within our population is decaying geometrically with each passing generation. If we assume that  $1/(2N) \ll 1$  then we can approximate this geometric decay by an exponential decay (see Question 2 below), such that

$$H_t = H_0 e^{-t/(2N)} \quad (3.3)$$

i.e. heterozygosity decays exponentially at a rate  $1/(2N)$ .

In Figure 3.3 we show trajectories through time for 40 independently simulated loci drifting in a population of 50 individuals. Each population was started from a frequency of 30% some drift up and some drift down eventually being lost or fixed from the population, but on average, across simulations, the allele frequency doesn't change. We also track heterozygosity, you can see that heterozygosity sometimes goes up, and sometimes goes down, but on average we are losing heterozygosity, and this rate of loss is well predicted by eqn. (3.2).



Figure 3.3: Change in allele frequency and loss of heterozygosity over time for 40 replicates. Simulations of genetic drift in a diploid population of 50 individuals, in the absence of new mutations. We start 40 independent, biallelic loci each with an initial allele at 30% frequency. The left panel shows the allele frequency over time and the right panel shows the heterozygosity over time, with the mean decay matching eqn. (3.2). Code here.

**Question 1.** You are in charge of maintaining a population of delta smelt in the Sacramento river delta. Using a large set of microsatellites you estimate that the mean level of heterozygosity in this population is 0.005. You set yourself a goal of maintaining a level of heterozygosity of at least 0.0049 for the next two hundred years. Assuming that the smelt have a generation time of 3 years, and that only genetic drift affects these loci, what is the smallest fully outbreeding population that you would need to maintain to meet this goal?

Note how this picture of decreasing heterozygosity stands in contrast to the consistency of Hardy-Weinberg equilibrium from the previous chapter. However, our Hardy-Weinberg *proportions* still hold in forming each new generation. As the offsprings' genotypes in the next generation ( $t + 1$ ) represent a random draw from the previous generation ( $t$ ), if the parental frequency is  $p_t$ , we *expect* a proportion  $2p_t(1 - p_t)$  of our offspring to be heterozygotes (and HW proportions for our homozygotes). However, because population size is finite, the observed genotype frequencies in the offspring will (likely) not match exactly with our expectations. As our genotype frequencies likely change slightly due to sampling, biologically this reflects random variation in family size and Mendelian segregation, the allele frequency will change. Therefore, while each generation represents a sample from Hardy-Weinberg proportions based on the generation before, our genotype proportions are not at an equilibrium (an unchanging state) as the underlying allele frequency changes over the generations. We'll develop some mathematical models for these allele frequency changes later on. For now, we'll simply note that under our simple model of drift (formally the Wright Fisher model), our allele count in the  $t + 1^{th}$  generation represents a binomial sample (of size  $2N$ ) from the popu-

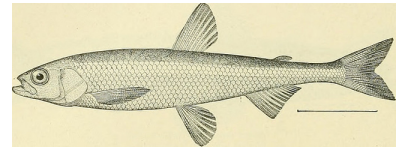


Figure 3.4: Pond smelt (*Hypomesus olidus*), a close relative of delta smelt. Bulletin of the United States Fish Commission, 1906. Image from the Biodiversity Heritage Library. Contributed by Smithsonian Libraries. Not in copyright.

lation frequency  $p_t$  in the previous generation. If you've read to here, please email Prof Coop a picture of JBS Haldane in a striped suit with the title "I'm reading the chapter 3 notes". (It's well worth googling JBS Haldane and to read more about his life; he's a true character and one of the last great polymaths. )



Figure 3.6: Loss of heterozygosity in the Black-footed Ferrets in their declining population. Numbers in brackets give estimated number of individuals alive at that time. Data from WISELY *et al.* (2002). Code here.



Figure 3.5: The black-footed ferret (*M. nigripes*).  
Wild animals of North America. The National geographical society, 1918. Image from the Biodiversity Heritage Library. Contributed by American Museum of Natural History Library. Not in copyright.

To see how a decline in population size can affect levels of heterozygosity, let's consider the case of black-footed ferrets (*Mustela nigripes*). The black-footed ferret population has declined dramatically through the twentieth century due to destruction of their habitat. In 1979, when the last known black-footed ferret died in captivity, they were thought to be extinct. In 1981, a very small wild population was rediscovered (40 individuals), but in 1985 this population suffered a number of disease outbreaks. All of the 18 remaining wild individuals were brought into captivity, 7 of which reproduced. Thanks to intense captive breeding efforts and conservation work, a wild population of over 300 individuals has been established since. However, because all of these individuals are descended from those 7 individuals who survived the bottleneck, diversity levels remain low. WISELY *et al.* measured heterozygosity at a number of microsatellites in individuals from museum collections, showing the sharp drop in diversity as population sizes crashed (see Figure 3.6).

**Question 2.** In mathematical population genetics, a commonly used approximation is  $(1 - x) \approx e^{-x}$  for  $x \ll 1$  (formally, this

follows from the Taylor series expansion of  $\exp(-x)$ , ignoring second order and higher terms of  $x$ ). This approximation is especially useful for approximating a geometric decay process by an exponential decay process, e.g.  $(1 - x)^t \approx e^{-xt}$ . Using your calculator, or R, check how good of an approximation this is compared to the exact expression for two values of  $x$ ,  $x = 0.1$ , and  $0.01$ , across two different values of  $t$ ,  $t = 5$  and  $t = 50$ . I.e. calculate both expressions for these values, hand in your answers and briefly comment on your results.

### 3.1.1 Levels of diversity maintained by a balance between mutation and drift

Next we're going to consider the amount of neutral polymorphism that can be maintained in a population as a balance between genetic drift removing variation and mutation introducing new neutral variation, see Figure 3.7 for an example. Note in our example, how no-one allele is maintained at a stable equilibrium, rather an equilibrium level of polymorphism is maintained by a constantly shifting case of alleles.

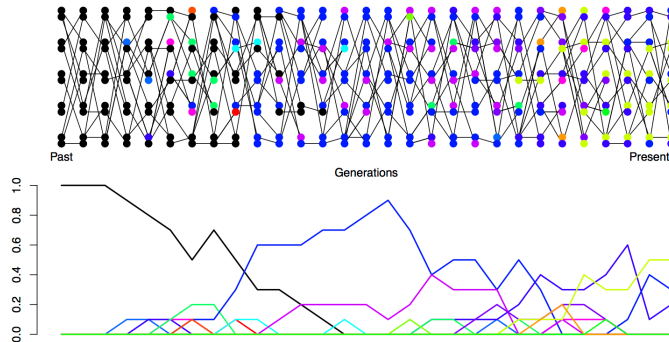


Figure 3.7: Mutation-drift balance. A diploid population of 5 individuals. In the first generation everyone has the same allele (black). Each generation the transmitted allele can mutate and we generate a new colour. In the bottom plot, I trace the frequency of alleles in our population over time. The mutation rate we use is very high, simply to maintain diversity in this small population. Code here.

*The neutral mutation rate.* We'll first want to consider the rate at which neutral mutations arise in the population. Thinking back to our discussion of the neutral theory of molecular evolution, let's suppose that there are only two classes of mutation that can arise in our genomic region of interest: neutral mutations and highly deleterious mutations. The total mutation rate at our locus is  $\mu_T$  per generation, i.e. per transmission from parent to child. A fraction  $C$  of our mutations are new alleles that are highly deleterious and so quickly removed from the population. We'll call this  $C$  parameter the constraint, and it will differ according to the genomic region we consider. The remaining fraction  $(1 - C)$  are our neutral mutations, such that our neutral mutation rate is

$$\mu = (1 - C)\mu_T \quad (3.4)$$

This is the per generation rate.

**Question 3.** It's worth taking a minute to get familiar with both how rare, and how common, mutation is. The per base pair mutation rate in humans is around  $1.5 \times 10^{-8}$  per generation. That means, on average, we have to monitor a site for  $\sim 66.6$  million transmissions from parent to child to see a mutation. Yet populations and genomes are big places, so mutations are common at these levels.

**A)** Your autosomal genome is  $\sim 3$  billion base pairs long ( $3 \times 10^9$ ). You have two copies, the one you received from your mum and one from your dad. What is the average (i.e. the expected) number of mutations that occurred in the transmission from your mum and your dad to you?

**B)** The current human population size is  $\sim 7$  billion individuals. How many times, at the level of the entire human population, is a single base-pair mutated in the transmission from one generation to the next?

*Levels of heterozygosity maintained as a balance between mutation and selection.* Looking backwards in time from one generation to the previous generation, we are going to say that two alleles which have the same parental allele (i.e. find their common ancestor) in the preceding generation have *coalesced*, and refer to this event as a *coalescent event*.

The probability that our pair of randomly sampled alleles have coalesced in the preceding generation is  $1/(2N)$ , the probability that our pair of alleles fail to coalesce is  $1 - 1/(2N)$ .

The probability that a mutation changes the identity of the transmitted allele is  $\mu$  per generation. So the probability of no mutation occurring is  $(1 - \mu)$ . We'll assume that when a mutation occurs it creates some new allelic type which is not present in the population. This assumption (commonly called the infinitely-many-alleles model) makes the math slightly cleaner, and also is not too bad an assumption biologically. See Figure 3.7 for a depiction of mutation-drift balance in this model over the generations.

This model lets us calculate when our two alleles last shared a common ancestor and whether these alleles are identical as a result of failing to mutate since this shared ancestor. For example, we can work out the probability that our two randomly sampled alleles coalesce 2 generations in the past (i.e. they fail to coalesce in generation 1 and then coalesce in generation 2), and that they are identical as

$$\left(1 - \frac{1}{2N}\right) \frac{1}{2N} (1 - \mu)^4 \quad (3.5)$$

Note the power of 4 is because our two alleles have to have failed to

mutate through 2 meioses each.

More generally, the probability that our alleles coalesce in generation  $t + 1$  (counting backwards in time) and are identical due to no mutation to either allele in the subsequent generations is

$$P(\text{coal. in } t+1 \& \text{ no mutations}) = \frac{1}{2N} \left(1 - \frac{1}{2N}\right)^t (1 - \mu)^{2(t+1)} \quad (3.6)$$

To make this slightly easier on ourselves let's further assume that  $t \approx t + 1$  and so rewrite this as:

$$P(\text{coal. in } t+1 \& \text{ no mutations}) \approx \frac{1}{2N} \left(1 - \frac{1}{2N}\right)^t (1 - \mu)^{2t} \quad (3.7)$$

This gives us the approximate probability that two alleles will coalesce in the  $(t + 1)^{\text{th}}$  generation. In general, we may not know when two alleles may coalesce: they could coalesce in generation  $t = 1, t = 2, \dots$ , and so on. Thus, to calculate the probability that two alleles coalesce in *any* generation before mutating, we can write:

$$\begin{aligned} P(\text{coal. in any generation \& no mutations}) &\approx P(\text{coal. in } t = 1 \& \text{ no mutations}) + \\ &\quad P(\text{coal. in } t = 2 \& \text{ no mutations}) + \dots \\ &= \sum_{t=1}^{\infty} P(\text{coal. in } t \text{ generations \& no mutation}) \end{aligned}$$

which follows from basic probability and the fact that coalescing in a particular generation is mutually exclusive with coalescing in a different generation.

While we could calculate a value for this sum given  $N$  and  $\mu$ , it's difficult to get a sense of what's going on with such a complicated expression. Here, we turn to a common approximation in population genetics (and all applied mathematics), where we assume that  $1/(2N) \ll 1$  and  $\mu \ll 1$ . This allows us to approximate the geometric decay as an exponential decay. Then, the probability two alleles coalesce in generation  $t + 1$  and don't mutate can be written as:

$$P(\text{coal. in } t+1 \& \text{ no mutations}) \approx \frac{1}{2N} \left(1 - \frac{1}{2N}\right)^t (1 - \mu)^{2t} \quad (3.8)$$

$$\approx \frac{1}{2N} e^{-t/(2N)} e^{-2\mu t} \quad (3.9)$$

$$= \frac{1}{2N} e^{-t(2\mu+1/(2N))} \quad (3.10)$$

Then we can approximate the summation by an integral, giving us:

$$\frac{1}{2N} \int_0^\infty e^{-t(2\mu+1/(2N))} dt = \frac{1/(2N)}{1/(2N) + 2\mu} = \frac{1}{1 + 4N\mu} \quad (3.11)$$

The equation above gives us the probability that our two alleles coalesce at some point in time, and do not mutate before reaching their common ancestor. Equivalently, this can be thought of as the probability our two alleles coalesce *before* mutating, i.e. that they are homozygous.

Then, the complementary probability that our pair of alleles are non-identical (or heterozygous) is simply one minus this. The following equation gives the equilibrium heterozygosity in a population at equilibrium between mutation and drift:

$$H = \frac{4N\mu}{1 + 4N\mu} \quad (3.12)$$

compound parameter  $4N\mu$ , the population-scaled mutation rate, will come up a number of times so we'll give it its own name:

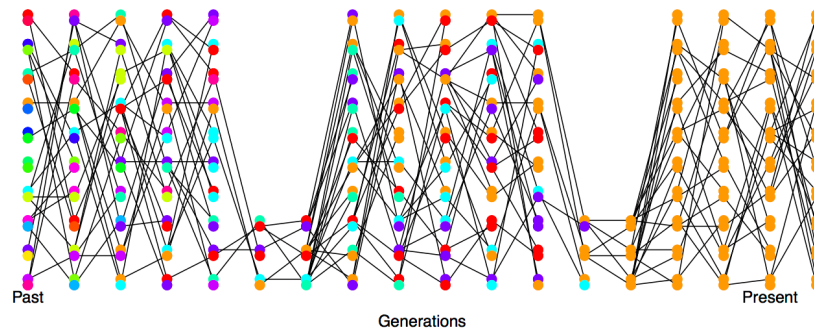
$$\theta = 4N\mu \quad (3.13)$$

So all else being equal, species with larger population sizes should have proportionally higher levels of neutral polymorphism.

**Question 4.** The sequence-level heterozygosity in *Capsella grandiflora* (grand shepherd's purse) is  $\sim 2\%$  per base. Assuming a mutation rate of  $10^{-9} bp^{-1}$  per generation, what is your estimate of the population size of *C. grandiflora*?

### 3.1.2 The effective population size

In practice, populations rarely conform to our assumptions of being constant in size with low variance in reproductive success. Real populations experience dramatic fluctuations in size, and there is often high variance in reproductive success. Thus rates of drift in natural populations are often a lot higher than the census population size would imply. See Figure 3.8 for a depiction of a repeatedly bottlenecked population losing diversity at a fast rate.



This result was derived by KIMURA and CROW (1964) and MALÉCOT (1948) (see MALÉCOT, 1969, for an English translation, the lack of earlier translation meant this result was missed). Technically we're assuming that every new mutation creates a new allele, the so-called "infinitely many alleles" model, otherwise our pair of sequences could be identical due to repeat or back mutation. See this GENETICS blog post and EWENS (2016) for a nice discussion of the history.

the effective population size ( $N_e$ ) is the population size that would result in the same rate of drift in an idealized population of constant size (following our modeling assumptions) as that observed in our true population .

Figure 3.8: Loss of heterozygosity over time in a bottlenecking population. A diploid population of 10 individuals, that bottlenecks down to three individuals repeatedly. In the first generation, I colour every allele a different colour so we can track their descendants. There are no new mutations. Code here.

To cope with this discrepancy, population geneticists often invoke the concept of an *effective population size* ( $N_e$ ). In many situations (but not all), departures from model assumptions can be captured by substituting  $N_e$  for  $N$ .

If population sizes vary rapidly in size, we can (if certain conditions are met) replace our population size by the harmonic mean population size. Consider a diploid population of variable size, whose size is  $N_t$   $t$  generations into the past. The probability our pairs of alleles have not coalesced by generation  $t$  is given by

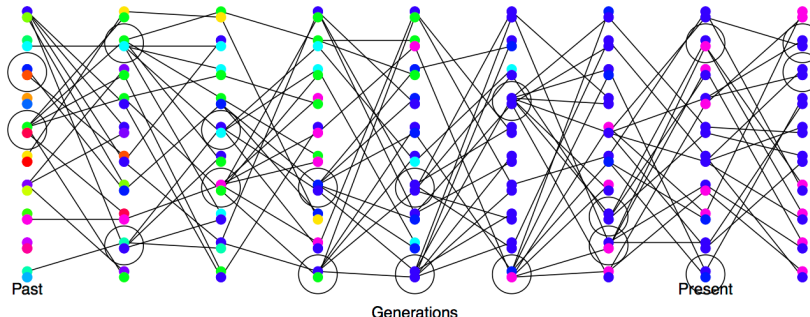
$$\prod_{i=1}^t \left(1 - \frac{1}{2N_i}\right) \quad (3.14)$$

Note that this simply collapses to our original expression  $(1 - \frac{1}{2N})^t$  if  $N_i$  is constant. Under this model, the rate of loss of heterozygosity in this population is equivalent to a population of effective size

$$N_e = \frac{1}{\frac{1}{t} \sum_{i=1}^t \frac{1}{N_i}}. \quad (3.15)$$

This is the harmonic mean of the varying population size.<sup>2</sup>

Thus our effective population size, the size of an idealized constant population which matches the rate of genetic drift, is the harmonic mean true population size over time. The harmonic mean is very strongly affected by small values, such that if our population size is one million 99% of the time but drops to 1000 every hundred or so generations,  $N_e$  will be much closer to 1000 than a million.



Variance in reproductive success will also affect our effective population size. Even if our population has a large constant size  $N$  individuals, if only small proportion of them get to reproduce, then the rate of drift will reflect this much smaller number of reproducing individuals. See Figure 3.9 for a depiction of the higher rate of drift in a population where there is high variance in reproductive success.

To see one example of this, consider the case where  $N_F$  of females get to reproduce and  $N_M$  males get reproduce. While every individual

<sup>2</sup> To see this, note that if  $1/(N_i)$  is small, then we can approximate (3.14) using the exponential approximation:

$$\prod_{i=1}^t \exp\left(-\frac{1}{2N_i}\right) = \exp\left(-\sum_{i=1}^t \frac{1}{2N_i}\right). \quad (3.16)$$

When we put the product inside the exponent, it becomes a sum. We can also write the probability of not coalescing by generation  $t$  in a population of constant size ( $N_e$ ) as an exponential, so that it takes the same form as the expression above on the right. Comparing the exponent in the two cases, we see

$$\frac{t}{2N_e} = \sum_{i=1}^t \frac{1}{2N_i} \quad (3.17)$$

So that if we want a constant effective population size ( $N_e$ ) that has the same rate of loss of heterozygosity as our variable population, we need to rearrange and solve this equation to give (3.15).

Figure 3.9: High variance on reproductive success increases the rate of genetic drift. A diploid population of 10 individuals, where the circled individuals have much higher reproductive success. In the first generation I colour every allele a different colour so we can track their descendants, there are no new mutations. Code here.

has a mother and a father, not every individual gets to be a parent. In practice, in many animal species far more females get to reproduce than males, i.e.  $N_M < N_F$ , as a few males get many mating opportunities and many males get no/few mating opportunities (see JANICKE *et al.*, 2016, for a broad analysis, and note that there are certainly many exceptions to this general pattern). When our two alleles pick an ancestor, 25% of the time our alleles were both in a female ancestor, in which case they are IBD with probability  $1/(2N_F)$ , and 25% of the time they are both in a male ancestor, in which case they coalesce with probability  $1/(2N_M)$ . The remaining 50% of the time, our alleles trace back to two individuals of different sexes in the prior generation and so cannot coalesce. Therefore, our probability of coalescence in the preceding generation is

$$\frac{1}{4} \left( \frac{1}{2N_M} \right) + \frac{1}{4} \left( \frac{1}{2N_F} \right) \quad (3.18)$$

i.e. the rate of coalescence is the harmonic mean of the two sexes' population sizes, equating this to  $\frac{1}{2N_e}$  we find

$$N_e = \frac{4N_F N_M}{N_F + N_M} \quad (3.19)$$

Thus if reproductive success is very skewed in one sex (e.g.  $N_M \ll N/2$ ), our effective population size will be much reduced as a result. For more on how different evolutionary forces affect the rate of genetic drift, and their impact on the effective population size, see CHARLESWORTH (2009).

**Question 5.** You are studying a population of 500 males and 500 females Hamadryas baboons. Assume that all of the females but only 1/10 of the males get to mate: **A)** What is the effective population size for the autosome?

**B)** Do you expect the *ratio* of X-chromosome to autosomal diversity to be higher or lower in this species compared to a species where the sexes have more similar variance in reproductive success? Explain the intuition behind your answer.

### 3.2 The Coalescent and patterns of neutral diversity

"Life can only be understood backwards; but it must be lived forwards." – Kierkegaard

*Pairwise Coalescent time distribution and the number of pairwise differences.* Thinking back to our calculations we made about the loss of neutral heterozygosity and equilibrium levels of diversity (in Sections 3.1 and 3.1.1), you'll note that we could first specify which



Figure 3.10: Male Hamadryas baboons. Up to ten females live in a harem with a single male.  
Brehm's Tierleben (Brehm's animal life).  
Brehm, A.E. 1893. Image from the Biodiversity Heritage Library. Contributed by University of Illinois Urbana-Champaign. Not in copyright.

generation a pair of sequences coalesce in, and then calculate some properties of heterozygosity based on that. That's because neutral mutations do not affect the probability that an individual transmits an allele, and so don't affect the way in which we can trace ancestral lineages back through the generations.

As such, it will often be helpful to consider the time to the common ancestor of a pair of sequences, and then think of the impact of that time to coalescence on patterns of diversity. See Figure 3.11 for an example of this.

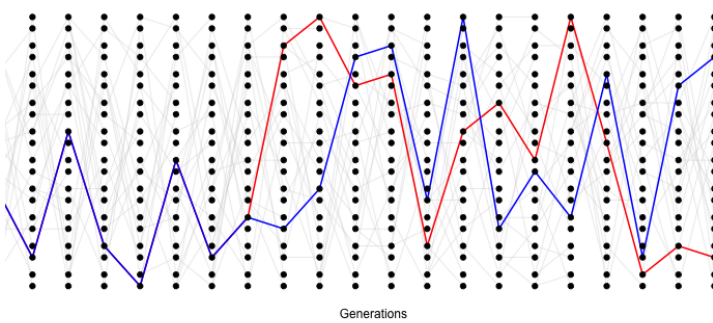


Figure 3.11: A simple simulation of the coalescent process. The simulation consists of a diploid population of 10 individuals (20 alleles). In each generation, each individual is equally likely to be the parent of an offspring (and the allele transmitted is indicated by a light grey line). We track a pair of alleles, chosen in the present day, back 14 generations until they find a common ancestor. [Code here](#).

The probability that a pair of alleles have failed to coalesce in  $t$  generations and then coalesce in the  $t + 1$  generation back is

$$P(T_2 = t + 1) = \frac{1}{2N} \left(1 - \frac{1}{2N}\right)^t \quad (3.20)$$

Thus the coalescent time of our pair of alleles is a Geometrically distributed random variable, where the probability of success is  $1/(2N)$ ; we denote this by  $T_2 \sim \text{Geo}(1/(2N))$ . The expected (i.e. the mean over many replicates) coalescent time of a pair of alleles is then

$$\mathbb{E}(T_2) = 2N \quad (3.21)$$

generations.

Conditional on a pair of alleles coalescing  $t$  generations ago, there are  $2t$  generations in which a mutation could occur. If the per generation mutation rate is  $\mu$ , then the expected number of mutations between a pair of alleles coalescing  $t$  generations ago is  $2t\mu$  (the alleles have gone through a total of  $2t$  meioses since they last shared a common ancestor). So we can write the expected number of mutations

Blurring our eyes a little, we can see that 3.20 is

$$\approx \frac{1}{2N} e^{-t/(2N)} \quad (3.22)$$

and so think of a continuous random variable, i.e. we could say that the coalescent time of a pair of sequences ( $T_2$ ) is approximately exponentially distributed with a rate  $1/(2N)$ , i.e.  $T_2 \sim \text{Exp}(1/(2N))$ . Formally we can do this by taking the limit of the discrete process more carefully.

$(S_2)$  separating two alleles drawn at random from the population as

$$\begin{aligned}\mathbb{E}(S_2) &= \sum_{t=0}^{\infty} \mathbb{E}(S_2|T_2 = t)P(T_2 = t) \\ &= \sum_{t=0}^{\infty} 2\mu t P(T_2 = t) \\ &= 2\mu \mathbb{E}(T_2) \\ &= 4\mu N\end{aligned}\tag{3.23}$$

We'll assume that mutation is rare enough that it never happens at the same basepair twice, i.e. no multiple hits, such that we get to see all of the mutation events that separate our pair of sequences.<sup>3</sup> Thus the number of mutations between a pair of sites is the observed number of differences between a pair of sequences. In the previous chapter we denote the observed number of pairwise differences at putatively neutral sites separating a pair of sequences as  $\pi$  (we usually average this over a number of pairs of sequences for a region). Therefore, under our simple, neutral, constant population-size model we expect

$$\mathbb{E}(\pi) = 4N\mu = \theta\tag{3.24}$$

So we can get an empirical estimate of  $\theta$  from  $\pi$ , let's call this  $\hat{\theta}_\pi$ , by setting  $\hat{\theta}_\pi = \pi$ , i.e. our observed level of pairwise genetic diversity. If we have an independent estimate of  $\mu$ , then from setting  $\pi = \hat{\theta}_\pi = 4N\mu$  we can furthermore obtain an estimate of the population size  $N$  that is consistent with our levels of neutral polymorphism. If we estimate the population size this way, we should call it the effective coalescent population size ( $N_e$ ). It's best to think about  $N_e$  estimated from neutral diversity as a long-term, effective population size for the species, but there's a boat load of caveats that come along with that assumption. For example, past bottlenecks and population expansions are all subsumed into a single number and so this estimated  $N_e$  may not be very representative of the population size at any time. That said, it's not a bad place to start when thinking about the rate of genetic drift for neutral diversity in our population over long time-periods.<sup>4</sup>

Lets take a moment to distinguish our expected heterozygosity (eqn. 3.12) from our expected number of pairwise differences ( $\pi$ ). Our expected heterozygosity is the probability that two alleles at a locus, sampled from a population at random, are different from each other. If one or more mutations have occurred since a pair of alleles last shared a common ancestor, then our sequences will be different from each other. On the other hand, our  $\pi$  measure keeps track of the average total number of differences between our loci. As such,  $\pi$  is often a more useful measure, as it records the number of differences between

<sup>3</sup> This is called the infinitely-many-sites assumption, which should be fine if  $N\mu_{BP} \ll 1$ , where  $\mu_{BP}$  is the mutation rate per base pair.

<sup>4</sup> Up to this point we've been describing only neutral processes, however, selection can also alter levels of polymorphism. For example, if some synonymous sites directly experience selection, then even if we use  $\pi$  calculated for on synonymous changes we may underestimate the coalescent effective population size. As we'll see later in the notes, selection at linked sites can also impact neutral diversity. As such, if we can, we may want to use genomic sites subject to the weakest selective constraints, and also far from gene-dense or otherwise very constrained regions of the genome, to estimate  $N_e$  from  $\pi$ . But even then caution is warranted.

the sequences, not just whether they are different from each other (however, for certain types of loci, e.g. microsatellites, heterozygosity is often used as we cannot usually count up the minimum number of mutations in a sensible way). In the case where our locus is a single basepair, the two measures will usually be close to one another, as  $H \approx \theta$  for small values of  $\theta$ . For example, comparing two sequences at random in humans,  $\pi \approx 1/1000$  per basepair, and the probability that a specific base pair differs between two sequences is  $\approx 1/1000$ . However, these two quantities start to differ from each other when we consider regions with higher mutation rates. For example, if we consider a 10kb region, our mutation rate will 10,000 times larger than a single base pair. For this length of sequence the probability that two randomly chosen haplotypes differ is quite different from the number of mutational differences between them. (Try a mutation rate of  $10^{-8}$  per base and a population size of 10, 000 in our calculations of  $\mathbb{E}[\pi]$  and  $H$  to see this.)

**Question 6.** ROBINSON *et al.* (2016) found that the endangered Californian Channel Island fox on San Nicolas had very low levels of diversity ( $\pi = 0.000014\text{bp}^{-1}$ ) compared to its close relative the California mainland gray fox ( $0.0012\text{bp}^{-1}$ ).

**A)** Assuming a mutation rate of  $2 \times 10^{-8}$  per bp, what effective population sizes do you estimate for these two populations?

**B)** Why is the effective population size of the Channel Island fox so low? [Hint: quickly google Channel island foxes to read up on their history, also to see how ridiculously cute they are.]

**Question 7.** In your own words describe why the coalescent time of a pair of lineages scales linearly with the (effective) population size.

*More details on the pairwise coalescent and the randomness of mutation.* We've derived the expected number of differences between a pair of sequences and talked about how variable the coalescent time is for a pair of sequences. The mutation process is also very variable; even if two sequences coalesce in the very distant past by chance, they may still be identical in the present if there was no mutation during that time.

Conditional on the coalescent time  $t$ , the probability that our pair of alleles are separated by  $S_2$  mutations since they last shared a common ancestor is

$$P(S_2|T_2 = t) = \binom{2t}{j} \mu^j (1 - \mu)^{2t-j} \quad (3.25)$$

i.e. mutations happen in  $j$  generations and do not happen in  $2t - j$  generations (with  $\binom{2t}{j}$  ways this combination of events can possibly



Figure 3.12: Gray Fox, *Urocyon cinereoargenteus*.

Diseases and enemies of poultry. Pearson and Warren. (1897) Image from the Biodiversity Heritage Library. Contributed by University of California Libraries. Not in copyright.

happen). Assuming that  $\mu \ll 1$  and that  $2t - j \approx 2t$ , then we can approximate the probability that we have  $S_2$  mutations as a Poisson distribution:

$$P(S_2|T_2 = t) = \frac{(2\mu t)^j e^{-2\mu t}}{j!} \quad (3.26)$$

i.e. a Poisson with mean  $2\mu t$ . We'll not make much use of this result, but it is very useful in thinking about how to simulate the process of mutation.

### 3.3 The coalescent process of a sample of alleles.

Usually we are not just interested in pairs of alleles, or the average pairwise diversity. Generally we are interested in the properties of diversity in samples of a number of alleles drawn from the population. Instead of just following a pair of lineages back until they coalesce, we can follow the history of a sample of alleles back through the population.

Consider first sampling three alleles at random from the population. The probability that all three alleles choose exactly the same ancestral allele one generation back is  $1/(2N)^2$ . If  $N$  is reasonably large, then this is a very small probability. As such, it is very unlikely that our three alleles coalesce all at once, and in a moment we'll see that it is safe to ignore such unlikely events.

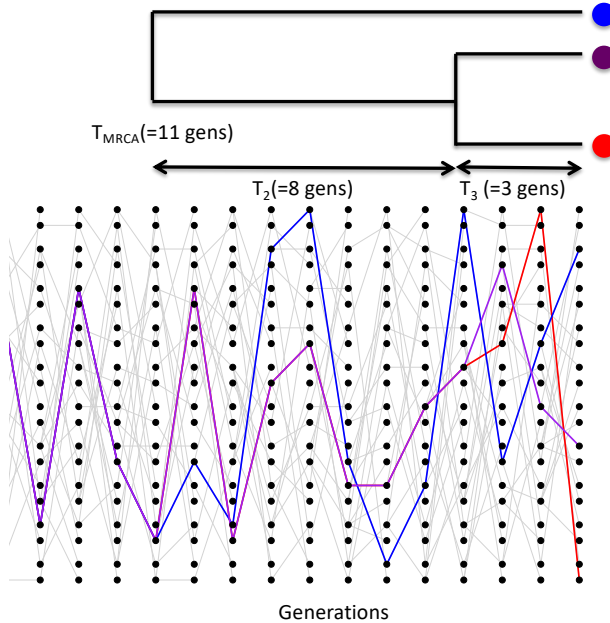


Figure 3.13: A simple simulation of the coalescent process for three lineages. We track the ancestry of three modern-day alleles, the first pair (blue and purple) coalesce four generations back, after which there are only two independent lineages we are tracking. This pair then coalesces twelve generations in the past. Note that different random realizations of this process will differ from each other a lot. The  $T_{MRCA}$  is  $T_3 + T_2$ . The total time in the tree is  $T_{tot} = 3T_3 + 2T_2 = 25$  generations. Code here.

The probability that a specific pair of alleles find a common ancestor in the preceding generation is still  $1/(2N)$ . There are three possible

pairs of alleles, so the probability that no pair finds a common ancestor in the preceding generation is

$$\left(1 - \frac{1}{2N}\right)^3 \approx \left(1 - \frac{3}{2N}\right) \quad (3.27)$$

In making this approximation we are multiplying out the right hand-side and ignoring terms of  $1/N^2$  and higher. See Figure 3.13 for a random realization of this process.

More generally, when we sample  $i$  alleles there are  $\binom{i}{2}$  pairs,<sup>5</sup> i.e.  $i(i - 1)/2$  pairs. Thus, the probability that no pair of alleles in a sample of size  $i$  coalesces in the preceding generation is

$$\left(1 - \frac{1}{(2N)}\right)^{\binom{i}{2}} \approx \left(1 - \frac{\binom{i}{2}}{2N}\right) \quad (3.28)$$

while the probability any pair coalesces is  $\approx 2N/\binom{i}{2}$ .

We can ignore the possibility that more than pairs of alleles (e.g. tripletons) simultaneously coalesce at once as terms of  $1/N^2$  and higher can be ignored as they are vanishingly rare. Obviously in reasonable sample sizes there are many more triples ( $\binom{i}{3}$ ) and higher order combinations than there are pairs ( $\binom{i}{2}$ ), but if  $i \ll N$  then we are safe to ignore these terms.

When there are  $i$  alleles, the probability that we wait until the  $t + 1$  generation before any pair of alleles coalesces is

$$P(T_i = t + 1) = \frac{\binom{i}{2}}{2N} \left(1 - \frac{\binom{i}{2}}{2N}\right)^t \quad (3.29)$$

Thus the waiting time to the first coalescent event while there are  $i$  lineages is a geometrically distributed random variable with probability of success  $\binom{i}{2}/2N$ , which we denote by

$$T_i \sim \text{Geo}\left(\frac{\binom{i}{2}}{2N}\right). \quad (3.30)$$

The mean waiting time till any of pair within our sample coalesces is

$$\mathbb{E}(T_i) = \frac{2N}{\binom{i}{2}} \quad (3.31)$$

After a pair of alleles first finds a common ancestral allele some number of generations back in the past, we only have to keep track of that common ancestral allele for the pair when looking further into the past. Thus when a pair of alleles in our sample of  $i$  alleles coalesces, we then switch to having to follow  $i - 1$  alleles back in time. Then when a pair of these  $i - 1$  alleles coalesce, we then only have to follow  $i - 2$  alleles back. This process continues until we coalesce back to a sample of two, and from there to a single most recent common ancestor (MRCA).

<sup>5</sup> said as “i choose 2”

To see the continuous time version of this, note that (3.29) is

$$\approx \frac{\binom{i}{2}}{2N} \exp\left(-\frac{\binom{i}{2}}{2N} t\right) \quad (3.32)$$

The waiting time  $T_i$  to the first coalescent event in a sample of  $i$  alleles is thus exponentially distributed with rate  $\binom{i}{2}/2N$ , i.e.  $T_i \sim \text{Exp}\left(\frac{\binom{i}{2}}{2N}\right)$ .

*Simulating a coalescent genealogy* To simulate a coalescent genealogy at a locus for a sample of  $n$  alleles we therefore simply follow the following algorithm:

1. Set  $i = n$ .
2. Simulate a random variable to be the time  $T_i$  to the next coalescent event from  $T_i \sim \text{Exp}((\frac{i}{2})/2N)$
3. Choose a pair of alleles to coalesce at random from all possible pairs.
4. Set  $i = i - 1$
5. Continue looping steps 1-3 until  $i = 1$ , i.e. the most recent common ancestor of the sample is found.

By following this algorithm we are generating realizations of the genealogy of our sample.

### 3.3.1 Expected properties of coalescent genealogies and mutations.

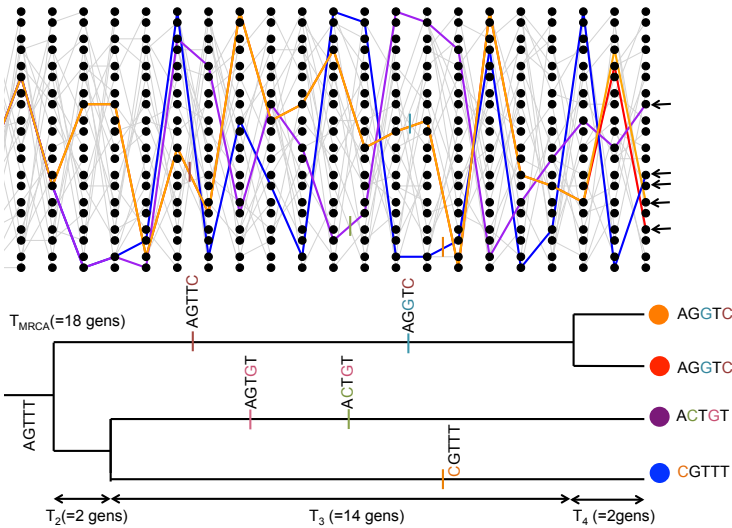


Figure 3.14: A simple coalescent tree from a single coalescent simulation, tracing the genealogy of 4 alleles with mutational changes marked with dashes showing transitions away from the MRCA sequence (AGTTT). The  $T_{MRCA}$  is  $T_4 + T_3 + T_2$ . The total time in the tree is  $T_{tot} = 4T_4 + 3T_3 + 2T_2 = 54$  generations. [Code here.](#)

*The expected time to the most recent common ancestor.* We will first consider the time to the most recent common ancestor of the entire sample ( $T_{MRCA}$ ). This is

$$T_{MRCA} = \sum_{i=n}^2 T_i \quad (3.33)$$

generations back, where we are summing from  $i = n$  alleles counting backwards to  $i = 2$  alleles (see Figure 3.14 for example). As our coalescent times for different  $i$  are independent, the expected time to the most recent common ancestor is

$$\mathbb{E}(T_{MRCA}) = \sum_{i=n}^2 \mathbb{E}(T_i) = \sum_{i=n}^2 2N / \binom{i}{2} \quad (3.34)$$

Using the fact that  $\frac{1}{i(i-1)} = \frac{1}{i-1} - \frac{1}{i}$  and a bit of rearrangement, we can rewrite this as

$$\mathbb{E}(T_{MRCA}) = 4N \left( 1 - \frac{1}{n} \right) \quad (3.35)$$

So the average  $T_{MRCA}$  scales linearly with population size  $N$ . Interestingly, as we move to larger and larger samples (i.e.  $n \gg 1$ ), the average time to the most recent common ancestor converges on  $4N$ . What's happening here is that in large samples our lineages typically coalesce rapidly at the start and very soon coalesce down to a much smaller number of lineages.

**Question 8.** Assume an autosomal effective population of 10,000 individuals (roughly the long-term human estimate) and a generation time of 30 years. What is the expected time to the most recent common ancestor of a sample of 20 people? What is this time for a sample of 500 people?

*The expected total time in a genealogy and the number of segregating sites.* Mutations fall on specific lineages of the coalescent genealogy and are transmitted to all descendants of their lineage. Furthermore, under the infinitely-many-sites assumption, each mutation creates a new segregating site. The mutation process is a *Poisson process*, and the longer a particular lineage, i.e. the more generations of meioses it represents, the more mutations that can accumulate on it. The total number of segregating sites in a sample is thus a function of the *total* amount of time in the genealogy of the sample, or the sum of all the branch lengths on the genealogical tree,  $T_{tot}$ . Our total amount of time in the genealogy is

$$T_{tot} = \sum_{i=n}^2 iT_i \quad (3.36)$$

as when there are  $i$  lineages, each contributes a time  $T_i$  to the total time (see Figure 3.14 for an example). Taking the expectation of the total time in the genealogy,

$$\mathbb{E}(T_{tot}) = \sum_{i=n}^2 i \frac{2N}{\binom{i}{2}} = \sum_{i=n}^2 \frac{4N}{i-1} = \sum_{i=n-1}^1 \frac{4N}{i} \quad (3.37)$$

we see that our expected total amount of time in the genealogy scales linearly with our population size  $N$ . Our expected total amount of time is also increasing with sample size  $n$ , but is doing so very slowly.

This again follows from the fact that in large samples, the initial coalescence usually happens very rapidly, so that extra samples add little to the total amount of time in the genealogical tree.

We saw above that the number of mutational differences between a pair of alleles that coalescence  $T_2$  generations ago was Poisson with a mean of  $2\mu T_2$ , where  $2T_2$  is the total branch length in this simple 2-sample genealogical tree. A mutation that occurs on any branch of our genealogy will cause a segregating polymorphism in the sample (meeting our infinitely-many-sites assumption). Thus, if the total time in the genealogy is  $T_{tot}$ , there are  $T_{tot}$  generations for mutations. So the total number of mutations segregating in our sample ( $S$ ) is Poisson with mean  $\mu T_{tot}$ . Thus the expected number of segregating sites in a sample of size  $n$  is

$$\mathbb{E}(S) = \mu \mathbb{E}(T_{tot}) = \sum_{i=n-1}^1 \frac{4N\mu}{i} = \theta \sum_{i=n-1}^1 \frac{1}{i} \quad (3.38)$$

Note that this is growing with the sample size  $n$ , albeit very slowly (roughly at the rate of the log of the sample size). We can use this formula to derive another estimate of the population scaled mutation rate  $\theta$ , by setting our observed number of segregating sites in a sample ( $S$ ) equal to this expectation. We'll call this estimator  $\hat{\theta}_W$ :

$$\hat{\theta}_W = \frac{S}{\sum_{i=n-1}^1 1/i} \quad (3.39)$$

This estimator of  $\theta$  was devised by WATTERSON (1975), hence the  $W$ .

*The neutral site-frequency spectrum.* We can use our coalescent process to find the expected number of derived alleles present  $i$  times out of a sample size  $n$ , e.g. how many singletons ( $i = 1$ ) do we expect to find in our sample? For example, in Figure 3.14 in our sample of four sequences, there are 3 singletons and 2 doubletons. The number of sites with these different allele frequencies depends on the lengths of specific genealogical branches. A mutation that falls on a branch with  $i$  descendants will create a derived allele with frequency  $i$ . For example, in our example tree in Figure 3.14, the total number of generations where a mutation could arise and be a doubleton is  $T_3 + 2T_2$ , the total length of the branch ancestral to just the orange and red allele ( $T_3 + T_2$ ) plus the branch ancestral to just the blue and purple allele ( $T_2$ ).

To get a better sense of how  $T_{tot}$  grows with the sample size, we can approximate the sum 3.37 by an integral, which will work for large  $n$ . The result is  $\int_1^{n-1} \frac{4N}{i} di = 4N \log(n - 1)$ .



Figure 3.15: A tree for three samples; note that this is the only possible tree shape (treating the tips as unlabeled, i.e. I don't care which pair of sequences carry a doubleton, just that any two sequences carry a derived allele).

To see how we could go about working this out, lets start by considering the simple coalescent tree, shown in Figure 3.15, for sample of 3 alleles drawn from a population. Mutations that fall on the branches coloured in black will be derived singletons, while mutations that fall along the orange branch will be doubletons in the sample. The total number of generations where a singleton mutation could arise is  $3T_3 + T_2$ . Note that we only count the time where there are two lineages ( $T_2$ ) once. So our expected number of singletons, using eqn (3.31), is

$$\mathbb{E}(S_i) = \mu (3\mathbb{E}(T_3) + \mathbb{E}(T_2)) = \mu \left( 3 \frac{2N}{3} + 2N \right) = \theta \quad (3.40)$$

By similar logic, the time where doubletons could arise is  $T_2$  and our expected number of doubletons is  $\mathbb{E}(S_i) = \theta/2$ . Thus, there are on average half as many doubletons as singletons.

Extending this logic to larger samples might be doable, but is tedious (I mean really tedious: for 10 alleles there are thousands of possible tree shapes and the task quickly gets impossible even computationally). A nice, relatively simple proof of the neutral site frequency spectrum is given by HUDSON, but we won't give this here. The general form is:

$$\mathbb{E}(S_i) = \frac{\theta}{i} \quad (3.41)$$

i.e. there are twice as many singletons as doubletons, three times as many singletons as tripletons, and so on. The other thing that will be helpful for us to know is that neutral alleles at intermediate frequency tend to be old, and those that are rare in the sample are young. We expect to see a lot more rare alleles in our sample than common alleles.

**Question 9.** There are two possible tree shapes that could relate four samples. Draw both of them and separately colour (or otherwise mark) the branches by where singletons, doubletons, and tripleton derived alleles could arise.

We can also ask the probability of observing a derived allele segregating at frequency  $i/n$  given that the site is polymorphic in our sample of size  $n$  (i.e. given that  $0 < i < n$ ). We can obtain this probability by dividing the expected number of sites segregating for an allele at frequency  $i$  by the expected number segregating at all of the possible allele frequencies for polymorphisms in our sample

$$P(i|0 < i < n) = \frac{\mathbb{E}(S_i)}{\sum_{j=1}^{n-1} \mathbb{E}(S_j)} = \frac{1/i}{\sum_{j=1}^{n-1} 1/j}. \quad (3.42)$$

We can interpret this probability as the fraction of polymorphic sites we expect to find at a frequency  $i/n$ .

*tests based on the site frequency spectrum* Population geneticists have proposed a variety of ways to test whether an observed site frequency spectrum conforms to its neutral, constant-population expectations. These tests are useful for detecting population size changes using data across many loci, or for detecting the signal of selection at individual loci. One of the first tests was proposed by TAJIMA, and is called Tajima's  $D$ . Tajima's  $D$  is

$$D = \frac{\theta_\pi - \theta_W}{C} \quad (3.43)$$

where the numerator is the difference between the estimate of  $\theta$  based on pairwise differences and that based on segregating sites. As these two estimators both have expectation  $\theta$  under the neutral, constant-population model, the expectation of  $D$  is zero. The denominator  $C$  is a positive constant; it's the square-root of an estimator of the variance of this difference under the constant population size, neutral model. This constant was chosen for  $D$  to have mean zero and variance 1 under the null model, so we can test for departures from this simple null model.

An excess of rare alleles compared to the constant-population, neutral model will result in a negative Tajima's  $D$ , because each additional rare allele increases the number of segregating sites by 1, but only has a small effect on the number of pairwise differences between samples. In contrast, a positive Tajima's  $D$  reflects an excess of intermediate frequency alleles relative to the constant-population, neutral expectation. Alleles at intermediate-frequency increase pairwise diversity more per segregating site than typical, thus increasing  $\theta_\pi$  more than  $\theta_W$ .

### 3.3.2 Demography and the coalescent

We've already seen how changes in population size can change the rate at which heterozygosity is lost from the population (see the discussion around eqn. (3.14)). If the population size in generation  $i$  is  $N_i$ , the probability that a pair of lineages coalesce is  $1/2N_i$ ; this conforms to our intuition that if the population size is small, the rate at which pairs of lineages find their common ancestor is faster. We can potentially accommodate rapid random fluctuations in population size by simply using the effective population size  $N_e$  in place of  $N$ . However, longer term more systematic changes in population size will distort the coalescent genealogies, and hence patterns of diversity, in more systematic ways.

We can see how demography potentially distorts the observed frequency spectrum away from the neutral expectation in a very large sample of humans shown in Figure 3.20. For comparison, the neu-

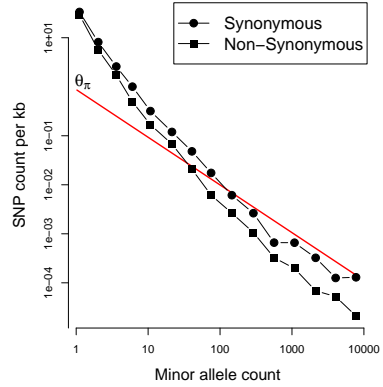


Figure 3.16: Data from 202 genes from 14002 people of European ancestry (28004 alleles). Note the double log-scale. The red line gives the neutral, constant population size estimate of the site frequency spectrum, our equation (3.41), using a  $\theta$  estimated from  $\pi$ . Note how the non-synonymous changes are even more skewed towards rare alleles, that's likely due to selection against non-synonymous alleles acting to push them towards rare frequency. Data from NELSON *et al.* (2012). Code here.

tral frequency spectrum, eqn (3.41), is shown as a red line. There are vastly more rare alleles than expected under our neutral, constant-population-size model, but the neutral prediction and reality agree somewhat more for alleles that are more common.



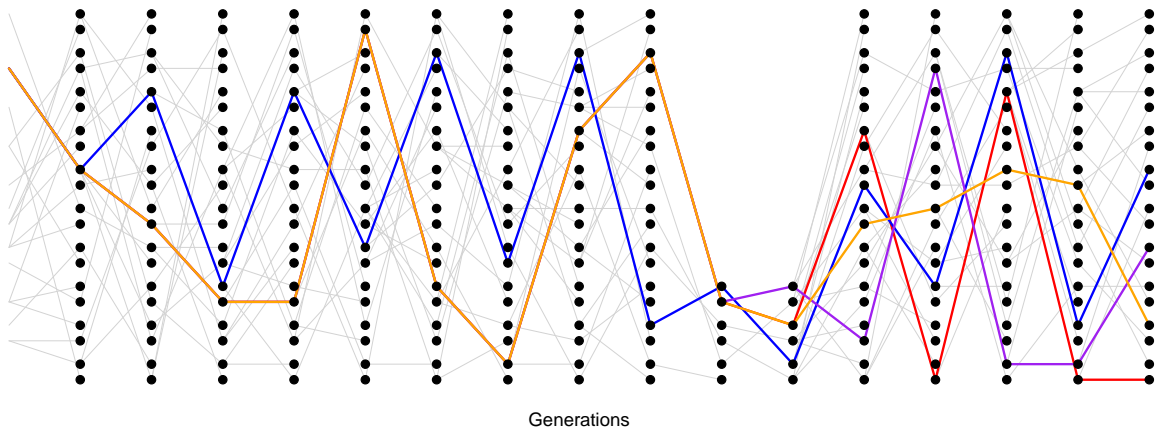
Why is this? Well, these patterns are likely the result of the very recent explosive growth in human populations. If the population has grown rapidly, then the pairwise-coalescent rate in the past may be much higher than the coalescent rate closer to the present. (see Figure 3.17).

One consequence of a recent population expansion is that there is much less genetic diversity in the population than you'd predict using the census population size. Humans are one example of this effect; there are 7 billion of us alive today, but this is due to very rapid population growth over the past thousand to tens of thousands of years. Our level of genetic diversity is very much lower than you'd predict given our census size, reflecting our much smaller ancestral population. A second consequence of recent population expansion is that the deeper coalescent branches are much more squished together in time, compared to those in a constant population. Mutations on deeper branches are the source of alleles at more intermediate frequencies, and so there are even fewer intermediate-frequency alleles in growing populations. That's why there are so many rare alleles, especially singletons, in this large sample of Europeans.

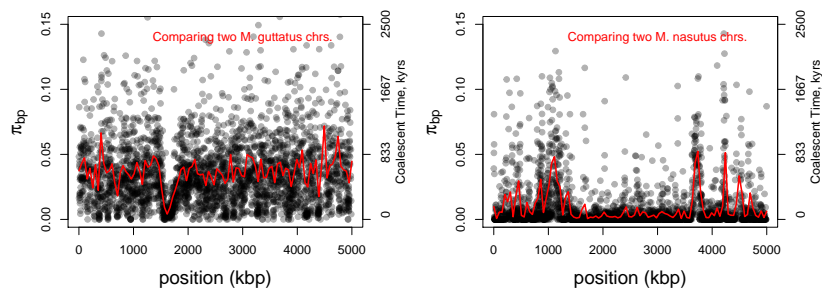
Another common demographic scenario is a population bottleneck. In a bottleneck, the population size crashes dramatically, and sub-

Figure 3.17: A realization of the coalescent process in a growing population. The population underwent a period of doubling every generation. The initial population size of just two individuals, maintained for a number of generations, is obviously highly unrealistic but serves our purpose. [Code here.](#)

sequently recovers. For example, our population may have had size  $N_{\text{Big}}$  and crashed down to  $N_{\text{Small}}$ . One example of a bottleneck is shown in Figure 3.18. Looking at a sample of lineages drawn from the



population today, if the bottleneck was somewhat recent ( $\ll N_{\text{Big}}$  generations in the past) many of our lineages will not have coalesced before reaching the bottleneck, moving backward in time. But during the bottleneck our lineages coalesce at a much higher rate, such that many of our lineages will coalesce if the bottleneck lasts long enough ( $\sim N_{\text{Small}}$  generations). If the bottleneck is very strong, then all of our lineages will coalesce during the bottleneck, and the resulting site frequency spectrum may look very much like our population growth model (i.e. an excess of rare alleles). However, if some pairs of lineages escape coalescing during the bottleneck, they will coalesce much more deeply in time (e.g. the blue and orange ancestral lineages in 3.18).



An example of this is shown Figure 3.19, data from BRANDVAIN *et al.*. *Mimulus nasutus* is a selfing species that arose recently from an out-crossing progenitor *M. guttatus*, and experienced a strong bottleneck. *M. guttatus* has a very high levels of genetic diversity ( $\pi = 4\%$  at synonymous sites), but *M. nasutus* has lost much of this diversity

Figure 3.18: A realization of the coalescent process in a bottlenecked population. Our population underwent a bottleneck eight generations in the past. Code here.

Figure 3.19: Diversity along the *Mimulus* genome. Black dots give  $\pi$  in 1kb windows between chromosomes sampled from two individuals, the red line is a moving average (data from BRANDVAIN *et al.*). Pairwise coalescent times ( $t$ ) estimated assuming  $t = \pi/2\mu$  using  $\mu_{BP} = 10^{-9}$ . Code here.



Figure 3.20: Yellow Monkeyflower *M. guttatus*. Choix des plus belles fleurs et des plus beaux fruits. Pierre-Joseph Redouté. (1833). Contributed to Flickr by Swallowtail Garden Seeds. Public Domain.

( $\pi = 1\%$ ). Looking along the genome, between a pair of *M. guttatus* chromosomes, levels of diversity are fairly uniformly high.

But in comparing two *M. nasutus* chromosomes, diversity is low because the pair of lineages generally coalesce recently. Yet in a few places we see levels of diversity comparable to *M. guttatus*; these regions correspond to genomic sites where our pair of lineages fail to coalesce during the bottleneck and subsequently coalesce much more deeply in the ancestral *M. guttatus* population.

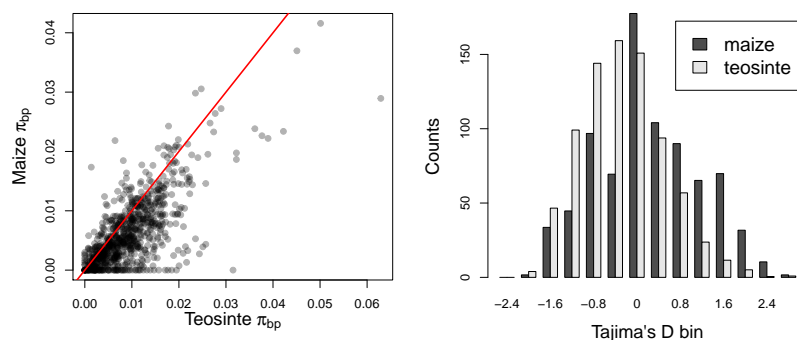


Figure 3.21: Data for polymorphism from Maize and Teosinte: 774 genes from WRIGHT *et al.* (2005). **Left)** Genetic diversity levels in maize and Teosinte samples at each of these genes. Note how diversity levels are lower in maize than teosinte, i.e. most points are below the red  $x = y$  line. **Right)** The distribution of Tajima's D in maize and teosinte, see how the maize distribution is shifted towards positive values. Code here.

Mutations that arise on deeper lineages will be at intermediate frequency in our sample, and so mild bottlenecks can lead to an excess of intermediate frequency alleles compared to the standard constant-population model. This can skew Tajima's D, see eqn 3.43, towards positive values and away from its expectation of zero. One example of this skew is shown in Figure 3.21. Maize ((*Zea mays* subsp.*mays*) was domesticated from its wild progenitor teosinte ((*Zea mays* subsp.*parviglumis*) roughly ten thousand years ago. We can see how the bottleneck associated with domestication has resulted in a loss of genetic diversity in maize, compared to teosinte, and the polymorphism that remains is somewhat skewed towards intermediate frequencies resulting in more positive values of Tajima's D.

**Question 10.** VOIGHT *et al.* (2005) sequenced 40 autosomal regions from 15 diploid samples of Hausa people from Yaounde, Cameroon. The average length of locus they sequenced for each region was 2365bp. They found that the average number of segregating sites per locus was  $S = 11.1$  and the average  $\pi = 0.0011$  per base over the loci. Is Tajima's D positive or negative? Is a demographic model with a bottleneck or growth more consistent with this result?



Figure 3.22: Maize (*Zea mays*). Prof. Dr. Thomé's Flora von Deutschland. 1886. Thomé, O. W. Image from the Biodiversity Heritage Library. Contributed by New York Botanical Garden. Not in copyright.

### 3.4 Molecular Evolution and the fixation of neutral alleles

"history is just one damn thing after another" -Arnold Toynbee

It is very unlikely that a rare neutral allele accidentally drifts up to fixation; more likely, such an allele will be eventually lost from the population. However, populations experience a large and constant influx of rare alleles due to mutation, so even if it is very unlikely that an individual allele fixes within the population, some neutral alleles will fix by chance.

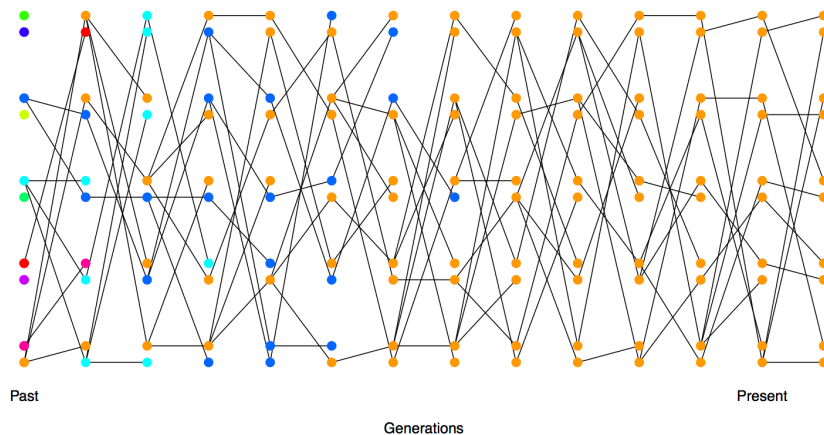


Figure 3.23: Each allele initially present in a small diploid population is given a different colour so we can track their descendants over time. By the 9th generation, all of the alleles present in the population can trace their ancestry back to the orange allele. [Code here.](#)

*Probability of the eventual fixation of a neutral allele* An allele which reaches fixation within a population is an ancestor to the entire population. In a particular generation there can only be a single allele that all other alleles at the locus in a later generation can claim as an ancestor (See Figure 3.23). At a neutral locus, the actual allele does not affect the number of descendants that the allele has (this follows from the definition of neutrality: neutral alleles don't leave more or less descendants on average than other neutral alleles). An equivalent way to state this is that the allele labels don't affect anything; thus the alleles are *exchangeable*. As a consequence of being exchangeable, any allele is equally likely to be the ancestor of the entire population. In a diploid population of size  $N$ , there are  $2N$  alleles, all of which are equally likely to be the ancestor of the entire population at some later time point. So if our allele is present in a single copy, the chance that it is the ancestor to the entire population in some future generation is  $1/(2N)$ , i.e. the chance our neutral allele is eventually fixed is  $1/(2N)$ . In Figure 3.23, our orange allele in the first generation is one of 10 differently coloured alleles, and so has a  $1/10$  chance of being the ancestor of the entire population at some later time point (and

in this simulation it does become the common ancestor, by the 9th generation).

More generally, if our neutral allele is present in  $i$  copies in the population, of  $2N$  alleles, the probability that this allele becomes fixed is  $i/(2N)$ , i.e. the probability that a neutral allele is eventually fixed is simply given by its frequency ( $p$ ) in the population. (We can also derive this result by letting  $Ns \rightarrow 0$  in eqn. (7.11), a result we'll encounter later.)

A newly arisen mutation only becomes a fixed difference if it is lucky enough to be the ancestor of the entire population. As we saw above, this occurs with probability  $1/(2N)$ .

How long does it take on average for such an allele to fix within our population? Well, in developing equation (3.35) we've seen that it takes  $4N$  generations for a large sample of alleles to all trace their ancestry back to a single most recent common ancestral allele. Any single-base pair change which arose as a single mutation at a locus, and fixed in the population, must have been present in the sequence transmitted by the most recent common ancestor of the population at that locus. Thus it must take roughly  $4N$  generations for a neutral allele present in a single copy within the population to the ancestor of all alleles within our population. This argument can be made more precise, but in general we would still find that it takes  $\approx 4N$  generations for a neutral allele to go from its introduction to fixation with the population.

*Rate of substitution of neutral alleles* A substitution between populations that do not exchange gene flow is simply a fixation event within one population. The rate of substitution is therefore the rate at which new alleles fix in the population, so that the long-term substitution rate is the rate at which mutations arise that will eventually become fixed within our population.

Lets assume, based on our discussion of the neutral theory of molecular evolution, that there are only two classes of mutational changes that can occur with a region, highly deleterious mutations and neutral mutations. A fraction  $C$  of all mutational changes are highly deleterious, and cannot possibly contribute to substitution nor polymorphism. The other  $1 - C$  fraction of mutations are neutral. If our mutation rate is  $\mu$  per transmitted allele per generation, then a total of  $2N\mu(1 - C)$  neutral mutations enter our population each generation.

Each of these neutral mutations has a  $1/(2N)$  probability chance of eventually becoming fixed in the population. Therefore, the rate at which neutral mutations arise that eventually become fixed within our population is

$$2N\mu(1 - C)\frac{1}{2N} = \mu(1 - C) \quad (3.44)$$

Thus the rate of substitution, under a model where newly arising alleles are either highly deleterious or neutral, is simply given by the mutation rate of neutral alleles, i.e.  $\mu(1 - C)$ .

Consider a pair of species that have diverged for  $T$  generations, i.e. orthologous sequences shared between the species last shared a common ancestor  $T$  generations ago. If these species have maintained a constant  $\mu$  over that time, they will have accumulated an average of

$$2\mu(1 - C)T \quad (3.45)$$

neutral substitutions. This assumes that  $T$  is a lot longer than the time it takes to fix a neutral allele, such that the total number of alleles introduced into the population that will eventually fix is the total number of substitutions.

This is a really pretty result as the population size has completely canceled out of the neutral substitution rate. However, there is another way to see this in a more straight forward way. If I look at a sequence in me compared to, say, a particular chimp, I'm looking at the mutations that have occurred in both of our germlines since they parted ways  $T$  generations ago. Since neutral alleles do not alter the probability of their transmission to the next generation, we are simply looking at the mutations that have occurred in  $2T$  generations worth of transmissions. Thus the average number of neutral mutational differences separating our pair of species is simply  $2\mu(1 - C)T$ .

A number of observations follow under this model, from equation (3.45), the first is that a primary determinant of patterns of molecular evolution in a genomic region is the level of constraint ( $C$ ). This pattern generally seems to hold empirically: non-coding regions often evolve more rapidly than coding regions; synonymous substitutions accumulate faster than nonsynonymous; nonsynonymous changes faster in less vital proteins than ones that are absolutely necessary for early development. Note that this is not a unique prediction of the neutral model, e.g. lower pleiotropy means that less constrained regions may be better able to evolve adaptively. However, it is a fantastically useful general insight, e.g. it allows us to spot putatively functional non-coding regions by looking for genomic regions that have very low levels of divergence among distantly related species.

"functionally less important molecules or parts of a molecule evolve faster than more important ones."

— KIMURA and OHTA (1974)



Figure 3.24: The numbers of substitutions between various pairs of groups, for three proteins, plotted against the time these groups shared a common ancestor in the fossil record. Data from DICKERSON (1971). The number of observed amino-acid differences is corrected for multiple hits to obtain the corrected number of changes estimated to occur. The lines give the linear regression, constrained to pass through the origin, for each protein. The slope of the regression is given next to the protein name. Code here. See (ROBINSON *et al.*, 2016) who revisited this classic study and confirmed the conclusions.

The second important insight, and critical for the development of the neutral theory, is that equation (3.45) is seemingly consistent with ZUCKERKANDL and PAULING (1965)'s hypothesis of a surprisingly constant, protein molecular clock. The protein molecular clock is the observation that for some proteins there's a linear relationship between the number of non-synonymous substitutions and the time species last shared a common ancestor in the fossil record. DICKERSON (1971) provided an early example of this observation (Figure 3.24), by comparing various organisms whose molecular sequences were available to him. For example, he found that humans and rattlesnakes, who last share a common ancestor in the fossil record around 300 million years, are separated by roughly 15 NS substitutions per 100 sites in the Cytochrome c protein. While, humans and dog fish, which diverged around 400 million years, are separated by 19 NS substitutions per 100 sites in this gene.

In equation (3.45) we double the amount of time separating a pair of species  $T$ , we double the number of substitutions predicted. Note that for this to be true  $T$  must be measured in generations. To explain a protein molecular clock between species that clearly differed dramatically in generation time it was hypothesized that the mutation rate actually scaled with generation time, i.e. short-lived organisms introduced less mutations per generation, e.g. as they had fewer rounds of mitosis. This generation-time assumption meant that the mutation rate per year could be constant, such that  $\mu T$  would be a constant for pairs of species that had diverged for similar geological



Figure 3.25: Eastern diamondback rattlesnake (*Crotalus adamanteus*). North American herpetology. Holbrook, J. E. Image from the Biodiversity Heritage Library. Contributed by Smithsonian Libraries. Licensed under CC BY-2.0.

times, which are measured in years, even if the organisms differed in generation time. This assumption would allow neutral theory to be consistent with a protein molecular clock measured in years. We now know that this critical generation time assumption is false, organisms with shorter generation times have somewhat higher mutation rates per year, and so a strict neutral model is inconsistent with the protein molecular clock. We'll return to these ideas when we discuss the fate of very weakly selected mutations in Chapter 7 and OHTA (1973)'s Nearly Neutral theory. If you are still reading this send Graham a picture of Tomoko Ohta receiving the Crafoord Prize, an analog of the Nobel prize for biology, for her contributions to molecular evolution.

*The contribution of ancestral polymorphism to divergence.* If we are considering  $T$  to represent the divergence between long-separated species, then we can think of  $T$  as the time that the species split. However, for more recently diverged populations and species, we need to include the fact that the sorting of ancestral polymorphism contributes to divergence among species. In Figure 3.26, we see our two populations split  $T_s$  generations ago. However, the coalescence of our A and B lineage is necessarily deeper in time than  $T_s$ . The top mutation was polymorphic in the ancestral population but now contributes to the divergence between A and B. Assuming that our ancestral population had effective size  $N_A$  individuals, and that our populations split cleanly with no subsequent gene flow, then

$$T = T_s + 2N_A. \quad (3.46)$$

If our species split time is very large compared to  $2N$  then we can think of  $T$  as the split time.

**Question 11.** For this, and the next question, assume that humans and chimp diverged around  $5.5 \times 10^6$  years ago, have a generation time 20 years, that the speciation occurred instantaneously in allopatry with no subsequent gene flow, and the ancestral effective population size of the human and chimp common ancestor population was 10,000 individuals.

Nachman and Crowell sequenced 12 pseudogenes in human and chimp and found substitutions at 1.3% of sites.

- A) What is the mutation rate per site per generation at these genes?
- B) All of the pseudogenes they sequenced are on the autosomes. What would your prediction be for pseudogenes on the X and Y chromosomes, given that there are fewer rounds of replication in the female germline than in the male germline.

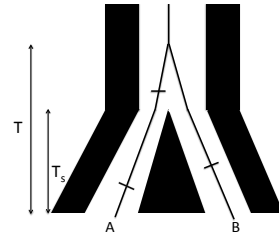


Figure 3.26: The genealogy of two alleles one sampled from population A and B. Mutations on the lineages are shown as dashes. The pair of alleles coalesce in the ancestral population of A and B. The two populations split  $T_s$  generations ago, with no subsequent gene flow, but the two lineages must coalesce deeper in time.

### 3.5 Tests of molecular evolution.

#### 3.5.1 Comparing the rates of non-synonymous to synonymous substitutions $d_N/d_S$

One common tool in molecular evolution is to compare the estimated number (or rates) of substitutions in different classes of genomic sites, for example the ratio of the number of non-synonymous to synonymous substitutions in a given gene. The simplest way to calculate  $d_N$  is to count up the non-synonymous changes and divide by the total number of positions in the gene where a non-synonymous point mutation could occur. We can do likewise for synonymous changes  $d_S$ , and then take the ratio  $d_N/d_S$ . This is a helpful conceptual way to think about what  $d_N/d_S$  represents, however, this ignores the fact that some changes are more likely to occur by mutation than others and also does not account for multiple hits (multiple mutations at the same bp position). Therefore, in practice the ratio  $d_N/d_S$  is more typically calculated by model-based likelihood and bayesian methods that can account for these features.

For the vast majority of protein-coding genes in the genome we see that  $d_N/d_S < 1$ . This observation is consistent with the view that non-synonymous sites are much more constrained than synonymous sites, i.e. that most non-synonymous mutations are deleterious and quickly removed from the population. If we are willing to make the assumption that all synonymous changes are neutral,  $d_S = 2T\mu$ , then we can estimate the degree of constraint on non-synonymous sites. (Note that synonymous changes can sometimes be subject to both positive and negative selection, but this neutral assumption is a useful starting place.)

Assume that a fraction  $C$  of non-synonymous changes are too deleterious to contribute to polymorphism. Then, after  $T$  generations of divergence have elapsed between two populations, we'd expect  $d_N$  neutral non-synonymous substitutions, where

$$d_N = 2T(1 - C)\mu \quad (3.47)$$

Dividing by  $d_S$ , we find

$$d_N/d_S = (1 - C) \quad (3.48)$$

Therefore, if we assume that non-synonymous mutations can only be strongly deleterious or neutral, we estimate the fraction of mutational changes that are constrained by negative selection as  $C = 1 - d_N/d_S$ .  $C$  has the interpretations of being the fraction of non-synonymous mutations that are quickly weeded out of the population by selection, and so do not contribute to divergence among species.

We can test whether our gene is evolving in a constrained way at the protein level by estimating  $d_N/d_S$  and testing whether this is significantly less than 1. A  $d_N/d_S$  test can provide evolutionary evidence that a stretch of DNA proposed to be protein-coding is subject to selective constraint, and so likely does encode for a functional protein. We can also perform a  $d_N/d_S$  test on specific branches of a phylogeny for a gene, to test on which branches the gene is subject to constraint, or to test for changes in the level of constraint across the phylogeny.

*Loss of constraint at pseudogenes.* While most protein genes evolve under constraint, we can find examples of genes that are evolving in a less constrained manner. The simplest example of this is where the gene has lost function. Genes can lose function because of inactivating mutations that stop them being transcribed or translated into functional proteins. Such genes are called 'pseudogenes'. When a gene completely loses function there is no longer selection against non-synonymous changes and so such mutations are just as free to accumulate as synonymous changes, and so  $d_N/d_S = 1$ . Pseudogenes are a wonderful example of the extension of Darwin's ideas about vestigial traits ('Rudimentary organs') to the DNA level; we can still recognize a once useful word (gene) whose spelling is slowly degrading. Our genomes are filled with old pseudogenes whose original meanings (functional protein coding sequences) are slowly being eroded through the accumulation of neutral substitutions. One nice example of a gene that has repeatedly lost function, i.e. become repeatedly pseudogenized, is the Enamlin gene from the study of MEREDITH *et al.* (2009).

|                             | 818         | 827      | 1239      | 1247      | 2501   | 2512         | 2533  | 2542 | 4028  | 4039 |  |
|-----------------------------|-------------|----------|-----------|-----------|--------|--------------|-------|------|-------|------|--|
| <i>Sus</i>                  | ...AAATCAA  | CT       | TGTTTACTA | ..ACATGCC | ATGCA  | GGGGCACAGTTT |       |      |       |      |  |
| <i>Hippopotamus</i>         | ...AAATCAA  | CT       | TGTTTACTA | ..ACATGCC | ATGCA  | GGGGCACAGTTT |       |      |       |      |  |
| <i>Eubalaena glacialis</i>  | ...AAATCAA  | CT       | TGTTTACTA | ..ATA     | TGCA   | GGGGCACAGTTT |       |      |       |      |  |
| <i>Eubalaena australis</i>  | ...AAATCAA  | CT       | TGTTTACTA | ..ATA     | TGCA   | GGGGCACAGTTT |       |      |       |      |  |
| <i>Megaptera</i>            | ...AAATCAA  | CT       | TGTTTACTA | ..ATA     | TGCA   | GGGGCACAGTTT |       |      |       |      |  |
| <i>Caperea</i>              | ...AAATCAA  | CT       | TGTTTACTA | ..ATA     | TGCA   | GGGGCACAGTTT |       |      |       |      |  |
| <i>Eschrichtius</i>         | ...AAATCAA  | CT       | TGTTTACTA | ..ATA     | TGCA   | GGGGCACAGTTT |       |      |       |      |  |
| <i>Kogia sima</i>           | ...AAATCAA  | CT       | TGTTTACTA | ..ATA     | TGCA   | GGGGCACAGTTT |       |      |       |      |  |
| <i>Kogia breviceps</i>      | ...AAATCAA  | CT       | TGTTTACTA | ..ATA     | TGCA   | GGGGCACAGTTT |       |      |       |      |  |
| <b>D</b>                    |             |          |           |           |        |              |       |      |       |      |  |
|                             | 918         | 935      | 1584      | 1593      | 1614   | 1620         | 2499  | 2507 | 4017  | 4023 |  |
| <i>Sus</i>                  | ...GGGA-GTC | AAAGAGCC | ACCTTCC   | ..CAAAAC  | CAACAT | GGC          | GCT   | -AGC |       |      |  |
| <i>Bradypterus</i>          | ...???      | ???      | ???       | ???       | ???    | ???          | ???   | ???  |       |      |  |
| <i>Choloepus didactylus</i> | ...ACT      | TCGC     | ..CAAAAC  | CAAP      | TTGC   | ..GTT        | AGC   |      |       |      |  |
| <i>Choloepus hoffmanni</i>  | ...???      | ???      | ???       | ???       | ???    | ???          | ???   | ???  |       |      |  |
| <i>Myrmecophaga</i>         | ...GTGA-TTC | CGAGAAC  | GTCT      | ..CAAAAC  | CAAP   | TTGC         | ..GTT | AGC  |       |      |  |
| <i>Tamandua</i>             | ...GAGAA    | TTC      | CGAGAAC   | ..ATT     | TGCA   | ..CAAAAC     | CAAP  | TTGC | ..GTT | AGC  |  |
| <i>Cyclopes</i>             | ...GAGA     | TTC      | CGAGAAC   | ..ATT     | TGCA   | ..CAAAAC     | CAAP  | TTGC | ..GTT | AGC  |  |
| <i>Dasypus</i>              | ...GAGA     | TTC      | CGAGAAC   | ..ATT     | TGCA   | ..CAAAAC     | CAAP  | TTGC | ..GTT | AGC  |  |
| <i>Tolypeutes</i>           | ...GAGA     | -CTC     | AAAGAGTC  | ..GTC     | TGCA   | ..CAAAAC     | CAAP  | TTGC | ..GTT | AGA  |  |
| <i>Chaetophractus</i>       | ...GAGA     | -CTC     | AAAGAGTC  | ..GTC     | TGCA   | ..CAAAAC     | CAAP  | TTGC | ..GTT | AGG  |  |
| <i>Euphractus</i>           | ...GAGA     | -CTC     | AAAGAGTC  | ..GTC     | TGCA   | ..CAAAAC     | CAAP  | TTGC | ..GTT | AGG  |  |

The protein Enamlin is a key structural protein involved in the outer cap of enamel on teeth. Various mammals have secondarily evolved diets that do not require hard teeth, and so greatly reduced the selection pressure for hard enamel, or even teeth at all. For ex-

"Rudimentary organs may be compared with the letters in a word, still retained in the spelling, but become useless in the pronunciation, but which serve as a clue .. for its derivation." – DARWIN (1859) pg. 455

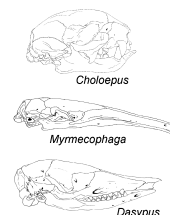
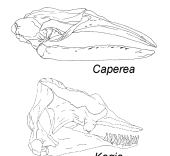


Figure 3.27: Examples of frameshift mutations (insertions blue, deletions red) and premature stop codons in Enamlin in Cetacea and Xenarthra. Figure from MEREDITH *et al.* (2009), licensed under CC BY 4.0.



Figure 3.28: Two-toed sloth (*Choloepus hoffmanni*). An introduction to the study of mammals, living and extinct. 1891. Flower W. H. and Lydekker R. Image from the Biodiversity Heritage Library. Contributed by University of Toronto. Not in copyright.

ample, two-toed sloths (*Choloepus*), Pygmy sperm whales (*Kogia*), and aardvark (*Orycteropus*) all lack enamel on teeth. Other mammals have lost their teeth entirely, e.g. giant anteaters (*Myrmecophaga*) and Baleen whales. Due to this relaxation of constraint on the phenotype, the Enamlin gene has accumulated pseudogenizing substitutions such as premature stop codons and frameshift mutations (see Figure 3.27 for examples). MEREDITH *et al.* sequenced Enamlin across a range of species and found that none of the species with enamel have frameshift mutations in Enamlin, while 17/20 of species that lack enamel or teeth have frameshifts in Enamlin, and all of them carry premature stop codons (Figure 3.29).



Figure 3.29: The tooth symbol next to each taxon shows whether they have teeth with enamel, lack enamel, or lack teeth. Branches of the phylogeny are coloured by whether their Enamlin is functional (black), pre-mutation (blue), mixed (purple), or pseudogenized (red). The black and white vertical bars on branches show frameshift mutations. The numbers after taxon names indicate minimum number of stop codons in the sequence divided by the length of the sequence. Figure from MEREDITH *et al.* (2009), licensed under CC BY 4.0.

The branches of the Enamlin phylogeny with a functional Enamlin gene (black) had an estimated  $d_N/d_S = 0.51$ , consistent with the protein evolving in a constrained manner. In contrast, the branches with a pseudogenized Enamlin (red) had  $d_N/d_S = 1.02$ , consistent with the gene evolving an unconstrained way. The branches where the gene was likely transitioning from a functional to non-function state, i.e. pre-mutation (blue) and mixed (purple), had intermediate values of  $d_N/d_S = 0.83 - 0.98$ , consistent with a transition from a constrained to unconstrained mode of protein evolution somewhere along these branches of the phylogeny.

*Adaptive evolution and  $d_N/d_S$ .* Clearly genes are not only subject to neutral and deleterious mutations; beneficial mutations must also arise and fix from time to time. Let's assume that a fraction  $B$  of non-synonymous mutations that arise are beneficial such that  $2N\mu B$  beneficial mutations arise per generation. Newly arisen beneficial alleles are not destined to fix in the population, as they may be lost to genetic drift when they are rare in the population (we'll discuss how to calculate the fixation probability for beneficial alleles in Chapter 7). A newly arisen beneficial allele reaches fixation in the population with probability  $f_B$  from its initial frequency of  $1/2N$ . This fixation probability may be much higher than that of neutral mutations, but still much less than 1. If  $2T$  generations of divergence have elapsed between the two populations then a total of

$$dN = 2T(1 - C - B)\mu + 2T \times (2N\mu B) \times f_B \quad (3.49)$$

non-synonymous substitutions will have accumulated. Then

$$d_N/d_S = (1 - C - B) + 2NBf_B \quad (3.50)$$

assuming again that all synonymous mutations are neutral. Note that this means that our estimates of  $C$  using  $1 - d_N/d_S$  will be a lower bound on the true constraint if even a small fraction of mutations are beneficial. Those cases where the gene is evolving more rapidly at the protein level than at synonymous sites, i.e.  $d_N/d_S > 1$ , are potentially strong candidates for positive selection rapidly driving change at the protein level. We can identify genes that have  $d_N/d_S$  significantly greater than one, either on the complete gene phylogeny, or on particular branches. Note that is a very conservative test that few genes in the genome meet, as many genes that are fixing adaptive non-synonymous substitutions will have  $d_N/d_S < 1$ ; even if adaptive mutations are common, genes may still evolve in a constrained way (i.e.  $d_N/d_S < 1$ ) if the rapid fixation of beneficial mutations due to positive selection is outweighed by the loss of non-synonymous mutations to negative selection.

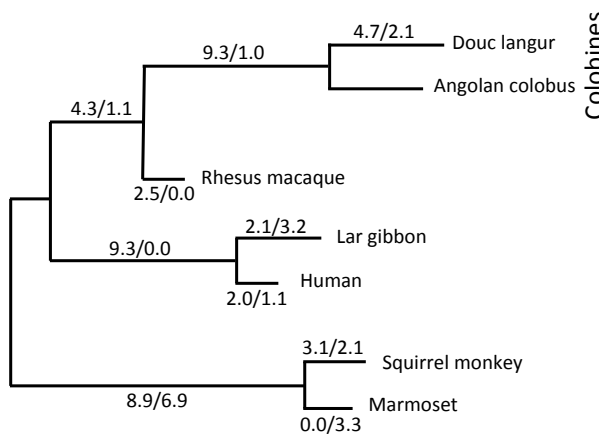


Figure 3.30: A phylogram for the primate lysozyme gene, data from YANG (1998). For each branch, the numbers give the estimated average number of non-synonymous to synonymous changes in the lysozyme protein.

A classic example for looking at adaptive evolution using  $dN/dS$  is the evolution of the lysozyme protein in primates (MESSIER and STEWART, 1997; YANG, 1998), see the phylogeny in Figure 3.30. The lysozyme protein is a key component for the breakdown of bacterial walls. It shows very fast protein evolution, notably on the lineages leading to apes (e.g. gibbons and humans) and Colobines (e.g. colobus and langur monkeys). Colobines have leaf-based diets. They digest these leaves by bacterial fermentation in their foregut, and then use lysozymes to break down the bacteria to extract energy from the leaves. In Colobines, the lysozyme protein has evolved to work well in the high-PH environment of the stomach. Remarkably, the Colobine lysozyme has convergently evolved this activity via very similar amino-acid changes at 5 key residuals in cows and Hoatzins (a leaf eating bird, KORNEGAY *et al.*, 1994)

*The McDonald-Kreitman test* As noted above, a big issue with using  $dN/dS$  to detect adaptation is that it is very conservative. For a more powerful test of rapid divergence, what we need to do is adjust for the level of constraint a gene experiences at non-synonymous sites. One way to do this is to use polymorphism data as an internal control. If we see little non-synonymous polymorphism at a gene, but a lot of synonymous polymorphism, we now know that there is likely strong constraint on the gene (i.e. high  $C$ ), thus we expect  $dN/dS$  to be low. McDONALD and KREITMAN (1991) devised a simple test of the neutral theory of molecular evolution at a gene based on this intuition (building on the conceptually similar HKA test HUDSON *et al.*, 1987). McDONALD and KREITMAN took the case where we have polymorphism data at a gene for one species and divergence to



Figure 3.31: Abyssinian black-and-white colobus (*Colobus guereza*). A member of the leaf-eating Colobines. Brehm's Tierleben, Brehm, A.E. 1893. Image from the Biodiversity Heritage Library. Contributed by University of Illinois Urbana-Champaign. Not in copyright.



Figure 3.32: (hoatzin (*Opisthocomus hoazin*)). A leaf-eating bird. A history of birds (1910) Pycraft, W.P. Image from the Biodiversity Heritage Library. Contributed by American Museum of Natural History Library. Not in copyright.

a closely related species. They partitioned polymorphism and fixed differences in their sample into non-synonymous and synonymous changes:

|          | Poly.     | Fixed     |
|----------|-----------|-----------|
| Non-Syn. | $P_N$     | $D_N$     |
| Syn.     | $P_S$     | $D_S$     |
| Ratio    | $P_N/P_S$ | $D_N/D_S$ |

Under neutral theory, we expect a smaller number of non-synonymous to synonymous fixed differences ( $D_N/D_S < 1$ ) and exactly the same expectation holds for polymorphism ( $P_N/P_S$ ). Let's consider a gene with  $L_S$  and  $L_N$  sites where synonymous and non-synonymous mutations could arise respectively. We can think of the underlying gene genealogy at our gene, see Figure 3.33, with the total time on the coalescent genealogy within the species as  $T_{tot}$  and the total time for fixed differences between our species as  $T'_{div}$ . Then under neutrality we expect  $\mu L_N(1 - C)T_{tot}$  non-synonymous polymorphisms (i.e. our number of segregating sites), and  $\mu L_N(1 - C)T'_{div}$  non-synonymous fixed differences. We can then fill out the rest of our table as follows:

|          | Poly.                   | Fixed                    |
|----------|-------------------------|--------------------------|
| Non-Syn. | $\mu L_N(1 - C)T_{tot}$ | $\mu L_N(1 - C)T'_{div}$ |
| Syn.     | $\mu L_N T_{tot}$       | $\mu L_S T'_{div}$       |
| Ratio    | $L_N(1 - C)/(L_S)$      | $L_N(1 - C)/(L_S)$       |

Therefore, we expect the ratio of non-synonymous to synonymous changes to be the same for polymorphism and divergence under a strict neutral model. We can test this expectation of equal ratios via the standard tests of a  $2 \times 2$  table. If the ratio of  $N/S$  is significantly higher for divergence than polymorphism we have evidence that non-synonymous substitutions are accumulating more rapidly than we would predict given levels of constraint alone.

As example of a McDonald-Kreitman table consider the work of FRENTIU *et al.* (2007) on the molecular evolution of L Photopigment opsin in Admiral (*Limenitis*) butterflies, responsible for colour vision in the long-wavelength part of the visual spectrum. FRENTIU *et al.* found that the sensitivity of this opsin had shifted towards blue-shifted in its sensitivity in *L. archippus archippus* (viceroy) compared to *L. arthemis astyanax*. To test whether this molecular evolution reflected positive selection they sequenced 24 *L. arthemis astyanax* individuals and one *L. archippus archippus* sequence. They identified 11 polymorphic sites in *L. arthemis astyanax* and 16 fixed differences, which break down as follows:

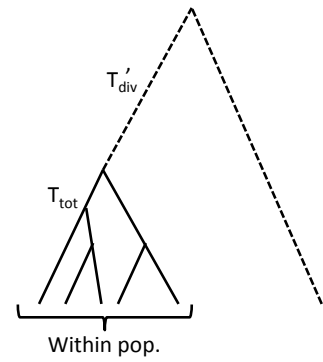


Figure 3.33: An example of a gene genealogy for a set of alleles sampled within a population and a single allele sampled from a distantly-related species.



Figure 3.34: White admiral (*Limenitis arthemis*). American entomology : a description of the insects of North America (1859). Say, T. Image from the Biodiversity Heritage Library. Contributed by Smithsonian Libraries. Not in copyright.

|          | Poly. | Fixed |
|----------|-------|-------|
| Non-Syn. | 2     | 12    |
| Syn.     | 9     | 4     |
| Ratio    | 2/9   | 3/1   |

Note the strong excess of non-synonymous to synonymous divergence compared to polymorphism (p-value of 0.006, Fisher's exact test), which is consistent with the gene evolving in an adaptive manner among the two species. We would expect roughly only 3 non-synonymous substitutions out of 16 substitutions if the gene was evolving neutrally ( $16 \times 2/11$ ).

### 3.6 Neutral diversity and population structure

We've considered alleles drawn from a randomly-mating population, and divergence among alleles drawn from two distantly-related populations. We'll now turn to consider divergence among more closely related populations. In thinking about the coalescent within populations we made the assumption that any pair of lineages is equally likely to coalesce with each other. However, when there is population structure this assumption is violated.

We have previously written the measure of population structure  $F_{ST}$  as

$$F_{ST} = \frac{H_T - H_S}{H_T} \quad (3.51)$$

where  $H_S$  is the probability that two alleles sampled at random from a subpopulation differ, and  $H_T$  is the probability that two alleles sampled at random from the total population differ.

*A simple population split model* Imagine a population of constant size of  $N_e$  diploid individuals that  $T$  generations in the past split into two daughter populations (sub-populations) each of size  $N_e$  individuals, which do not subsequently exchange migrants. In the current day we sample an equal number of alleles from both subpopulations.

Consider a pair of alleles sampled within one of our sub-populations and think about their per site heterozygosity. These alleles have experienced a population of size  $N_e$  and so the probability that they differ is  $H_S \approx 4N_e\mu$  (assuming that  $N_e\mu \ll 1$ , using our equation 3.12 for heterozygosity within a population ).

The heterozygosity in our total population is a little more tricky to calculate. Assuming that we equally sample both sub-populations, when we draw two alleles from our total sample, 50% of the time they are drawn from the same subpopulation and 50% of the time they are drawn from different subpopulations. Therefore, our total

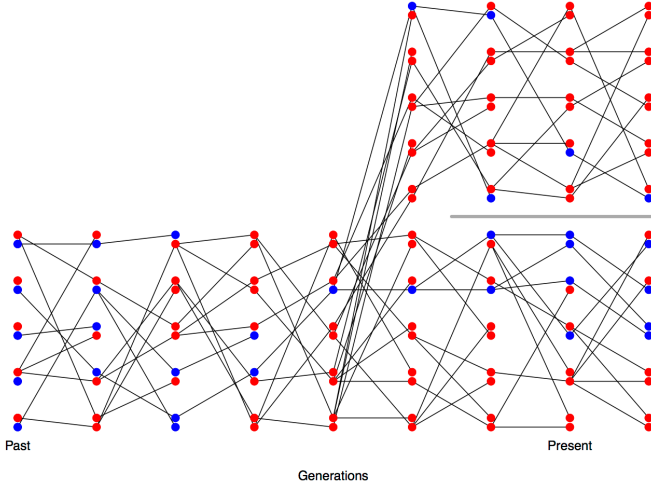


Figure 3.35: Change in allele frequencies following a population split. Code here.

heterozygosity is given by

$$H_T = \frac{1}{2}H_S + \frac{1}{2}H_B \quad (3.52)$$

where  $H_B$  is the probability that a pair of alleles drawn from our two different sub-populations differ from each other. A pair of alleles from different sub-populations cannot find a common ancestor with each other for at least  $T$  generations into the past as they are in distinct populations (not connected by migration). Once our alleles find themselves back in the combined ancestral population it takes them on average  $2N$  generations to coalesce. So the total opportunity for mutation between our pair of alleles sampled from different populations is  $2(T + 2N)$  generations of meioses, such that the probability that our pairs of alleles is different is

$$H_B \approx 2\mu(T + 2N) \quad (3.53)$$

We can plug this into our expression for  $H_T$ , and then that in turn into  $F_{ST}$ . Doing so we find that

$$F_{ST} \approx \frac{\mu T}{\mu T + 4N_e \mu} = \frac{T}{T + 4N_e} \quad (3.54)$$

Note that  $\mu$  cancels out of this equation. In this simple toy model,  $F_{ST}$  is increasing because the amount of between-population diversity increases with the divergence time of the two populations (initially linearly with  $T$ ).  $F_{ST}$  grows at a rate give by  $T/(4N_e)$  so that differentiation will be higher between populations separated by long divergence times or with small effective population sizes.

**Question 12.** The genome-wide  $F_{ST}$  between Bornean and Sumatran orang-utan species samples (*Pongo pygmaeus* and *Pongo abelii*)

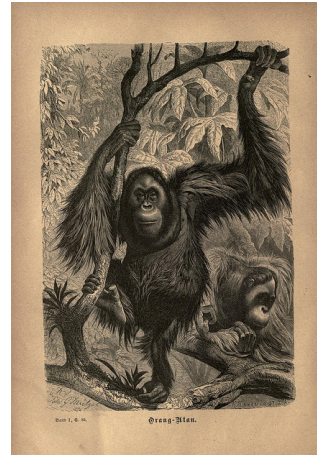


Figure 3.36: Orangutan (*Pongo*). Brehms thierleben, allgemeine kunde des thierreichs. Brehm, A. E. Image from the Biodiversity Heritage Library. Contributed by MBLWHOI Library. Not in copyright.

is  $\approx 0.37$  (LOCKE *et al.*, 2011), representing a deep population split between the species (potentially with little subsequent gene flow).

Within the populations the genome-wide average Watterson's  $\theta$  is  $\theta_W = 1.4\text{kb}^{-1}$ , estimated from the number of segregating sites. Assume a generation time of 20 years, and a mutation rate of  $2 \times 10^{-8}$  per base per generation. How far in the past did the two populations diverge?

*A simple model of migration between an island and the mainland.* We can also use the coalescent to think about patterns of differentiation under a simple model of migration-drift equilibrium. Let's consider a small island population that is relatively isolated from a large mainland population, where both of these populations are constant in size. We'll assume that the expected heterozygosity for a pair of alleles sampled on the mainland is  $H_M$ .

Our island has a population size  $N_I$  that is very small compared to our mainland population. Each generation some low fraction  $m$  of our individuals on the island have migrant parents from the mainland the generation before. Our island may also send migrants back to the mainland, but these are a drop in the ocean compared to the large population size on the mainland and their effect can be ignored.

If we sample an allele on the island and trace its ancestral lineage backward in time, each generation our ancestral allele has a low probability  $m$  of being descended from the mainland in the preceding generation (if we go back far enough the allele eventually has to be descended from an allele on the mainland). The probability that a pair of alleles sampled on the island are descended from a shared recent common ancestral allele on the island is the probability that our pair of alleles coalesces before either lineage migrates. For example, the probability that our pair of alleles coalesces  $t + 1$  generations back on the island is

$$\frac{1}{2N_I} (1-m)^{2(t+1)} \left(1 - \frac{1}{2N_I}\right)^t \approx \frac{1}{2N_I} \exp\left(-t\left(\frac{1}{2N_I} + 2m\right)\right), \quad (3.55)$$

with the approximation following from assuming that  $m \ll 1$  &  $\frac{1}{(2N_I)} \ll 1$  (note that this is very similar to our derivation of heterozygosity above). The probability that our alleles coalesce before either one of them migrates off the island, irrespective of the time, is

$$\int_0^\infty \frac{1}{2N_I} \exp\left(-t\left(\frac{1}{2N_I} + 2m\right)\right) dt = \frac{1/(2N_I)}{1/(2N_I) + 2m}. \quad (3.56)$$

Let's assume that the mutation rate is very low such that it is very unlikely that the pair of alleles mutate before they coalesce on the island. Therefore, the only way that the alleles can be different from

each other is if one or other of them migrates to the mainland, which happens with probability

$$1 - \frac{1/(2N_I)}{1/(2N_I) + 2m} \quad (3.57)$$

Conditional on one or other of our alleles migrating to the mainland, both of our alleles represent independent draws from the mainland and so differ from each other with probability  $H_M$ . Therefore, the level of heterozygosity on the island is given by

$$H_I = \left(1 - \frac{1/(2N_I)}{1/(2N_I) + 2m}\right) H_M \quad (3.58)$$

So the reduction of heterozygosity on the island compared to the mainland is

$$F_{IM} = 1 - \frac{H_I}{H_M} = \frac{1/(2N_I)}{1/(2N_I) + 2m} = \frac{1}{1 + 4N_I m}. \quad (3.59)$$

The level of inbreeding on the island compared to the mainland will be high if the migration rate is low and the effective population size of the island is low, as allele frequencies on the island are drifting and diversity on the island is not being replenished by migration. The key parameter here is the number individuals on the island replaced by immigrants from the mainland each generation ( $N_I m$ ).

We have framed this problem as being about the reduction in genetic diversity on the island compared to the mainland. However, if we consider collecting individuals on the island and mainland in proportion to their population sizes, the total level of heterozygosity would be  $H_T = H_M$ , as samples from our mainland would greatly outnumber those from our island. Therefore, considering the island as our sub-population, we have derived another simple model of  $F_{ST}$ .

**Question 13.** You are investigating a small river population of sticklebacks, which receives infrequent migrants from a very large marine population. At a set of putatively neutral biallelic markers the freshwater population has frequencies:

0.2, 0.7, 0.8

at the same markers the marine population has frequencies:

0.4, 0.5 and 0.7.

From studying patterns of heterozygosity at a large collection of markers, you have estimated the long term effective size of your freshwater population is 2000 individuals.

What is your estimate of the migration rate from the marine populations into the river?

*Incomplete lineage sorting* Because it can take a long time for an polymorphism to drift up or down in frequency, multiple population

splits may occur during the time an allele is still segregating. This can lead to incongruence between the overall population tree and the information about relationships present at individual loci. In Figure 3.37 and 3.38 we show simulations of three populations where the bottom population splits off from the other two first, followed by the subsequent splitting of the top and middle populations. We start both simulations with a newly introduced red allele being polymorphic in the combined ancestral population. The most likely fate of this allele is that it is quickly lost from the population, but sometimes the allele can drift up in frequency and be polymorphic when the populations split, as the alleles in our two figures have done. If the allele is lost/fixed in the descendant populations before the next population split, our allele configuration will agree with the population tree, as it does in Figure 3.37, and so too the gene tree will agree with population tree (as shown in the left side of Figure 3.39). However, if the allele persists as a polymorphism in the ancestral population till the top and the middle populations split, then the allele can fix in one of these populations and not the other. Such an event can lead to a substitution pattern that disagrees with the population tree, as in Figure 3.38. If we were to construct a phylogeny using the variation at this site we would see a disagreement between the gene tree and population tree. In Figure 3.38 an allele drawn from the top and the bottom populations are necessarily more closely related to each other than either is to an allele drawn from population 2; tracing our allelic lineages from the top and bottom populations back through time, they must coalesce with each other before we reach the point where the red mutation arose; in contrast, a lineage from the middle population cannot have coalesced with either other lineage until past the time the red mutation arose. An example of this 'incomplete lineage sorting' in terms of the underlying tree is shown on the right side of Figure 3.39 .

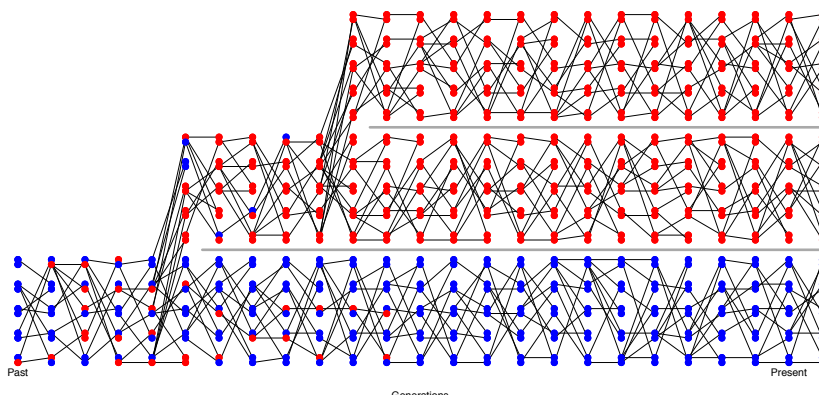


Figure 3.37: An example of alleles assorting among three populations such that there is no incomplete lineage sorting. Code here.

A natural pedigree analogy to incomplete lineage sorting is the fact



Figure 3.38: An example of alleles assorting among three populations leading to incomplete lineage sorting. Code here.



Figure 3.39: The population tree of three populations ((A, B), C) is shown blocked out with black shapes. Two different coalescent trees are relating a single allele drawn from A, B, and C are shown with thinner lines.

that while two biological siblings are more closely related to each other genealogically than either is to their cousin, at any given locus one of the siblings can share an allele IBD with their cousin that they do not share with their own sibling, due to the randomness of Mendelian segregation down their pedigree. In these cases, the average relatedness of the individuals/populations disagrees with the patterns of relatedness at a particular locus.

As an empirical example of incomplete lineage sorting, let's consider the work of JENNINGS and EDWARDS who sequenced a single allele from three different species of Australian grass finches (*Poephila*): two sister species of long-tailed finches (*Poephila acuticauda* and *P. hecki*) and the black-throated finch (*Poephila cincta*, see Figure 3.40). They collected sequence data for 30 genes, and constructed phylogenetic gene trees at each of these loci, resulting in 28 well-resolved gene trees. 16 of the gene trees showed *P. acuticauda* and *P. hecki* as sisters with *P. cincta* (the tree ((A,H),C)), while for twelve genes the gene tree was discordant with the population tree: for seven of their genes *P. hecki* fell as an outgroup to the other two and at five *P. acuticauda* fell as an outgroup (the trees ((A,C),H) and ((H,C),A) respectively).

Let's use the coalescent to understand this discordance between gene trees and species trees. Let's assume that two sister populations (A & B) split  $t_1$  generations in the past, with a deeper split from a



Figure 3.40: Banded Grass Finch (*P. cincta*). Illustration by Elizabeth Gould. Birds of Australia Gould J. 1840. CC BY 4.0 uploaded to Flickr by rawpixel.com.

third outgroup population (C)  $t_2$  generations in the past. We'll assume that there's no gene flow among our populations after each split. We can trace back the ancestral lineages of our three alleles. The first opportunity for the A & B lineages to coalesce is  $t_1$  generations ago. If they coalesce with each other in their shared ancestral population before  $t_2$  in the past (left side of Figure 3.39) their gene tree will definitely agree with the population tree. So the only way for the gene tree to disagree with the population tree is for the A & B lineages to fail to coalesce in their shared ancestral population between  $t_1$  and  $t_2$ ; this happens with probability  $(1 - 1/2N)^{t_2-t_1}$ . We'll get a discordant gene tree if A & B make it back to the shared ancestral population with C without coalescing, and then one or the other of them coalesces with the C lineage before they coalesce with each other. This happens with probability 2/3, as at the first pairwise-coalescent event there are three possible pairs of lineages that could coalesce, two of which (A & C and B & C) result in a discordant tree. So the probability that we get a coalescent tree that is discordant with the population tree is

$$\frac{2}{3} (1 - 1/2N)^{t_2-t_1}. \quad (3.60)$$

Thus we should expect gene-tree population-tree discordance when populations split in rapid succession and/or population sizes are large.

**Question 14.** Let's return to JENNINGS and EDWARDS's Australian grass finches example. They estimated that the ancestral population size of our two long-tailed finches was four hundred thousand. What is your best estimate of the inter-speciation time, i.e.  $t_2 - t_1$ ?

*Testing for gene flow.* We often want to test whether gene flow has occurred between populations. For example, we might want to establish a case that interbreeding between humans and Neanderthals occurred or demonstrate that gene flow occurred after two populations began to speciate. A broad range of methods have been designed to test for gene flow and to estimate gene flow rates, based on neutral expectations. Here we'll briefly just discuss one method based on some simple coalescent ideas. Above we assumed that gene-tree population-tree discordance was due to incomplete lineage sorting due to populations rapidly splitting. However, gene flow among populations can also lead to gene-tree discordance. While both ILS and gene flow can lead to discordance, under simplifying assumptions, ILS implies more symmetry in how these discordances manifest themselves.

Take a look at Figure 3.41. In both cases the lineages from A and B fail to coalesce in their initial shared ancestral population, and one or the other of them coalesces with the lineage from C before they

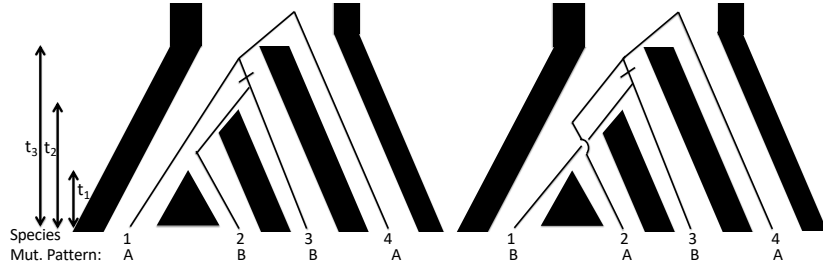


Figure 3.41: In both the left and right trees ILS has occurred between our single lineages sampled from populations A, B, and C. Imagine that population D is a somewhat distant outgroup such that the lineages from A through C (nearly) always coalesce with each other before any coalescence with D. The small dash on the branch indicates the mutation A → B occurring, giving rise to the ABBA or BABA mutational pattern shown at the bottom.

coalesce with each other. Each option is equally likely; therefore the mutational patterns ABBA and BABA are equally likely to occur under ILS.<sup>6</sup>

However, if gene flow occurs from population C into population B, in addition to ILS the lineage from B can more recently coalesce with the lineage from C, and so we should see more ABBAAs than BABAs. To test for this effect of gene flow, we can sample a sequence from each of our 4 populations and count up the number of sites that show the two mutational patterns consistent with the gene-tree discordance  $n_{ABBA}$  and  $n_{BABA}$  and calculate

$$\frac{n_{ABBA} - n_{BABA}}{n_{ABBA} + n_{BABA}} \quad (3.61)$$

This statistic will have expectation zero if the gene-tree discordance is due to ILS and will be skewed negative if gene flow occurred from C into B (and skewed positive if gene flow occurred from C into A).

<sup>6</sup> here we have to assume no structure in the ancestral population.

# 4

## *Phenotypic Variation and the Resemblance Between Relatives.*

THE DISTINCTION BETWEEN GENOTYPE AND PHENOTYPE is one of the most useful ideas in Biology.<sup>1</sup> The genotype of an individual (the genome), for most purposes, is decided when the sperm fertilizes egg. The phenotype of an individual represents any measurable aspect of an organism.

Your height, to the amount of RNA transcribed from a given gene, to what you ate last Tuesday: all of these are phenotypes. Nearly any phenotype we can choose to measure about an organism represents the outcome of the information encoded by their genome played out through an incredibly complicated developmental, physiological and/or behavioural processes that in turn interact with a myriad of environmental and stochastic factors. Honestly it boggles the mind how organisms work as well as they do, let alone that I managed to eat lunch last Tuesday.

There are many different ways to think about studying the path from genotype through to phenotype. The one we will take here is to think about how phenotypic variation among individuals in a population arises as a result of genetic variation in the population. One simple way to measure this genotype-phenotype relationship is to calculate the phenotypic mean for each genotype at a locus. For example, WANG *et al.* (2018) explored the genetic basis of budset time in European aspen (*Populus tremula*); the effect of one specific SNP on that phenotype is shown in Figure 4.2. Budset timing is a key trait underlying local adaptation to varying growing season length. The associated SNP falls in a gene (*PtFT2*) that is known to play a strong role in flowering time regulation in other plants.

One way for us to assess the relationship between genotype and phenotype is to find the best fitting linear line through the data, i.e. fit a linear regression of phenotypes for our individuals on their geno-

<sup>1</sup> JOHANNSEN, W., 1911 The Genotype Conception of Heredity. *The American Naturalist* 45(531): 129–159

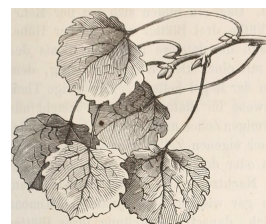


Figure 4.1: European aspen *P. tremula*.  
Der baum. H. Schacht. 1860. BHL Image from the Biodiversity Heritage Library. Contributed by The Library of Congress. Not in copyright.

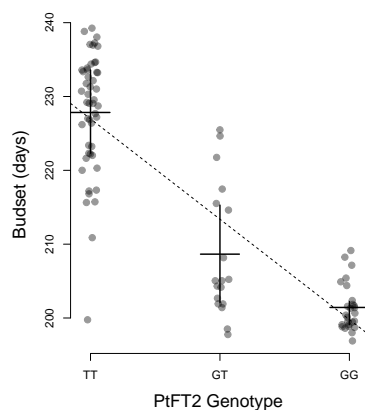


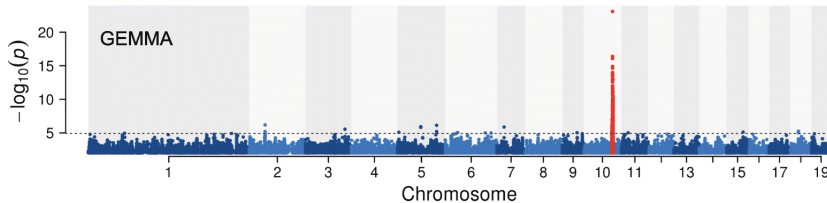
Figure 4.2: The effect of a flowering time gene (*PtFT2*) SNP on budset time in European aspen. Each dot gives the genotype-phenotype combination for an individual. The horizontal lines give the budset mean for each genotype and the vertical lines show the inter-quartile range. The dotted line gives the linear regression of phenotype on genotype. Thanks to Pär Ingvarsson for sharing these data from WANG *et al.* (2018).

types at a particular SNP ( $l$ ):

$$X \sim \mu + a_l G_l \quad (4.1)$$

In the equation above,  $X$  is a vector of the phenotypes of a set of individuals and  $G_l$  is our vector of genotypes at locus  $l$ , with  $G_{i,l}$  taking the value 0, 1, or 2 depending on whether our individual  $i$  is homozygote, heterozygote, or the alternate homozygote at our locus of interest. Here  $\mu$  is our phenotypic mean. The slope of this regression line ( $a_l$ ) has the interpretation of being the average effect of substituting a copy of allele 2 for a copy of allele 1. In our Aspen example the slope is  $-13.6$ , i.e. swapping a single  $T$  for a  $G$  allele moves the budset forward by 13.6 days, such that the  $GG$  homozygote is predicted to set buds 27.2 days earlier than the  $TT$  homozygote.

As a measure of the significance of this genotype-phenotype relationship, we can calculate the p-value of our regression. To try and identify loci that are associated with our trait genome-wide, we can conduct this regression at each SNP we genotype in the genome. One common way to display the results of such an analysis (called a genome-wide association study or GWAS for short) is to plot the logarithm of the p-value for each SNP along genome (a so-called Manhattan plot). Here's one from WANG *et al.* (2018) for their Aspen budset phenotype



The SNP with the most significant p-value is the PtFT2 SNP. Note that other SNPs in the surrounding region also light up as showing a significant association with budset timing. This is because loci that are in LD with a functional locus may in turn show an association, not because they directly affect the phenotype, but simply because the genotypes at the two loci are themselves non-randomly associated. Below is a zoomed in version (Figure 2 in WANG *et al.* (2018)) with SNPs coloured by the strength of their LD with the putatively functional SNP. Note how SNPs in strong LD with the functional allele (redder points) have more significant p-values.

Variation in some traits seems to have a relatively simple genetic basis. In our Aspen example there is one clear large-effect locus, which explains 62% of the variation in budset. Note that even in this case, where we have an allele with a very strong effect on a phenotype, this

Figure 4.3: Manhattan plot of the p-value of the linear association between genotype and budset in Aspen. Each dot represents the test at a single SNP, plotted at its physical coordinate in the genome. Different chromosomes are plotted in alternating colours. The SNPs surrounding the PtFT2 gene are shown in red. From WANG *et al.* (2018), licensed under CC BY 4.0.



Figure 4.4: The Manhattan plot zoomed in on the top-hit (red SNPs from Figure 4.3). SNPs are now coloured by their  $D/t$  value with the most significant SNP.  $D/t$  is the LD covariance between a pair of loci ( $D$ ) normalized by the largest value  $D$  can take given the allele frequencies. Figure from WANG *et al.* (2018), licensed under CC BY 4.0.

is not an allele *for* budset, nor is PtFT2 a gene *for* budset. It is an allele that is associated with budset in the sampled environments and populations. In a different set of environments, this allele's effects may be far smaller, and a different set of alleles may contribute to phenotype variation. PtFT2, the gene our focal SNP falls close to, is just one of many genes and molecular pathways involved in budset. A mutant screen for budset may uncover many genes with larger effects; this gene is just a locus that happens to be polymorphic in this particular set of genotyped individuals.

While phenotypic variation for some phenotypes has a relatively simple genetic basis, many phenotypes are likely much more genetically complex, involving the functional effect of many alleles at hundreds or thousands of polymorphic loci. For example hundreds of small effect loci affecting human height have been mapped in European populations to date. Such genetically complex traits are called polygenic traits.

In this chapter, we will use our understanding of the sharing of alleles between relatives to understand the phenotypic resemblance between relatives in quantitative phenotypes. This will allow us to understand the contribution of genetic variation to phenotypic variation. In the next chapter, we will then use these results to understand the evolutionary change in quantitative phenotypes in response to selection.

#### 4.0.1 A simple additive model of a trait

Let's imagine that the genetic component of the variation in our trait is controlled by  $L$  autosomal loci that act in an additive manner. The frequency of allele 1 at locus  $l$  is  $p_l$ , with each copy of allele 1 at this locus increasing your trait value by  $a_l$  above the population mean. The phenotype of an individual, let's call her  $i$ , is  $X_i$ . Her genotype at SNP  $l$  is  $G_{i,l}$ . Here  $G_{i,l} = 0, 1$ , or  $2$ , representing the number of

"All that we mean when we speak of a gene [allele] for pink eyes is, a gene which differentiates a pink eyed fly from a normal one —not a gene [allele] which produces pink eyes per se, for the character pink eyes is dependent on the action of many other genes." - STURTEVANT (1915)

copies of allele 1 she has at this SNP. Her expected phenotype, given her genotype at all  $L$  SNPs, is then

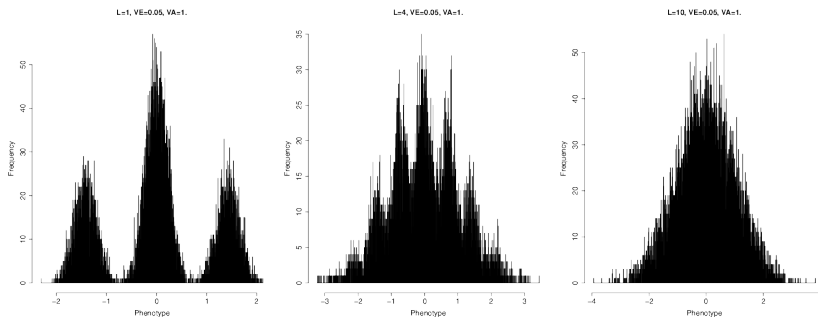
$$\mathbb{E}(X_i|G_{i,1}, \dots, G_{i,L}) = \mu + X_{A,i} = \mu + \sum_{l=1}^L G_{i,l}a_l \quad (4.2)$$

where  $\mu$  is the mean phenotype in our population, and  $X_{A,i}$  is the deviation away from the mean phenotype due to her genotype. Now in reality the phenotype is a function of the expression of those alleles in a particular environment. Therefore, we can think of this expected phenotype as being an average across a set of environments that occur in the population.

When we measure our individual's observed phenotype we see

$$X_i = \mu + X_{A,i} + X_{E,i} \quad (4.3)$$

where  $X_E$  is the deviation from the mean phenotype due to the environment. This  $X_E$  includes the systematic effects of the environment our individual finds herself in and all of the noise during development, growth, and the various random insults that life throws at our individual. If a reasonable number of loci contribute to variation in our trait then we can approximate the distribution of  $X_{A,i}$  by a normal distribution due to the central limit theorem (see Figure 4.5). Thus if we can approximate the distribution of the effect of environmental variation on our trait ( $X_{E,i}$ ) also by a normal distribution, which is reasonable as there are many small environmental effects, then the distribution of phenotypes within the population ( $X_i$ ) will be normally distributed (see Figure 4.5).



Note that as this is an additive model; we can decompose eqn. 4.3 into the effects of the two alleles at each locus and rewrite it as

$$X_i = \mu + X_{iM} + X_{iP} + X_{iE} \quad (4.4)$$

where  $X_{iM}$  and  $X_{iP}$  are the contribution to the phenotype of the alleles that our individual received from her mother (maternal alleles) and

**Figure 4.5:** The convergence of the phenotypic distribution to a normal distribution. Each of the three histograms shows the distribution of the phenotype in a large sample, for increasingly large numbers of loci ( $L = 1, 4$ , and  $10$ , with the proportion of variance explained held at  $V_A = 1$ ). I have simulated each individual's phenotype following equations 4.2 and 4.3. Specifically, we've simulated each individual's biallelic genotype at  $L$  loci, assuming Hardy-Weinberg proportions and that the allele is at 50% frequency. We assume that all of the alleles have equal effects and combine them additively together. We then add an environmental contribution, which is normally distributed with variance 0.05. Note that in the left two pictures you can see peaks corresponding to different genotypes due to our low environmental noise (in practice we can rarely see such peaks for real quantitative phenotypes). Code here.

father (paternal alleles) respectively. This will come in handy in just a moment when we start thinking about the phenotypic covariance of relatives.

Now obviously this model seems silly at first sight as alleles don't only act in an additive manner, as they interact with alleles at the same loci (dominance) and at different loci (epistasis). Later we'll relax this assumption, however, we'll find that if we are interested in evolutionary change over short time-scales it is actually only the "additive component" of genetic variation that will (usually) concern us. We will define this more formally later on, but for the moment we can offer the intuition that parents only get to pass on a single allele at each locus on to the next generation. As such, it is the effect of these transmitted alleles, averaged over possible matings, that is an individual's average contribution to the next generation (i.e. the additive effect of the alleles that their genotype consists of).

#### 4.0.2 Additive genetic variance and heritability

As we are talking about an additive genetic model, we'll talk about the additive genetic variance ( $V_A$ ), the phenotypic variance due to the additive effects of segregating genetic variation. This is a subset of the total genetic variance if we allow for non-additive effects.

The variance of our phenotype across individuals ( $V$ ) we can write as

$$V = \text{Var}(X_A) + \text{Var}(X_E) = V_A + V_E \quad (4.5)$$

In writing the phenotypic variance as a sum of the additive and environmental contributions, we are assuming that there is no covariance between  $X_{G,i}$  and  $X_{E,i}$  i.e. there is no covariance between genotype and environment.

Our additive genetic variance can be written as

$$V_A = \sum_{l=1}^L \text{Var}(G_{i,l}a_l) \quad (4.6)$$

where  $\text{Var}(G_{i,l}a_l)$  is the contribution of locus  $l$  to the additive variance among individuals. Assuming random mating, and that our loci are in linkage equilibrium, we can write our additive genetic variance as

$$V_A = \sum_{l=1}^L a_l^2 2p_l(1 - p_l) \quad (4.7)$$

where the  $2p_l(1 - p_l)$  term follows from the binomial sampling of two alleles per individual at each locus.

**Question 1.** You have two biallelic SNPs contributing to variance in human height. At the first SNP you have an allele with an additive

effect of 5cm which is found at a frequency of 1/10,000. At the second SNP you have an allele with an additive effect of  $-0.5\text{cm}$  segregating at 50% frequency. Which SNP contributes more to the additive genetic variance? Explain the intuition of your answer.

*An example of calculating polygenic scores.* Now we don't usually get to see the individual loci contributing to highly polygenic traits. Instead, we only get to see the distribution of the trait in the population. However, with the advent of GWAS in human genetics we can see some of the underlying genetics using the many trait-associated loci identified to date. Using the estimated effect sizes at each locus, each one of which is tiny, we can calculate the weighted sum over an individual's genotype as in equation 4.2. This weighted sum is called the individual's polygenic score. To illustrate how polygenic scores work, we can take a set of 1700 SNPs, each chosen as the SNP with the strongest signal of association with height in 1700 roughly independent bins spaced across the genome. The effects of these SNPs are tiny; the medium, absolute additive effect size is 0.07cm. Figure 4.6 shows the distribution of a thousand individuals' polygenic scores calculated using these 1700 SNPs (simulated genotypes using the UKBB frequencies). The standard deviation of these polygenic scores  $\sim 2\text{cm}$ . The individuals with higher polygenic scores for height are predicted to be taller than the individuals with lower polygenic scores.

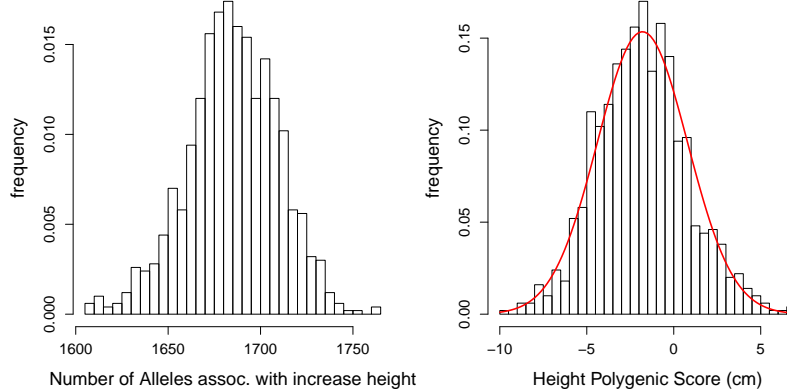


Figure 4.6: **Left)** The distribution of the number of height-increasing alleles that individuals carry at 1700 SNPs associated with height in the UK Biobank, for a sample of 1000 individuals. **right)** The distribution of the polygenic scores for these 1000 individuals. Plotted on top is a normal distribution with the same mean and variance. The empirical variance of these polygenic scores is 0.13, the additive genetic variance calculated by equation (4.7) is 0.135, so the two are in good agreement. Code here.

*The narrow sense heritability* We would like a way to think about what proportion of the variation in our phenotype across individuals is due to genetic differences as opposed to environmental differences. Such a quantity will be key in helping us think about the evolution of

phenotypes. For example, if variation in our phenotype had no genetic basis, then no matter how much selection changes the mean phenotype within a generation the trait will not change over generations.

We'll call the proportion of the variance that is genetic the *heritability*, and denote it by  $h^2$ . We can then write heritability as

$$h^2 = \frac{Var(X_A)}{V} = \frac{V_A}{V} \quad (4.8)$$

Remember that we are thinking about a trait where all of the alleles act in a perfectly additive manner. In this case our heritability  $h^2$  is referred to as the *narrow sense heritability*, the proportion of the variance explained by the additive effect of our loci. When we allow dominance and epistasis into our model, we'll also have to define the *broad sense heritability* (the total proportion of the phenotypic variance attributable to genetic variation).

The narrow sense heritability of a trait is a useful quantity; indeed we'll see shortly that it is exactly what we need to understand the evolutionary response to selection on a quantitative phenotype. We can calculate the narrow sense heritability by using the resemblance between relatives. For example, if the phenotypic differences between individuals in our population were solely determined by environmental differences experienced by these different individuals, we should not expect relatives to resemble each other any more than random individuals drawn from the population. Now the obvious caveat here is that relatives also share an environment, so may resemble each other due to shared environmental effects.

Note that the heritability is a property of a sample from the population in a particular set of environments at a particular time.

Changes in the environment may change the phenotypic variance.

Changes in the environment may also change how our genetic alleles are expressed through development and so change  $V_A$ . Thus estimates of heritability are not transferable across environments or populations.

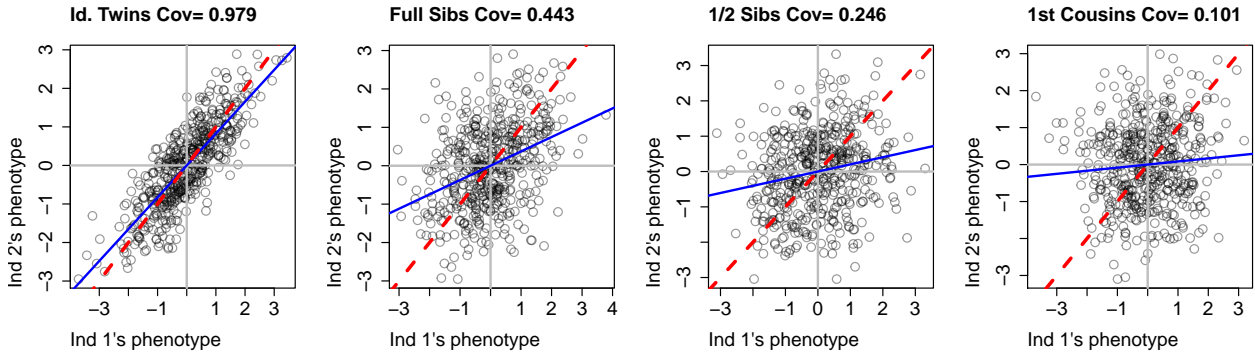
#### 4.0.3 The covariance between relatives

So we'll go ahead and calculate the covariance in phenotype between two individuals (1 and 2) who have phenotypes  $X_1$  and  $X_2$  respectively. To think about imagine plotting the phenotypes of, say, sisters against each other. The x and y coordinates of each point will be the, say, heights of the pair of siblings. Do tall women tend to have tall sisters, do short women tend to have short sisters? How much do their phenotypes covary. If some of the variation in our phenotype is genetic we expect identical twins to resemble each other more than full siblings, who in turn will resemble each other more than half-sibs and so on out (see Figure 4.7). Under our simple additive model of

phenotypes we can write the covariance as

$$\text{Cov}(X_1, X_2) = \text{Cov}((X_{1M} + X_{1P} + X_{1E}), ((X_{2M} + X_{2P} + X_{2E})) \quad (4.9)$$

We can expand this out in terms of the covariance between the various components in these sums.



To make our task easier, we will make two commonly made assumptions:

1. We can ignore the covariance of the environments between individuals (i.e.  $\text{Cov}(X_{1E}, X_{2E}) = 0$ )
2. We can ignore the covariance between the environment of one individual and the genetic variation in another individual (i.e.  $\text{Cov}(X_{1E}, (X_{2M} + X_{2P})) = 0$ ). (We can actually incorporate these effects in later if we choose too.)

The failure of these assumptions to hold can undermine our estimates of heritability, but we'll return to that later. Moving forward with these assumptions, we can simplify our original expression above and write our phenotypic covariance between our pair of individuals as

$$\text{Cov}(X_1, X_2) = \text{Cov}((X_{1M}, X_{2M}) + \text{Cov}(X_{1M}, X_{2P}) + \text{Cov}(X_{1P}, X_{2M}) + \text{Cov}(X_{1P}, X_{2P}) \quad (4.10)$$

This equation is saying that, under our simple additive model, we can see the covariance in phenotypes between individuals as the covariance between the maternal and paternal allelic effects in our individuals. We can use our results about the sharing of alleles between relatives to obtain these covariance terms. But before we write down the general case, let's quickly work through some examples.

*The covariance between identical twins* Let's first consider the case of a pair of identical twins from two unrelated parents. Our pair of

Figure 4.7: Covariance of phenotypes between pairs of individuals of a given relatedness. Each point gives the phenotypes of a different pair of individuals. The additive genetic variance is held constant at  $V_A = 1$ , such that the expected covariances ( $2F_{1,2}V_A$ ) should be 1, 0.5, 0.25, and 0.125 respectively din good agreement with the empirical covariances reported in the title of each graph. The data were simulated as described in the caption of Figure 4.5. The blue line shows  $x = y$  and the red line shows the best fitting linear regression line. Code here.

twins share their maternal and paternal allele identical by descent ( $X_{1M} = X_{2M}$  and  $X_{1P} = X_{2P}$ ). As their maternal and paternal alleles are not correlated draws from the population, i.e. have no probability of being IBD as we've said the parents are unrelated, the covariance between their effects on the phenotype is zero (i.e.  $Cov(X_{1P}, X_{2M}) = Cov(X_{1M}, X_{2P}) = 0$ ). In that case, eqn. 4.10 is

$$Cov(X_1, X_2) = Cov((X_{1M}, X_{2M}) + Cov(X_{1P}, X_{2P}) = 2Var(X_{1M}) = V_A \quad (4.11)$$

Now in general identical twins are not going to be super helpful for us in estimating  $h^2$ , because under models with non-additive effects, identical twins will have higher covariance than we'd expect just based on the alleles they share. This is because identical twins don't just share alleles, they share their entire genotypes, and thus resemble each other in phenotype also because of shared dominance effects.

*The covariance in phenotype between mother and child* If a mother and father are unrelated individuals (i.e. are two random draws from the population) then this mother and her child share one allele IBD at each locus (i.e.  $r_1 = 1$  and  $r_0 = r_2 = 0$ ). Half the time our mother (ind 1) transmits her paternal allele to the child (ind 2), in which case  $X_{P1} = X_{M2}$ , and so  $Cov(X_{P1}, X_{M2}) = Var(X_{P1})$ , and all the other covariances in eqn. 4.10 are zero. The other half of the time she transmits her maternal allele to the child, in which case  $Cov(X_{M1}, X_{M2}) = Var(X_{M1})$  and all the other terms are zero. By this argument,  $Cov(X_1, X_2) = \frac{1}{2}Var(X_{M1}) + \frac{1}{2}Var(X_{P1}) = \frac{1}{2}V_A$ .

*The covariance between general pairs of relatives under an additive model* The two examples above make clear that to understand the covariance between phenotypes of relatives, we simply need to think about the alleles they share IBD. Consider a pair of relatives (1 and 2) with a probability  $r_0$ ,  $r_1$ , and  $r_2$  of sharing zero, one, or two alleles IBD respectively. When they share zero alleles  $Cov((X_{1M} + X_{1P}), (X_{2M} + X_{2P})) = 0$ , when they share one allele  $Cov((X_{1M} + X_{1P}), (X_{2M} + X_{2P})) = Var(X_{1M}) = \frac{1}{2}V_A$ , and when they share two alleles  $Cov((X_{1M} + X_{1P}), (X_{2M} + X_{2P})) = V_A$ . Therefore, the general covariance between two relatives is

$$Cov(X_1, X_2) = r_0 \times 0 + r_1 \frac{1}{2}V_A + r_2 V_A = 2F_{1,2}V_A \quad (4.12)$$

So under a simple additive model of the genetic basis of a phenotype, to measure the narrow sense heritability we need to measure the covariance between pairs of relatives (assuming that we can remove the effect of shared environmental noise). From the covariance between relatives we can calculate  $V_A$ , and we can then divide this by the total phenotypic variance to get  $h^2$ .

**Question 2.** A) In polygynous red-winged blackbird populations (i.e. males mate with several females), paternal half-sibs can be identified. Suppose that the covariance of tarsus lengths among half-sibs is  $0.25 \text{ cm}^2$  and that the total phenotypic variance is  $4 \text{ cm}^2$ . Use these data to estimate  $h^2$  for tarsus length in this population.

B) Why might paternal half-sibs be preferable for measuring heritability than maternal half-sibs?

*Parent-midpoint offspring regression* Another way that we can estimate the narrow sense heritability is through the regression of child's phenotype on the parental mid-point phenotype. The parental mid-point phenotype is simply the average of the mum and dad's phenotype. We denote the child's phenotype by  $X_{kid}$  and mid-point phenotype by  $X_{mid}$ , so that if we take the regression  $X_{kid} \sim X_{mid}$  this regression has slope  $\beta = \text{Cov}(X_{kid}, X_{mid})/\text{Var}(X_{mid})$ . The covariance of  $\text{Cov}(X_{kid}, X_{mid}) = \frac{1}{2}V_A$ , and  $\text{Var}(X_{mid}) = \frac{1}{2}V$ , as by taking the average of the parents we have halved the variance, such that the slope of the regression is

$$\beta_{mid,kid} = \frac{\text{Cov}(X_{kid}, X_{mid})}{\text{Var}(X_{mid})} = \frac{V_A}{V} = h^2 \quad (4.13)$$

i.e. the regression of the child's phenotype on the parental midpoint phenotype is an estimate of the narrow sense heritability. This way of estimating heritability has the problem of not controlling for environmental correlations between relatives. But it's a useful way to think about heritability and will be directly relevant to our discussion of the response to selection in the next chapter.

Our regression allows us to attempt to predict the phenotype of the child given the phenotypes of the parents; how well we can do this depends on the slope. If the slope is close to zero then the parental phenotypes hold no information about the phenotype of the child, while if the slope is close to one then the parental mid-point is a good guess at the child's phenotype.

More formally, the expected phenotype of the child given the parental phenotypes is

$$\mathbb{E}(X_{kid}|X_{mum}, X_{dad}) = \mu + \beta_{mid,kid}(X_{mid} - \mu) = \mu + h^2(X_{mid} - \mu) \quad (4.14)$$

which follows from the definition of linear regression. So to find the child's predicted phenotype, we simply take the mean phenotype and add on the difference between our parental mid-point and the population mean, multiplied by our narrow sense heritability.

**Question 3.** Briefly explain what Galton meant by 'regression towards mediocrity', and why he observed this pattern in light of Mendelian inheritance.



Figure 4.8: Red-winged blackbird and Tricoloured Red-winged blackbirds (*Agelaius phoeniceus* and *Agelaius tricolor*).

Bird-lore (1899). National Association of Audubon Societies for the Protection of Wild Birds and Animals. Image from the Biodiversity Heritage Library. Contributed by American Museum of Natural History Library. Not in copyright.

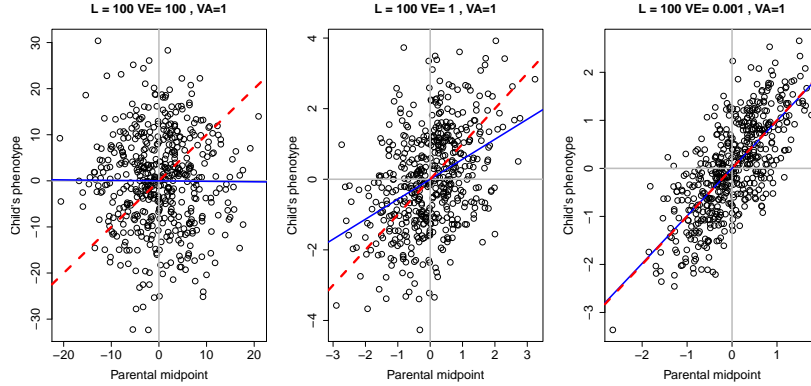


Figure 4.9: Regression of child's phenotype of the parental mid-point phenotype. The three panels show decreasing levels of environmental variance ( $V_E$ ) holding the additive genetic variance constant ( $V_A = 1$ ). In these figures, we simulate 100 loci, as described in the caption of Figure 4.5. We simulate the genotypes and phenotypes of the two parents, and then simulate the child's genotype following mendelian transmission. The blue line shows  $x = y$  and the red line shows the best fitting linear regression line. Code here.

*Estimating additive genetic variance across a variety of different relationships.* In many natural populations we may have access to individuals with a range of different relationships to each other (e.g. through monitoring of the paternity of individuals), but relatively few pairs of individuals for a specific relationship (e.g. sibs). We can try and use this information on various relatives as fully as possible in a mixed model framework. Building from equation 4.3, we can write an individual's phenotype  $X_i$  as

$$X_i = \mu + X_{A,i} + X_{E,i} \quad (4.15)$$

where  $X_{E,i} \sim N(0, V_E)$  and  $X_{A,i}$  is normally distributed across individuals with covariance matrix  $V_A A$ , where the entries for a pair of individuals i and j are  $A_{ij} = 2F_{i,j}$  and  $A_{ii} = 1$ . Given the matrix  $A$  we can estimate  $V_A$ . We can also add fixed effects into this model to account for generation effects, additional mixed effects could also be included to account for shared environments between particular individuals (e.g. a shared nest). This approach is sometimes called the “animal model”.

#### 4.1 Multiple traits

Traits often covary with each other, both due to environmentally induced effects (e.g. due to the effects of diet on multiple traits) and due to the expression of underlying genetic covariance between traits. Genetic covariance, in turn, can reflect pleiotropy, a mechanistic effect of an allele on multiple traits (e.g. variants that affect skin pigmentation often affect hair color), the genetic linkage of loci independently affecting multiple traits, or the effects of assortative mating.

Consider two traits  $X_{1,i}$  and  $X_{2,i}$  in an individual  $i$ . These traits could be, say, the individual's leg length and nose length. As before,

we can write these as

$$\begin{aligned} X_{1,i} &= \mu_1 + X_{1,A,i} + X_{1,E,i} \\ X_{2,i} &= \mu_2 + X_{2,A,i} + X_{2,E,i} \end{aligned} \quad (4.16)$$

As before we can talk about the total phenotypic variance ( $V_1, V_2$ ), environmental variance ( $V_{1,E}$  and  $V_{2,E}$ ), and the additive genetic variance for trait one and two ( $V_{1,A}, V_{2,A}$ ). But now we also have to consider the total covariance between trait one and trait two,  $V_{1,2} = \text{Cov}(X_1, X_2)$ , as well as the environmentally induced covariance ( $V_{E,1,2} = \text{Cov}(X_{1,E}, X_{2,E})$ ) and the additive genetic covariance ( $V_{A,1,2} = \text{Cov}(X_{1,A}, X_{2,A})$ ). To better understand the covariance arising due to pleiotropy, let's think about a set of  $L$  SNPs contributing to our two traits. If the additive effect of an allele at the  $i^{th}$  SNP is  $\alpha_{i,1}$  and  $\alpha_{i,2}$  on traits 1 and 2, then the additive covariance between our traits is

$$V_{A,1,2} = \sum_{i=1}^L 2\alpha_{i,1}\alpha_{i,2}p_i(1-p_i) \quad (4.17)$$

assuming our loci are in linkage disequilibrium. Thus a genetic correlation arises due to pleiotropy, because loci that tend to affect trait 1 also systematically affect trait 2. For example, alleles associated with later Age at Menarche (AAM) in European females also tend to be positively associated with height (see Figure 4.10), thereby creating a genetic correlation between AAM and height.

We can store our variance and covariance values in matrices, a way of gathering these terms that will be useful when we discuss selection:

$$\mathbf{V} = \begin{pmatrix} V_1 & V_{1,2} \\ V_{1,2} & V_2 \end{pmatrix} \quad (4.18)$$

and

$$\mathbf{G} = \begin{pmatrix} V_{1,A} & V_{A,1,2} \\ V_{A,1,2} & V_{2,A} \end{pmatrix} \quad (4.19)$$

Here we've shown the matrices for two traits, but we can generalize this to an arbitrary number of traits.

We can estimate these quantities, in a similar way as before, by studying the covariance in different traits between relatives:

$$\text{Cov}(X_{1,i}, X_{2,j}) = 2F_{i,j}V_{A,1,2} \quad (4.20)$$

We can also talk about the genetic correlation between two phenotypes

$$r_g = \frac{V_{A,1,2}}{\sqrt{V_{A,1}V_{A,2}}} \quad (4.21)$$

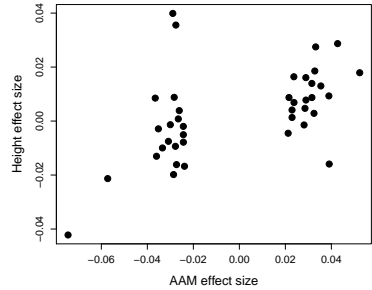


Figure 4.10: The additive effect sizes of loci associated with female Age at Menarche (AAM) and their effect size on Height in a European population. Data from PICKRELL *et al.* (2016). Code here.

where  $V_{A,1}$  and  $V_{A,2}$  are the additive genetic variance for trait 1 and 2 respectively. Here,  $r_g$  tells us to what extent the additive genetic variance in two traits is correlated.

One type of genetic covariance we often think about is the covariance of male and female phenotypes. For example, below is the relationship between the forehead patch size for Pied fly-catcher fathers and their sons and daughters. The phenotype has been standardized to have mean 0 and variance 1 in each group. The phenotypic covariance of the sample of fathers and sons is 0.35, while the phenotypic covariance of fathers and daughter is 0.23.

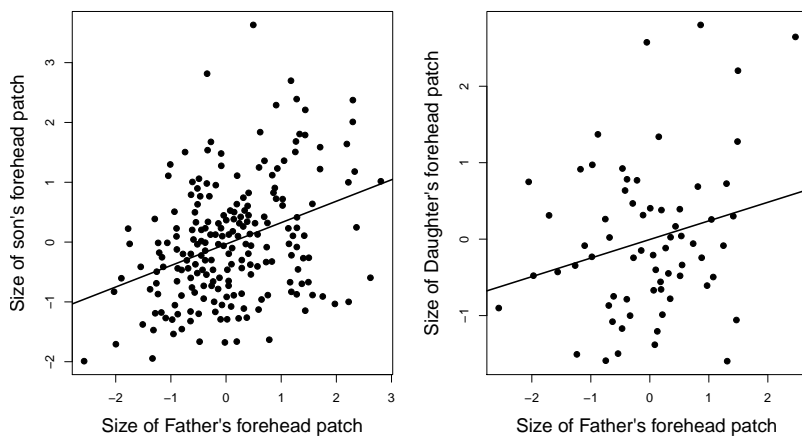


Figure 4.11: Relationship of standardized forehead patch size between fathers and sons and daughters in Pied fly-catchers. Data from POTTI and CANAL. Code here.



**Question 4.** Assume we can ignore the effect of the shared environment in our Pied fly-catcher example.

**A)** What is the additive genetic covariance between male and female patch size?

**B)** What is the additive genetic correlation of male and female patch size? You can assume that the additive genetic variance is the same in males and females.

#### 4.1.1 Non-additive variation.

Up to now we've assumed that our alleles contribute to our phenotype in an additive fashion. However, that does not have to be the case as there may be non-additivity among the alleles present at a locus (*dominance*) or among alleles at different loci (*epistasis*). We can accommodate these complications into our models. We do this by partitioning our total genetic variance into independent variance components.

Figure 4.12: *Ficedula hypoleuca*, Pied fly-catcher.  
Coloured illustrations of British birds, and their eggs (1842-1850). London :G.W. Nicklinson. Image from the Biodiversity Heritage Library. Contributed by Smithsonian Libraries. Not in copyright.

*Dominance.* To understand the effect of dominance, let's consider how the allele that a parent transmits influences their offspring's phenotype. A parent transmits one of their two alleles at a locus to their offspring. Assuming that individuals mate at random, this allele is paired with another allele drawn at random from the population. For example, assume your mother transmitted an allele 1 to you: with probability  $p$  it would be paired with another allele 1, and you would be a homozygote; and with probability  $q$  it's paired with a 2 allele and you're a heterozygote.

Now consider an autosomal biallelic locus  $\ell$ , with frequency  $p$  for allele 1, and genotypes 0, 1, and 2 corresponding to how many copies of allele 1 individuals carry. We'll denote the mean phenotype of an individual with genotype 0, 1, and 2 as  $\bar{X}_{\ell,0}$ ,  $\bar{X}_{\ell,1}$ ,  $\bar{X}_{\ell,2}$  respectively. This mean is taking an average phenotype over all the environments and genetic backgrounds the alleles are present on. We'll mean center (MC) these phenotypic values, setting  $\bar{X}'_{\ell,0} = \bar{X}_{\ell,0} - \mu$ , and likewise for the other genotypes.

We can think about the average (marginal) MC phenotype of an individual who received an allele 1 from their parent as the average of the MC phenotype for heterozygotes and 11 homozygotes, weighted by the probability that the individual has these genotypes, i.e. the probability they receive an additional allele 1 or an allele 2 from their other parent:

$$a_{\ell,1} = p\bar{X}'_{\ell,2} + q\bar{X}'_{\ell,1}, \quad (4.22)$$

Similarly, if your parent transmitted an 2 allele to you, your average MC phenotype would be

$$a_{\ell,2} = p\bar{X}'_{\ell,1} + q\bar{X}'_{\ell,0} \quad (4.23)$$

Let's now consider the average phenotype of an offspring of each of our three genotypes

|                         |                             |                             |                           |
|-------------------------|-----------------------------|-----------------------------|---------------------------|
| genotype:               | 0,                          | 1,                          | 2.                        |
| additive genetic value: | $a_{\ell,2} + a_{\ell,2}$ , | $a_{\ell,1} + a_{\ell,2}$ , | $a_{\ell,1} + a_{\ell,1}$ |

i.e. the mean phenotype of each genotypes' offspring averaged over all possible matings to other individuals in the population (assuming individuals mate at random). These are the additive MC genetic values (breeding values) of our genotypes. Here we are simply adding up the additive contributions of the alleles present in each genotype and ignoring any non-additive effects of genotype.

To illustrate this, in Figure 4.13 we plot two different cases of dominance relationships; in the top row an additive polymorphism and in the second row a fully dominant allele. The additive genetic values of the genotypes are shown as red dots. Note that the additive values of the genotypes line up with the observed MC phenotypic means in the



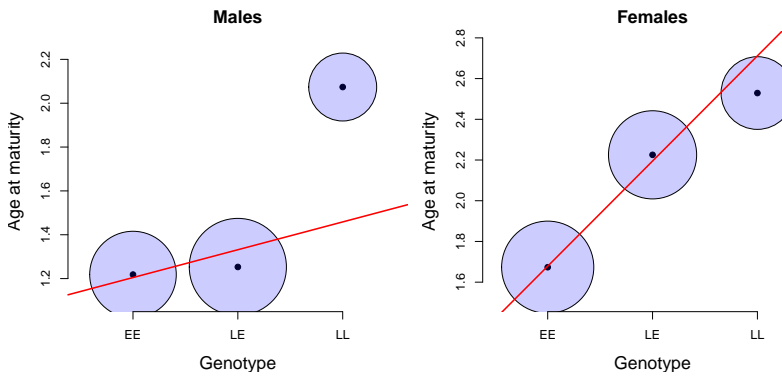
Figure 4.13: The average mean-centered (MC) phenotypes of each genotype. **Top Row:** Additive relationship between genotype and phenotype. **Bottom Row:** Allele 1 is dominant over allele 2, such that the heterozygote has the same phenotype as the 22 genotype (2). The area of each circle is proportion to the fraction of the population in each genotypic class ( $p^2$ ,  $2pq$ , and  $q^2$ ). One the left column  $p = 0.1$  and the right column is  $p = 0.9$ . The additive genetic values of the genotypes are shown as red dots. The regression between phenotype and additive genotype is shown as a red line. The black vertical arrows show the difference between the average MC phenotype and additive genetic value for each genotype. Code here.

top row, when our alleles interact in a completely additive manner. Our additive genetic values always fall along a linear line (the red line in our figure). The additive values are falling along the best fitting line of linear regression for our population, when phenotype is regressed against the additive genotype (0, 1, 2 copies of allele 1) across all individuals in our population. Note in the dominant case the additive genetic values differ from the observed phenotypic means, and are closer to the observed values for the genotypes that are most common in the population.

The difference in the additive effect of the two alleles  $a_{\ell,2} - a_{\ell,1}$  can be interpreted as an average effect of swapping an allele 1 for an allele 2; we'll call this difference  $\alpha_\ell = a_{\ell,2} - a_{\ell,1}$ . Our  $\alpha_\ell$  is also the slope of the regression of phenotype against genotype (the red line in Figure 4.13). Note that the slope of our regression of phenotype on genotype ( $\alpha_\ell$ ) does not depend on the population allele frequency for our completely additive locus (top row of 4.13). In contrast, when there is dominance, the slope between genotype and phenotype ( $\alpha_\ell$ ) is a function of allele frequency (bottom row of 4.13). When a dominant allele (1) is rare there is a strong slope of phenotype on genotype, bottom left Figure 4.13. This strong slope is because replacing a single copy of the 2 allele with a 1 allele in an individual has a big effect on average phenotype, as it will most likely move an individual from being a 22 homozygote to being a 12 heterozygote. In contrast, when the dominant allele (1) is common in the population, replacing a 2 allele by a 1 allele in an individual on average has little phenotypic effect,

leading to a weak slope bottom right Figure 4.13. This small effect is because as we are mainly turning heterozygotes into homozygotes (11), who have the same mean phenotype as each other.

As an example of how dominance and population allele frequencies can change the additive effect of an allele, let's consider the genetics of the age of sexual maturity in Atlantic Salmon. A single allele of large effect segregates in Atlantic Salmon that influences the sexual maturation rate in salmon (AYLLON *et al.*, 2015; BARSON *et al.*, 2015), and hence the timing of their return from the sea to spawn (sea age). The allele falls close to the autosomal gene VGLL3 (COUSMINER *et al.*, 2013, variation at this gene in humans also influences the timing of puberty). The left side of Figure 4.15 shows the age at sexual maturity in males. The allele (E) associated with slower sexual maturity is recessive in males. While the LL homozygotes mature on average a whole year later, the additive effect of the allele is weak while the L allele is rare in the population. The right panel shows the effect of the L allele in females. Note how the allele is much more dominant in females, and has a much more pronounced additive effect. The dominance of an allele is not a fixed property of the allele but rather a statement of the relationship of genotype to phenotype, such that the dominance relationship between alleles may vary across phenotypes and contexts (e.g. sexes).



The variance in the population phenotype due to these additive breeding values at locus  $\ell$ , assuming HW proportions, is

$$\begin{aligned}
 V_{A,\ell} &= p^2(2a_{\ell,2})^2 + 2pq(a_{\ell,1} + a_{\ell,2})^2 + q^2(2a_{\ell,0})^2 \\
 &= 2(pa_{\ell,1}^2 + qa_{\ell,2}^2) \\
 &= 2pq\alpha_{\ell}^2
 \end{aligned} \tag{4.24}$$

The total additive variance for the whole genotype can be found by

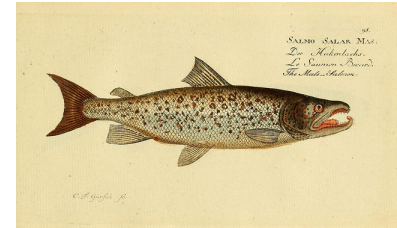


Figure 4.14: Atlantic Salmon (*Salmo salar*).

Histoire naturelle des poissons. 1796. Bloch, M. E. Image from the Biodiversity Heritage Library. Contributed by Ernst Mayr Library, Museum of Comparative Zoology. Not in copyright.

Figure 4.15: The average age at sexual maturity for each genotype, broken down by sex. The area of each circle is proportional to the fraction of the population in each genotypic class. The regression between phenotype and additive genotype is shown as a red line. Data from BARSON *et al.* (2015). Code here.

summing the individual additive genetic variances over loci

$$V_A = \sum_{\ell=1}^L V_{A,\ell} = \sum_{\ell=1}^L 2p_\ell q_\ell \alpha_\ell^2. \quad (4.25)$$

Having assigned the additive genetic variance to be the variance explained by the additive contribution of the alleles at a locus, we define the dominance variance as the population variance among genotypes at a locus due to their deviation from additivity. We can calculate how much each genotypic mean deviates away from its additive prediction at locus  $\ell$  (the length of the arrows in Figure 4.13). For example, the heterozygote deviates

$$d_{\ell,1} = \bar{X}'_{\ell,1} - (a_{\ell,1} + a_{\ell,2}) \quad (4.26)$$

away from its additive genetic value, with similar expressions for each of the homozygotes ( $d_{\ell,0}$  and  $d_{\ell,2}$ ). We can then write the dominance variance at our locus as the genotype-frequency weighted sum of our squared dominance deviations

$$V_{D,\ell} = p^2 d_{\ell,0}^2 + 2pq d_{\ell,1}^2 + q^2 d_{\ell,2}^2. \quad (4.27)$$

Writing our total dominance variance as the sum across loci

$$V_D = \sum_{\ell=1}^L V_{D,\ell}. \quad (4.28)$$

Having now partitioned all of the genetic variance into additive and dominant terms, we can write our total genetic variance as

$$V_G = V_A + V_D. \quad (4.29)$$

We can do this because by construction the covariance between our additive and dominant deviations for the genotypes is zero. We can define the narrow sense heritability as before  $h^2 = V_A/V_P = V_A/(V_G + V_E)$ , which is the proportion of phenotypic variance due to additive genetic variance. We can also define the total proportion of the phenotypic variance due to genetic differences among individuals, as the broad-sense heritability  $H^2 = V_G/(V_G + V_E)$ .

| Relationship (i,j)*           | $Cov(X_i, X_j)$   |
|-------------------------------|-------------------|
| parent-child                  | $1/2V_A$          |
| full siblings                 | $1/2V_A + 1/4V_D$ |
| identical (monozygotic) twins | $V_A + V_D$       |
| 1 <sup>st</sup> cousins       | $1/8V_A$          |

Table 4.1: Phenotypic covariance between some pairs of relatives, include the dominance variation. \* Assuming this is the only relationship the pair of individuals share (above that expected from randomly sampling individuals from the population).

When dominance is present in the loci influencing our trait ( $V_D > 0$ ), we need to modify our phenotype covariance among relatives to

account for this non-additivity. Specifically, our equation for the covariance among a general pair of relatives (eqn. 4.12 for additive variation) becomes

$$\text{Cov}(X_1, X_2) = 2F_{1,2}V_A + r_2V_D \quad (4.30)$$

where  $r_2$  is the probability that the pair of individuals share 2 alleles identical by descent, making the same assumptions (other than additivity) that we made in deriving eqn. 4.12. In table 4.1 we show the phenotypic covariance for some common pairs of relatives. The regression of offspring phenotype on parental midpoint still has a slope  $V_A/V_P$ .

Full sibs and parent-offspring have the same covariance if there is no dominance variance (as they have the same kinship coefficient  $F_{1,2}$ ). However, when dominance is present ( $V_D > 0$ ), full-sibs resemble each other more than parent-offspring pairs. That's because parents and offspring share precisely one allele, while full-sibs can share both alleles (i.e. the full genotype at a locus) identical by descent. We can attempt to estimate  $V_D$  by comparing different sets of relationships. For example, non-identical twins (full sibs born at same time) should have 1/2 the phenotypic covariance of identical twins if  $V_D = 0$ . Therefore, we can attempt to estimate  $V_D$  by looking at whether identical twins have more than twice the phenotypic covariance than non-identical twins.

The most important aspect of this discussion for thinking about evolutionary genetics is that the parent-offspring covariance is still only a function of  $V_A$ . This is because our parent (e.g. the mother) transmits only a single allele, at each locus, to its offspring. The other allele the offspring receives is random (assuming random mating), as it comes from the other unrelated parent (the father). Therefore, the average effect on the child's phenotype of an allele the child receives from their mother is averaged over all possible random alleles the child could receive from their father (weighted by their frequency in the population). Thus we only care about the additive effect of the allele, as parents transmit only alleles (not genotypes) to their offspring. This means that the short-term response to selection, as described by the breeder's equation, depends only on  $V_A$  and the additive effect of alleles. Therefore, if we can estimate the narrow-sense heritability we can predict the short-term response. However, if alleles display dominance, our value of  $V_A$  will change as alleles at our loci change in frequency, e.g. as dominant alleles become common in the population their contribution to  $V_A$  decreases. Therefore, if there is dominance our value of  $V_A$  will not be constant across generations.

Up to this point we have only considered dominance and not epistasis. However, we can include epistasis in a similar manner (for ex-

ample among pairs of loci). This gets a little tricky to think about, so we will only briefly explain it. We can first estimate the additive effect of the alleles by considering the effect of the alleles averaging over their possible genetic backgrounds (including the other interacting alleles they are possibly paired with), just as before. We can then calculate the additive genetic variance from this. We can estimate the dominance variance, by calculating the residual variance among genotypes at a locus unexplained by the additive effect of the loci. We can then estimate the epistatic variance by estimating the residual variance left unexplained among the two locus genotypes after accounting for the additive and dominant deviations calculated from each locus separately. In practice these high variance components are hard to estimate, and usually small as much of our variance is assigned to the additive effect. Again we would find that we mostly care about  $V_A$  for predicting short-term evolution, but that the contribution of loci to the additive genetic variance will depend on the epistatic relationships among loci.

**Question 5.** How could you use 1/2 sibs vs. full-sibs to estimate  $V_D$ ? Why might this be difficult in practice? Why are identical vs. non-identical twins better suited for this?

**Question 6.** Can you construct a case where  $V_A = 0$  and  $V_D > 0$ ? You need just describe it qualitatively; you don't need to work out the math. (tricker question).



# 5

## *The Response to Phenotypic Selection*

Evolution by natural selection requires:

1. Variation in a phenotype
2. That survival is non-random with respect to this phenotypic variation.
3. That this variation is heritable.

Points 1 and 2 encapsulate our idea of Natural Selection, but evolution by natural selection will only occur if the 3rd condition is also met.

<sup>1</sup> It is the heritable nature of variation that couples change within a generation due to natural selection to change across generations (evolutionary change).

Let's start by thinking about the change within a generation due to directional selection, where selection acts to change the mean phenotype within a generation. For example, a decrease in mean height within a generation, due to taller organisms having a lower chance of surviving to reproduction than shorter organisms. Specifically, we'll denote our mean phenotype at reproduction by  $\mu_S$ , i.e. after selection has acted, and our mean phenotype before selection acts by  $\mu_{BS}$ . This second quantity may be hard to measure, as obviously selection acts throughout the life-cycle, so it might be easier to think of this as the mean phenotype if selection hadn't acted. So the change in mean phenotype within a generation is  $\mu_S - \mu_{BS} = S$ .

We are interested in predicting the distribution of phenotypes in the next generation. In particular, we are interested in the mean phenotype in the next generation to understand how directional selection has contributed to evolutionary change. We'll denote the mean phenotype in offspring, i.e. the mean phenotype in the next generation before selection acts, as  $\mu_{NG}$ . The change across generations we'll call the response to selection  $R$  and put this equal to  $\mu_{NG} - \mu_{BS}$ .

The mean phenotype in the next generation is

$$\mu_{NG} = \mathbb{E}(\mathbb{E}(X_{kid}|X_{mom}, X_{dad})) \quad (5.1)$$

See LEWONTIN (1970). Note that these requirements are not specific to DNA, i.e. the concept of evolution by natural selection is substrate independent.

<sup>1</sup> Some people consider natural selection to only operate on heritable phenotype variation and so require all three conditions to say that natural selection occurs. This is mostly a semantic point, however, it is useful to be able to distinguish the action of selection from a possible response.

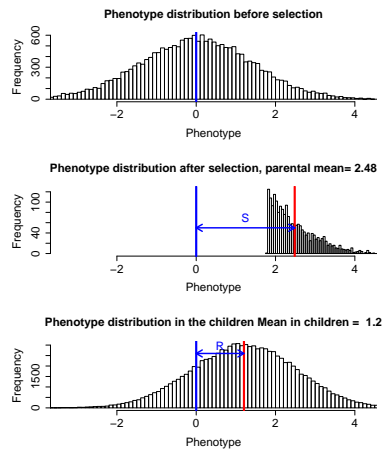


Figure 5.1: **Top.** Distribution of a phenotype in the parental population prior to selection,  $V_A = V_E = 1$ . **Middle.** Only individuals in the top 10% of the phenotypic distribution are selected to reproduce; the resulting shift in the phenotypic mean is  $S$ . **Bottom.** Phenotypic distribution of children of the selected parents; the shift in the mean phenotype is  $R$ . Code here.

where the outer expectation is over possible pairs of randomly mating individuals who survive to reproduce. We can use eqn. 4.14 to obtain an expression for this expectation:

$$\mu_{NG} = \mu_{BS} + \beta_{mid,kid}(\mathbb{E}(X_{mid}) - \mu_{BS}) \quad (5.2)$$

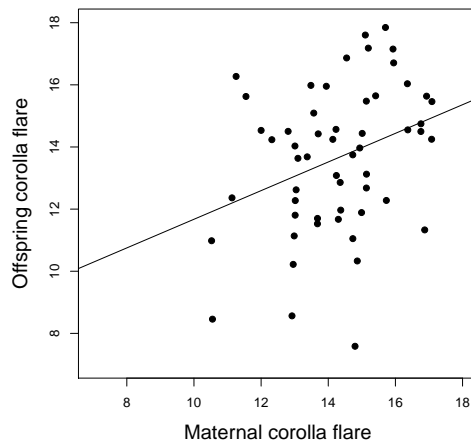
So to obtain  $\mu_{NG}$  we need to compute  $\mathbb{E}(X_{mid})$ , the expected mid-point phenotype of pairs of individuals who survive to reproduce. Well this is just the expected phenotype in the individuals who survived to reproduce ( $\mu_S$ ), so

$$\mu_{NG} = \mu_{BS} + h^2(\mu_S - \mu_{BS}) \quad (5.3)$$

So we can write our response to selection as

$$R = \mu_{NG} - \mu_{BS} = h^2(\mu_S - \mu_{BS}) = h^2S \quad (5.4)$$

So our response to selection is proportional to our selection differential, and the constant of proportionality is the narrow sense heritability. This equation is sometimes termed the Breeder's equation. It is a statement that the evolutionary change across generations ( $R$ ) is proportional to the change caused by directional selection within a generation ( $S$ ), and that the strength of this relationship is determined by the narrow sense heritability ( $h^2$ ).



**Question 1.** GALEN (1996) explored selection on flower shape in *P. viscosum*. She found that plants with larger corolla flare had more bumblebee visits, which resulted in higher seed set and a 17% increase in corolla flare in the plants contributing to the next generation. Based on the data in the caption of Figure 5.3 what is the expected response in the next generation?

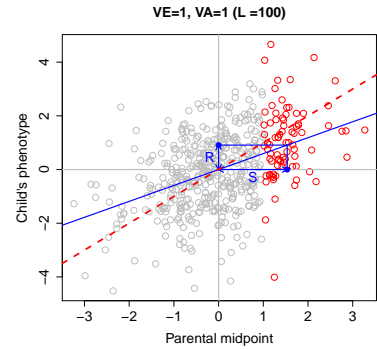


Figure 5.2: A visual representation of the Breeder's equation. Regression of child's phenotype on parental midpoint phenotype ( $V_A = V_E = 1$ ). Under truncation selection, only individuals with phenotypes  $> 1$  (red) are bred. Code here.

Figure 5.3: The relationship between maternal and offspring corolla flare (flower width) in *P. viscosum*. From GALEN's data the covariance of mother and child is 1.3, while the variance of the mother is 2.8. Data from GALEN (1996). Code here.



Figure 5.4: Sticky jacob's ladder (*Polemonium viscosum*). Flowers of Mountain and Plain (1920). Clements, E. Image from the Biodiversity Heritage Library. Contributed by New York Botanical Garden, Mertz Library. Not in copyright. Cropped from original.

To understand the genetic basis of the response to selection take a look at Figure 5.5. The setup is the same as in our previous simulation figures. The individuals who are selected to form our next

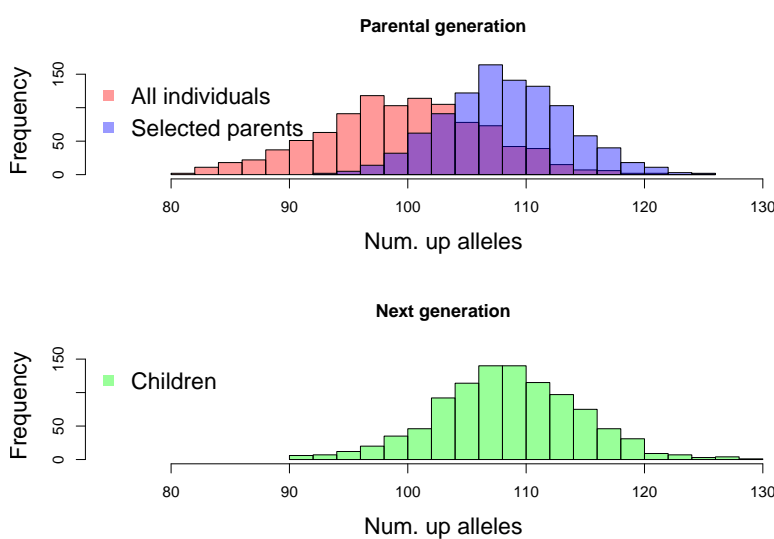


Figure 5.5: **Top.** Distribution of the number of up alleles in the parental population prior to selection (red), for the selected individuals the top 10% of the population (blue) **Bottom.** The same distribution for the offspring of the selected parents in the next generation (green). Code here.

generation carry more alleles that increase the phenotype, in the current range of environments currently experienced by the population. The average individual before selection carried 100 of these ‘up’ alleles, the average individual surviving selection 108 ‘up’ alleles. As individuals faithfully transmit their alleles to the next generation the average child of the selected parents carries 108 up alleles. Note that the variance has changed little, the children have plenty of variation in their genotype, such that selection can readily drive evolution in future generations. The average frequency of an ‘up’ allele has changed from 50% to 54%. Our gains due to selection will be stably inherited to future generations.

*The long-term response to selection* If our selection pressure is sustained over many generations, we can use our breeder’s equation to predict the response. If we are willing to assume that our heritability does not change and we maintain a constant selection gradient, then after  $n$  generations our phenotype mean will have shifted

$$nh^2S \quad (5.5)$$

i.e. our population will keep up a linear response to selection.

**Question 2.** A population of red deer were trapped on Jersey (an island off of England) during the last inter-glacial period. From the

fossil record <sup>2</sup> we can see that the population rapidly adapted to their new conditions. Within 6,000 years they evolved from an estimated mean weight of the population of 200kg to an estimated mean weight of 36kg (a 6 fold reduction)! You estimate that the generation time of red deer is 5 years and, from a current day population, that the narrow sense heritability of the phenotype is 0.5.

**A)** Estimate the mean change per generation in the mean body weight.

**B)** Estimate the change in mean body weight caused by selection within a generation. State your assumptions.

**C)** Assuming we only have fossils from the founding population and the population after 6000 years, should we assume that the calculations accurately reflect what actually occurred within our population?

*Alternative formulations of the Breeder's equation.* A change in mean phenotype within a generation occurs because of the differential fitness of our organisms. To think more carefully about this change within a generation, let's think about a simple fitness model where our phenotype affects the viability of our organisms (i.e. the probability they survive to reproduce). The probability that an individual has a phenotype  $X$  before selection is  $p(X)$ , so that the mean phenotype before selection is

$$\mu_{BS} = \mathbb{E}[X] = \int_{-\infty}^{\infty} xp(x)dx \quad (5.6)$$

The probability that an organism with a phenotype  $X$  survives to reproduce is  $w(X)$ , and we'll think about this as the fitness of our organism. The probability distribution of phenotypes in those who do survive to reproduce is

$$\mathbb{P}(X|\text{survive}) = \frac{p(x)w(x)}{\int_{-\infty}^{\infty} p(x)w(x)dx}. \quad (5.7)$$

where the denominator is a normalization constant which ensures that our phenotypic distribution integrates to one. The denominator also has the interpretation of being the mean fitness of the population, which we'll call  $\bar{w}$ , i.e.

$$\bar{w} = \int_{-\infty}^{\infty} p(x)w(x)dx. \quad (5.8)$$

Therefore, we can write the mean phenotype in those who survive to reproduce as

$$\mu_S = \frac{1}{\bar{w}} \int_{-\infty}^{\infty} xp(x)w(x)dx \quad (5.9)$$

<sup>2</sup> LISTER, A., 1989 Rapid dwarfing of red deer on Jersey in the last interglacial. *Nature* 342(6249): 539

If we mean center our population, i.e. set the phenotype before selection to zero, then

$$S = \frac{1}{\bar{w}} \int_{-\infty}^{\infty} xp(x)w(x)dx \quad (5.10)$$

Inspecting this more closely, we can see that  $S$  has the form of a covariance between our phenotype  $X$  and our fitness  $w(X)$  ( $S = Cov(X, w(X))$ ). Thus our change in mean phenotype is directly a measure of the covariance of our phenotype and our fitness. Rewriting our breeder's equation using this observation we see

$$R = \frac{V_A}{V} Cov(X, w(X)) \quad (5.11)$$

we see that the response to selection is due to the fact that our fitness (viability) of our organisms/parents covaries with our phenotype, and that our child's phenotype is correlated with our parent's phenotype.

The phenotype-fitness covariance divided by the phenotypic variance,  $Cov(X, w(X))/V$ , is the slope of the linear regression of phenotype on fitness. Let's call this slope the fitness gradient and denote it by  $\beta$ . Then, equivalently, we can write the breeder's equation as

$$R = V_A \beta \quad (5.12)$$

i.e. we'll see a directional response to selection if there is a linear relationship of phenotype on fitness, and if there is additive genetic variance for the phenotype.

As one example of a fitness gradient, in Figure 5.7 the lifetime reproductive success (LRS) of male Red Deer is plotted against the weight of their antlers. The red line gives the linear regression of fitness (LRS) on antler mass and the slope of this line is the fitness gradient ( $\beta$ ).

### 5.0.1 The response of multiple traits to selection, the multivariate breeder's equation.

We can generalize these results for multiple traits, to ask how selection on multiple phenotypes plays out over short time intervals.<sup>3</sup> Considering two traits we can write our responses in both traits as

$$\begin{aligned} R_1 &= V_{A,1}\beta_1 + V_{A,1,2}\beta_2 \\ R_2 &= V_{A,2}\beta_2 + V_{A,1,2}\beta_1 \end{aligned} \quad (5.13)$$

where the 1 and 2 index our two different traits. Here  $V_{A,1,2}$  is our additive covariance between our traits. Our selection gradient for trait 1,  $\beta_1$ , represents the change in fitness changing trait 1 alone holding



Figure 5.6: Red deer (*Cervus elaphus*).

British mammals. Thorburn, A. (1920) Image from the Biodiversity Heritage Library. Contributed by Field Museum of Natural History Library. Licensed under CC BY-2.0.

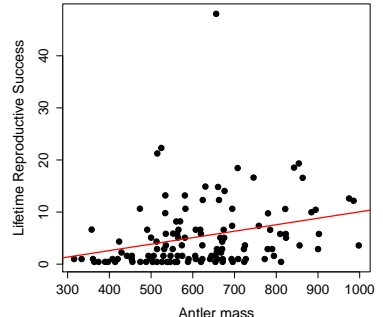


Figure 5.7: Lifetime reproductive success (LRS) of male Red Deer as a function of their antler mass. Data from KRUUK *et al.* (2002), see the paper for discussion of the complexities of equating this selection gradient with the evolutionary response. Code here..

<sup>3</sup> LANDE, R., 1979 Quantitative genetic analysis of multivariate evolution, applied to brain: body size allometry. Evolution 33(1Part2): 402–416

everything else constant. This is a statement that our response in any one phenotype is modified by selection on other traits that covary with that trait. This offers a good way to think about how genetic trade offs play out over short-term evolution.

We can also write this in matrix form. We can write our change in the mean of our multiple phenotypes within a generation as the vector  $\mathbf{S}$  and our response across multiple generations as the vector  $\mathbf{R}$ . These two quantities are related by

$$\mathbf{R} = \mathbf{GV}^{-1}\mathbf{S} = \mathbf{G}\boldsymbol{\beta} \quad (5.14)$$

where  $\mathbf{V}$  and  $\mathbf{G}$  are our matrices of the variance-covariance of phenotypes and additive genetic values (eqn. (4.19) (4.18)) and  $\boldsymbol{\beta}$  is a vector of selection gradients (i.e. the change within a generation as a fraction of the total phenotypic variance).

**Question 3.** You collect observations of red deer within a generation, recording an individual's number of offspring and phenotypes for a number of traits which are known to have additive genetic variation. Using your data, you construct the plots shown in Figure 5.8 (standardizing the phenotypes). Answer the following questions by choosing one of the bold options. Briefly justify each of your answers with reference to the breeder's equation and multi-trait breeder's equation.

**A)** Looking just at figure 5.8 A, in what direction do you expect male antler size to evolve?

**Insufficient information, increase, decrease.**

**B)** Looking just at figures 5.8 B and C, in what direction do you expect male antler size to evolve?

**Insufficient information, increase, decrease.**

**C)** Looking at figures 5.8 A, B, and C, in what direction do you expect male antler size to evolve?

**Insufficient information, increase, decrease.**

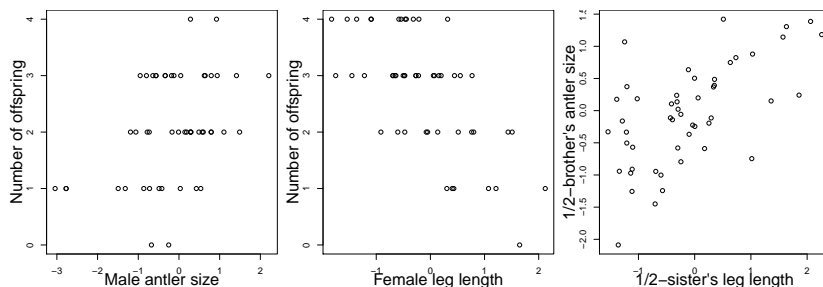


Figure 5.8: Observations of red deer within a generation; recording an individual's number of offspring and phenotypes (simulated data), which are known to have additive genetic variation. The figures left to right are A-C. (Data are simulated. Code here.)

As an example of correlated responses to selection, consider the WILKINSON (1993) selection experiment on Stalk-eyed flies (*Cryptodiopsis dalmanni*). Stalk-eyed flies have evolved amazingly long

eye-stalks. In the lab, WILKINSON established six populations of wild-caught flies and selected up and down on males eye-stalk to body size ratio for 10 generations (left plot in Figure 5.9). Despite the fact that he did not select on females, he saw a correlated response in the females from each of the lines (right plot), because of the genetic correlation between male and female body proportions.

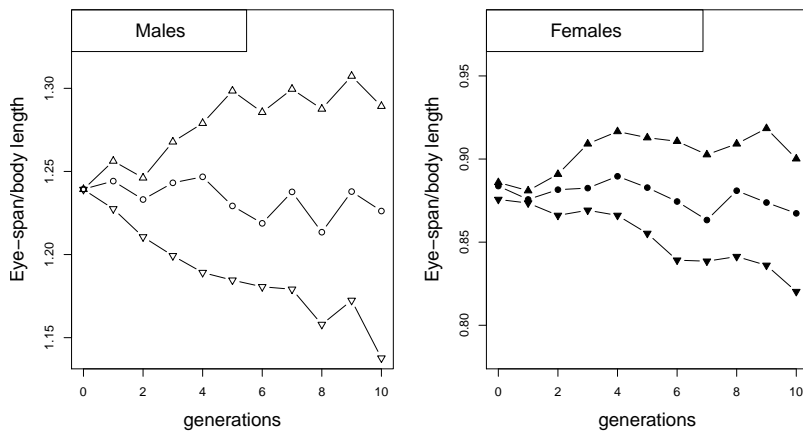


Figure 5.9: WILKINSON selected two of populations for flies for increased and eye-stalk to body length ratio in males (mean shown as up triangles), and two for a decreased ratio (down triangles), by taking the top 10 males with the highest (lowest) ratio out of 50 measures. He also established two control populations (circles). He constructed each generation of females by sampling 10 at random from each population. Data from WILKINSON (1993). Code here.

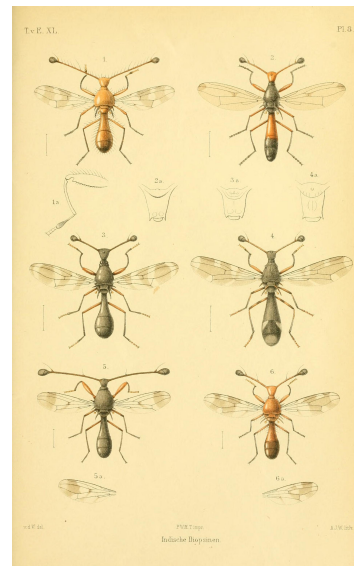


Figure 5.10: Stalk-eyed Flies (*Diopsidae*).  
Diptera. van der Wulp. 1898. Image from the Biodiversity Heritage Library. Contributed by Smithsonian Libraries. Not in copyright.

#### Question 4.

At the end of ten generations in WILKINSON's experiment (Figure 5.9), the males from the up- and down-selected lines had mean eye-stalk to body ratios of 1.29 and 1.14 respectively, while the females from the up- and down-selected lines had means of 0.9 and 0.82.

A) WILKINSON estimated that by selecting the top/bottom 10 males, he had on average shifted the mean body ratio by 0.024 within each generation. What is the male heritability of eye-stalk to body-length ratio?

B) Assume that the additive genetic variance of male and female phenotypes are equal and that there is no direct selection on female body-proportion in this experiment, i.e. that all of the response in females is due to correlated selection. Can you estimate the male-female genetic correlation of the eye-stalk ratio?

### 5.1 Some applications of the multivariate trait breeder's equation

The multivariate breeders equation has a lot of different uses in understanding the response of multiple traits to selection. It also offers some insights into kin selection and sexual selection. We'll discuss these

next.

#### *Hamilton's Rule and the evolution of altruistic and selfish behaviours*

Individuals frequently behave in ways that sacrifice their own fitness for the benefit of others. That selection favours such apparent acts of altruism is puzzling at first sight. HAMILTON (1964a,b) supplied the first general evolutionary explanation of such altruism. His intuition was that while an individual is losing out of some reproductive output, the alleles underlying an altruistic behaviour can still spread in the population if this cost is outweighed by benefits gained through the transmission of these alleles through a related individual. Note that this means that the allele is not acting in an self-sacrificing manner, even though individuals may act as a result.

Altruism reflects social interactions. So as a simple model let's imagine that individuals interact in pairs, with our focal individual  $i$  being paired with an individual  $j$ . This could be pairs of siblings interacting. Imagine that individuals have two possible phenotypes  $X = 1$  or  $0$ , corresponding to providing or withholding some small act of 'altruism' (we could just as easily flip these labels and call them an unselfish act and a selfish act respectively). Our pairs of individuals interacting could, for example, be siblings sharing a nest. The altruistic trait could be as simple as growing at a slightly slower rate so as to reducing sibling-competition for food from parents, or more complicated acts of altruism such as children foregoing their own reproduction so as to help their parents raise their siblings.

Providing the altruistic act has a cost  $C$  to the fitness of our individual and failing to provide this act has no cost. Receiving this altruistic act confers a fitness benefit  $B$  over individuals who did not receive this act. HAMILTON's rule states that such a trait will spread through the population if

$$2FB > C \quad (5.15)$$

where  $F$  is the average kinship coefficient between the interacting individuals ( $i$  and  $j$ ). In the usual formulation of Hamilton's Rule our  $2F$  is replaced by the 'Coefficient of relationship', which is the proportion of alleles shared between the individuals. Here we use two times the kinship coefficient to keep things inline with our notation for these chapters. Note that if our individuals are themselves inbred we need to do a little more careful to reconcile these two measures. So the altruistic behaviour will spread even if it is costly to the individual if its cost is paid off by the benefit to sufficiently related individuals.

As one example of kin-selection consider KRAKAUER (2005)'s work on co-operative courtship in wild turkeys (*Meleagris gallopavo*). Male turkeys often form display partnerships, with a subordinate male

MAYNARD SMITH (1964) coined the name kin selection to describe Hamilton's approach to this problem. It's also sometimes called the inclusive fitness approach, as we need to include not just one individual's fitness but the weighted sum of all the fitness of all their relatives.

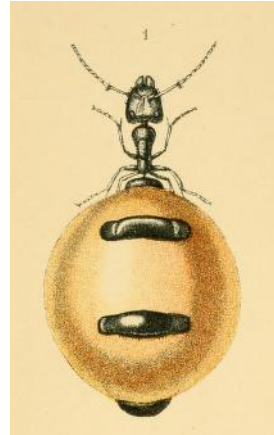


Figure 5.11: Australian Honey-pot Ant (*Camponotus inflatus*). Honey ants are gorged with honeydew collected by their nest mates, till they swell to the size of grapes, and used as a food storage device.  
Ants, bees, and wasps: a record of observations on the habits of the social Hymenoptera (1897) Lubbock, J. Image from the Biodiversity Heritage Library. Contributed by Smithsonian Libraries. Not in copyright.

helping a dominant male with displaying to females and defending the females from other groups of males.

These pairs are often full brothers ( $F = 0.25$ ), with the subordinate male often being the younger of the two. The subordinate male often loses out on mating opportunities over their entire lifetime by acting as a wingman to their older brothers. KRAKAUER (2005) estimated that dominant males gained an extra 6.1 offspring when they display with a partner than males who display alone. While the subordinate males lose out on fathering 0.9 offspring compared to solitary males. Thus the costs of helping by subordinate males is more than compensated by the fitness gains of their brothers ( $(2 \times 0.25) \times 6.1 > 0.9$ ), and so the evolution of this altruistic helping in co-operative courtship is potentially well explained by kin-selection (see AKÇAY and VAN CLEVE, 2016, for more analysis).

**Question 5.** How would this answer be changed if the male Turkey partnerships were only  $1/2$  sibs, or first cousins?

Where does this result come from? Well, we can use our quantitative genetics framework to gain some intuition by deriving a simple version of Hamilton's Rule by thinking about the phenotypes of an individual's kin as genetically correlated phenotypes. To sketch a proof of this result, let's assume that our focal  $i$  individual's fitness can be written as

$$W(i, j) = W_0 + W_i + W_j \quad (5.16)$$

where  $W_i$  is the contribution of the fitness of the individual  $i$  due to their own phenotype, and  $W_j$  is the contribution to our individual  $i$ 's fitness due to the interacting individual  $j$ 's behaviour (i.e.  $j$ 's phenotype). With the benefit  $B$  and cost  $C$ , our  $W(i, j)$  are depicted in Figure 5.13.

Following our multivariate breeder's equation, we can write the expected change of our behavioural phenotype as

$$R = \beta_i V_A + \beta_j V_{A,i,j}, \quad (5.17)$$

Our altruistic phenotype is increasing in the population if  $R > 0$ , i.e. if

$$\beta_i V_A + \beta_j V_{A,i,j} > 0 \quad (5.18)$$

The slope  $\beta_i$  of the regression of our focal individual's behavioural phenotype on fitness is proportional to  $-C$ . The slope  $\beta_j$  of the regression of our interacting partner's phenotype on our focal individual's fitness is proportional to  $B$  (with the same constant of proportionality). Therefore, our altruistic phenotype is increasing in the



Figure 5.12: Turkey (*Meleagris gallopavo*).  
Bilder-atlas zur Wissenschaftlich-populären Naturgeschichte der Vögel in ihren sämtlichen Hauptformen (1864). Wien,K.K. Hof Image from the Biodiversity Heritage Library.  
Contributed by Smithsonian Libraries. Not in copyright.

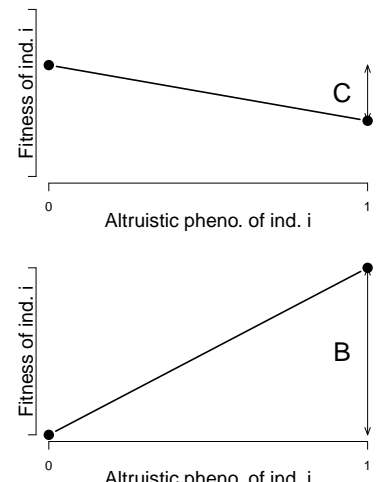


Figure 5.13: **Top)** The fitness of individual  $i$  as a function of their behavioural phenotype, where altruistic/non-altruistic behavioural phenotypes are encoded as 1 and 0 respectively. The direct fitness cost of behaving altruistically is  $C$ . **Bottom)** The fitness of our focal individual  $i$  as a function of the behavioural phenotype of their interacting partner ( $j$ ). Our focal individual gets an increase  $B$  in fitness if their partner behaves altruistically. Code here.

Here we've following a simplified version of QUELLER (1992)'s treatment, to re-derive Hamilton's rule in a quantitative genetics framework (Hamilton's original papers did this in a population genetics framework).

population if

$$\begin{aligned} \beta_i V_A + \beta_j V_{A,i,j} &> 0 \\ B \frac{V_{A,i,j}}{V_A} &> C \end{aligned} \quad (5.19)$$

So what's the average genetic covariance between individual  $i$  and  $j$ 's altruistic phenotype? Well it's the same behavioural phenotype in both individuals, so the phenotypes are genetically correlated if our individuals are related to each other. The covariance of the same phenotype between two individuals is just  $2F_{i,j}V_A$  (see (4.12)). So our altruistic phenotype is increasing in the population if

$$\begin{aligned} B \frac{2F_{i,j}V_A}{V_A} &> C \\ 2F_{i,j}B &> C \end{aligned} \quad (5.20)$$

Seen from this perspective, HAMILTON's rule is simply a statement that altruistic behaviours can spread via kin-selection, if the average cost to an individual of carrying altruistic alleles is paid back through the average benefit of interacting with altruistic relatives (kin)

*Sexual selection and the evolution of mate preference by indirect benefits.* Organisms often put an enormous effort into finding and attracting mates, sometimes at a considerable cost to their chances of survival. Why are individuals so choosy about who they mate with, particularly when their choice seems to be based on elaborate characters and arbitrary displays that surely lower the viability of their mates?

One major reason why individuals evolve to be choosy about who they mate with is that it can directly impact their fitness. By choosing a mate with particular characteristics, individuals can gain more parental care for their offspring, avoid parasites, or be choosing a mate with higher fertility. For example, female glow-worms flash at night to attract males flying by. Females with larger, brighter lanterns have higher fecundity, so males with a preference for brighter flashes will gain a direct benefit to their own fitness. (Note that males will benefit even if these differences in female fecundity are entirely driven by differences in environment, and so non-heritable.) Indeed male glow worms have evolved to be attracted to brighter flashing lures.

However, even in the absence of direct benefits of choice, selection can still indirectly favour the evolution of choosiness. These indirect benefits occur because individuals can have higher fitness offspring by choosing a mate whose phenotype indicates high viability (the so-called good genes hypothesis), or by choosing a mate whose phenotype is simply attractive, and likely to produce similarly attractive offspring (the 'runaway' or sexy sons hypothesis).

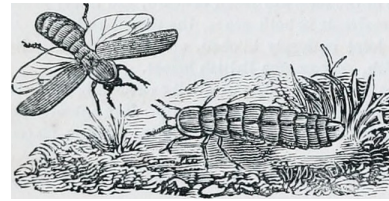


Figure 5.14: Male (left) and female (right) common glow worm (*Lampyris noctiluca*).  
The animal kingdom : arranged after its organization; forming a natural history of animals, and an introduction to comparative anatomy. (1863) Cuvier, G. Image from the Biodiversity Heritage Library. Contributed by University of Toronto - Gerstein Science Information Centre. Not in copyright.

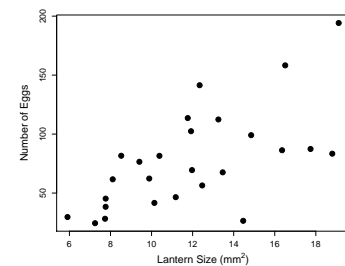


Figure 5.15: Female Glow worms who have the largest, and therefore brightest, lanterns have the highest fecundity. Data from HOPKINS *et al.* (2015). Code here.

We'll denote a display trait, e.g. tail length, in males by  $\sigma$  and a preference trait in females by  $\varphi$ . Our display trait is under direct selection in males, such that its response to selection can be written as

$$R_{\sigma} = \beta_{\sigma} V_{A,\sigma} \quad (5.21)$$

Let's assume that the female preference trait, the degree to which females are attracted to long tails, is not under direct selection  $\beta_{\varphi} = 0$ . Then the response to selection of the preference trait can be written as

$$R_{\varphi} = \beta_{\varphi} V_{A,\varphi} + \beta_{\sigma} V_{A,\varphi\sigma} = \beta_{\sigma} V_{A,\varphi\sigma} \quad (5.22)$$

So the female preference will respond to selection if it is genetically correlated with the male trait, i.e. if  $V_{A,\varphi\sigma}$  is not zero. There's a number of different ways this genetic correlation could arise; the simplest is that the loci underlying the male trait may have a pleiotropic effect on female preference. However, female preference may often have quite a distinct genetic basis from male display traits.

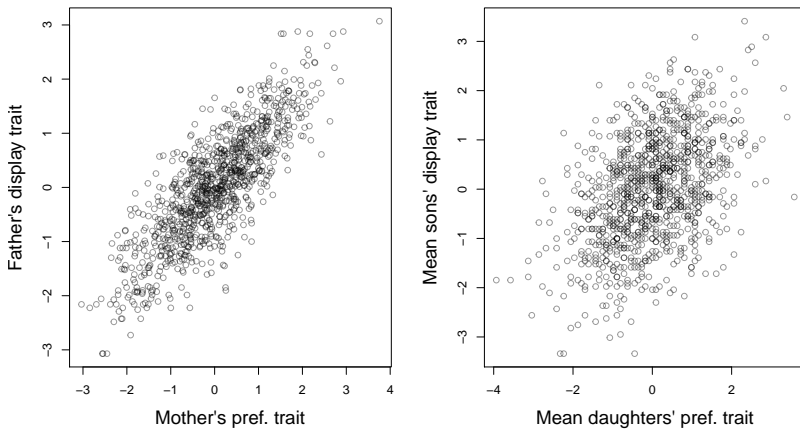


Figure 5.16: **Left)** Assortative mating between males and females. Males vary in a display trait (e.g. tail length), females vary in their preference for this trait. We see evidence of assortative mating as females with a preference for a particular value of the male trait tend to mate with those males. **Right)** As both male trait and female preference are genetic this establishes a genetic correlation in the next generation. This is simulated data. Code here.

A more general way in which trait-preference genetic correlations may arise is through assortative mating. As females vary in their tail-length preference, the ones with a preference for longer tails will mate with long-tailed males and the opposite for females with a preference for shorter-tails. Therefore, a genetic correlation between mates display and preference traits will become established (see Figure 5.16).

The males with the longer tails will also carry the alleles associated with the preference for longer tails, as their long-tailed dads tended to mate with females with a genetic preference for long tails. Similarly, the males with shorter tails will carry alleles associated with the preference for shorter tails. Thus if there is direct selection for

males with longer tails, then the female preference for longer tails will increase too, as it is genetically correlated via assortative mating.

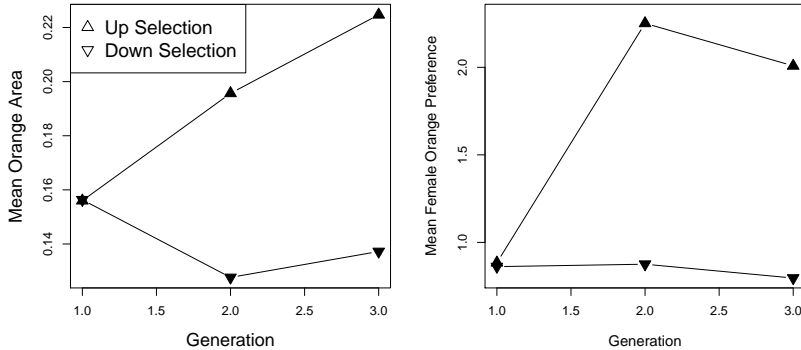


Figure 5.17: Mean phenotypes for the two up- and two down-selected populations of Guppies. Left panel: A response to selection was seen due to the direct selection on male colouration. Right panel: An indirect, correlated response was also seen in female preference. Data from HOUDE (1994). Code here.

As an example of how direct selection on display traits can drive the evolution of preference traits, let's consider some data from guppies. Guppies (*Poecilia reticulata*) are a classic system for studying the interplay of natural and sexual selection. In some populations of guppies, females show a preference for males with more orange colouration.

HOUDE established four replicate population pairs of guppies and selected one of each pair for an increased or decreased orange coloration in males, selecting the top/bottom 20 out of 50 males. She randomly chose females from each population to form the next generation, and so did not exert direct selection on females. She measured the response to selection on male colouration and on female preference for orange (left and right panels of Figure 5.1 respectively). In the lines that were selected for more orange males females showed an increased preference for orange. While in those lines that she selected males for less orange in their display females showed a decreased preference for orange. This is consistent with indirect selection on female orange preference as a response to selection on male colouration, due to a genetic correlation between female preference and male trait. It is *a priori* unlikely that pleiotropy is the source of the genetic correlation between these traits, rather it is likely caused by females assortative mating with males that match their colour preference.

Returning to our bird tail example, what could drive the direct selection on male tail length? The selection for longer tails in males could come about because longer tails are genetic correlated with higher male viability, for example perhaps only males who gather an excess of food have the resources to invest in growing long tail, i.e. a long tail is an honest signal. This would be a good genes explanation



Figure 5.18: Guppy (*Poecilia reticulata*).

From a set of 1962 stamps of Hungary. Contributed to wikimedia by Darjac, not covered by copyright

of female mate choice evolution.

There's another subtler way that selection could favour our male trait. Imagine that the variation in female preference trait is because some females have no strong preference for the male-tail length, but some females have a strong preference for males with longer tails. Males with longer tails would then have higher fecundity than the short-tailed males as there's a subset of females who are strongly attracted to long tails, and these males also get to mate with the other females. Thus selection favours long-tailed males, and so indirectly favours female preference for longer tails; females with a preference for longer-tails have sons who in turn who are more attractive. This model is sometimes called the sexy-son model. It is also called the Fisherian runaway model (FISHER, 1915), as female preference and male trait can coevolve in an escalating fashion driving more and more extreme preferences for arbitrary traits. Thus many extravagant display traits in males and females may exist purely because individuals find them beautiful and are attracted to them.

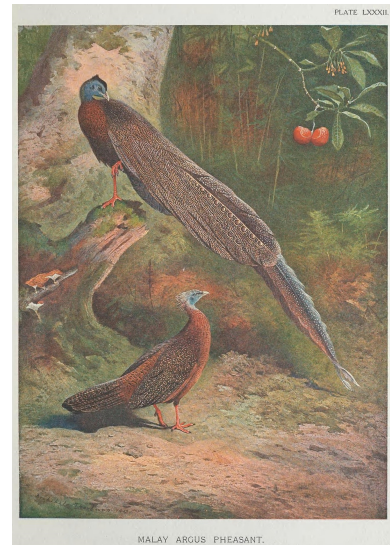


Figure 5.19: Argus Pheasant.  
A monograph of the pheasants. (1918). Beebe, W. Image from the Biodiversity Heritage Library. Contributed by Smithsonian Institution Libraries. Licensed under CC BY-2.0.

“The case of the male Argus Pheasant is eminently interesting, because it affords good evidence that the most refined beauty may serve as a sexual charm, and for no other purpose.” – DARWIN (1888)



# 6

## *One-Locus Models of Selection*

"Socrates consisted of the genes his parents gave him, the experiences they and his environment later provided, and a growth and development mediated by numerous meals. For all I know, he may have been very successful in the evolutionary sense of leaving numerous offspring. His phenotype, nevertheless, was utterly destroyed by the hemlock and has never since been duplicated. The same argument holds also for genotypes. With Socrates' death, not only did his phenotype disappear, but also his genotype.[...] The loss of Socrates' genotype is not assuaged by any consideration of how prolifically he may have reproduced. Socrates' genes may be with us yet, but not his genotype, because meiosis and recombination destroy genotypes as surely as death." –WILLIAMS (1966)

Individuals are temporary, their phenotypes are temporary, and their genotypes are temporary. However, the alleles that individuals transmit across generations have permanence. Sustained phenotypic evolutionary change due to natural selection occurs because of changes in the allelic composition of the population. To understand these changes, we need to understand how the frequency of alleles (genes) changes over time due to natural selection.

As we have seen, natural selection occurs when there are differences between individuals in fitness. We may define fitness in various ways. Most commonly, it is defined with respect to the contribution of a phenotype or genotype to the next generation. Differences in fitness can arise at any point during the life cycle. For instance, different genotypes or phenotypes may have different survival probabilities from one stage in their life to the stage of reproduction (viability), or they may differ in the number of offspring produced (fertility), or both. Here, we define the absolute fitness of a genotype as the expected number of offspring of an individual of that genotype. Differences in fitness among genotypes drive allele frequency change. In this chapter we'll study the dynamics of alleles at a single locus. In this chapter we'll ignore the effects of genetic drift, and just study the deterministic dynamics of selection. We'll return to discuss the interaction of

selection and drift in the next chapter.

### 6.0.1 Haploid selection model

We start out by modeling selection in a haploid model, as this is mathematically relatively simple. Let the number of individuals carrying alleles  $A_1$  and  $A_2$  in generation  $t$  be  $P_t$  and  $Q_t$ . Then, the relative frequencies at time  $t$  of alleles  $A_1$  and  $A_2$  are  $p_t = P_t/(P_t + Q_t)$  and  $q_t = Q_t/(P_t + Q_t) = 1 - p_t$ . Further, assume that individuals of type  $A_1$  and  $A_2$  on average produce  $W_1$  and  $W_2$  offspring individuals, respectively. We call  $W_i$  the absolute fitness.

Therefore, in the next generation, the absolute number of carriers of  $A_1$  and  $A_2$  are  $P_{t+1} = W_1 P_t$  and  $Q_{t+1} = W_2 Q_t$ , respectively. The mean absolute fitness of the population at time  $t$  is

$$\bar{W}_t = W_1 \frac{P_t}{P_t + Q_t} + W_2 \frac{Q_t}{P_t + Q_t} = W_1 p_t + W_2 q_t, \quad (6.1)$$

i.e. the sum of the fitness of the two types weighted by their relative frequencies. Note that the mean fitness depends on time, as it is a function of the allele frequencies, which are themselves time dependent.

As an example of a rapid response to selection on an allele in a haploid population, we can consider some data on the evolution of drug resistant viruses. FEDER *et al.* (2017) studied viral dynamics in a macaque infected with a strain of simian immunodeficiency virus (SHIV) that carries the HIV-1 reverse transcriptase coding region. The viral load of the macaque's blood plasma is shown as a black line in Figure 6.1. Twelve weeks after infection, the macaque was treated with an anti-retroviral drug that targeted the the virus' reverse transcriptase protein. Note how the viral load initially starts to drop once the drug is administered, suggesting that the absolute fitness of the original strain is less than one ( $W_2 < 1$ ) in the presence of the drug (as their numbers are decreasing). However, the viral population rebounds as a mutation that confers drug resistance to the anti-retroviral drug arises in the SHIV and starts to spread. Viruses carrying this mutation (let's call them allele 1) likely have absolute fitness  $W_1 > 1$ . The frequency of the drug-resistant allele is shown in red; it quickly spreads from being undetectable in week 13, to being fixed in the SHIV population in week 20.

The rapid spread of this drug-resistant allele through the population is driven by the much greater relative fitness of the drug-resistant allele over the original strain in the presence of the anti-retroviral drug.

The main focus of FEDER *et al.*'s work was modeling the complicated spatial dynamics of drug-resistant SHIV adaptation in different organ systems.

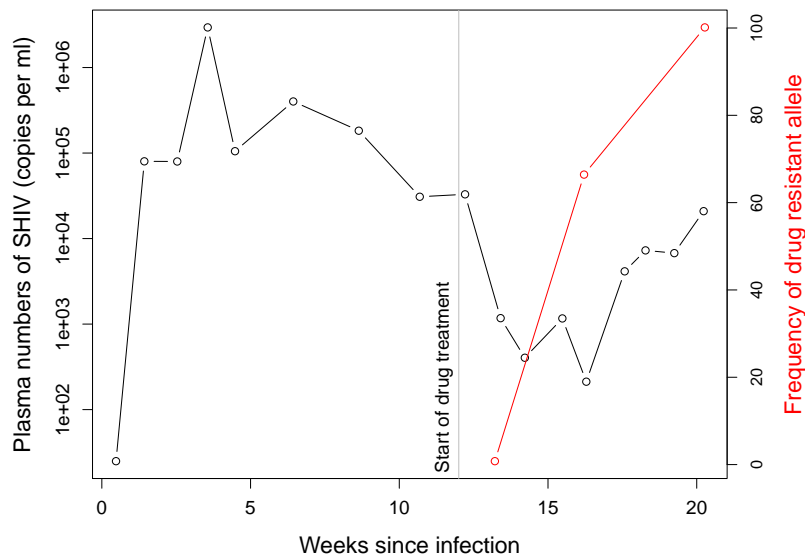


Figure 6.1: The rapid evolution of drug-resistant SHIV. The viral load of SHIV in the blood of a macaque (black line), the frequency of a drug resistance mutation (red line). Data from FEDER *et al.* (2017). Code here.

The frequency of allele  $A_1$  in the next generation is given by

$$p_{t+1} = \frac{P_{t+1}}{P_{t+1} + Q_{t+1}} = \frac{W_1 P_t}{W_1 P_t + W_2 Q_t} = \frac{W_1 p_t}{W_1 p_t + W_2 q_t} = \frac{W_1}{\bar{W}_t} p_t. \quad (6.2)$$

Importantly, eqn. (6.2) tells us that the change in  $p$  only depends on a ratio of fitnesses. Therefore, we need to specify fitness only up to an arbitrary constant. As long as we multiply all fitnesses by the same value, that constant will cancel out and eqn. (6.2) will hold.

Based on this argument, it is very common to scale absolute fitnesses by the absolute fitness of one of the genotypes, e.g. the most or the least fit genotype, to obtain relative fitnesses. Here, we will use  $w_i$  for the relative fitness of genotype  $i$ . If we choose to scale by the absolute fitness of genotype  $A_1$ , we obtain the relative fitnesses  $w_1 = W_1/W_1 = 1$  and  $w_2 = W_2/W_1$ .

Without loss of generality, we can therefore rewrite eqn. (6.2) as

$$p_{t+1} = \frac{w_1}{\bar{w}} p_t, \quad (6.3)$$

dropping the subscript  $t$  for the dependence of the mean fitness on time in our notation, but remembering it. The change in frequency from one generation to the next is then given by

$$\Delta p_t = p_{t+1} - p_t = \frac{w_1 p_t}{\bar{w}} - p_t = \frac{w_1 p_t - \bar{w} p_t}{\bar{w}} = \frac{w_1 p_t - (w_1 p_t + w_2 q_t) p_t}{\bar{w}} = \frac{w_1 - w_2}{\bar{w}} p_t q_t, \quad (6.4)$$

recalling that  $q_t = 1 - p_t$ .

Assuming that the fitnesses of the two alleles are constant over time, the number of the two allelic types  $\tau$  generations after time  $t$  are

$P_{t+\tau} = (W_1)^\tau P_t$  and  $Q_{t+\tau} = (W_2)^\tau Q_t$ , respectively. Therefore, the relative frequency of allele  $A_1$  after  $\tau$  generations past  $t$  is

$$p_{t+\tau} = \frac{(W_1)^\tau P_t}{(W_1)^\tau P_t + (W_2)^\tau Q_t} = \frac{(w_1)^\tau P_t}{(w_1)^\tau P_t + (w_2)^\tau Q_t} = \frac{p_t}{p_t + (w_2/w_1)^\tau q_t}, \quad (6.5)$$

where the last step includes dividing the whole term by  $(w_1)^\tau$  and switching from absolute to relative allele frequencies.

Rearranging eqn. (6.5) and setting  $t = 0$ , we can work out the time  $\tau$  for the frequency of  $A_1$  to change from  $p_0$  to  $p_\tau$ . First, we write

$$p_\tau = \frac{p_0}{p_0 + (w_2/w_1)^\tau q_0} \quad (6.6)$$

and rearrange this to obtain

$$\frac{p_\tau}{q_\tau} = \frac{p_0}{q_0} \left( \frac{w_1}{w_2} \right)^\tau. \quad (6.7)$$

Solving this for  $\tau$  yields

$$\tau = \log \left( \frac{p_\tau q_0}{q_\tau p_0} \right) / \log \left( \frac{w_1}{w_2} \right). \quad (6.8)$$

In practice, it is often helpful to parametrize the relative fitnesses  $w_i$  in a specific way. For example, we may set  $w_1 = 1$  and  $w_2 = 1 - s$ , where  $s$  is called the selection coefficient. Using this parametrization,  $s$  is simply the difference in relative fitnesses between the two alleles. Equation (6.5) becomes

$$p_{t+\tau} = \frac{p_t}{p_t + q_t(1-s)^\tau}, \quad (6.9)$$

as  $w_2/w_1 = 1 - s$ . Then, if  $s \ll 1$ , we can approximate  $(1-s)^\tau$  in the denominator by  $\exp(-s\tau)$  to obtain

$$p_{t+\tau} \approx \frac{p_t}{p_t + q_t e^{-s\tau}}. \quad (6.10)$$

This equation takes the form of a logistic function. That is because we are looking at the relative frequencies of two ‘populations’ (of alleles  $A_1$  and  $A_2$ ) that are growing (or declining) exponentially, under the constraint that  $p$  and  $q$  always sum to 1.

Moreover, eqn. (6.7) for the number of generations  $\tau$  it takes for a certain change in frequency to occur becomes

$$\tau = -\log \left( \frac{p_\tau q_0}{q_\tau p_0} \right) / \log(1-s). \quad (6.11)$$

Assuming again that  $s \ll 1$ , this simplifies to

$$\tau \approx \frac{1}{s} \log \left( \frac{p_\tau q_0}{q_\tau p_0} \right). \quad (6.12)$$

One particular case of interest is the time it takes to go from an absolute frequency of 1 to near fixation in a population of size  $N$ . In this case, we have  $p_0 = 1/N$ , and we may set  $p_\tau = 1 - 1/N$ , which is very close to fixation. Then, plugging these values into eqn. (6.12), we obtain

$$\begin{aligned}\tau &= \frac{1}{s} \log \left( \frac{1 - 2/N + 1/N^2}{1/N^2} \right) \\ &\approx \frac{1}{s} (\log(N) + \log(N - 2)) \\ &\approx \frac{2}{s} \log(N)\end{aligned}\tag{6.13}$$

where we make the approximations  $N^2 - 2N + 1 \approx N^2 - 2N$  and later  $N - 2 \approx N$ .

**Question 1.** In our example of the evolution of drug resistance, the drug-resistant SHIV virus spread from undetectable frequencies to  $\sim 65\%$  frequency by 16 weeks post infection. An estimated effective population size of SHIV is  $1.5 \times 10^5$ , and its generation time is  $\sim 1$  day. Assuming that the mutation arose as a single copy allele very shortly the start of drug treatment at 12 weeks, what is the selection coefficient favouring the drug resistance allele?

*Haploid model with fluctuating selection* Selection pressures may change while a polymorphism persists in the population due to environmental changes. We can use our haploid model to consider this case where the fitnesses depend on time (DEMPSTER, 1955), and say that  $w_{1,t}$  and  $w_{2,t}$  are the fitnesses of the two types in generation  $t$ . The frequency of allele  $A_1$  in generation  $t + 1$  is

$$p_{t+1} = \frac{w_{1,t}}{\bar{w}_t} p_t,\tag{6.14}$$

which simply follows from eqn. (6.3). The ratio of the frequency of allele  $A_1$  to that of allele  $A_2$  in generation  $t + 1$  is

$$\frac{p_{t+1}}{q_{t+1}} = \frac{w_{1,t}}{w_{2,t}} \frac{p_t}{q_t}.\tag{6.15}$$

Therefore, if we think of the two alleles starting in generation  $t$  at frequencies  $p_t$  and  $q_t$ , then  $\tau$  generations later,

$$\frac{p_{t+\tau}}{q_{t+\tau}} = \left( \prod_{i=t}^{\tau-1} \frac{w_{1,i}}{w_{2,i}} \right) \frac{p_t}{q_t}.\tag{6.16}$$

The question of which allele is increasing or decreasing in frequency comes down to whether  $\left( \prod_{i=t}^{\tau-1} w_{1,i}/w_{2,i} \right)$  is  $> 1$  or  $< 1$ . As it is a little

hard to think about this ratio, we can instead take the  $\tau^{\text{th}}$  root of it and consider

$$\sqrt[\tau]{\left(\prod_{i=t}^{\tau-1} \frac{w_{1,i}}{w_{2,i}}\right)} = \frac{\sqrt[\tau]{\prod_{i=t}^{\tau-1} w_{1,i}}}{\sqrt[\tau]{\prod_{i=t}^{\tau-1} w_{2,i}}}. \quad (6.17)$$

The term  $\sqrt[\tau]{\prod_{i=t}^{\tau-1} w_{1,i}}$  is the geometric mean fitness of allele  $A_1$  over the  $\tau$  generations past generation  $t$ . Therefore, allele  $A_1$  will only increase in frequency if it has a higher geometric mean fitness than allele  $A_2$  (at least in our simple deterministic model).

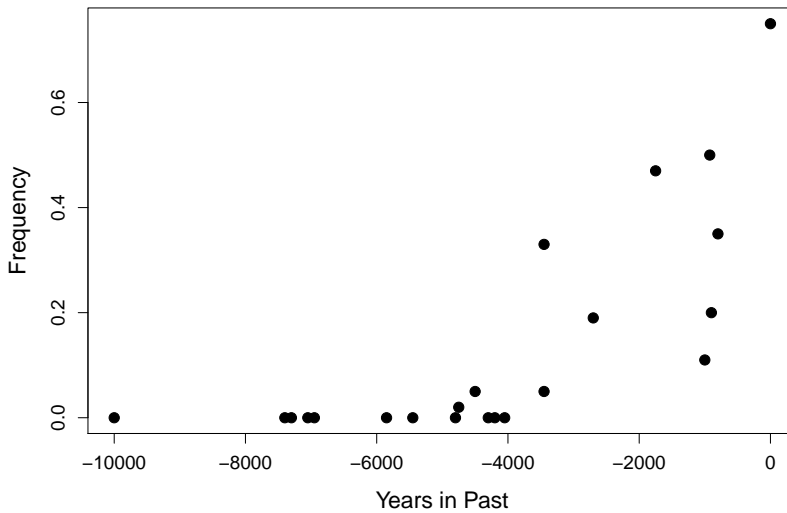


Figure 6.2: Frequency of the Lactase persistence allele in ancient and modern samples from Central Europe. Data compiled by MARCINIAK and PERRY (2017) from various sources. Thanks to Stephanie Marciniak for sharing these data. Code here.

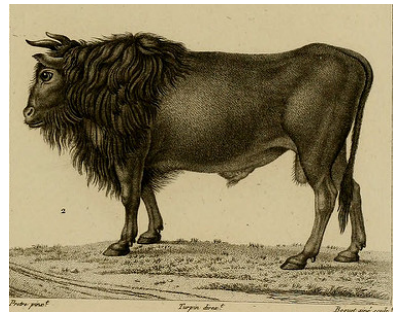


Figure 6.3: Auroch (*Bos primigenius*). Aurochs are an extinct species of large wild cattle that cows were domesticated from.  
Dictionnaire des sciences naturelles. 1816  
Cuvier, F.G. Image from the Internet Archive.  
Contributed by NCSU Libraries. No known  
copyright restrictions.

### 6.0.2 Diploid model

We will now move on to a diploid model of a single locus with two segregating alleles. As an example of the change in the frequency of an allele driven by selection, let's consider the evolution of Lactase persistence. A number of different human populations that historically have raised cattle have convergently evolved to maintain the expression of the protein Lactase into adulthood (in most mammals the protein is switched off after childhood), with different lactase-persistence mutations having arisen and spread in different pastoral human populations. This continued expression of Lactase allows adults to break down Lactose, the main carbohydrate in milk, and so benefit nutritionally from milk-drinking. This seems to have offered a strong fitness benefit to individuals in pastoral populations.

With the advent of techniques to sequence ancient human DNA,

researchers can now potentially track the frequency of selected mutations over thousands of years. The frequency of a Lactase persistence allele in ancient Central European populations is shown in Figure 6.2. The allele is absent more than 5,000 years ago, but now found at frequency of upward of 70% in many European populations.

We will assume that the difference in fitness between the three genotypes comes from differences in viability, i.e. differential survival of individuals from the formation of zygotes to reproduction. We denote the absolute fitnesses of genotypes  $A_1A_1$ ,  $A_1A_2$ , and  $A_2A_2$  by  $W_{11}$ ,  $W_{12}$ , and  $W_{22}$ . Specifically,  $W_{ij}$  is the probability that a zygote of genotype  $A_iA_j$  survives to reproduction. Assuming that individuals mate at random, the number of zygotes that are of the three genotypes and form generation  $t$  are

$$Np_t^2, \quad N2p_tq_t, \quad Nq_t^2. \quad (6.18)$$

The mean fitness of the population of zygotes is then

$$\bar{W}_t = W_{11}p_t^2 + W_{12}2p_tq_t + W_{22}q_t^2. \quad (6.19)$$

Again, this is simply the weighted mean of the genotypic fitnesses.

How many zygotes of each of the three genotypes survive to reproduce? An individual of genotype  $A_1A_1$  has a probability of  $W_{11}$  of surviving to reproduce, and similarly for other genotypes. Therefore, the expected number of  $A_1A_1$ ,  $A_1A_2$ , and  $A_2A_2$  individuals who survive to reproduce is

$$NW_{11}p_t^2, \quad NW_{12}2p_tq_t, \quad NW_{22}q_t^2. \quad (6.20)$$

It then follows that the total number of individuals who survive to reproduce is

$$N(W_{11}p_t^2 + W_{12}2p_tq_t + W_{22}q_t^2). \quad (6.21)$$

This is simply the mean fitness of the population multiplied by the population size (i.e.  $N\bar{w}$ ).

The relative frequency of  $A_1A_1$  individuals at reproduction is simply the number of  $A_1A_1$  genotype individuals at reproduction ( $NW_{11}p_t^2$ ) divided by the total number of individuals who survive to reproduce ( $N\bar{w}$ ), and likewise for the other two genotypes. Therefore, the relative frequency of individuals with the three different genotypes at reproduction is

$$\frac{NW_{11}p_t^2}{N\bar{w}}, \quad \frac{NW_{12}2p_tq_t}{N\bar{w}}, \quad \frac{NW_{22}q_t^2}{N\bar{w}} \quad (6.22)$$

(see Table 6.1).

As there is no difference in the fecundity of the three genotypes, the allele frequencies in the zygotes forming the next generation are simply

|                                | $A_1 A_1$               | $A_1 A_2$                 | $A_2 A_2$               |
|--------------------------------|-------------------------|---------------------------|-------------------------|
| Absolute no. at birth          | $Np_t^2$                | $N2p_tq_t$                | $Nq_t^2$                |
| Fitnesses                      | $W_{11}$                | $W_{12}$                  | $W_{22}$                |
| Absolute no. at reproduction   | $NW_{11}p_t^2$          | $NW_{12}2p_tq_t$          | $NW_{22}q_t^2$          |
| Relative freq. at reproduction | $\frac{W_{11}}{W}p_t^2$ | $\frac{W_{12}}{W}2p_tq_t$ | $\frac{W_{22}}{W}q_t^2$ |

Table 6.1: Relative genotype frequencies after one episode of viability selection.

the allele frequency among the reproducing individuals of the previous generation. Hence, the frequency of  $A_1$  in generation  $t + 1$  is

$$p_{t+1} = \frac{W_{11}p_t^2 + W_{12}p_tq_t}{\bar{W}}. \quad (6.23)$$

Note that, again, the absolute value of the fitnesses is irrelevant to the frequency of the allele. Therefore, we can just as easily replace the absolute fitnesses with the relative fitnesses. That is, we may replace  $W_{ij}$  by  $w_{ij} = W_{ij}/W_{11}$ , for instance.

Each of our genotype frequencies is responding to selection in a manner that depends just on its fitness compared to the mean fitness of the population. For example, the frequency of the 11 homozygotes increases from birth to adulthood in proportion to  $W_{11}/\bar{W}$ . In fact, we can estimate this fitness ratio for each genotype by comparing the frequency at birth compared to adults. As an example of this calculation, we'll look at some data from sticklebacks.

Marine threespine stickleback (*Gasterosteus aculeatus*) independently colonized and adapted to many freshwater lakes as glaciers receded following the last ice age, making sticklebacks a wonderful system for studying the genetics of adaptation. In marine habitats, most of the stickleback have armour plates to protect them from predation, but freshwater populations repeatedly evolve the loss of armour plates due to selection on an allele at the Ectodysplasin gene (EDA). This allele is found as a standing variant at very low frequency marine populations; BARRETT *et al.* took advantage of this fact and collected and bred a population of marine individuals carrying both the low- (L) and completely-plated (C) alleles. They introduced the offspring of this cross into four freshwater ponds and monitored genotype frequencies<sup>1</sup> over their life courses:

|                                     | CC   | LC   | LL   |
|-------------------------------------|------|------|------|
| Juveniles                           | 0.55 | 0.23 | 0.22 |
| Adults                              | 0.21 | 0.53 | 0.26 |
| Adults/Juv. ( $W_\bullet/\bar{W}$ ) | 0.4  | 2.3  | 1.2  |
| rel. fitness ( $W_\bullet/W_{12}$ ) | 0.17 | 1.0  | 0.54 |

The heterozygotes have increased in frequency dramatically in the population as their fitness is more than double the mean fitness of the population. We can also calculate the relative fitness of each genotype by dividing through by the fitness of the fittest genotype, the

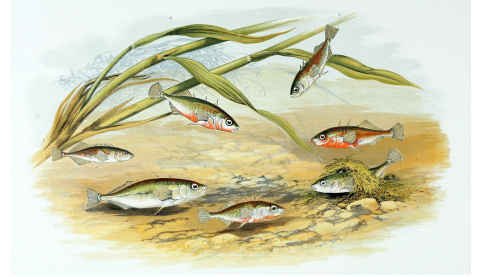


Figure 6.4: Freshwater threespine Stickleback (*G. aculeatus*). British fresh-water fishes. Houghton W 1879. Image from the Biodiversity Heritage Library. Contributed by Ernst Mayr Library, Harvard.. Not in copyright.

<sup>1</sup> The actual dynamics observed by BARRETT *et al.* are more complicated as in the very young fish selection reverses direction.

heterozygote in this case (doing this cancels through  $\bar{W}$ ). The relative fitness of the  $CC$  is  $\sim 1/5$  of the heterozygote. Note that this calculation does not rely on the genotype frequencies being at their HWE in the juveniles.

**Question 2.** **A** What is the frequency of the low-plated EDA allele ( $L$ ) at the start of the stickleback experiment?

**B** What is the frequency in the adults?

**Question 3.** For many generations you have been studying an annual wildflower that has two color morphs, orange and white. You have discovered that a single bi-allelic locus controls flower color, with the white allele being recessive. The pollinator of these plants is an almost blind bat, so individuals are pollinated at random with respect to flower color. Your population census of 200 individuals showed that the population consisted of 168 orange-flowered individuals, and 32 white-flowered individuals.

Heavy February rainfall creates optimal growing conditions for an exotic herbivorous beetle with a preference for orange-flowered individuals. This year it arrives at your study site with a ravenous appetite. Only 50% of orange-flowered individuals survive its wrath, while 90% of white-flowered individuals survive until the end of the growing season.

**A** What is the initial frequency of the white allele, and what do you have to assume to obtain this?

**B** What is the frequency of the white allele in the seeds forming the next generation?

The change in frequency from generation  $t$  to  $t + 1$  is

$$\Delta p_t = p_{t+1} - p_t = \frac{w_{11}p_t^2 + w_{12}p_tq_t}{\bar{w}} - p_t. \quad (6.24)$$

To simplify this equation, we will first define two variables  $\bar{w}_1$  and  $\bar{w}_2$  as

$$\bar{w}_1 = w_{11}p_t + w_{12}q_t, \quad (6.25)$$

$$\bar{w}_2 = w_{12}p_t + w_{22}q_t. \quad (6.26)$$

These are called the marginal fitnesses of allele  $A_1$  and  $A_2$ , respectively. They are so called as  $\bar{w}_1$  is the average fitness of an allele  $A_1$ , i.e. the fitness of  $A_1$  in a homozygote weighted by the probability it is in a homozygote ( $p_t$ ) plus the fitness of  $A_1$  in a heterozygote weighted by the probability it is in a heterozygote ( $q_t$ ). We further note that the mean relative fitness can be expressed in terms of the marginal fitnesses as

$$\bar{w} = \bar{w}_1p_t + \bar{w}_2q_t, \quad (6.27)$$

where, for notational simplicity, we have omitted subscript t for the dependence of mean and marginal fitnesses on time.

We can then rewrite eqn. (6.24) using  $\bar{w}_1$  and  $\bar{w}_2$  as

$$\Delta p_t = \frac{(\bar{w}_1 - \bar{w}_2)}{\bar{w}} p_t q_t. \quad (6.28)$$

The sign of  $\Delta p_t$ , i.e. whether allele  $A_1$  increases or decreases in frequency, depends only on the sign of  $(\bar{w}_1 - \bar{w}_2)$ . The frequency of  $A_1$  will keep increasing over the generations so long as its marginal fitness is higher than that of  $A_2$ , i.e.  $\bar{w}_1 > \bar{w}_2$ , while if  $\bar{w}_1 < \bar{w}_2$ , the frequency of  $A_1$  will decrease. Note the similarity between eqn. (6.28) and the respective expression for the haploid model in eqn. (6.4). (We will return to the special case where  $\bar{w}_1 = \bar{w}_2$  shortly).

We can also rewrite (6.24) as

$$\Delta p_t = \frac{1}{2} \frac{p_t q_t}{\bar{w}} \frac{d\bar{w}}{dp}, \quad (6.29)$$

the demonstration of which we leave to the reader. This form shows that the frequency of  $A_1$  will increase ( $\Delta p_t > 0$ ) if the mean fitness is an increasing function of the frequency of  $A_1$  (i.e. if  $\frac{d\bar{w}}{dp} > 0$ ). On the other hand, the frequency of  $A_1$  will decrease ( $\Delta p_t < 0$ ) if the mean fitness is a decreasing function of the frequency of  $A_1$  (i.e. if  $\frac{d\bar{w}}{dp} < 0$ ). Thus, although selection acts on individuals, under this simple model, selection is acting to increase the mean fitness of the population. The rate of this increase is proportional to the variance in allele frequencies within the population ( $p_t q_t$ ).

**Question 4.** Show that eqns. (6.29) and (6.28) are equivalent.  
(Trickier question.)

So far, our treatment of the diploid model of selection has been in terms of generic fitnesses  $w_{ij}$ . In the following, we will use particular parametrizations to gain insight about two specific modes of selection: directional selection and heterozygote advantage.

### 6.0.3 Diploid directional selection

Directional selection means that one of the two alleles always has higher marginal fitness than the other one. Let us assume that  $A_1$  is the fitter allele, so that  $w_{11} \geq w_{12} \geq w_{22}$ , and hence  $\bar{w}_1 > \bar{w}_2$ . As we are interested in changes in allele frequencies, we may use relative fitnesses. We parameterize the reduction in relative fitness in terms of a selection coefficient, similar to the one we met in the haploid selection section, as follows:

| genotype                    | $A_1A_1$                 | $A_1A_2$                 | $A_2A_2$                 |
|-----------------------------|--------------------------|--------------------------|--------------------------|
| absolute fitness            | $W_{11}$                 | $\geq W_{12} \geq$       | $W_{22}$                 |
| relative fitness (generic)  | $w_{11} = W_{11}/W_{11}$ | $w_{12} = W_{12}/W_{11}$ | $w_{22} = W_{22}/W_{11}$ |
| relative fitness (specific) | 1                        | $1 - sh$                 | $1 - s.$                 |

Here, the selection coefficient  $s$  is the difference in relative fitness between the two homozygotes, and  $h$  is the dominance coefficient. For selection to be directional, we require that  $0 \leq h \leq 1$  holds. The dominance coefficient allows us to move between two extremes. One is when  $h = 0$ , such that allele  $A_1$  is fully dominant and  $A_2$  fully recessive. In this case, the heterozygote  $A_1A_2$  is as fit as the  $A_1A_1$  homozygote genotype. The inverse holds when  $h = 1$ , such that allele  $A_1$  is fully recessive and  $A_2$  fully dominant.

We can then rewrite eqn. (6.28) as

$$\Delta p_t = \frac{p_t h s + q_t s(1-h)}{\bar{w}} p_t q_t, \quad (6.30)$$

where

$$\bar{w} = 1 - 2p_t q_t sh - q_t^2 s. \quad (6.31)$$

**Question 5.** Throughout the Californian foothills are old copper and gold-mines, which have dumped out soils that are polluted with heavy metals. While these toxic mine tailings are often depauperate of plants, *Mimulus guttatus* and a number of other plant species have managed to adapt to these harsh soils. WRIGHT *et al.* (2015) have mapped one of the major loci contributing to the adaptation to soils at two mines near Copperopolis, CA. WRIGHT *et al.* planted homozygote seedlings out in the mine tailings and found that only 10% of the homozygotes for the non-copper-tolerant allele survived to flower, while 40% of the copper-tolerant seedlings survived to flower.

**A)** What is the selection coefficient acting against the non-copper-tolerant allele on the mine tailing?

**B)** The copper-tolerant allele is fairly dominant in its action on fitness. If we assume that  $h = 0.1$ , what percentage of heterozygotes should survive to flower?

**Question 6.** Comparing the red ( $h = 0$ ) and black ( $h = 0.5$ ) trajectories in Figure 6.5, provide an explanation for why  $A_1$  increases faster initially if  $h = 0$ , but then approaches fixation more slowly compared to the case of  $h = 0.5$ .

To see how dominance affects the trajectory of a real polymorphism, we'll consider an example from a colour polymorphism in red foxes (*Vulpes vulpes*). There are three colour morphs of red foxes: silver, cross, and red (see Figure 6.8), with this difference primarily

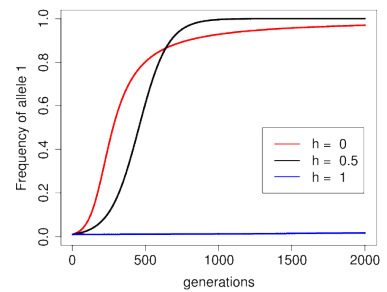


Figure 6.5: The trajectory of the frequency of allele  $A_1$ , starting from  $p_0 = 0.01$ , for a selection coefficient  $s = 0.01$  and three different dominance coefficients. The recessive beneficial allele ( $h = 1$ ) will eventually fix in the population, but it takes a long time. Code here.

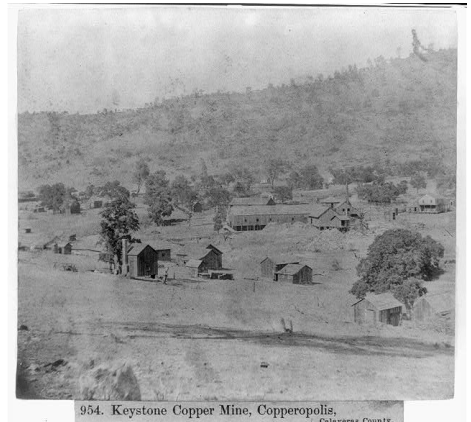


Figure 6.6: Keystone Copper Mine 1866, Copperopolis, Calaveras County. Image from picryl. Source Library of Congress, Public Domain.

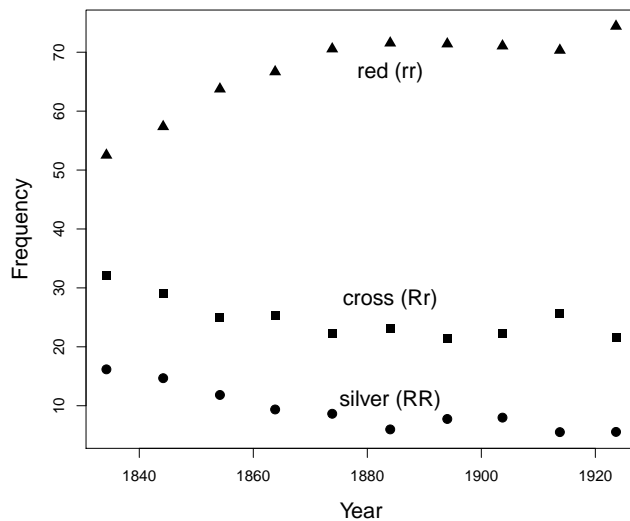


Figure 6.7: The frequency of red, cross, and silver fox morphs over the decades in Eastern Canada. These data are well described by recessive selection acting against the silver fox morph. Data from ELTON (1942), compiled by ALLENDORF and HARD (2009). [Code here.](#)

controlled by a single polymorphism with genotypes RR, Rr, and rr respectively. The fur pelts of the silver morph fetched three times the price for hunters compared to cross (a smoky red) and red pelts, the latter two being seen as roughly equivalent in worth. Thus the desirability of the pelts acts as a recessive trait, with much stronger selection against the silver homozygotes. As a result of this price difference, silver foxes were hunted more intensely and declined as a proportion of the population in Eastern Canada, see Figure 6.7, as documented by ELTON, from 16% to 5% from 1834 to 1937. HALDANE reanalyzed these data and showed that they were consistent with recessive selection acting against the silver morph alone.

Note how the heterozygotes (cross) decline somewhat as a result of selection on the silver homozygotes, but overall the R allele is slow to respond to selection as it is ‘hidden’ from selection in the heterozygote state.

*Directional selection on an additive allele.* A special case is when  $h = 0.5$ . This case is the case of no dominance, as the interaction among alleles with respect to fitness is strictly additive. Then, eqn. (6.30) simplifies to

$$\Delta p_t = \frac{1}{2} \frac{s}{\bar{w}} p_t q_t. \quad (6.32)$$

If selection is very weak, i.e.  $s \ll 1$ , the denominator ( $\bar{w}$ ) is close to 1 and we have

$$\Delta p_t = \frac{1}{2} s p_t q_t. \quad (6.33)$$



Figure 6.8: Three colour morphs in red fox *V. vulpes*, cross, red, and silver foxes from left to right.  
The previous black and silver gray foxes are mostly color phase, occurring in flocks of the underfur did not last too long, page 410  
E.W., Fuertes, L.A. 1916. Image from the Biodiversity Heritage Library. Contributed by Cornell University Library. No known copyright restrictions.

It is instructive to compare eqn. (6.33) to the respective expression under the haploid model. To this purpose, start from the generic term for  $\Delta p_t$  under the haploid model in eqn. (6.4) and set  $w_1 = 1$  and  $w_2 = 1 - s$ . Again, assume that  $s$  is small, so that eqn. (6.4) becomes  $\Delta p_t = sp_t q_t$ . Hence, if  $s$  is small, the diploid model of directional selection without dominance is identical to the haploid model, up to a factor of 1/2. That factor is due to the choice of the parametrisation; we could have set  $w_{11} = 1$ ,  $w_{12} = 1 - s$ , and  $w_{22} = 1 - 2s$  in our diploid model instead, in which case the agreement with the haploid model would be perfect.

From this analogy, we can borrow some insight we gained from the haploid model. Specifically, the trajectory of the frequency of allele  $A_1$  in the diploid model without dominance follows a logistic growth curve similar to (6.10). From this similarity, we can extrapolate from Equation (6.12) to find the time it takes for our diploid, beneficial, additive allele ( $A_1$ ) to move from frequency  $p_0$  to  $p_\tau$ :

$$\tau \approx \frac{2}{s} \log \left( \frac{p_\tau q_0}{q_\tau p_0} \right) \quad (6.34)$$

generations; this just differs by a factor of 2 from our haploid model. Using this result we can find the time it takes for our favourable, additive allele ( $A_1$ ) to transit from its entry into the population ( $p_0 = 1/(2N)$ ) to close to fixation ( $p_\tau = 1 - 1/(2N)$ ):

$$\tau \approx \frac{4}{s} \log(2N) \quad (6.35)$$

generations. Note the similarity to eqn. 6.13 for the haploid model, with a difference by a factor of 2 due to the choice of parametrization (and that the number of alleles is  $2N$  in the diploid model, rather than  $N$ ). Doubling our selection coefficient halves the time it takes for our allele to move through the population.

**Question 7.** Gulf killifish (*Fundulus grandis*) have rapidly adapted to the very high pollution levels in the Houston shipping canal since the 1950s. One of the ways that they've adapted is through the deletion of their aryl hydrocarbon receptor (AHR) gene. Oziolor et al. estimated that individuals who were homozygote for the intact AHR gene had a relative fitness of 20% of that of homozygotes for the deletion. Assuming an effective population size of 200 thousand individuals, how long would it take for the deletion to reach fixation, starting as a single copy in this population?

Directional selection on genotypes is expected to remove variation from populations, yet we see plentiful phenotypic and genetic variation in every natural population. Why is this? Three broad explanations for the maintenance of polymorphisms are

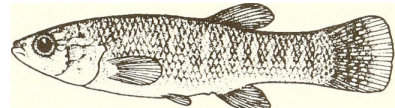


Figure 6.9: Gulf killifish (*Fundulus grandis*).

Distribution and abundance of fishes and invertebrates in Gulf of Mexico estuaries. Nelson D M and Pattillo M E Image from the Biodiversity Heritage Library. Contributed by MBLWHOI Library. No known copyright restrictions.

1. Variation is maintained by a balance of genetic drift and mutation (we discussed this explanation in Chapter 3).
2. Selection can sometimes act to maintain variation in populations (balancing selection).
3. Deleterious variation can be maintained in the population as a balance between selection removing variation and mutation constantly introducing new variation into the population.

We'll turn to these latter two explanations through the rest of the chapter. Note that these explanations are not mutually exclusive, and each of them will explain some proportion of the variation.

#### 6.0.4 Heterozygote advantage

One form of balancing selection occurs when the heterozygotes are fitter than either of the homozygotes. In this case, it is useful to parameterize the relative fitnesses as follows:

| genotype                    | $A_1A_1$                 | $A_1A_2$                 | $A_2A_2$                 |
|-----------------------------|--------------------------|--------------------------|--------------------------|
| absolute fitness            | $w_{11}$                 | $\langle w_{12} \rangle$ | $w_{22}$                 |
| relative fitness (generic)  | $w_{11} = W_{11}/W_{12}$ | $w_{12} = W_{12}/W_{12}$ | $w_{22} = W_{22}/W_{12}$ |
| relative fitness (specific) | $1 - s_1$                | 1                        | $1 - s_2$                |

Here,  $s_1$  and  $s_2$  are the differences between the relative fitnesses of the two homozygotes and the heterozygote. Note that to obtain relative fitnesses we have divided absolute fitness by the heterozygote fitness. We could use the same parameterization as in the model of directional selection, but the reparameterization we have chosen here makes the math easier.

In this case, when allele  $A_1$  is rare, it is often found in a heterozygous state, while the  $A_2$  allele is usually in the homozygous state, and so  $A_1$  is more fit and increases in frequency. However, when the allele  $A_1$  is common, it is often found in a less fit homozygous state, while the allele  $A_2$  is often found in a heterozygous state; thus it is now allele  $A_2$  that increases in frequency at the expense of allele  $A_1$ . Thus, at least in the deterministic model, neither allele can reach fixation and both alleles will be maintained at an equilibrium frequency as a balanced polymorphism in the population.

We can solve for this equilibrium frequency by setting  $\Delta p_t = 0$  in eqn. (6.28), i.e.  $p_t q_t (\bar{w}_1 - \bar{w}_2) = 0$ . Doing so, we find that there are three equilibria, all of which are stable. Two of them are not very interesting ( $p = 0$  or  $q = 0$ ), but the third one is the polymorphic equilibrium, where  $\bar{w}_1 - \bar{w}_2 = 0$  holds. Using our  $s_1$  and  $s_2$  parametrization

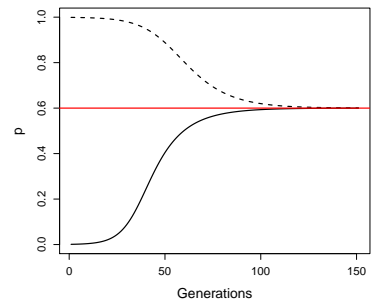
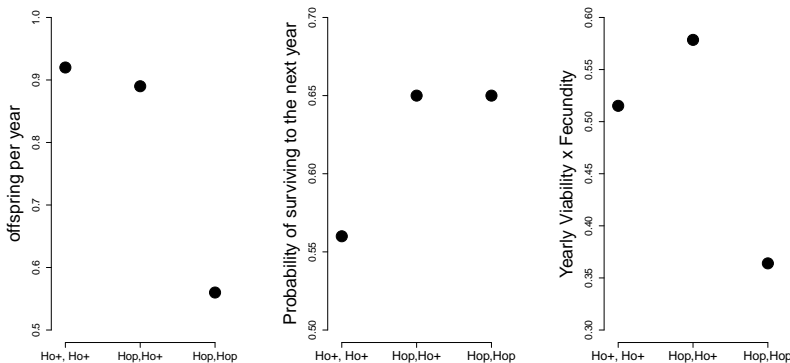


Figure 6.10: Two allele frequency trajectories of the  $A_1$  allele subject to heterozygote advantage ( $w_{11} = 0.9$ ,  $w_{12} = 1$ , and  $w_{22} = 0.85$ ). In one simulation the allele is started from being rare in the population ( $p = 1/1000$ , solid line) and increases in frequency. In the other simulation the allele is almost fixed ( $p = 999/1000$ , dashed line). In both cases the frequency moves toward the equilibrium frequency. The red line shows the equilibrium frequency ( $p_e$ ). Code here.

above, we see that the marginal fitnesses of the two alleles are equal when

$$p_e = \frac{s_2}{s_1 + s_2} \quad (6.36)$$

for the equilibrium frequency of interest. This is also the frequency of  $A_1$  at which the mean fitness of the population is maximized. The highest possible fitness of the population would be achieved if every individual was a heterozygote. However, Mendelian segregation of alleles in the gametes of heterozygotes means that a sexual population can never achieve a completely heterozygote population. This equilibrium frequency represents an evolutionary compromise between the advantages of the heterozygote and the comparative costs of the two homozygotes.



One example of a polymorphism maintained by heterozygote advantage is a horn-size polymorphism found in Soay sheep, a population of feral sheep on the island of Soay (about 40 miles off the coast of Scotland). The horns of the soay sheep resemble those of the wild Mouflon sheep, and the male Soay sheep use their horns to defend females during the rut. JOHNSTON *et al.* (2013) found a large-effect locus, at the RXFP2 gene, that controls much of the genetic variation for horn size. Two alleles  $Ho^p$  and  $Ho^+$  segregate at this locus. The  $Ho^+$  allele is associated with growing larger horns, while the  $Ho^p$  allele is associated with smaller horns, with a reasonable proportion of  $Ho^p$  homozygotes developing no horns at all. JOHNSTON *et al.* (2013) found that the  $Ho$  locus had substantial effects on male, but not female, fitness (see Figure 6.13).

The  $Ho^p$  allele has a mostly recessive effect on male fecundity, with the  $Ho^p$  homozygotes having lower yearly reproductive success presumably due to the fact that they perform poorly in male-male competition (left plot Figure 6.13). Conversely, the  $Ho^+$  has a mostly recessive effect on viability, with  $Ho^+$  homozygotes having lower yearly

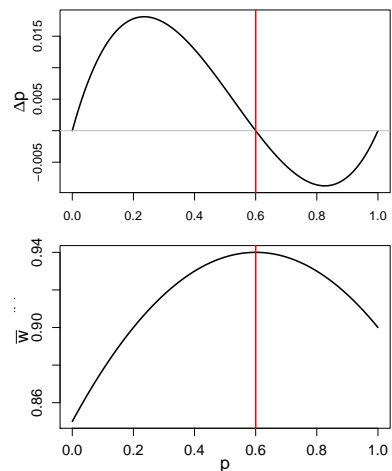


**Figure 6.11:** **Top)** The change in frequency of an allele with heterozygote advantage within a generation ( $\Delta p$ ) as a function of the allele frequency. Fitnesses as in Figure 6.10. Note how the frequency change is positive below the equilibrium frequency ( $p_e$ ) and negative above. **Bottom)** Mean fitness ( $\bar{w}$ ) as a function of the allele frequency. The red line shows the equilibrium frequency ( $p_e$ ). Code here.

**Figure 6.12:** For the three Soay sheep genotypes: the offspring per year (left), the probability of surviving a year (middle), and the product of the two (right). Thanks to Susan Johnston for supplying these simplified numbers from JOHNSTON *et al.* (2013). Code here.

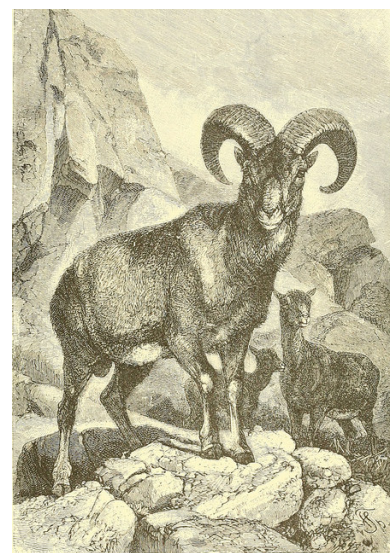


**Figure 6.13:** Mouflon (*Ovis orientalis orientalis*). Animate creation. (1898). Wood, J. G. Image from the Biodiversity Heritage Library. Contributed by Smithsonian Libraries. Not in copyright.

survival (middle plot Figure 6.13), likely because they spend little time feeding during the rut and so lose substantial body weight. Thus both of the homozygotes suffer from trade-offs between viability and fecundity. As a result, the  $\text{Ho}^P\text{Ho}^+$  heterozygotes have the highest fitness (right plot Figure 6.13). The allele is thus balanced at intermediate frequency (50%) in the population due to this trade off between fitness at different life history stages.

**Question 8.** Assume that the frequency of the  $\text{Ho}^P$  allele is 10%, that there are 1000 males at birth, and that individual adults mate at random.

**A)** What is the expected number of males with each of the three genotypes in the population at birth?

**B)** Assume that a typical male individual of each genotype has the following probability of surviving to adulthood:

| $\text{Ho}^+$ | $\text{Ho}^P$ | $\text{Ho}^+ \text{Ho}^P$ | $\text{Ho}^P \text{Ho}^P$ |
|---------------|---------------|---------------------------|---------------------------|
| 0.5           | 0.8           | 0.8                       |                           |

Making the assumptions from above, how many males of each genotype survive to reproduce? **C)** Of the males who survive to reproduce, let's say that males with the  $\text{Ho}^+ \text{Ho}^+$  and  $\text{Ho}^P \text{Ho}^P$  genotype have on average 2.5 offspring, while  $\text{Ho}^P \text{Ho}^P$  males have on average 1 offspring. Taking into account both survival and reproduction, how many offspring do you expect each of the three genotypes to contribute to the total population in the next generation?

**D)** What is the frequency of the  $\text{Ho}^+$  allele in the sperm that will form this next generation?

**E)** How would your answers to B-D change if the  $\text{Ho}^P$  allele was at 90% frequency?

The fitnesses here are chosen to roughly match those of the real Soay sheep example, as a full model would require us to more carefully model the life-histories of the sheep.

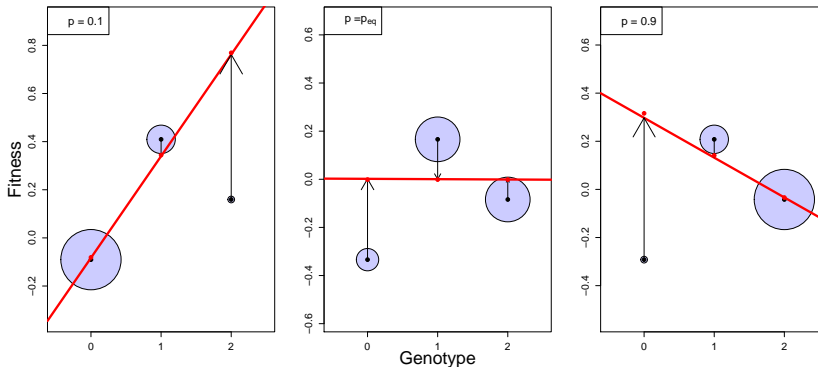


Figure 6.14: The deviation of the fitness of each genotype away from the mean population fitness (0) is shown as black dots. The area of each circle is proportion to the fraction of the population in each genotypic class ( $p^2$ ,  $2pq$ , and  $q^2$ ). The additive genetic fitness of each genotype is shown as a red dot. The linear regression between fitness and additive genotype is shown as a red line. The black vertical arrows show the difference between the average mean-centered phenotype and additive genetic value for each genotype. The left panel shows  $p = 0.1$  and the right panel shows  $p = 0.9$ ; in the middle panel the frequency is set to the equilibrium frequency. Code here.

To push our understanding of heterozygote advantage a little further, note that the marginal fitnesses of our alleles are equivalent to the additive effects of our alleles on fitness. Recall from our discussion of non-additive variation (Section 4.1.1) that the difference in the

additive effects of the two alleles gives the slope of the regression of additive genotypes on fitness, and that there is additive variance in fitness when this slope is non-zero. So what's happening here in our heterozygote advantage model is that the marginal fitness of the  $A_1$  allele, the additive effect of allele  $A_1$  on fitness, is greater than the marginal fitness of the  $A_2$  allele ( $\bar{w}_1 > \bar{w}_2$ ) when  $A_1$  is at low frequency in the population. In this case, the regression of fitness on the number of  $A_1$  alleles in a genotype has a positive slope. This is true when the frequency of the  $A_1$  allele is below the equilibrium frequency. If the frequency of  $A_1$  is above the equilibrium frequency, then the marginal fitness of allele  $A_2$  is higher than the marginal fitness of allele  $A_1$  ( $\bar{w}_1 < \bar{w}_2$ ) and the regression of fitness on the number of copies of allele  $A_1$  that individuals carry is negative. In both cases there is additive genetic variance for fitness ( $V_A > 0$ ) and the population has a directional response. Only when the population is at its equilibrium frequency, i.e. when  $\bar{w}_1 = \bar{w}_2$ , is there no additive genetic variance ( $V_A = 0$ ), as the linear regression of fitness on genotype is zero.

*Underdominance.* Another case that is of potential interest is the case of fitness underdominance, where the heterozygote is less fit than either of the two homozygotes. Underdominance can be parametrized as follows:

| genotype                    | $A_1A_1$                 | $A_1A_2$                 | $A_2A_2$                 |
|-----------------------------|--------------------------|--------------------------|--------------------------|
| absolute fitness            | $w_{11}$                 | $> w_{12} <$             | $w_{22}$                 |
| relative fitness (generic)  | $w_{11} = W_{11}/W_{12}$ | $w_{12} = W_{12}/W_{12}$ | $w_{22} = W_{22}/W_{12}$ |
| relative fitness (specific) | $1 + s_1$                | 1                        | $1 + s_2$                |

Underdominance also permits three equilibria:  $p = 0$ ,  $p = 1$ , and a polymorphic equilibrium  $p = p_U$ . However, now only the first two equilibria are stable, while the polymorphic equilibrium is unstable. If  $p < p_U$ , then  $\Delta p_t$  is negative and allele  $A_1$  will be lost, while if  $p > p_U$ , allele  $A_1$  will become fixed.

While underdominant alleles might not spread within populations (if  $p_U \gg 0$  and selection is reasonably strong), they are of interest in the study of speciation and hybrid zones. That is because alleles  $A_1$  and  $A_2$  may have arisen in a stepwise fashion, i.e. not by a single mutation, but in separate subpopulations. In this case, heterozygote disadvantage will play a potential role in species maintenance, if isolation of the subpopulations is not complete.

**Question 9.** You are studying the polymorphism that affects flight speed in butterflies. The polymorphism does not appear to affect fecundity. Homozygotes for the B allele are slow in flight and so only



Figure 6.15: In *Pseudacraea eurytus* there are two homozygotes morphs that mimic a different blue and orange butterfly; the heterozygote fails to mimic either successfully and so suffers a high rate of predation (OWEN and CHANTER, 1972). Illustrations of new species of exotic butterflies (1868) Hewitson. Image from the Biodiversity Heritage Library. Contributed by Smithsonian Libraries. Not in copyright.

40% of them survive to have offspring. Heterozygotes for the polymorphism ( $Bb$ ) fly quickly and have a 70% probability of surviving to reproduce. The homozygotes for the alternative allele ( $bb$ ) fly very quickly indeed, but often die of exhaustion, with only 10% of them making it to reproduction.

- A)** What is the equilibrium frequency of the  $B$  allele?
- B)** Calculate the marginal absolute fitnesses of the  $B$  and the  $b$  allele at the equilibrium frequency.

**Question 10.** OPTIONAL trickier question.

Imagine a randomly-mating population of hermaphrodites. In this population, a derived allele ( $D$ ) segregates that distorts transmission in its favour over the ancestral allele ( $d$ ) in the production of all the gametes of heterozygotes. The drive leads to a fraction  $r$  of the gametes of heterozygotes ( $D/d$ ) to carry the  $D$  allele ( $r > 0.5$ ). The  $D$  allele causes viability problems in the homozygous state, such that the relative fitnesses are  $w_{dd} = 1$ ,  $w_{Dd} = 1$ ,  $w_{DD} = 1 - e$ . The  $D$  allele is currently at frequency  $p$  in the population at birth. Assume that the population is very large and no mutation occurs:

- A)** What is the frequency of the  $D$  allele in the next generation, before selection has had a chance to act?
- B)** What conditions do you need for a polymorphic equilibrium to be maintained? What is the equilibrium frequency of this balanced polymorphism?
- C)** Imagine the cost of the driver were additive:  $w_{dd} = 1$ ,  $w_{Dd} = 1 - e$ ,  $w_{DD} = 1 - 2e$ . Under what conditions can the driver invade the population? Can a polymorphic equilibrium be maintained?

*Diploid fluctuating fitness* Selection pressures fluctuate over time and can potentially maintain polymorphisms in the population. Two examples of polymorphisms fluctuating in frequency in response to temporally-varying selection are shown in Figure 6.16; thanks to the short lifespan of *Drosophila* we can see seasonally-varying selection. The first example is an inversion allele in *Drosophila pseudoobscura* populations. Throughout western North America, two orientations of the chromosome, two 'inversion alleles', exist: the Chiricahua and Standard alleles. DOBZHANSKY (1943) and WRIGHT and DOBZHANSKY (1946) investigated the frequency of these inversion alleles over four years at a number of locations and found that their frequency fluctuated systematically over the seasons in response to selection (left side of 6.16). If you're still reading these notes send Prof. Coop a picture of Dobzhansky; Dobzhansky was one of the most important evolutionary geneticists of the past century and spent a bunch of time at UC Davis in his later years. Our second example is an

insertion-deletion polymorphism in the Insulin-like Receptor gene in *Drosophila melanogaster*. PAABY *et al.* (2014) tracked the frequency of this allele over time and found it oscillated with the seasons (right side of 6.16). She and her coauthors also determined that these alleles had large effects on traits such as developmental time and fecundity, which could mediate the maintenance of this polymorphism through life-history trade-offs.

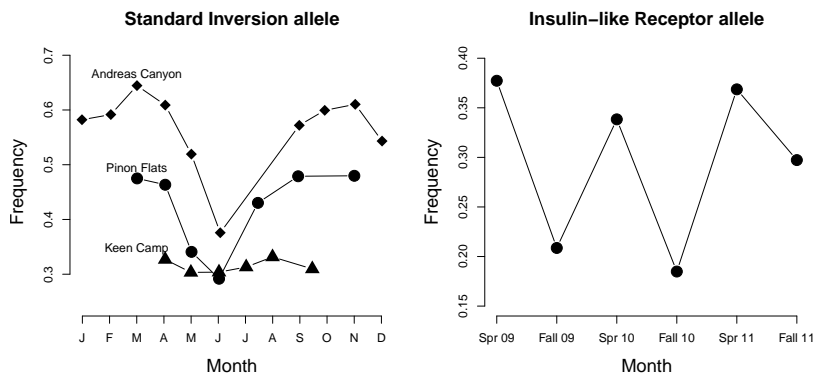


Figure 6.16: **Left**) Seasonal variation in the frequency of the ‘Standard’ inversion allele in *Drosophila pseudoobscura* for three populations from Mount San Jacinto, CA. These frequencies are an average over four years. Data from WRIGHT and DOBZHANSKY (1946). **Right**) The frequency of an allele at the Insulin-like Receptor gene over three years in *Drosophila melanogaster* samples from an Orchard in Pennsylvania. Data from PAABY *et al.* (2014). Code here.

To explore temporal fluctuations in fitness, we’ll need to think about the diploid absolute fitnesses being time-dependent, where the three genotypes have fitnesses  $w_{11,t}$ ,  $w_{12,t}$ , and  $w_{22,t}$  in generation  $t$ . Modeling the diploid case with time-dependent fitness is much less tractable than the haploid case, as segregation makes it tricky to keep track of the genotype frequencies. However, we can make some progress and gain some intuition by thinking about how the frequency of allele  $A_1$  changes when it is rare (following the work of HALDANE and JAYAKAR, 1963).

When  $A_1$  is rare, i.e.  $p_t \ll 1$ , the frequency of  $A_1$  in the next generation (6.23) can be approximated as

$$p_{t+1} \approx \frac{w_{12}}{\bar{w}} p_t. \quad (6.37)$$

To obtain this equation, we have ignored the  $p_t^2$  term (because it is very small when  $p_t$  is small) and we have assumed that  $q_t \approx 1$  in the numerator. Following a similar argument to approximate  $q_{t+1}$ , we can write

$$\frac{p_{t+1}}{q_{t+1}} = \frac{w_{12,t}}{w_{22,t}} \frac{p_t}{q_t}. \quad (6.38)$$

Starting from out from  $p_0$  and  $q_0$  in generation 0, then  $t+1$  generations later we have

$$\frac{p_{t+1}}{q_{t+1}} = \left( \prod_{i=0}^t \frac{w_{12,i}}{w_{22,i}} \right) \frac{p_0}{q_0}. \quad (6.39)$$

From this we can see, following our haploid argument from above, that the frequency of allele  $A_1$  will increase when rare only if

$$\frac{\sqrt[t]{\prod_{i=0}^t w_{12,i}}}{\sqrt[t]{\prod_{i=0}^t w_{22,i}}} > 1, \quad (6.40)$$

i.e. if the heterozygote has higher geometric mean fitness than the  $A_2A_2$  homozygote.

The question now is whether allele  $A_1$  will approach fixation in the population, or whether there are cases in which we can obtain a balanced polymorphism. To investigate that, we can simply repeat our analysis for  $q \ll 1$ , and see that in that case

$$\frac{p_{t+1}}{q_{t+1}} = \left( \prod_{i=0}^t \frac{w_{11,i}}{w_{12,i}} \right) \frac{p_0}{q_0}. \quad (6.41)$$

Now, for allele  $A_1$  to carry on increasing in frequency and to approach fixation, the  $A_1A_1$  genotype has to be out-competing the heterozygotes. For allele  $A_1$  to approach fixation, we need the geometric mean of  $w_{11,i}$  to be greater than the geometric mean fitness of heterozygotes ( $w_{12,i}$ ). At the same time, if heterozygotes have higher geometric mean fitness than the  $A_1A_1$  homozygotes, then the  $A_2$  allele will increase in frequency when it is rare.

Intriguingly, we can thus have a balanced polymorphism even if the heterozygote is never the fittest genotype in any generation, as long as the heterozygote has a higher geometric mean fitness than either of the homozygotes. In this case, the heterozygote comes out ahead when we think about long-term fitness across heterogeneous environmental conditions, despite never being the fittest genotype in any particular environment.

As a toy example of this type of balanced polymorphism, consider a plant population found in one of two different environments each generation. These occur randomly;  $1/2$  of time the population experiences the dry environment and with probability  $1/2$  it experiences the wet environment. The absolute fitnesses of the genotypes in the different environments are as follows:

| Environment     | AA   | Aa  | aa   |
|-----------------|------|-----|------|
| Wet             | 6.25 | 5.0 | 3.75 |
| Dry             | 3.85 | 5.0 | 6.15 |
| arithmetic mean | 5.05 | 5.0 | 4.95 |

Let's write  $w_{AA,\text{dry}}$  and  $w_{AA,\text{wet}}$  for the fitnesses of the AA homozygote in the two environments. Then, if the two environments are equally common,  $\prod_{i=0}^t w_{AA,i} \approx w_{AA,\text{dry}}^{t/2} w_{AA,\text{wet}}^{t/2}$  for large values of  $t$ . To obtain an estimate of this product normalized over the  $t$  generations, we can take the  $t^{\text{th}}$  root to obtain the geometric mean fitness.

This example is loosely based on the work of SCHEMSKE and BIERZYCHUDEK (2001) on *Linanthus parryae*, a desert annual, endemic to California. There are blue- and a white-flowered colour morphs polymorphic many populations, with this polymorphism being controlled by a single dominant allele. The blue-flowered plants produce more seeds in dry years, i.e. they have higher fitness in these years, while the white-flowered plants have higher seed production in wet years. Thus both morphs can potentially be maintained in the population. See TURELLI *et al.* (2001) for a more detailed analysis.

Taking the  $t^{th}$  root, we find the geometric mean fitness of the AA allele is  $w_{AA,\text{dry}}^{1/2} w_{AA,\text{wet}}^{1/2}$ . Doing this for each of our genotypes, we find the geometric mean fitnesses of our alleles to be:

|                | AA   | Aa  | aa   |
|----------------|------|-----|------|
| Geometric mean | 4.91 | 5.0 | 4.80 |

i.e. the heterozygote has higher geometric mean fitnesses than either of the homozygotes, despite not being the fittest genotype in either environment (nor having the highest arithmetic mean fitness). So the  $A_1$  allele can invade the population when it is rare as it spread thanks to the higher fitness of the heterozygotes. Similarly the  $A_2$  allele can invade the population when it is rare. Thus both alleles will persist in the population due to the environmental fluctuations, and the higher geometric mean fitness of the heterozygotes.

*Negative frequency-dependent selection.* In the models and examples above, heterozygote advantage maintains multiple alleles in the population because the common allele has a disadvantage compared to the other rarer allele. In the case of heterozygote advantage, the relative fitnesses of our three genotypes are not a function of the other genotypes present in the population. However, there's a broader set of models where the relative fitness of a genotype depends on the genotypic composition of the population; this broad family of models is called frequency-dependent selection. Negative frequency-dependent selection, where the fitness of an allele (or phenotype) decreases as it becomes more common in the population, can act to maintain genetic and phenotypic diversity within populations. While cases of long-term heterozygote advantage may be somewhat rare in nature, negative frequency-dependent selection is likely a common form of balancing selection.

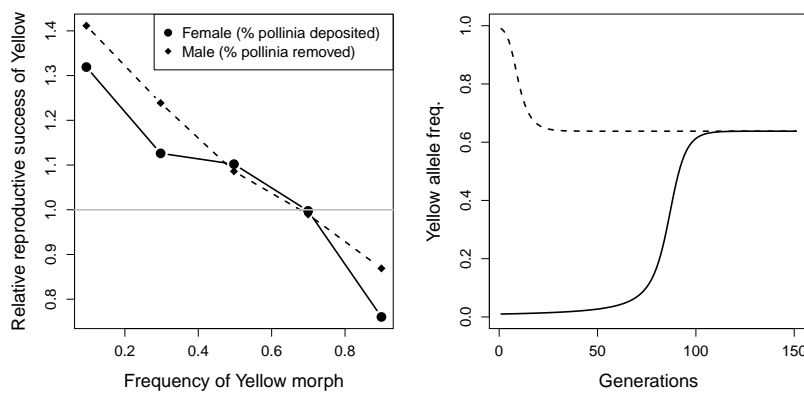
One common mechanism that may create negative frequency-dependent selection is the interaction between individuals within or among species. For example, negative frequency-dependent dynamics can arise in predator-prey or pathogen-host dynamics, where alleles conferring common phenotypes are at a disadvantage because predators or pathogens learn or evolve to counter the phenotypic effects of common alleles.

As one example of negative frequency-dependent selection, consider the two flower colour morphs in the deceptive Elderflower orchid (*Dactylorhiza sambucina*). Throughout Europe, there are populations of these orchids polymorphic for yellow- and purple-flowered individuals, with the yellow flower corresponding to a recessive allele. Neither of these morphs provide any nectar or pollen reward to their bumblebee pollinators. Thus these plants are typically polli-



Figure 6.17: Elderflower orchid (*Dactylorhiza sambucina*). Abbildungen der in Deutschland und den angrenzenden gebieten vorkommenden grundformen der orchideenarten (1904). Müller, W. Image from the Biodiversity Heritage Library. Contributed by New York Botanical Garden. Not in copyright.

nated by newly emerged bumblebees who are learning about which plants offer food rewards, with the bees alternating to try a different coloured flower if they find no food associated with a particular flower-colour morph (SMITHSON and MACNAIR, 1997). GIGORD *et al.* (2001) explored whether this behaviour by bees could result in negative frequency-dependent selection; out in the field, the researchers set up experimental orchid plots in which they varied the frequency of the two colour morphs. Figure 6.18 shows their measurements of the relative male and female reproductive success of the yellow morph across these experimental plots. When the yellow morph is rare, it has higher reproductive success than the purple morph, as it receives a disproportionate number of visits from bumblebees that are dissatisfied with the purple flowers. This situation is reversed when the yellow morph becomes common in the population; now the purple morph outperforms the yellow morph. Therefore, both colour morphs are maintained in this population, and presumably Europe-wide, due to this negative frequency-dependent selection.



Negative frequency-dependent selection can also maintain different breeding strategies due to interactions amongst individuals within a population. One dramatic example of this occurs in ruffs (*Philomachus pugnax*), a marsh-wading sandpiper that summers in Northern Eurasia. The males of this species lek, with the males gathering on open ground to display and attract females. There are three different male morphs differing in their breeding strategy. The large majority of males are ‘Independent’, with black or chestnut ruff plumage, and try to defend and display on small territories. ‘Satellite’ males, with white ruff plumage, make up ~ 16% of males and do not defend territories, but rather join in displays with Independent males and opportunistically mate with females visiting the lek. Finally, the rare ‘Faeder’

Figure 6.18: **Left)** Measures of the relative male- and female- reproductive success of the yellow Elderflower orchid morph as a function of the yellow morph in experimental plots. **Right)** Two allele frequency trajectories of the Yellow allele subject to negative frequency scheme given in the left plot (for an initial frequency of 0.01 and 0.99, solid and dotted line respectively). Note that the yellow Male reproductive success is measured in terms of the % of pollinia removed front a plant and female reproductive success is measured in terms of the % of stigmas receiving pollinia on a plant. These measures are made relative by dividing the reproductive success of the yellow morph by the mean of the yellow and purple morphs. Pollinia are the pollen masses of orchids, and other plants, where individual pollinium are transferred as a single unit by pollinators. Data from GIGORD *et al.* (2001). Code here.

morph was only discovered in 2006 (JUKEMA and PIERSMA, 2006) and makes up less than 1% of males. These Faeder males are female mimics who hang around the territories of Independents and try to 'sneak' in matings with females. Faeder males have plumage closely resembling that of females and a smaller body size than other males, but with larger testicles (presumably to take advantage of rare mating opportunities). All three of these morphs, with their complex behavioural and morphological differences, are controlled by three alleles at a single autosomal locus, with the Satellite and Faeder alleles being genetically dominant over the high frequency Independent allele. The



Figure 6.19: Lekking Ruffs (*Philomachus pugnax*). Three Independent males, one Satellite male, and one female (or Faeder male?).

Painting by Johann Friedrich Naumann (1780–1857). Public Domain, wikimedia.

genetic variation for these three morphs is potentially maintained by negative frequency-dependent selection, as all three male strategies are likely at an advantage when they are rare in the population. For example, while the Satellites mostly lose out on mating opportunities to Independents, they may have longer life-spans and so may have equal life-time reproductive success (WIDEMO, 1998). However, Satellite and Faeder males are totally reliant on the lekking Independent males, and so both of these alternative strategies cannot become overly common in the population. The locus controlling these differences has been mapped, and the underlying alleles have persisted for roughly four million years (KÜPPER *et al.*, 2016; LAMICHHANEY *et al.*, 2016). While this mating system is bizarre, the frequency dependent dynamics mean that it has been around longer than we've been using stone tools.

While these examples may seem somewhat involved, they must be simple compared to the complex dynamics that maintain the hundreds of alleles present at the genes in the Major histocompatibility complex (MHC). MHC genes are key to the coordination of the vertebrate immune system in response to pathogens, and are likely caught in an endless arms race with pathogens adapting to common MHC alleles,

allowing rare MHC alleles to be favoured. Balancing selection at the MHC locus has maintained some polymorphisms for tens of millions of years, such that some of your MHC alleles may be genetically more closely related to MHC alleles in other primates than they are to alleles in your close human friends.

### 6.0.5 Mutation-selection balance

Mutation is constantly introducing new alleles into the population. Therefore, variation can be maintained within a population not only if selection is balancing (e.g. through heterozygote advantage or fluctuating selection over time, as we have seen in the previous section), but also due to a balance between mutation introducing deleterious alleles and selection acting to purge these alleles from the population (HALDANE, 1937). To study mutation-selection balance, we return to the model of directional selection, where allele  $A_1$  is advantageous, i.e.

| genotype         | $A_1A_1$     | $A_1A_2$           | $A_2A_2$         |
|------------------|--------------|--------------------|------------------|
| absolute fitness | $W_{11}$     | $\geq W_{12} \geq$ | $W_{22}$         |
| relative fitness | $w_{11} = 1$ | $w_{12} = 1 - sh$  | $w_{22} = 1 - s$ |

We'll begin by considering the case where allele  $A_2$  is not completely recessive ( $h > 0$ ), so that the heterozygotes suffer at least some disadvantage. We denote by  $\mu = \mu_{1 \rightarrow 2}$  the mutation rate per generation from  $A_1$  to the deleterious allele  $A_2$ , and assume that there is no reverse mutation ( $\mu_{2 \rightarrow 1} = 0$ ). Let us assume that selection against  $A_2$  is relatively strong compared to the mutation rate, so that it is justified to assume that  $A_2$  is always rare, i.e.  $q_t = 1 - p_t \ll 1$ . Compared to previous sections, for mathematical clarity, we also switch from following the frequency  $p_t$  of  $A_1$  to following the frequency  $q_t$  of  $A_2$ . Of course, this is without loss of generality. The change in frequency of  $A_2$  due to selection can be written as

$$\Delta_S q_t = \frac{\bar{w}_2 - \bar{w}_1}{\bar{w}} p_t q_t \approx -hsq_t. \quad (6.42)$$

This approximation can be found by assuming that  $q^2 \approx 0$ ,  $p \approx 1$ , and that  $\bar{w} \approx w_1$ . All of these assumptions make sense if  $q \ll 1$ . From eqn. (6.42) we see that selection acts to reduce the frequency of  $A_2$  (as both  $h$  and  $s$  are positive), and it does so geometrically across the generations. That is, if the initial frequency of  $A_2$  is  $q_0$ , then its frequency at time  $t$  is approximately

$$q_t = q_0(1 - hs)^t. \quad (6.43)$$

We will now consider the change in frequency induced by mutation. Recalling that  $\mu$  is the mutation rate from  $A_1$  to  $A_2$  per generation, the frequency of  $A_2$  after mutation is

$$q' = \mu p_t + q_t = \mu(1 - q_t) + q_t. \quad (6.44)$$

Assuming that  $\mu \ll 1$  and that  $q \ll 1$ , the change in the frequency of allele  $A_2$  due to mutation ( $\Delta_M q_t$ ) can be approximated by

$$\Delta_M q_t = q' - q_t = \mu. \quad (6.45)$$

Hence, when  $A_2$  is rare and the mutation rate is low, mutation acts to linearly increase the frequency of the deleterious allele  $A_2$ .

If selection is to balance deleterious mutation, their combined effect over one generation has to be zero. Therefore, to find the mutation–selection equilibrium, we set

$$\Delta_M q_t + \Delta_S q_t = 0, \quad (6.46)$$

insert eqns. (6.42) and (6.45), and solve for  $q$  to obtain

$$q_e = q_t = \frac{\mu}{hs}. \quad (6.47)$$

We see that the frequency of the deleterious allele  $A_2$  is balanced at a frequency equal to the mutation rate ( $\mu$ ) divided by the reduction in relative fitness in the heterozygote ( $hs$ ).

It is worth pointing out that the fitness of the  $A_2 A_2$  homozygote has not entered this calculation, as  $A_2$  is so rare that it is hardly ever found in the homozygous state. Therefore, if  $A_2$  has any deleterious effect in a heterozygous state (i.e. if  $h > 0$ ), it is this effect that determines the frequency at which  $A_2$  is maintained in the population. Also, note that by writing the total change in allele frequency as  $\Delta_M q_t + \Delta_S q_t$  we have implicitly assumed that we can ignore terms of order  $\mu \times s$ . That is, we have assumed that mutation and selection are both relatively weak. This assumption is valid under our prior assumption that both  $\mu$  and  $s$  are small.

If an allele is truly recessive (although few likely are), we have  $h = 0$ , and so eqn. (6.47) is not valid. However, we can make an argument similar to the one above to show that, for truly recessive alleles,

$$q_e = \sqrt{\frac{\mu}{s}}. \quad (6.48)$$

**Question 11.** Oblong-winged katydids (*Amblycorypha oblongifolia*) are usually green. However, some are bright pink, thanks to an erythrism mutation (a nice example of early Mendelian reasoning in a wonderfully titled paper<sup>2</sup>). This pink condition is thought to be due to a dominant mutation (Crew, 2013). Assume that roughly one in ten thousand katydids is bright pink and that the mutation rate at the gene underlying this condition is  $10^{-5}$ . What is the relative fitness of heterozygotes for the pink mutation?



Figure 6.20: Oblong-winged katydid. Field book of insects (1918). Lutz, F.E. Image from the Biodiversity Heritage Library. Contributed by MBLWHOI Library. Not in copyright.

<sup>2</sup> WHEELER, W. M., 1907 Pink Insect Mutants. The American Naturalist 41(492): 773–780

*The genetic load of deleterious alleles* What effect do such deleterious mutations at mutation–selection balance have on the population? It is common to quantify the effect of deleterious alleles in terms of a reduction of the mean relative fitness of the population. For a single site at which a deleterious mutation is segregating at frequency  $q_e = \mu/(hs)$ , the population mean relative fitness is reduced to

$$\bar{w} = 1 - 2p_e q_e hs - q_e^2 s \approx 1 - 2\mu. \quad (6.49)$$

Somewhat remarkably, the drop in mean fitness due to a site segregating at mutation–selection balance is independent of the selection coefficient against the heterozygote; it depends only on the mutation rate. Intuitively this is because, given a fixed mutation rate, less deleterious alleles can rise to a higher equilibrium frequency, and thus contribute the same total load as more deleterious (rarer) alleles, but this load is spread across more individuals in the population. Note that this result applies only if the mutation is not totally recessive, i.e. if  $h > 0$ .

A fitness reduction of  $2\mu$  is very small, given that the mutation rate of a gene is likely  $< 10^{-5}$ . However, if there are many loci segregating at mutation–selection balance, small fitness reductions can accumulate to a substantial so-called genetic load, a major cause of variation in fitness-related traits among individuals. For example, the human genome contains over twenty thousand genes, and many other functional regions, the vast majority of which will be subject to purifying selection against mutations that disrupt their function. In humans, most loss of function (LOF) variants, which severely disrupt a protein-coding gene, are found at low frequencies. However, each human genome typically carries over a hundred LOF variants (MACARTHUR *et al.*, 2012; LEK *et al.*, 2016). Not every LOF allele will be deleterious; some could even be advantageous. However, the combined load of these LOF alleles must on average lower our fitness, otherwise selection wouldn't be removing them from the population. Each one of us carries a unique set of these LOF alleles, usually in a heterozygous state. We differ slightly in how many of these alleles we carry. For example, the left side of Figure 6.21 shows the distribution of the number of LOF alleles carried by 769 individuals of Dutch ancestry. The individuals who carry fewer of these LOF alleles will on average have higher fitness than those individuals with more.

How do these differences across individuals in total LOF mutations mount up? Well, if we are willing to assume that the fitness costs of deleterious alleles interact multiplicatively, we can make some progress. If an individual who carries one LOF mutation has a fitness  $1 - hs$ , then an individual who's heterozygote for two LOF mutations would have fitness  $(1 - hs)^2$ , and an individual who is heterozygote

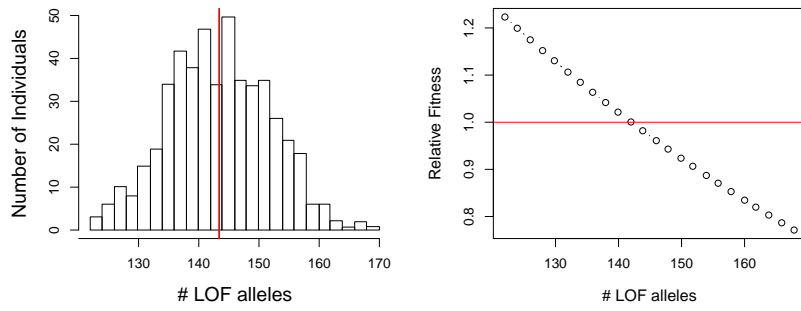


Figure 6.21: **Left)** The distribution of LOF alleles in 769 individuals from the Genome of the Netherlands project. Data from FRANCIOLI *et al.*. The average individual (red line) carries 144 LOF alleles. **Right).** The relative fitness of individuals carrying these varying numbers of LOF alleles, assuming multiplicative selection and a selection coefficient of  $sh = 10^{-2}$  acting against these alleles (CASSA *et al.*, 2017). Code here.

for  $L$  LOF alleles would have fitness  $(1 - hs)^L$ . The right-hand side of Figure 6.21 shows the predicted fitness of individuals carrying varying number of LOF alleles, relative to the mean fitness of the sample, using this multiplicative model. We don't yet know how much lower the fitness of these individuals really is, nor do we know how most of these LOF alleles manifest their fitness consequences through disease and other mechanisms. However, it's a reasonable guess that this variation in LOF alleles, presumably maintained by mutation-selection balance, is a major source of variation in fitness.

### 6.0.6 Inbreeding depression

All else being equal, eqn. (6.47) suggests that mutations that have a smaller effect in the heterozygote can segregate at higher frequency under mutation-selection balance. As a consequence, alleles that have strongly deleterious effects in the homozygous state can still segregate at low frequencies in the population, as long as they do not have too strong a deleterious effect in heterozygotes. Thus, outbred populations may have many alleles with recessive deleterious effects segregating within them.

**Question 12.** Assume that a deleterious allele has a relative fitness .99 in heterozygotes and a relative fitness 0.2 when present in the homozygote state. Assume that the deleterious allele is at a frequency  $10^{-3}$  at birth and the genotype frequencies follow from HWE. Only considering the fitness effects of this locus, and measuring fitness relative to the most fit genotype, answer the following questions:

- A)** What is the average fitness of an individual in the population?
- B)** What is the average fitness of the child of a full-sib mating?

One consequence of segregating for low-frequency recessive deleterious alleles is that inbreeding can reduce fitness. In typically outbred populations, the mean fitness of individuals decreases with the in-

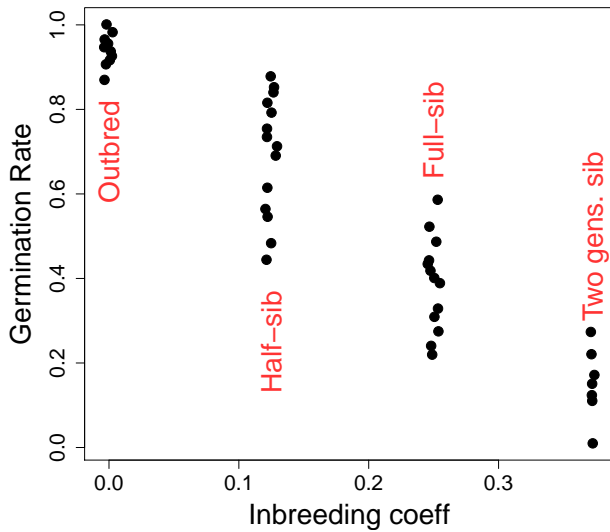


Figure 6.22: Data showing inbreeding depression over different degrees of inbreeding in *S. latifolia*. Each point is the mean seed germination rates for different family crosses. Data from RICHARDS. Code here.

breeding coefficient, i.e. so-called 'inbreeding depression' is a common observation. This wide-spread observation dates back to systematic surveys of inbreeding depression by DARWIN (1876). Inbreeding depression is likely primarily a consequence of being homozygous at many loci for alleles with recessive deleterious effects.

One example of inbreeding depression is shown in Figure 6.22. White campion (*Silene latifolia*) is a dioecious flowering plant; dioecious means that the males and females are separate individuals. RICHARDS performed crosses to create offspring who were outbred, the offspring of half-sibs, full-sibs, and of two generations of full-sib mating. He measured their germination success, which is plotted in Figure 6.22. Note how the fitness of individuals declines with increased inbreeding.

*Purging the inbreeding load.* Populations that regularly inbreed over sustained periods of time are expected to partially purge this load of deleterious alleles. This is because such populations have exposed many of these alleles in a homozygous state, and so selection can more readily remove these alleles from the population.

If the population has sustained inbreeding, such that individuals in the population have an inbreeding coefficient  $F$ , deleterious alleles at each locus will find a new equilibrium frequency. Assuming the mutation-selection model, now with inbreeding, the equilibrium frequency is

$$q_e = \frac{\mu}{(h(1 - F) + F)s} \quad (6.50)$$

The frequency of the deleterious allele is decreased due to the al-

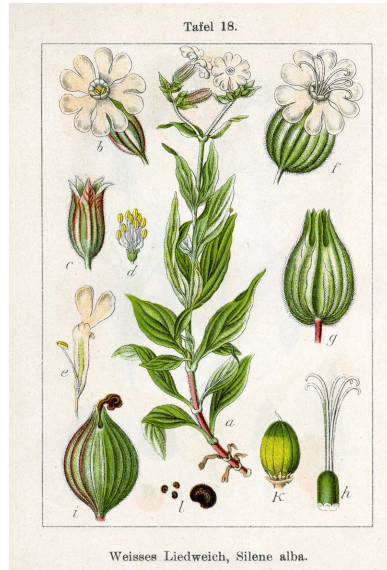


Figure 6.23: White campion (*S. latifolia*).  
Deutschlands Flora in Abbildungen (1796).  
Johann Georg Sturm (Painter: Jacob Sturm).  
Public Domain, wikimedia.

lele now being expressed in homozygotes, and therefore exposed to selection, more often due to inbreeding. Thus, all else being equal, populations with a high degree of inbreeding will purge their load.

#### 6.0.7 Migration-selection balance

Another reason for the persistence of deleterious alleles in a population is that there is a constant influx of maladaptive alleles from other populations where these alleles are locally adaptive. Migration-selection balance seems unlikely to be as broad an explanation for the persistence of deleterious alleles genome-wide as mutation-selection balance. However, a brief discussion of such alleles is worthwhile, as it helps to inform our ideas about local adaptation.

Local adaptation can occur over a range of geographic scales. Local adaptation is relatively unimpeded by migration at broad geographically scales, where selection pressures change more slowly than distances over which individuals typically migrate over a number of generations. Adaptation can, however, potentially occur on much finer geographic scales, from kilometers down to meters in some species. On such small scales, dispersal is surely rapidly moving alleles between environments, but local adaptation is maintained by the continued action of selection. An example of adaptation at fine-scales is shown in Figure 6.25 . JAIN and BRADSHAW (1966) studied the patterns of heavy-metal resistance in plants on mine tailings and in nearby meadows, a set of classic studies of population differences maintained by local adaptation to different soils. Even at these very short geo-



Figure 6.24: Sweet vernal grass (*Anthoxanthum odoratum*).  
Billeder af nordens flora (1917). Mentz, A & Ostenfeld, C H. Image from the Biodiversity Heritage Library. Contributed by New York Botanical Garden. Not in copyright.

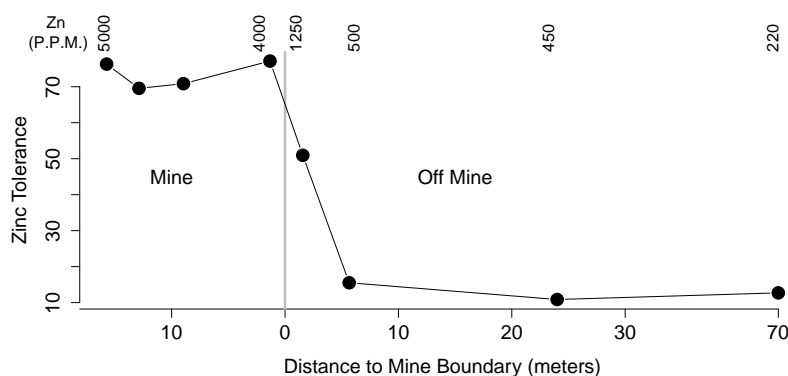


Figure 6.25: Data showing the Zinc tolerance of *Anthoxanthum odoratum* on and off of the Trelogan Mine, Flintshire, North Wales. The numbers along the top give the soil contamination of Zinc in parts per million. Data from JAIN and BRADSHAW (1966). Code here.

ically scales, over which seed and pollen will definitely move, we see strong local adaptation. Zinc-intolerant alleles are nearly absent from the mine tailings because they prevent plants from growing on these zinc-heavy soils; conversely, zinc-tolerant alleles do not spread into the meadow populations, likely due to some trade-off or fitness cost of

zinc-tolerance.

As a first pass at developing a model of local adaptation, let's consider a haploid two-allele model with two different populations, see Figure 6.26, where the relative fitnesses of our alleles are as follows

| allele       | 1   | 2   |
|--------------|-----|-----|
| population 1 | 1   | 1-s |
| population 2 | 1-s | 1   |

As a simple model of migration, let's suppose within a population a fraction of  $m$  individuals are migrants from the other population, and  $1 - m$  individuals are from the same population.

To quickly sketch an equilibrium solution to this scenario, we'll take an approach analogous to our mutation-selection balance model. To do this, let's assume that selection is strong compared to migration ( $s \gg m$ ), such that allele 1 will be almost fixed in population 1 and allele 2 will be almost fixed in population 2. If that is the case, migration changes the frequency of allele 2 in population 1 ( $q_1$ ) by

$$\Delta_{Mig.} q_1 \approx m \quad (6.51)$$

while as noted above  $\Delta_S q_1 = -sq_1$ , so that migration and selection are at an equilibrium when  $0 = \Delta_S q_1 + \Delta_{Mig.} q_1$ , i.e. an equilibrium frequency of allele 2 in population 1 of

$$q_{e,1} = \frac{m}{s} \quad (6.52)$$

Here, migration is playing the role of mutation and so migration-selection balance (at least under strong selection) is analogous to mutation-selection balance.

We can use this same model by analogy for the case of migration-selection balance in a diploid model. For the diploid case, we replace our haploid  $s$  by the cost to heterozygotes  $hs$  from our directional selection model, resulting in a diploid migration-selection balance equilibrium frequency of

$$q_{e,1} = \frac{m}{hs} \quad (6.53)$$

As an example of fine-scale local adaptation due to a single locus, consider the case of the rock pocket mice adapting to lava flows. Throughout the deserts of the American Southwest there are old lava flows, where the rocks and soils are much dark than the surrounding desert.

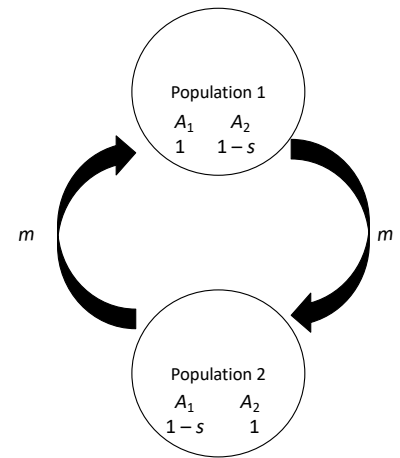


Figure 6.26: Setup of a two-population haploid model of local adaptation.

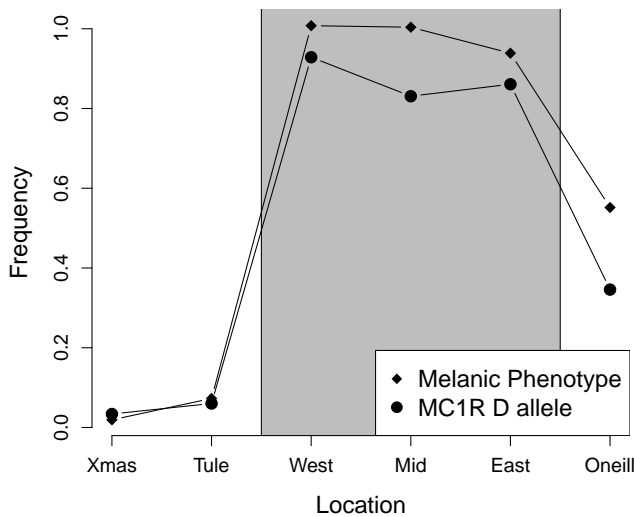


Figure 6.27: Frequency of melanic mice on the lava flow, and at nearby locations (diamonds). Frequency of MC1R melanic allele at same locations. Data from HOEKSTRA *et al.* (2004). Code here.

Many populations of small animals that live on these flows have evolved darker pigmentation to be cryptic against this dark substrate and better avoid visual predators. One example of such a locally adapted population are the rock pocket mice (*Chaetodipus intermedius*) who live on the Pinacate lava flow on the Arizona-Mexico border, studied by HOEKSTRA *et al.* (2004). These mice have much darker, more melanic pelts than the mice who live on nearby rocky outcrops (see Figure 6.27). NACHMAN *et al.* (2003) determined that a dominant allele (*D*) at MC1R is the primary determinant of this melanic phenotype. The frequency of this allele across study sites is shown in Figure 6.27. HOEKSTRA *et al.* (2004) found that other, unlinked markers showed little differentiation over these populations, suggesting that the migration rate is high.

**Question 13.** HOEKSTRA *et al.* (2004) found that the dark *D* allele was at 3% frequency at the Tule Mountains study site. Using  $F_{ST}$ -based approaches, for unlinked markers, they estimated that the per individual migration rate was  $m = 7.0 \times 10^{-4}$  per generation between this site and the Pinacate lava flow. What is the selection coefficient acting against the dark *D* allele at the Tule Mountains site?

*The width of a genetic cline.* We can also extend these ideas beyond our discrete model to a model of a population spread out on a land-



Figure 6.28: Two species from the genus *Chaetodipus*, pocket mice, formerly known as *Perognathus*. Wild animals of North America, intimate studies of big and little creatures of the mammal kingdom (1918), Nelson, E. W. Image from the Biodiversity Heritage Library. Contributed by American Museum of Natural History Library. Not in copyright.

scape where individuals migrate in a more continuous fashion. For simplicity, let's assume a one dimensional habitat, where the habitat makes a sharp transition in the middle of our region. You could imagine this to be a set of populations sampled along a transect through some environmental transition. Our individuals disperse to live on average  $\sigma$  miles away from where they were born (we can think of this as our individuals migrating a random distance drawn from a normal distribution, with mean zero, and  $\sigma$  being the standard deviation of this distribution). . We'll think of a bi-allelic model where the homozygotes for allele 1 have an additive selective advantage  $s$  over allele 2 homozygotes to the east of our habitat transition (left of zero in Figure 6.29). This flips to allele 2 having the same advantage  $s$  west of the transition (right of zero). If you've read this send Prof Coop a picture of the East and West Beast.

"Upon an island hard to reach, the East Beast sits upon his beach. Upon the west beach sits the West Beast. Each beach beast thinks he's the best beast." – Theodor Seuss Geisel

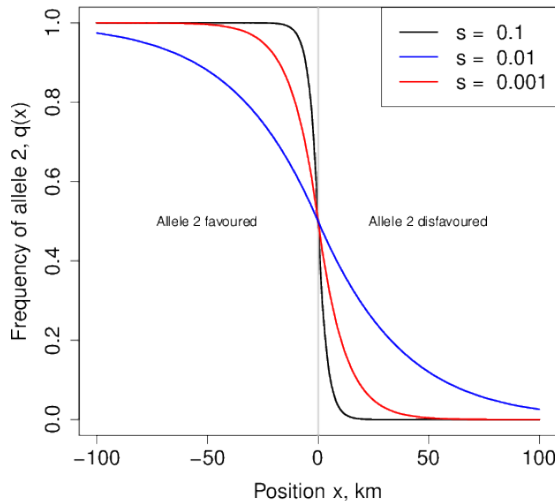


Figure 6.29: An equilibrium cline in allele frequency (the frequency of allele 2,  $q(\cdot)$ ) is shown). Our individuals disperse an average distance of  $\sigma = 1$  miles per generation, and our allele 2 has a relative fitness of  $1 + s$  and  $1 - s$  on either side of the environmental change at  $x = 0$ . Code here.

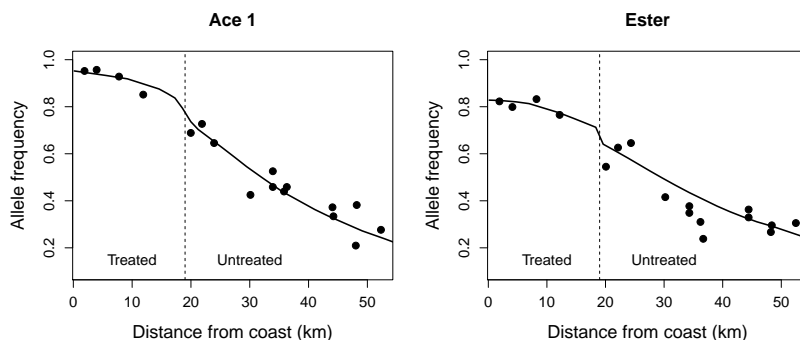
With this setup, we get an equilibrium distribution of our two alleles, where to the left of zero our allele 2 is at higher frequency, while to the right of zero allele 1 predominates. As we cross from the left to the right side of our range, the frequency of our allele 2 decreases in a smooth cline. The frequency of allele 2,  $q(\cdot)$ , is shown as a function of location along the cline for a variety of selection coefficients ( $s$ ) in Figure 6.29. The width of this cline, i.e. the geographic distance over which the allele frequency changes, depends on the relative strengths of dispersal and selection. If selection is strong compared to dispersal, then selection acts to remove maladaptive alleles much faster than migration acts to move alleles across the environmental transition. Thus the allele frequency transition would be very rapid, and the cline

narrow, as we move across the environmental transition. In contrast, if individuals disperse long distances and selection is weak, many alleles are being moved back and forth over the environmental transition much faster than selection can act against these alleles and so the cline would be very wide.

The width of our cline, i.e. the distance over which we make this shift from allele 2 to allele 1 predominating, can be defined in a number of different ways. One way to define the cline width, which is simple to define but perhaps hard to measure accurately, is via the slope (i.e. the tangent) of  $q(x)$  at  $x = 0$ . See Figure 6.30. Under this definition, the cline width is approximately

$$0.6\sigma/\sqrt{s} \text{ miles}, \quad (6.54)$$

note that the units are miles here just because we defined the average dispersal distance ( $\sigma$ ) in miles above. Thus the cline will be wider if individuals disperse further, higher  $\sigma$ , and if selection is weaker, smaller  $s$ . The appendix below talks through the math underlying these ideas in more detail.



LENORMAND *et al.* (1999) collected mosquitoes (*Culex pipiens*) in a north–south transect moving away from the Southern French coast. Areas near the coast were treated with pesticides, and the mosquitos have evolved resistance, but areas just a few tens of kilometers from the coast were untreated. LENORMAND *et al.* estimated the frequency of two unlinked, pesticide-resistance alleles, and found them at high frequency near the coast but found that their frequencies declined rapidly moving inland. LENORMAND *et al.* fit migration-selection cline models to their data, similar to those in Figure 6.29, with the pesticide-resistance alleles having an selection advantage ( $s$ ) in treated areas an a cost ( $c$ ) in untreated areas (they didn't enforce the selective advantage and cost being symmetric).

They estimated that a higher selective advantage for the Ace 1 allele than Ester allele ( $s = 0.33$  and  $s = 0.19$  respectively) and a

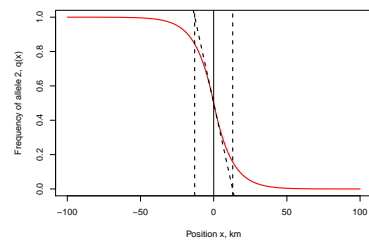


Figure 6.30: An equilibrium cline in allele frequency from Figure 6.29,  $s = 0.01$ . Vertical lines show the cline width. The diagonal line show the tangent to the cline at its midpoint. Code here.

Figure 6.31: Allele frequency clines of two pesticide resistance alleles, at the Ace 1 and Ester genes, in the mosquito *Culex pipiens*. The dotted line shows where we move from pesticide-treated to untreated areas as we move away from the French coast. The dots show observed allele frequencies, the solid lines clines fit under a migration-selection balance model of a cline. These allele frequencies represent collections over two summers, the frequencies of the alleles are substantially reduced in the winter due to the reduced use of pesticides. Data from LENORMAND *et al.* (1999). Code here.

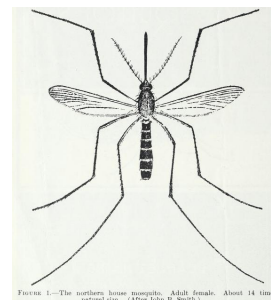


Figure 6.32: mosquito (*Culex pipiens*). Domestic mosquitoes (1939), Bishopp, F. C. Image from the Biodiversity Heritage Library. Contributed by U.S. Department of Agriculture, National Agricultural Library. Not in copyright.

higher cost to the Ace 1 allele than Ester allele in untreated areas ( $c = 0.11$  and  $c = 0.7$  respectively) potentially explaining the less extreme cline for Ester allele than the Ace 1 allele. Despite these strong selection pressures we still see a cline over tens of kilometers because dispersal is relatively high ( $\sigma = 6.6\text{km}$  per generation).

*Appendix: Some theory of the spatial distribution of allele frequencies under deterministic models of selection*

Imagine a continuous haploid population spread out along a line. Each individual disperses a random distance  $\Delta x$  from its birthplace to the location where it reproduces, where  $\Delta x$  is drawn from the probability density  $g(\cdot)$ . To make life simple, we will assume that  $g(\Delta x)$  is normally distributed with mean zero and standard deviation  $\sigma$ , i.e. migration is unbiased and individuals migrate an average distance of  $\sigma$ .

The frequency of allele 2 at time  $t$  in the population at spatial location  $x$  is  $q(x, t)$ . Assuming that only dispersal occurs, how does our allele frequency change in the next generation? Our allele frequency in the next generation at location  $x$  reflects the migration from different locations in the proceeding generation. Our population at location  $x$  receives a contribution  $g(\Delta x)q(x + \Delta x, t)$  of allele 2 from the population at location  $x + \Delta x$ , such that the frequency of our allele at  $x$  in the next generation is

$$q(x, t+1) = \int_{-\infty}^{\infty} g(\Delta x)q(x + \Delta x, t)d\Delta x. \quad (6.55)$$

To obtain  $q(x + \Delta x, t)$ , let's take a Taylor series expansion of  $q(x, t)$ :

$$q(x + \Delta x, t) = q(x, t) + \Delta x \frac{dq(x, t)}{dx} + \frac{1}{2}(\Delta x)^2 \frac{d^2q(x, t)}{dx^2} + \dots \quad (6.56)$$

then

$$q(x, t+1) = q(x, t) + \left( \int_{-\infty}^{\infty} \Delta x g(\Delta x) d\Delta x \right) \frac{dq(x, t)}{dx} + \frac{1}{2} \left( \int_{-\infty}^{\infty} (\Delta x)^2 g(\Delta x) d\Delta x \right) \frac{d^2q(x, t)}{dx^2} + \dots \quad (6.57)$$

Because  $g(\cdot)$  has a mean of zero,  $\int_{-\infty}^{\infty} \Delta x g(\Delta x) d\Delta x = 0$ , and has because  $g(\cdot)$  has variance  $\sigma^2$ ,  $\int_{-\infty}^{\infty} (\Delta x)^2 g(\Delta x) d\Delta x = \sigma^2$ . All higher order terms in our Taylor series expansion cancel out (as all high moments of the normal distribution are zero). Looking at the change in allele frequency,  $\Delta q(x, t) = q(x, t+1) - q(x, t)$ , so

$$\Delta q(x, t) = \frac{\sigma^2}{2} \frac{d^2q(x, t)}{dx^2} \quad (6.58)$$

This is a diffusion equation, so that migration is acting to smooth out allele frequency differences with a diffusion constant of  $\frac{\sigma^2}{2}$ . This is exactly analogous to the equation describing how a gas diffuses out to equal density, as both particles in a gas and our individuals of type 2 are performing Brownian motion (blurring our eyes and seeing time as continuous).

We will now introduce fitness differences into our model and set the relative fitnesses of allele 1 and 2 at location  $x$  to be 1 and  $1 + s\gamma(x)$ . To make progress in this model, we'll have to assume that selection isn't too strong, i.e.  $s\gamma(x) \ll 1$  for all  $x$ . The change in frequency of allele 2 obtained within a generation due to selection is

$$q'(x, t) - q(x, t) \approx s\gamma(x)q(x, t)(1 - q(x, t)) \quad (6.59)$$

i.e. logistic growth of our favoured allele at location  $x$ . Putting our selection and migration terms together, we find the total change in allele frequency at location  $x$  in one generation is

$$q(x, t+1) - q(x, t) = s\gamma(x)q(x, t)(1 - q(x, t)) + \frac{\sigma^2}{2} \frac{d^2q(x, t)}{dx^2} \quad (6.60)$$

In deriving this result, we have essentially assumed that migration acted upon our original allele frequencies before selection, and in doing so have ignored terms of the order of  $\sigma s$ .

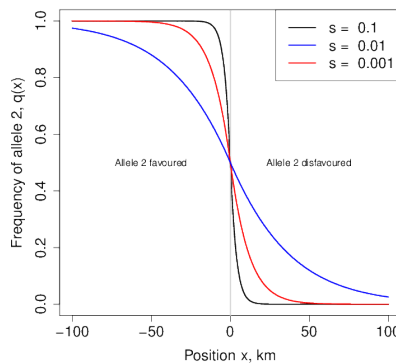


Figure 6.33: An equilibrium cline in allele frequency. Our individuals disperse an average distance of  $\sigma = 1$  km per generation, and our allele 2 has a relative fitness of  $1 + s$  and  $1 - s$  on either side of the environmental change at  $x = 0$ .

*The cline in allele frequency associated with a sharp environmental transition.* To make progress, let's consider a simple model of local adaptation where the environment abruptly changes. Specifically, we assume that  $\gamma(x) = 1$  for  $x < 0$  and  $\gamma(x) = -1$  for  $x \geq 0$ , i.e. our allele 2 has a selective advantage at locations to the left of zero, while this allele is at a disadvantage to the right of zero. In this case we can get an equilibrium distribution of our two alleles, where to the left of zero

our allele 2 is at higher frequency, while to the right of zero allele 1 predominates. As we cross from the left to the right side of our range, the frequency of our allele 2 decreases in a smooth cline.

Our equilibrium spatial distribution of allele frequencies can be found by setting the left-hand side of eqn. (6.60) to zero to arrive at

$$s\gamma(x)q(x)(1-q(x)) = -\frac{\sigma^2}{2} \frac{d^2q(x)}{dx^2} \quad (6.61)$$

We then could solve this differential equation with appropriate boundary conditions ( $q(-\infty) = 1$  and  $q(\infty) = 0$ ) to arrive at the appropriate functional form for our cline. While we won't go into the solution of this equation here, we can note that by dividing our distance  $x$  by  $\ell = \sigma/\sqrt{s}$ , we can remove the effect of our parameters from the above equation. This compound parameter  $\ell$  is the characteristic length of our cline, and it is this parameter which determines over what geographic scale we change from allele 2 predominating to allele 1 predominating as we move across our environmental shift.

# 7

## *The Impact of Genetic Drift on Selected Alleles*

“Natural selection is a mechanism for generating an exceedingly high degree of improbability.” –R.A. Fisher

In the previous chapter we assumed that the selection acting on our alleles was strong enough that we could ignore the action of genetic drift in shaping allele frequencies. However, genetic drift affects all alleles, and so in this chapter we explore the interaction of selection and drift. Strongly selected alleles can be lost from the population via drift when they are rare in the population, while both weakly beneficial and weakly deleterious alleles are subject to the random whims of genetic drift throughout their entire time in the population. Understanding the interaction of selection and genetic drift is key to understanding the extent to which small populations may be mutation-limited in their rates of adaptation, and how rates of molecular and genome evolution may differ across taxa.

### *7.1 Stochastic loss of strongly selected alleles*

Even strongly beneficial alleles can be lost from the population when they are sufficiently rare. This is because the number of offspring left by individuals to the next generation is fundamentally stochastic. A selection coefficient of  $s=1\%$  is a strong selection coefficient, which can drive an allele through the population in a few hundred generations once the allele is established. However, if individuals have on average a small number of offspring per generation, the first individual to carry our beneficial allele, who has on average 1% more children than their peers, could easily have zero offspring, leading to the loss of our allele before it ever gets a chance to spread.

To take a first stab at this problem, let’s think of a very large haploid population in which a single individual starts with the selected allele, and ask about the probability of eventual loss of our selected allele starting from this single copy. To derive this probability of loss ( $p_L$ ), we’ll make use of a simple argument (derived from branching

processes FISHER, 1923; HALDANE, 1927). Our selected allele will be eventually lost from the population if every individual with the allele fails to leave descendants. Well we can think about different cases:

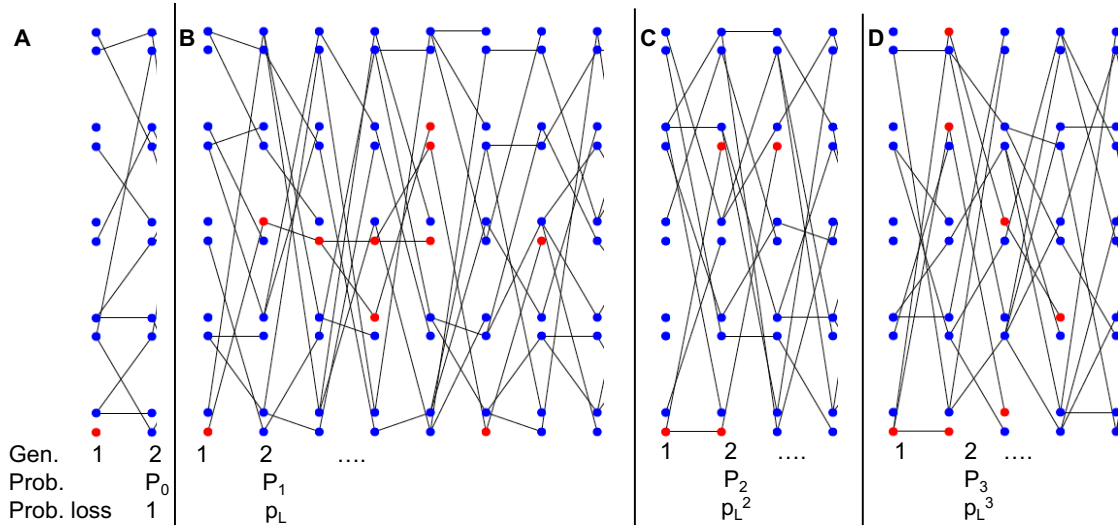


Figure 7.1: Four different outcomes of a selected allele present as a single copy in the population, leaving zero, one, two, three offspring in the next generation.

1. In our first generation, with probability  $P_0$  our individual allele leaves no copies of itself to the next generation, in which case our allele is lost (Figure 7.1A).
2. Alternatively, our allele could leave one copy of itself to the next generation (with probability  $P_1$ ), in which case with probability  $p_L$  this copy eventually goes extinct (Figure 7.1B).
3. Our allele could leave two copies of itself to the next generation (with probability  $P_2$ ), in which case with probability  $p_L^2$  both of these copies eventually go extinct (Figure 7.1C).
4. More generally, our allele could leave  $k$  copies ( $k > 0$ ) of itself to the next generation (with probability  $P_k$ ), in which case with probability  $p_L^k$  all of these copies eventually go extinct (e.g. Figure 7.1D).

Summing over these probabilities, we see that

$$p_L = \sum_{k=0}^{\infty} P_k p_L^k \quad (7.1)$$

We'll now need to specify  $P_k$ , the probability that an individual carrying our selected allele has  $k$  offspring. In order for this population to stay constant in size, we'll assume that individuals without the selected mutation have on average one offspring per generation, while

individuals with our selected allele have on average  $1 + s$  offspring per generation. We'll assume that the number of offspring an individual has is Poisson distributed with mean given by 1 or  $1 + s$ , i.e. the probability that an individual with the selected allele has  $i$  children is

$$P_i = \frac{(1+s)^i e^{-(1+s)}}{i!} \quad (7.2)$$

Substituting  $P_k$  into the equation above, we see

$$\begin{aligned} p_L &= \sum_{k=0}^{\infty} \frac{(1+s)^k e^{-(1+s)}}{k!} p_L^k \\ &= e^{-(1+s)} \left( \sum_{k=0}^{\infty} \frac{(p_L(1+s))^k}{k!} \right) \end{aligned} \quad (7.3)$$

The term in the brackets is itself an exponential expansion, so we can rewrite this equation as

$$p_L = e^{(1+s)(p_L - 1)} \quad (7.4)$$

Solving for  $p_L$  would give us our probability of loss for any selection coefficient. Let's rewrite our result in terms of the probability of escaping loss,  $p_F = 1 - p_L$ . We can rewrite eqn. (7.4) as

$$1 - p_F = e^{-p_F(1+s)} \quad (7.5)$$

To gain an approximate solution for this result, let's consider a small selection coefficient  $s \ll 1$  such that  $p_F \ll 1$  and then use a Taylor series to expand out the exponential on the right hand side (ignoring terms of higher order than  $s^2$  and  $p_F^2$ ):

$$1 - p_F \approx 1 - p_F(1 + s) + p_F^2(1 + s)^2/2 \quad (7.6)$$

Solving this we find that

$$p_F = 2s. \quad (7.7)$$

Thus even an allele with a 1% selection coefficient has a 98% probability of being lost when it is first introduced into the population by mutation.

If the mutation rate towards our advantageous allele is  $\mu$ , and there are  $N$  individuals in our haploid population, then  $N\mu$  advantageous mutations arise per generation. Each of these new beneficial mutations has a probability  $p_F$  of fixing. Thus the number of advantageous mutations arising per generation that will eventually fix in the population is  $N\mu p_F$ , and the waiting time for a mutation that will fix to arise is the reciprocal of this:  $1/N\mu p_F$ . Thus, in adapting to a novel selection pressure via new mutations, the population size, the mutational target size, and the selective advantage of new mutations all matter. One

reason why combinations of drugs are used against viruses like HIV and malaria is that, even if the viruses adapt to one of the drugs, the viral load ( $N$ ) of the patient is greatly reduced, making it very unlikely that the population will manage to fix a second drug-resistant allele.

*Diploid model of stochastic loss of strongly selected alleles.* We can also adapt this result to a diploid setting. Assuming that heterozygotes for the 1 allele have on average  $1 + hs$  children, the probability allele 1 is not lost, starting from a single copy in the population, is

$$p_F = 2hs \quad (7.8)$$

for  $h > 0$ . Note this is a slightly different parameterization from our diploid model in the previous chapter; here  $h$  is the dominance of our positively selected allele, with  $h = 1$  corresponding to the full selective advantage expressed in an individual with only a single copy. Thus the probability that a beneficial allele is not lost depends just on the relative fitness advantage of the heterozygote; this is because when the allele is rare it is usually present in heterozygotes and so its probability of escaping loss just depends on the fitness of these individuals compared to homozygotes for the ancestral allele (assuming an outbred population).

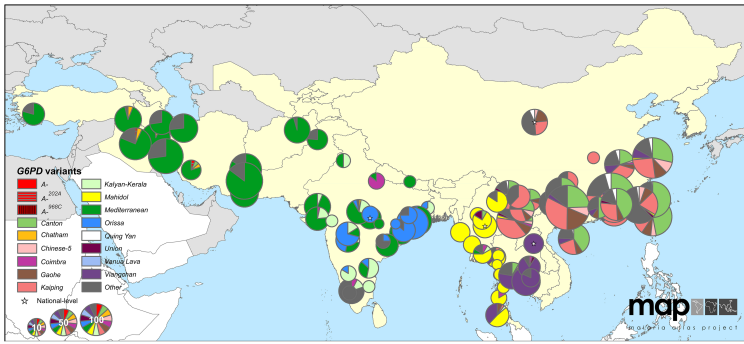


**Figure 7.2: Map of G6PD-deficiency allele frequencies across Asia.** The pie chart shows the frequency of G6PD-deficiency alleles. The size of the pie chart indicates the number of G6PD-deficient individuals sampled. Countries with endemic malaria are colored yellow. Figure from HOWES *et al.* (2013), licensed under CC BY 4.0.

Over roughly the past ten thousand years, adaptive alleles conferring resistance to malaria have arisen in a number of genes and spread through human populations in areas where malaria is endemic (KWIATKOWSKI, 2005). One particularly impressive case of convergent evolution in response to selection pressures imposed by malaria are the numerous changes throughout the G6PD gene, which include at least 15 common variants in Central and Eastern Asia alone that lower the activity of the enzyme (HOWES *et al.*, 2013). These alleles are now found at a combined frequency of around 8% frequency in malaria endemic areas, rarely exceeding 20% (HOWES

*et al.*, 2012). Whether these variants *all* confer resistance to malaria is unknown, but a number of these alleles have demonstrated effects against malaria and are thought to have a selective advantage to heterozygotes  $sh > 5\%$  where malaria is endemic (RUWENDE *et al.*, 1995; TISHKOFF *et al.*, 2001; LOUICHAROEN *et al.*, 2009).

With a 5% advantage in heterozygotes, a G6PD allele present as a single copy would only have a 10% probability of fixing in the population. If that's so, how come malaria adaptation has repeatedly occurred via changes at G6PD? Well, maybe adaptation didn't start from a single copy of the selected allele. How many copies of the G6PD-deficiency alleles do we expect were segregating in the population before selection pressures changed?

In the absence of malaria, these G6PD alleles are deleterious with carriers suffering from G6PD deficiency, leading to hemolytic anemia when individuals are exposed to a variety of different compounds, notably those present in fava beans. There's upward of one hundred bases where G6PD-deficiency alleles can arise, so assuming a mutation rate of  $\approx 10^{-8}$  per base pair per generation, we can roughly estimate the rate of mutations arising that affect the G6PD gene as  $\mu \approx 10^{-6}$  per generation. In the absence of malaria, the selective cost of being a heterozygote carrier of a G6PD-deficient allele must have been on the order of 5% or more, and thus the frequency of the allele under mutation-selection balance would have been  $\approx 10^{-6}/0.05 = 2 \times 10^{-5}$ .

Assuming an effective population size of 2 – 20 million individuals, roughly five to ten thousand years ago that means that there would have been forty to four hundred copies of the G6PD-deficiency allele present in the population when selection pressures shifted at the introduction of malaria. The chance that one of these newly adaptive alleles is lost is 90% but the chance that they're all lost is  $< (0.9)^{40} \approx 0.02$ , i.e. there would have been a greater than 98% chance that adaptation would occur via one or more alleles at G6PD. How many alleles would escape drift? Well with 40 – 400 copies of the allele pre-malaria, and each of them having a 10% probability of escaping drift, we expect between 4 and 40 G6PD alleles to escape drift and contribute to adaptation. We see 15 common G6PD alleles in Eurasia, so our simple model of adaptation from mutation-selection balance seems reasonable.

**Question 1.** ‘Haldane’s sieve’ is the name for the idea that the mutations that contribute to adaptation are likely to be dominant or at least co-dominant.

**A)** Briefly explain this argument with a verbal model relating to the results we've developed in the last two chapters.

**B)** Haldane’s sieve is thought to be less important for adaptation from previously deleterious standing variation, than adaptation from



Figure 7.3: Pythagoras's “just say no to fava beans” campaign. Pythagoras prohibited the consumption of fava beans by his followers; perhaps because favism, the anemia induced in G6PD-deficient individuals by fava beans, is relatively common in the Mediterranean due to adaptation to endemic malaria. French early 16th Century. Woodner Collection, National Gallery of Art. Public Domain, wikimedia.

A full analysis of this case requires modeling of G6PD's X chromosome inheritance, and the randomness in the number of copies of the allele present at mutation-selection balance (RALPH and COOP, 2015).



Figure 7.4: Haldane’s sieve. To our knowledge Haldane never wore a sieve, but we assume he owned one. Sieve, Flickr licensed under CC BY 2.0. Haldane, Public Domain, wikimedia.

new mutation. Can you explain the intuition behind of this idea?

C) Haldane's sieve is likely to be less important in inbred, e.g. selfing, populations. Why is this?

**Question 2.** Melanic squirrels suffer a higher rate of predation (due to hawks) than normally pigmented squirrels. Melanism is due to a dominant, autosomal mutation. The frequency of melanic squirrels at birth is  $4 \times 10^{-5}$ .

A) If the mutation rate to new melanic alleles is  $10^{-6}$ , assuming the melanic allele is at mutation-selection equilibrium, what is the reduction in fitness of the heterozygote?

Suddenly levels of pollution increase dramatically in our population, and predation by hawks now offers an equal (and opposite) advantage to the dark individuals as it once offered to the normally pigmented individuals.

B) What is the probability that a single copy of this allele (present just once in the population) is lost?

C) If the population size of our squirrels is a million individuals, and is at mutation-selection balance, what is the probability that the population adapts from one or more allele(s) from the standing pool of melanic alleles?

## 7.2 The interaction between genetic drift and weak selection.

For strongly selected alleles, once the allele has escaped initial loss at low frequencies, its path will be determined deterministically by its selection coefficients. However, if selection is weak compared to genetic drift, the stochasticity of reproduction can play a role in the trajectory an allele takes even when it is common in the population. If selection is sufficiently weak compared to genetic drift, then genetic drift will dominate the dynamics of alleles and they will behave like they're effectively neutral. Thus, the extent to which selection can shape patterns of molecular evolution will depend on the relative strengths of selection and genetic drift. But how weak must selection on an allele be for drift to overpower selection? And do these interactions between selection and drift have longterm consequences for genome-wide patterns evolution?

To model selection and drift each generation, we can first calculate the deterministic change in our allele frequency due to selection using our deterministic formula. Then, using our newly calculated expected allele frequency, we can binomially sample two alleles for each of our offspring to construct the next generation. This approach to jointly modeling genetic drift and selection is called the Wright-Fisher model.

Under the Wright-Fisher model, we will calculate the expected



Figure 7.5: cress bug (*Asellus aquaticus*) in the isopod family *Asellidae*. Brehms Tierleben. Allgemeine kunde des Tierreichs (1911). Brehm A.E. Image from the Biodiversity Heritage Library. Contributed by Smithsonian Libraries. Not in copyright.

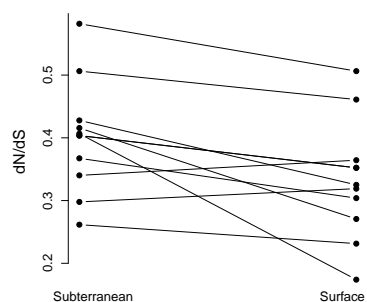


Figure 7.6: Asellid isopods have repeatedly invaded subterranean, ground-water habitats from surface-water habitats, and leading to a genome-wide increase in  $dN/dS$  and larger genomes (Data from LEFÉBURE *et al.*, 2017, comparing independent isopod species pairs). One possible explanation of this is that the longterm effective population sizes of the subterranean species are lower and so these species are less able to prevent mildly deleterious

change in allele frequency due to selection and the variance around this expectation due to drift. To make our calculations simpler, let's assume an additive model, i.e.  $h = 1/2$ , and that  $s \ll 1$  so that  $\bar{w} \approx 1$ . Using our directional selection deterministic model, from Chapter 6, and these approximations gives us our deterministic change due to selection

$$\Delta_{sp} = \mathbb{E}(\Delta p) = \frac{s}{2}p(1-p) \quad (7.9)$$

To obtain our new frequency in the next generation,  $p_1$ , we binomially sample from our new deterministic frequency  $p' = p + \Delta_{sp}$ , so the variance in our allele frequency change from one generation to the next is given by

$$Var(\Delta p) = Var(p_1 - p) = Var(p_1) = \frac{p'(1-p')}{2N} \approx \frac{p(1-p)}{2N}. \quad (7.10)$$

where the previous allele frequency  $p$  drops out because it is a constant and the variance in our new allele frequency follows from the fact that we are binomially sampling  $2N$  new alleles from a frequency  $p'$  to form the next generation.

To get our first look at the relative effects of selection vs. drift we can simply look at when our change in allele frequency caused by selection within a generation is reasonably faithfully passed down through the generations. In particular, if our expected change in allele frequency is much greater than the variance around this change, genetic drift will play little role in the fate of our selected allele (once the allele is not at low copy number within the population). When does selection dominant genetic drift? This will happen if  $\mathbb{E}(\Delta p) \gg Var(\Delta p)$ , i.e. when  $|Ns| \gg 1$ . Conversely, any hope of our selected allele following its deterministic path will be quickly undone if our change in allele frequencies due to selection is much less than the variance induced by drift. So if the absolute value of our population-size-scaled selection coefficient  $|Ns| \ll 1$ , then drift will dominate the fate of our allele.

To make further progress on understanding the fate of alleles with selection coefficients of the order  $1/N$  requires more careful modeling. However, under our diploid model, with an additive selection coefficient  $s$ , we can obtain the probability that allele 1 fixes within the population, starting from a frequency  $p$  :

$$p_F(p) = \frac{1 - e^{-2Ns}}{1 - e^{-2Ns}} \quad (7.11)$$

The proof of this result is sketched out below (see Section 7.2.1). A new allele that arrives in the population at frequency  $p = 1/(2N)$  has a probability of reaching fixation of

$$p_F\left(\frac{1}{2N}\right) = \frac{1 - e^{-s}}{1 - e^{-2Ns}} \quad (7.12)$$

To see this denote our new count of allele 1 by  $i$ , then

$$\begin{aligned} Var(p_1 - p) &= Var\left(\frac{i}{2N} - p\right) = Var\left(\frac{i}{2N}\right) \\ &= \frac{Var(i)}{(2N)^2} \end{aligned}$$

and from binomial sampling  $Var(i) = 2Np'(1-p')$  and so we arrive at our answer. Assuming that  $s \ll 1$ ,  $p' \approx p$ , then in practice we can use

$$Var(\Delta p) = Var(p' - p) \approx p(1-p)/2N.$$

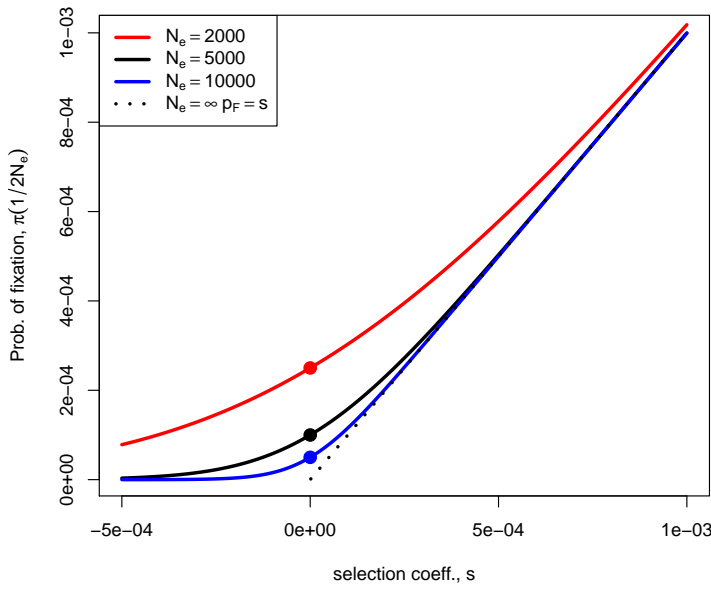


Figure 7.7: The probability of the fixation of a new mutation with selection coefficient  $s$  ( $h = 1/2$ ) in a diploid population of effective size  $N_e$ . The dashed line gives the infinite population solution. The dots give the solution for  $s \rightarrow 0$ , i.e. the neutral case, where the probability of fixation is  $1/(2N_e)$ . [Code here.](#)

If  $s \ll 1$  but  $Ns \gg 1$  then  $p_F(\frac{1}{2N}) \approx s$ , which nicely gives us back the result that we obtained above for an allele under strong selection (eqn. (7.8)). Our probability of fixation (eqn. (7.12)) is plotted as a function of  $s$  and  $N$  in Figure 7.8. To recover our neutral result, we can take the limit  $s \rightarrow 0$  to obtain our neutral fixation probability,  $1/(2N)$ .

In the case where  $Ns$  is close to 1, then

$$p_F\left(\frac{1}{2N}\right) \approx \frac{s}{1 - e^{-2Ns}} \quad (7.13)$$

This is greater than our earlier result  $p_F = s$  from the branching process argument (using our additive model of  $h = 1/2$ ), increasingly so for smaller  $N$ . Why is this? The reason why is that  $p_F$  is really the probability of "never being lost" in an infinitely large population. So to persist indefinitely, the allele has to escape loss permanently, by never being absorbed by the zero state. When the population size is finite, to fix we only need to reach a size  $2N$  individuals. Weakly beneficial mutations ( $Ns > 1$ ) are slightly more likely to fix than the  $s$  probability, as they only have to reach  $2N$  to never be lost.

If, for selection to operate on an allele, we need the selection coefficient to satisfy  $|Ns| \gg 1$ , then that holds if  $|s| \gg 1/N$ . Well, effective population sizes are often reasonably large, on the order of hundreds of thousands or millions of individuals, thus selection coefficients on the order of  $10^{-5}$  to  $10^{-6}$  can be effectively selected upon, i.e. selection equivalent to individuals have incredibly slight advantages in

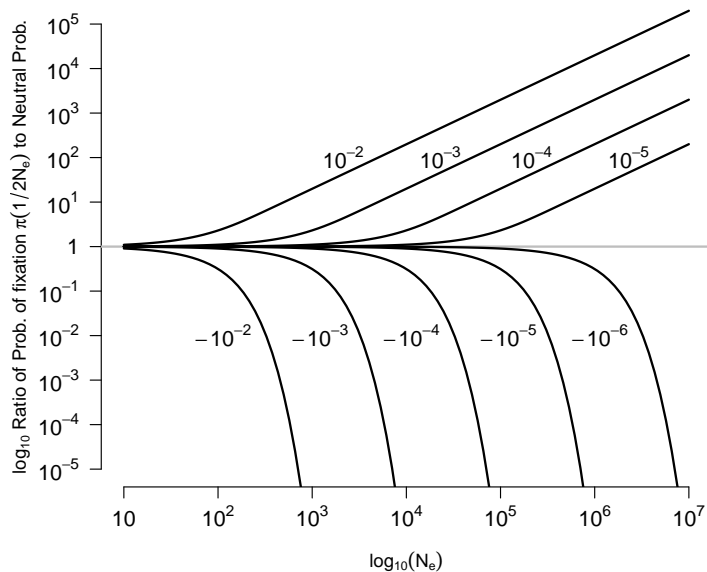


Figure 7.8: The probability of the fixation of a new mutation with selection coefficient  $s$  relative to the neutral fixation probability ( $1/2N_e$ ) as a function of the effective size  $N_e$ . The selection coefficient is shown next to the line. Note how quickly the probabilities move away from the neutral expectation as  $N_e s$  moves passed 1. [Code here.](#)

terms of the number of offspring they leave to the next generation. While we are incapable of detecting measuring all but the large fitness effect sizes, except in some elegant experiments (e.g. in microbes), such small effects are visible to selection in large populations. Thus, if consistent selection pressures are exerted over long time periods, natural selection can potentially finely tune various aspects of an organism.

As one example of this fine-tuning, consider how carefully crafted and optimized the sequence of codons is for translation. Due to the degeneracy of the protein code, multiple codons code for the same amino-acid. For example, there are six different codons that can code leucine. While these synonymous codons are equivalent at the protein level, cells do differ in the number of tRNA molecules that bind these codons and so the efficacy and accuracy with which proteins can be formed through translation and folding. These slight differences in translation rates likely often correspond to tiny differences in fitness, but do they matter?

In many organisms there is a strong bias in the codons to encode particular amino-acids, see Figure 7.9, with the most abundant codon matching the most abundant tRNA in cells. This 'codon bias' likely reflects the combined action of weak selection and mutational pressure, pushing the codon composition of the genome and tRNA abundances towards an adaptive compromise. These selection pressures have acted over long time periods, as codon usage patterns are often very simi-

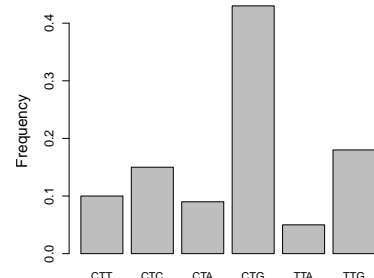


Figure 7.9: Data from *Drosophila melanogaster* on the frequency of different codons for Leucine. Data from Genscript. [Code here.](#)

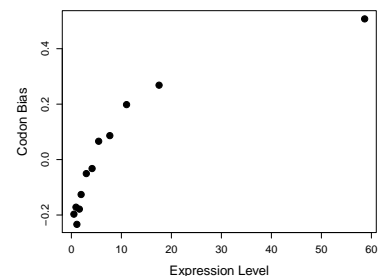


Figure 7.10: A measure of unequal codon frequencies ( $F$ ) plotted in bins of gene expression ( $E$ ) for genes across the *Drosophila melanogaster* genome. Data from HEY and KLIMAN (2002). [Code here.](#)

lar for species that diverged over many tens of millions of years ago. Compared to other genes, highly expressed genes show a strong bias towards using codons matching abundant tRNAs, consistent with the idea that the synonymous codon content of highly expressed genes is evolving to optimize their translation (see Figure 7.10 for an early example). These patterns likely represent the action of selection pressures that are incredibly weak on average, but that have played out over vast time-periods.

*The fixation of slightly deleterious alleles.* From Figure 7.8 we can see that weakly deleterious alleles can also fix, especially in small populations. To understand how likely it is that deleterious alleles by chance reach fixation by genetic drift, let's assume a diploid model with additive selection (with a selection coefficient of  $-s$  against our allele 2).

If  $Ns \gg 1$  then our deleterious allele (allele 2) cannot possibly reach fixation. However, if  $Ns$  is not large, then the probability of fixation

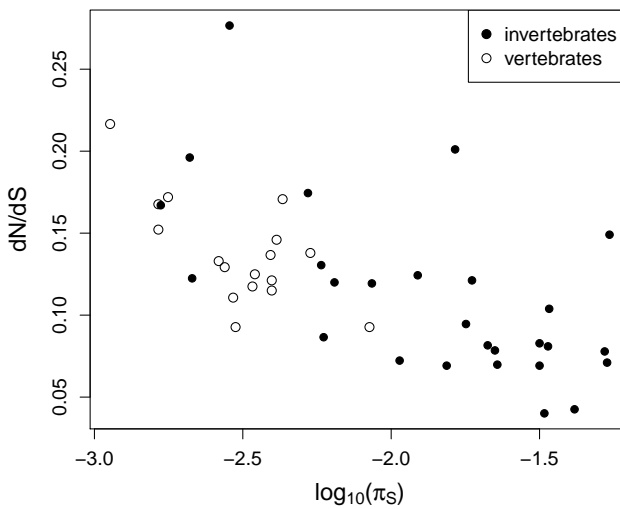
$$p_F \left( \frac{1}{2N} \right) \approx \frac{s}{e^{2Ns} - 1} \quad (7.14)$$

for our single-copy deleterious allele. So deleterious alleles can fix within populations (albeit at a low rate) if  $Ns$  is not too large. As above, this is because while deleterious mutations will never escape loss in infinite populations, they can become fixed in finite population by reaching  $2N$  copies.

**Question 3.** An additive mutation arises that lowers the relative fitness of heterozygotes by  $10^{-5}$ . What is the probability that this mutation fixes in a diploid population with effective size of  $10^4$ ? What is the probability it fixes in a population of effective size  $10^6$ ? By comparing both to their neutral probability describe the intuition behind this result.

OHTA proposed the ‘nearly-neutral’ theory of molecular evolution in a series of papers<sup>1</sup>. She suggested that a reasonable fraction of newly arising functional mutations may have very weak selection coefficients, such that species with smaller effective population sizes may have higher rates of fixation of these very weakly deleterious alleles. In effect, her suggestion is that the constraint parameter  $C$  of a functional region is not a fixed property, but rather depends on the ability of the population to resist the influx of very weakly deleterious mutations.

<sup>1</sup> OHTA, T., 1972 Population size and rate of evolution. *Journal of Molecular Evolution* 1(4): 305–314; OHTA, T., 1973 Slightly deleterious mutant substitutions in evolution. *Nature* 246(5428): 96; and OHTA, T., 1987 Very slightly deleterious mutations and the molecular clock. *Journal of Molecular Evolution* 26(1–2): 1–6



Across species, genome-wide averages of  $d_N/d_S$  do seem to be correlated with measures of the effective population size (such as synonymous diversity), see Figure 7.11. This evidence supports the idea that in species with smaller effective population sizes (lower  $\pi_S$ ), proteins may be subject to lower degrees of constraint, as very weakly deleterious mutations are able to fix. Thus, some reasonable proportion of functional substitutions in populations with small effective population sizes, such as humans, may be mildly deleterious.

### 7.2.1 Appendix: The fixation probability of weakly selected alleles

What is the probability a weakly beneficial or deleterious additive allele fixes in our population? We'll let  $P(\Delta p)$  be the probability that our allele frequency shifts by  $\Delta p$  in the next generation. Using this, we can write our probability  $p_F(p)$  in terms of the probability of achieving fixation averaged over the frequency in the next generation

$$p_F(p) = \int p_F(p + \Delta p)P(\Delta p)d(\Delta p) \quad (7.15)$$

This is very similar to the technique that we used when deriving our probability of escaping loss in a very large population above.

So we need an expression for  $p_F(p + \Delta p)$ . To obtain this, we'll do a Taylor series expansion of  $p_F(p)$ , assuming that  $\Delta p$  is small:

$$p_F(p + \Delta p) \approx p_F(p) + \Delta p \frac{dp_F(p)}{dp} + (\Delta p)^2 \frac{d^2 p_F(p)}{dp^2}(p) \quad (7.16)$$

Figure 7.11: Data from 44 metazoan species from Cuttlefish to Sifakas. Each dot represents the average of over many genes plotting  $d_N/d_S$  against synonymous diversity ( $\pi_S$ ). Data from GALTIER (2016). Code here.



Figure 7.12: Common Cuttlefish (*Sepia officinalis*). Cefalopodi viventi nel Golfo di Napoli (1896). Jatta G. Image from the Biodiversity Heritage Library. Contributed by Smithsonian Libraries. Licensed under CC BY-2.0.

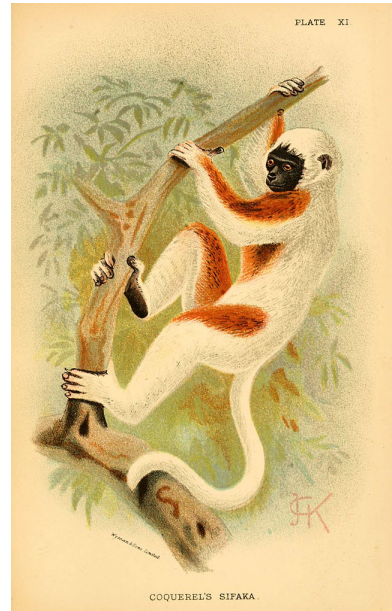


Figure 7.13: Coquerel's Sifaka (*Propithecus coquereli*). A hand-book to the primates (1894). Forbes, H. O. Image from the Biodiversity Heritage Library. Contributed by Smithsonian Libraries. Licensed under CC BY-2.0.

ignoring higher order terms.

Taking the expectation over  $\Delta p$  on both sides, as in eqn. 7.15, we obtain

$$p_F(p) = p_F(p) + \mathbb{E}(\Delta p) \frac{dp_F(p)}{dp} + \mathbb{E}((\Delta p)^2) \frac{d^2 p_F(p)}{dp^2} \quad (7.17)$$

Well,  $\mathbb{E}(\Delta p) = \frac{s}{2}p(1-p)$  and  $Var(\Delta p) = \mathbb{E}((\Delta p)^2) - \mathbb{E}^2(\Delta p)$ , so if  $s \ll 1$  then  $\mathbb{E}^2(\Delta p) \approx 0$ , and  $\mathbb{E}(\Delta p)^2 = \frac{p(1-p)}{2N}$ . Substituting in these values and subtracting  $p$  from both sides of our equation, this leaves us with

$$0 = \frac{s}{2}p(1-p) \frac{dp_F(p)}{dp} + \frac{p(1-p)}{2N} \frac{d^2 p_F(p)}{dp^2} \quad (7.18)$$

and we can specify the boundary conditions to be  $p_F(1) = 1$  and  $p_F(0) = 0$ . Solving this differential equation is a somewhat involved process, but in doing so we find that

$$p_F(p) = \frac{1 - e^{-2Ns p}}{1 - e^{-2Ns}} \quad (7.19)$$

This proof can be extended to alleles with arbitrary dominance, however, this does not lead to a analytically tractable expression so we do not pursue this here.

## *The Effects of Linked Selection.*

GENETIC DRIFT IS NOT THE ONLY SOURCE OF RANDOMNESS in the dynamics of alleles. Alleles also experience random fluctuations in frequency due to the fact that they present on a set of random genetic backgrounds with different fitnesses. For example, when a beneficial allele arises via a single mutation, it arises on a particular genetic background, i.e. a particular haplotype (Figure 8.1A). Imagine this mutation arising in a region with no recombination, or in an organism where genetic exchange is rare. If our beneficial allele becomes established in the population, i.e. escapes loss by genetic drift in those first few generations, it will start to increase in frequency rapidly. As it rises in frequency, so will the alleles that happened to be present on the haplotype that the mutation arose on (if those other alleles are neutral or at least not too deleterious). These other alleles are getting to 'hitchhiking' along. The alleles that are not on that particular background are swept out of the population, so the net effect of this selective sweep is to remove genetic diversity from the population. Diversity will eventually recover, as new mutations arise and some slowly drift up in frequency. But in the short-term, selective sweeps remove genetic variation from populations.

WILLIAMS and PENNINGS (2019) have visualized selective sweeps in HIV. In Figure 8.1B) we see a set of HIV haplotypes sampled from a patient before and after of a selective sweep of a drug-resistant mutation. The patient is taking a retrotransposase inhibitor (Efavirenz), but sadly within 161 days a drug-resistant mutation that changes the HIV retrotransposase protein has arisen and spread. Note how a particular haplotype is now fixed in the sample, and little genetic diversity remains, due to the hitchhiking effect of the strong selective sweep of this allele.

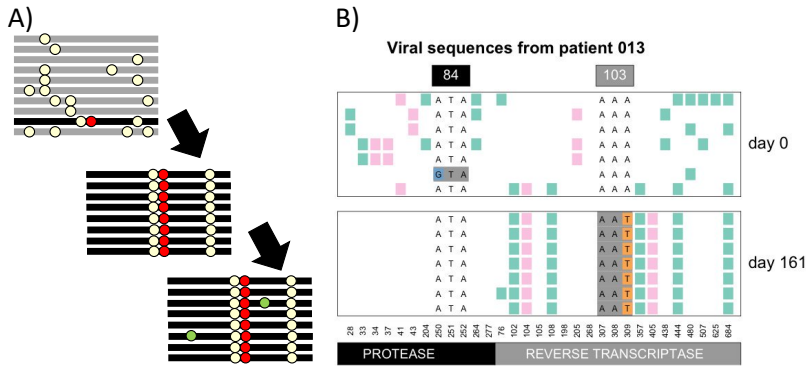


Figure 8.1: **A)** In the top panel, a selected mutation (red dot) arises on a particular haplotype in the population. It sweeps to fixation, carrying with it the haplotype on which it arose, middle panel, erasing the standing genetic diversity in the region. The bottom panel is some time after the selective sweep when some new neutral alleles (green dots) have started to drift up in frequency. **B)** Top panel: HIV sequences from a patient at the start of drug treatment in the protease and retrotransposase coding regions. Bottom panel: A sample 161 days later, after a drug resistant mutation has spread, the  $A \rightarrow T$  in the 103<sup>rd</sup> codon of retrotransposase. Each row is a haplotype, with the alleles present shown as coloured blocks. Figure B from WILLIAMS and PENNINGS (2019), licensed under CC BY 4.0.

To better understand hitchhiking, first let's imagine examining variation at a locus fully linked to our selected locus, just after our sweep reached fixation. Neutral alleles sampled at this locus must trace their ancestral lineages back to the neutral allele on whose background the selected allele initially arose (Figure 8.6). This is because that background neutral allele, which existed  $\tau$  generations ago, is the ancestor of the entire population at this fully linked locus. Our individuals who carry the beneficial allele are, from the perspective of these alleles, experiencing a rapidly expanding population. Therefore, a pair of neutral alleles sampled at our linked neutral locus will be forced to coalesce  $\approx \tau$  generations ago. A newly derived allele with an additive selection coefficient  $s$  will take a time  $\tau = 4 \log(2N)/s$  generations to reach fixation within our population (see eqn. (6.35)). This is a very short-time scale compared to the average neutral coalescent time of  $2N$  generations for a pair of alleles. Thus we expect little variation, as few mutations will have arisen on these very short branches, and those that have done will likely be singletons in our sample.

Now let's think about a sweep in a recombining region. Again the selected mutation arises on a particular haplotype, and it and its haplotype starts to increase in frequency in the population. However, now recombination events can occur between haplotypes carrying and not carrying the selected allele, in individuals who are heterozygote for the selected allele. These recombination events allow alleles that were not present on the original selected haplotype to avoid being swept out of the population, and also decouple the selected allele somewhat from hitchhiking alleles, preventing many of them from hitchhiking all the way to fixation. Far out from the selected site, the recombination rate is high enough that alleles that were present on the original background barely get to hitchhike along at all, as recombination breaks up their association with the selected allele very

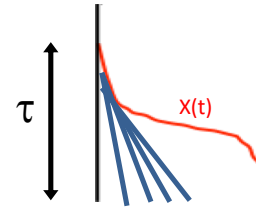


Figure 8.2: The coalescent of 4 lineages, marked in blue, at a locus completed linked to our selected allele. The frequency trajectory of the selected allele  $X(t)$  is shown in red.

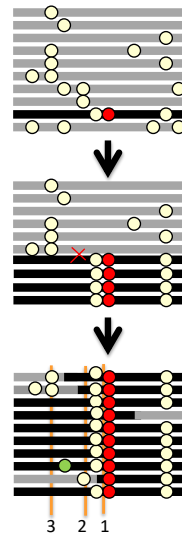
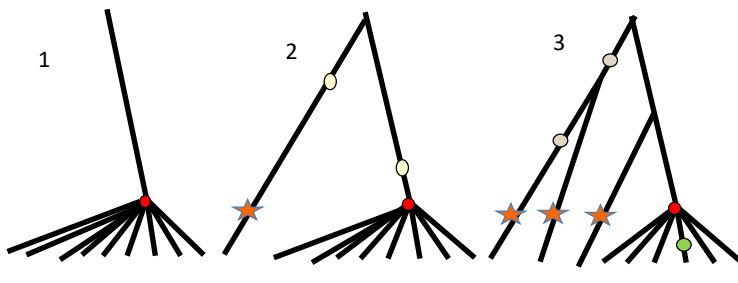


Figure 8.3: A cartoon depiction of a sweep of a red beneficial allele over three time points. The haplotype that the beneficial arose on by mutation is shown in black. The three vertical orange lines mark the loci shown in Figure 8.4. Neutral alleles segregating prior to the sweep appear as white circles, new mutations after the sweep as green circles.

rapidly.



What do the coalescent genealogies look like at loci various distances away from the selected site? Well, close to the selected site all our alleles in the present day trace back to a most recent common ancestral allele present on that selected haplotype, and so are all forced to coalesce around  $\tau$  generations ago (locus 1). Slightly further out from the selected site (locus 2), we have lineages that don't trace their ancestry back to the original selected haplotype, but instead are descended from recombinant haplotypes that recombined onto the sweep (the haplotype 2 from the bottom). These lineages can coalesce neutrally with the other ancestral lineages over far deeper time scales and mutations on these deeper lineages correspond to the standing diversity present in our population prior to the sweep. As we move even further out from the selected site (locus 3), we encounter more and more lineages descended from recombinant haplotypes that coalesce neutrally much deeper in time than  $\tau$ , allowing diversity to recover to background levels as we move away from the selected site.

Figure 8.4: Coalescent genealogies at three loci different distances along the genome from a selective sweep. The locations of these three loci along the genome are marked in Figure 8.3. The selected mutation is shown in red. Lineages descended from recombination events during the sweep are marked in stars. Neutral mutations close to each of the loci are shown on the genealogy.

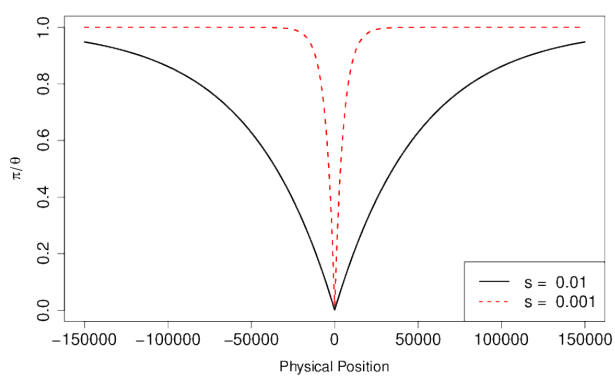


Figure 8.5: The expected reduction in diversity compared to its neutral expectation as a function of the distance away from a site where a selected allele has just gone to fixation. The sweeps associated with two different strengths of selection are shown, corresponding to a short timescale ( $\tau$ ) for the sweep and long one. The recombination rate is  $r_{BP} = 1 \times 10^{-8}$ . Code here.

To model the expected pattern of diversity surrounding a selected site, we can think about a pair of alleles sampled at a neutral locus a recombination distance  $r$  away from our selected site. Our pair of

alleles will be forced to coalesce  $\approx \tau$  generations if neither of them of are descended from recombinant haplotypes.

We know that in the present day our neutral lineage is linked to the selected allele. The probability that our lineage, in some generation  $t$  back in time, is in a heterozygote is  $1 - X(t)$ , and the probability that a recombination occurs in that individual is  $r$ . So the probability that our neutral lineage is descended from a recombinant haplotype  $t$  generations back is

$$r(1 - X(t)) \quad (8.1)$$

So the probability ( $p_{NR}$ ) that our lineage is not descended from a recombinant haplotype from a recombination event in the  $\tau$  generations it takes our selected allele to move through the population is

$$p_{NR} = \prod_{t=1}^{\tau} (1 - r(1 - X(t))) \quad (8.2)$$

Assuming that  $r$  is small, then  $(1 - r(1 - X(t))) \approx e^{-r(1-X(t))}$ , such that

$$p_{NR} = \prod_{t=1}^{\tau} (1 - r(1 - X(t))) \approx \exp\left(-r \sum_{t=1}^{\tau} 1 - X(t)\right) = \exp\left(-r\tau(1 - \hat{X})\right) \quad (8.3)$$

where  $\hat{X}$  is the average frequency of the derived beneficial allele across its trajectory as it sweeps up in frequency,  $\hat{X} = \frac{1}{\tau} \sum_{t=1}^{\tau} X(t)$ . As our allele is additive, its trajectory for frequencies  $< 0.5$  is the mirror image of its trajectory for frequencies  $> 0.5$ , therefore its average frequency  $\hat{X} = 0.5$ . This simplifies our expression to

$$p_{NR} = e^{-r\tau/2}. \quad (8.4)$$

The probability that neither of our lineages is descended from a recombinant haplotype, and hence are forced to coalesce, is  $p_{NR}^2$  (assuming that they coalesce at a time close to  $\tau$  so that they recombine independently of each other for times  $< \tau$ ).

If one or other of our lineages is descended from a recombinant haplotype, it will take them on average  $\approx 2N$  generations to find a common ancestor, as we are back to our neutral coalescent probabilities. Thus, the expected time till our pair of lineages find a common ancestor is

$$\mathbb{E}(T_2) = \tau \times p_{NR}^2 + (1 - p_{NR}^2)(\tau + 2N) \approx (1 - p_{NR}^2) 2N \quad (8.5)$$

where this last approximation assumes that  $\tau \ll 2N$ . So the expected pairwise diversity for neutral alleles at a recombination distance  $r$  away from the selected sweep ( $\pi_r$ ) is

$$\mathbb{E}(\pi_r) = 2\mu\mathbb{E}(T_2) \approx \pi_0 (1 - e^{-r\tau}) \quad (8.6)$$

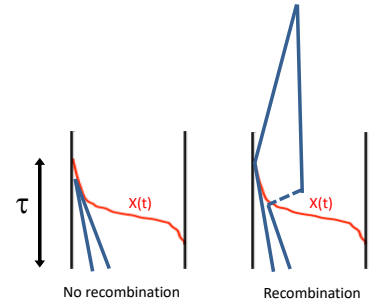
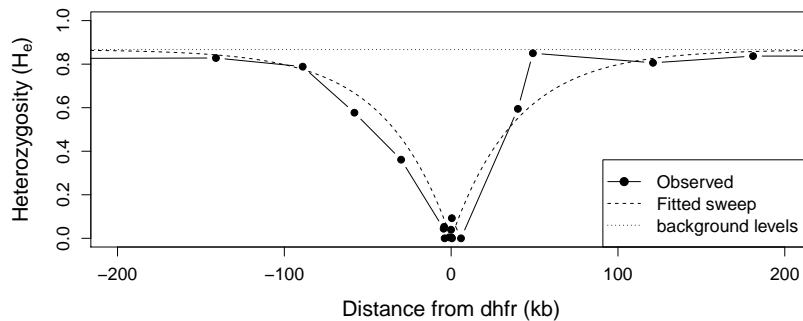


Figure 8.6:

So diversity increases as we move away from the selected site, slowly and exponentially plateauing to its neutral expectation  $\pi_0$ .

The malaria pathogen (*Plasmodium falciparum*) has evolved drug resistance to anti-malaria drugs, often by changes at the dhfr gene. Figure 8.8 shows levels of genetic diversity (heterozygosity) at a set of markers moving out from the dhfr gene in a set of drug resistant malaria sequences collected in Thailand (NASH *et al.*, 2005). We see the characteristic dip in diversity around the gene, with zero diversity at a number of the loci very close to the gene, suggesting a strong selective sweep. Fitting our simple model of a sweep to this data, we estimate that  $\tau \approx 40$  generations, corresponding to the drug-resistance allele fixing in very short time period.



To get a sense of the physical scale over which diversity is reduced, consider a region where recombination occurs at a rate  $r_{BP}$  per base pair per generation, and a locus  $\ell$  base pairs away from the selected site, such that  $r = r_{BP}\ell$  (where  $r_{BP}\ell \ll 1$  so we don't need to worry about more than one recombination event occurring per generation). Typical recombination rates are on the order of  $r_{BP} = 10^{-8}$ . In Figure 8.5 we show the reduction in diversity, given by eqn. (8.6), for two different selection coefficients.

For our expected diversity level to recover to 50% of its neutral expectation  $\mathbb{E}(\pi_r)/\theta = 0.5$ , requires a physical distance  $\ell^*$  such that  $\log(0.5) = -r_{BP}\ell^*\tau$ , and by re-arrangement,

$$\ell^* = \frac{-\log(0.5)}{r_{BP}\tau}. \quad (8.7)$$

As  $\tau$  depends inversely on the selection  $s$  (eqn. (6.35)), the width of our trough of reduced diversity depends on  $s/r_{BP}$ . All else being equal, we expect stronger sweeps or sweeps in regions of low recombination to have a larger hitchhiking effect. For example, in a genomic region with a recombination rate  $r_{BP} = 10^{-8}\text{bp}^{01}$  a selection coefficient of  $s = 0.1\%$  would reduce diversity over 10's of kb, while a sweep of  $s = 1\%$  would affect  $\sim 100\text{kb}$ .

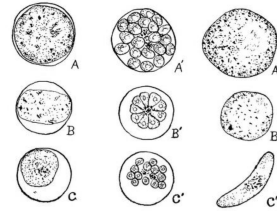


FIG. 47. Comparison of three species of malaria parasites  $\times 2000$  (figures selected largely from Manson). A, A' and A'', *Plasmodium vivax*; B, B' and B'', *Plasmodium vivax*; C, C' and C'', *Plasmodium falciparum*. A, B and C, mature parasites in red corpuscles. A', B' and C', segmented parasites ready to leave corpuscles. A'', B'' and C'', mature gameteocytes.

A, B and C, mature parasites in red corpuscles.

A', B' and C', segmented parasites ready to leave corpuscles.

A'', B'' and C'', mature gameteocytes.

Figure 8.7: Three species of malaria parasites (*Plasmodium*) in red blood cells.

Animal parasites and human disease (1918). Chandler, A.C. Image from the Biodiversity Heritage Library. Contributed by Cornell University Library. Not in copyright.

Figure 8.8: Levels of heterozygosity at a set of microsatellite markers surrounding the dhfr gene in samples of drug-resistant malaria (*Plasmodium falciparum*) from Thailand. The dotted horizontal line gives the average level of heterozygosity found at these markers in a set of drug-resistant malaria; we take this background as our  $\pi_0$ . The dashed line shows our fitted hitchhiking model from equation 8.6 with  $\tau \approx 40$ , fitted by non-linear least squares. The recombination rate in *P. falciparum* is  $r_{BP} \approx 10^{-6}\text{bp}^{-1}$ . Data from NASH *et al.* (2005). Code here.

**Question 1.** VAN'T HOF *et al.* (2011) identified the genetic basis of melanism in the peppered moth (*Biston betularia*). This allele swept to fixation in northern parts of the UK; a classic case of adaptation to industrial pollution (made famous by the work of KETTLEWELL, see MAJERUS (2009) and COOK *et al.* (2012)). The genetic basis of melanism is a transposable element (TE) inserted into a pigmentation gene. VAN'T HOF *et al.* found that diversity is suppressed in a broad region around the TE. Specifically, on the background of the TE, it takes roughly 200 kb in either direction for diversity levels to recover to 50% of genome-wide levels.

Random facts: In all moths and butterflies only males recombine; chromosomes are transmitted without recombination in females. The recombination rate in males is 2.9 cM/Mb. Peppered moths have an effective population size of roughly a hundred thousand individuals. Kettlewell used to eat moths when out collecting them in the field (personal communication, Art. Shapiro).

**A)** Briefly explain how this pattern offers further evidence that the melanistic allele was favoured by selection.

**B)** Using this information, and assuming the allele's effects on fitness are additive, what is your estimate of the age of the allele?

**C)** What is your estimate of the selection coefficient favouring this melanistic allele?

*Other signals of selective sweeps* The primary signal of a recently completed selective sweep is the characteristic reduction in diversity surrounding the selected site. However, sweeps do leave other signals and these have also often been used to identify loci undergoing selection. For example, neutral alleles further away from the selected site may hitchhiking only part of the way to fixation if recombination occurs during the sweep, which can lead to an excess of high-frequency derived alleles at intermediate distances away from the selected site, a pattern lasting for a short time after a sweep (FAY and WU, 2000; PRZEWORSKI, 2002; KIM, 2006). Also, as neutral diversity levels slowly recover through an influx of new mutations after a sweep, there is a strong skew towards low frequency derived alleles, a pattern that persists for many generations (BRAVERMAN *et al.*, 1995; PRZEWORSKI, 2002; KIM, 2006). The excess of rare alleles, compared to a neutral model, can be captured by statistics such as Tajima's D (which we encountered back in our discussion of the neutral site frequency eqn 3.43). Thus one way to look for loci that have undergone selective sweeps is to calculate Tajima's D from data in windows along the genome and look for strong departures from the null distribution.



Figure 8.9: peppered moth (*Biston betularia*), non-melanistic morph  
Les papillons dans la nature (1934). Robert, P.-A. Image from the Biodiversity Heritage Library. Contributed by University of Illinois Urbana-Champaign. Not in copyright.

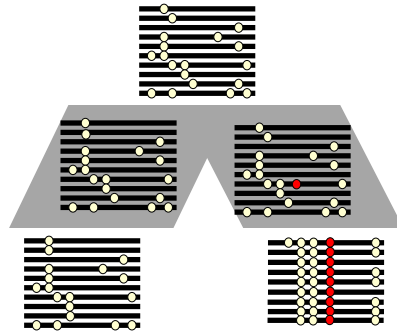


Figure 8.10: Two populations descended from a common ancestral population. A beneficial mutation has occurred in population and swept to fixation.

We can also use comparisons among multiple populations to look for evidence of sweeps occurring in one of the populations, for example to identify alleles involved in local adaptation (see 8.11). A selective sweep will decrease the within-population diversity ( $H_S$ ) surrounding the selected site, without affecting the diversity between different populations. Thus local sweeps create peaks of  $F_{ST}$  between weakly differentiated populations.

HOHENLOHE *et al.* (2010) studied genome-wide patterns of  $F_{ST}$  between marine and freshwater populations of threespine stickleback (*Gasterosteus aculeatus*). Between different marine populations, they found no strong peaks of  $F_{ST}$ ; however, between the marine and freshwater comparisons they found a number of high  $F_{ST}$  peaks that were replicated over a number of freshwater-marine comparisons. They identified a number of novel regions responsible for the adaptation of sticklebacks to freshwater environments and also a number of loci previously identified in crosses between marine and freshwater populations. For example, the first peak of Linkage Group IV includes Ectodysplasin A (Eda), a gene involved in the adaptive loss of armour plating in freshwater environments.

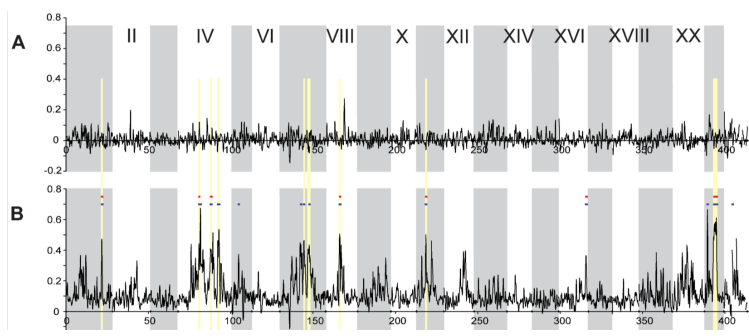


Figure 8.11:  $F_{ST}$  across the stickleback genome, with colored bars indicating significantly elevated ( $p \leq 10^{-5}$ , blue;  $p \leq 10^{-7}$ , red) and reduced ( $p \leq 10^{-5}$ , green) values. The alternating white and grey panels indicate different linkage groups. **A)**  $F_{ST}$  between two oceanic populations **B)** Average  $F_{ST}$  between a freshwater population and the two marine populations. Figure and caption text from HOHENLOHE *et al.* (2010), licensed under CC BY 4.0.

*Soft Sweeps from multiple mutations and standing variation.* In our sweep model above, we assumed that selection favoured a beneficial allele from the moment it entered the population as a single copy mutation (left panel, Figure 8.12). However, when a novel selection pressure switches on, multiple mutations at the same gene may start to sweep, such that no one of these alleles sweeps to fixation (middle panel, Figure 8.12). These sweeps involving multiple mutations significantly soften the impact of selection on genomic diversity, and so are called 'soft sweeps'.

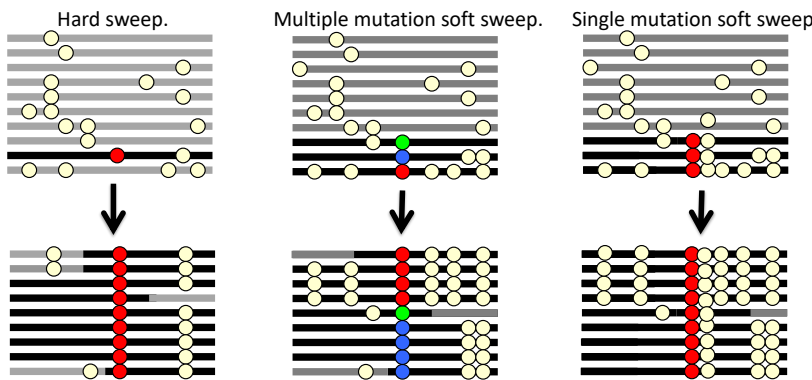


Figure 8.12: Three types of sweeps.

Another way that the impact of a sweep can be softened is if our allele was segregating in the population for some time before it became beneficial. That additional time means that our allele can have recombined onto various haplotype backgrounds, such that when selection pressures switch, the selected allele sweeps up in frequency on multiple different haplotypes (right panel, Figure 8.12). Detecting and differentiating these different types of sweeps is an active area of empirical research and theory in population genomics (see HERMISSON and PENNINGS (2017) for an overview of developments in this area).

### 8.1 The genome-wide effects of linked selection.

To what extent are patterns of variation along the genome and among species shaped by linked selection, such as selective sweeps? We can hope to identify individual cases of strong selective sweeps along the genome, but how do they contribute to broader patterns of variation?

Two observations have puzzled population geneticists since the inception of molecular population genetics. The first is the relatively high level of genetic variation observed in most obligately sexual species. The neutral theory of molecular evolution was developed in part to explain these high levels of diversity. As we saw in Chapter 3, under a simple neutral model, with constant population size, we

should expect the amount of neutral genetic diversity to scale with the product of the population size and mutation rate. The second observation, however, is the relatively narrow range of polymorphism across species with vastly different census sizes (see Figure 2.2 and LEFFLER *et al.* (2012) for a recent review). As highlighted by LEWONTIN (1974) in his discussion of the paradox of variation, this observation seemingly contradicts the prediction of the neutral theory that genetic diversity should scale with the census population size. There are a number of explanations for the discrepancy between genetic diversity levels and census population sizes. The first is that the effective size of the population ( $N_e$ ) is often much lower than the census size, due to high variance in reproductive success and frequent bottlenecks (as discussed in Chapter 3). The second major explanation, put forward by MAYNARD SMITH and HAIGH (1974), is that neutral levels of diversity are also systematically reduced by the effects of linked selection. In large populations, selective sweeps and other forms of linked selection may come to dominate over genetic drift as a source of stochasticity in allele frequencies, potentially establishing an upper limit to levels of diversity (KAPLAN *et al.*, 1989; GILLESPIE, 2000).

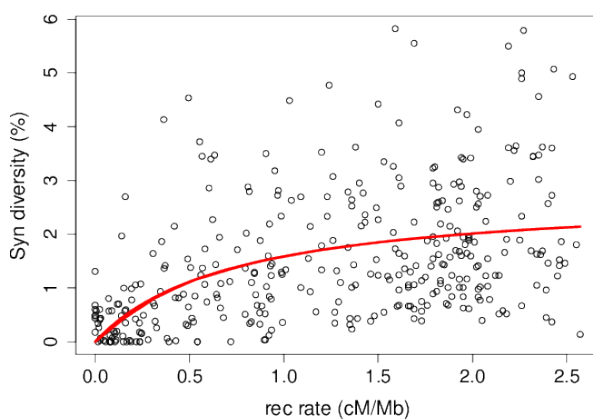


Figure 8.13: The relationship between (sex-averaged) recombination rate and synonymous site pairwise diversity ( $\pi$ ) in *Drosophila melanogaster*. The curve is the predicted relationship between  $\pi$  and recombination rate, obtained by fitting the recurrent hitchhiking equation (8.13) to this data using non-linear least squares via the `nls()` function in R. Data from (SHAPIRO *et al.*, 2007), kindly provided by Peter Andolfatto, see SELLA *et al.* (2009) for details. Code here.

One strong line of evidence for the action of linked selection in reducing levels of polymorphism is the positive correlation between putatively neutral diversity and recombination seen in a number of species, as, all else being equal, linked selection should remove diversity more quickly in regions of low recombination (AGUADÉ *et al.*, 1989; BEGUN and AQUADRO, 1992; WIEHE and STEPHAN, 1993b; CUTTER and CHOI, 2010; CAI *et al.*, 2009). For example, *Drosophila melanogaster* diversity levels are much lower in genomic regions of low recombination (see Figure 8.13). This pattern can not

be explained by differences in mutation rate between low and high recombination regions as this pattern is not seen strongly in divergence data among species.

These patterns could reflect the action of selective sweeps happening recurrently along the genome. In the next section we'll present a model for how levels of genetic diversity should depend on recombination and the density of functional sites under a model of recurrent selective sweeps. However, other forms of linked selection can impact genetic diversity in similar ways. For example, linked genetic diversity is continuously lost from natural populations due to the removal of haplotypes that carry deleterious alleles (CHARLESWORTH *et al.*, 1995; HUDSON and KAPLAN, 1995b); this is called the 'background selection' model. Below we'll discuss the background selection model and its basic predictions.

More generally, a wide range of models of selection predict the removal of neutral diversity linked to selected sites. This is because the diversity-reducing effects of high variance in reproductive success are compounded over the generations when there is heritable variance in fitness (ROBERTSON, 1961; SANTIAGO and CABALLERO, 1995, 1998; BARTON, 2000). Many different modes of linked selection likely contribute to these genome-wide patterns of diversity; the present challenge is how to differentiate among these different modes.

### 8.1.1 A simple recurrent model of selective sweeps

To explain how a constant influx of sweeps could impact levels of diversity, here we will develop a model of recurrent selective sweeps.

Imagine we sample a pair of neutral alleles at a locus a genetic distance  $r$  away from a locus where sweeps are initiated within the population at some very low rate  $\nu$  per generation. The waiting time between sweeps at our locus is exponentially distributed  $\sim \text{Exp}(\nu)$ . Each sweep rapidly transits through the population in  $\tau$  generations, such that each sweep is finished long before the next sweep ( $\tau \ll 1/\nu$ ).

As before, the chance that our neutral lineage fails to recombine off the sweep is  $p_{NR}$ , such that the probability that our pair of lineages are forced to coalesce by a sweep is  $e^{-r\tau}$ . Our lineages therefore have a very low probability

$$\nu e^{-r\tau} \tag{8.8}$$

of being forced to coalesce by a sweep per generation. If our lineages do not coalesce due to a sweep, they coalesce at a neutral rate of  $1/2N$  per generation. Thus the average waiting time till a coalescent event between our neutral pair of lineages due to either a sweep or a neutral coalescent event is

$$\mathbb{E}(T_2) = \frac{1}{\nu e^{-r\tau} + 1/2N} \tag{8.9}$$

Now imagine that the sweeps don't occur at a fixed location with respect to our locus of interest, but now occur uniformly at random across our genome. The sweeps are initiated at a very low rate of  $\nu_{BP}$  per basepair per generation. The rate of coalescence due to sweeps at a locus  $\ell$  basepairs away from our neutral loci is  $\nu_{BP}e^{-r_{BP}\ell\tau}$ . If our neutral locus is in the middle of a chromosome that stretches  $L$  basepairs in either direction, the total rate of sweeps per generation that could force our pair of lineages to coalesce is

$$2 \int_0^L \nu_{BP} e^{-r_{BP}\ell\tau} d\ell = \frac{2\nu_{BP}}{r_{BP}\tau} (1 - e^{-r_{BP}\tau L}) \quad (8.10)$$

so that if  $L$  is very large ( $r_{BP}\tau L \gg 1$ ), the rate of coalescence per generation due to sweeps is  $2\nu_{BP}/r_{BP}\tau$ . The total rate of coalescence for a pair of lineages per generation is then

$$\frac{2\nu_{BP}}{r_{BP}\tau} + \frac{1}{2N} \quad (8.11)$$

So our average time till a pair of lineages coalesce is

$$\mathbb{E}(T_2) = \frac{1}{\frac{2\nu_{BP}}{r_{BP}\tau} + 1/2N} = \frac{r_{BP}2N}{4N\nu_{BP}/\tau + r_{BP}} \quad (8.12)$$

such that our expected pairwise diversity ( $\pi = 2\mu\mathbb{E}(T_2)$ ) in a region with recombination rate  $r_{BP}$  that experiences sweeps at rate  $\nu_{BP}$  is

$$\mathbb{E}(\pi) = \pi_0 \frac{r_{BP}}{\frac{4N\nu_{BP}}{\tau} + r_{BP}} \quad (8.13)$$

where  $\pi_0$  is our expected diversity without any selective sweeps, ( $pi_0 = \theta = 4N\mu$ ). The expected diversity increases with  $r_{BP}$ , as higher recombination rates decrease the likelihood a neutral allele hitchhikes along with a sweep and is thus forced to coalesce by the sweep. Expected diversity decreases with  $\nu_{BP}$ , as a greater density of functional sites experiencing sweeps increases the chance of being linked to a nearby sweep. As we move to high  $r_{BP}$ , assuming that  $\nu_{BP}$  doesn't increase with  $r_{BP}$ , our level of diversity should plateau to  $\theta$ , the level of genetic diversity of a neutral site completely unlinked to any selected loci. If we assume that our genome experiences a constant rate of sweeps of a given strength, i.e. that  $4N\nu_{BP}/\tau$  is a constant, we can fit the variation in  $\pi$  across regions that vary in their recombination rate ( $r_{BP}$ ) to estimate a population's rate of recurrent sweeps per basepair. An example of fitting this curve to data from *Drosophila melanogaster* is shown in Figure 8.13; see WIEHE and STEPHAN (1993a) for an early example of fitting a similar recurrent hitchhiking model to such data. The parameter giving us this best-fitting curve is  $4N\nu_{BP}/\tau \approx 7 \times 10^{-9}$ . With an effect population size of a million and assuming that the sweeps take a thousand generations to reach fixation,

we find this implies  $\nu_{BP} \approx 10^{-12}$ . Thus, a really low rate of moderately strong sweeps, roughly one every megabase every million generations, is all we need to explain the profound dip in diversity seen in regions of the genome with low recombination. However, sweeps from positively selected alleles are not the only cause of genome-wide signals of linked selection. Selection against deleterious alleles can also drive these patterns.

### 8.1.2 Background selection

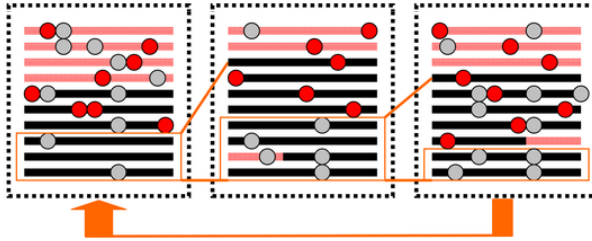
Populations experience a constant influx of deleterious mutations at functional loci while selection acts to purge them from the population, thus preventing deleterious substitutions and maintaining function at these loci. As we discussed in Chapter 6, this balance between mutation and selection results in a constant level of deleterious variation in the population. The constant selection against this deleterious variation has effects on diversity at linked sites. Each deleterious mutation arises at random on a haplotype in the population, and as selection purges this mutation, it removes with it any neutral alleles that were also on this haplotype. This constant removal of linked alleles from the population acts to reduce diversity in regions surrounding functional loci (HUDSON and KAPLAN, 1995a; NORDBORG *et al.*, 1996), an effect known as background selection (BGS).

What proportion of our haplotypes are free of deleterious mutations in any given generation, and so free to contribute to future generations? Well, under mutation-selection balance, a constrained locus with a mutation rate  $\mu$  towards deleterious alleles that experience a selection coefficient  $sh$  against them in heterozygotes, will result in  $\mu/sh$  chromosomes carrying the deleterious allele. Some of these haplotypes may be passed on to the next generation, but if they are fully linked to the deleterious locus they will all eventually be lost because they carry a deleterious mutation at a site under constraint. Thus, for a neutral polymorphism completely linked to a constrained locus, only  $2N(1 - \mu/sh)$  alleles get to contribute to future generations. Therefore, the level of pairwise diversity in a constant population due to BGS at such a locus will be

$$\mathbb{E}[\pi] = 2\mu \times 2N(1 - \mu/sh) = \pi_0(1 - \mu/sh) \quad (8.14)$$

where  $\pi_0 = 4N\mu$ , the level of neutral pairwise diversity in the absence of linked selection.

The effects of background selection are more pronounced in regions of low recombination, where neutral alleles are less able to recombine off the background of deleterious alleles. Thus, under background selection, we also expect to see reduced diversity in regions of lower recombination.



For a neutral locus that is a recombination fraction  $r$  away from a locus subject to constraint, the level of diversity is

$$\mathbb{E}[\pi] = \pi_0 \left(1 - \frac{\mu sh}{2(r+sh)^2}\right) \quad (8.15)$$

As we move away from a locus experiencing purifying selection, we increase  $r$ , and diversity should recover. For example, moving away from genic regions in the maize genome we see the average level of diversity recover. This occurs in both maize and teosinte, the wild progenitor of maize. The dip in diversity around non-synonymous sites is stronger in teosinte, perhaps because the accelerated drift due to the bottleneck in maize may have somewhat released constraint on sites where very weakly deleterious alleles segregated previously at mutation-selection balance.

More generally, if a neutral locus is surrounded by  $L$  loci experiencing purifying selection at recombination distances  $r_1, \dots, r_L$ , then compounding equation (8.16) across these loci, the expected reduced diversity is approximately

$$\mathbb{E}[\pi] = \pi_0 \prod_{i=1}^L \left(1 - \frac{\mu sh}{2(r_i+sh)^2}\right) \approx \exp\left(\sum_{i=1}^L \frac{\mu sh}{2(r_i+sh)^2}\right) \quad (8.16)$$

To model an average neutral locus in a genomic region with a given recombination rate, we can imagine that our neutral locus is situated in the center of a large region with total recombination rate  $R$  and total deleterious mutation rate  $U$ , where  $U = \mu L$ . Then our expression for diversity, equation (8.16), simplifies to

$$\mathbb{E}[\pi] \approx \pi_0 \exp(-U/(sh+R)) \approx \pi_0 \exp(-U/R). \quad (8.17)$$

In this last approximation, we assume that we're looking at a large region, with  $R \gg sh$ . Note that much like genetic load, equation (6.49), this expression depends only on the total deleterious mutation rate. Any dependence on the selection coefficient drops out, as weakly selected mutations segregate in the population at higher frequencies, but are also removed from the population more slowly, allowing more of the genome to recombine off the deleterious background.

Figure 8.14: A cartoon depiction of a region for 10 haplotypes experiencing background selection. Neutral mutations are shown as gray circles, and deleterious mutations in red. Over time, chromosomes carrying deleterious mutations are removed from the population, such that most individuals are descended from a subset of chromosomes free of deleterious alleles (highlighted here by orange boxes). Mutation is constantly generating new deleterious alleles on the background of chromosomes previously free of deleterious alleles. Figure modified from SELLA *et al.* (2009), licensed under CC BY 4.0.

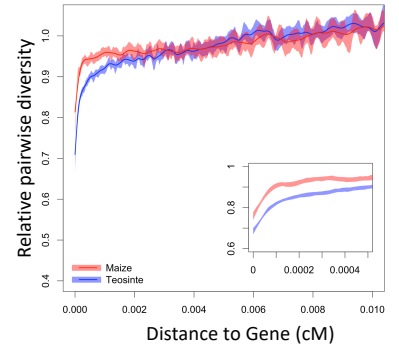


Figure 8.15: Relative diversity compared to the mean diversity in windows  $\geq 0.01$  cM as a function of the distance to the nearest gene. See (BEISSINGER *et al.*, 2016) for details. Figure licensed under CC BY 4.0 by Jeff Ross-Ibarra.

For a first go at fitting this to genome-wide data, we could look at diversity in windows of length  $W$  bp (as in Figure 8.16). If we assume that there is a constant rate of deleterious mutation per base pair,  $\mu_{BP}$ , then  $U = \mu_{BP}W$ . Furthermore, if our genomic window has a recombination rate  $r_{BP}$  per base-pair, our total genetic length is  $R = r_{BP}W$ . Making these substitutions in equation (8.17), our window size cancels out to give

$$\mathbb{E}[\pi] \approx \pi_0 \exp(-\mu_{BP}/r_{bp}) \quad (8.18)$$

Looking across windows that vary in their recombination rate, i.e.  $r_{BP}$ , we can fit equation (8.18) to data to estimate  $\mu_{BP}$ . An example of doing this to data from *D. melanogaster* is shown in Figure 8.16, yielding an estimate of the deleterious mutation rate of  $\mu_{BP} \approx 3.2 \times 10^{-9}$ . This is roughly on the same order as the mutation rate per base pair in *D. melanogaster*, and so this deleterious mutation rate estimate is somewhat high as it would require most of the genome to be constrained, but as a first approximation it's not terrible. Note how similar the fit is to a model of hitchhiking, suggesting that both BGS and hitchhiking are capable of explaining the broad relationship between diversity and recombination seen in *D. melanogaster* and other species.

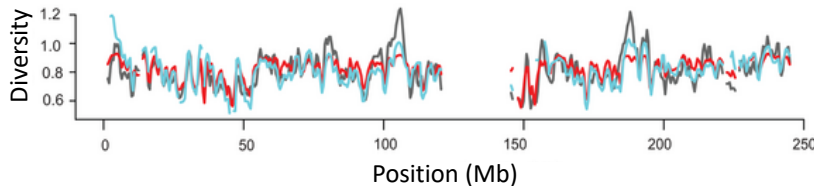


Figure 8.16: The relationship between recombination rate and synonymous site pairwise diversity ( $\pi$ ) in *D. melanogaster*, as in Figure 8.13. The red curve is the predicted relationship between  $\pi$  and recombination rate, obtained by fitting the BGS equation (8.17) to this data using non-linear least squares via the `nls()` function in R. The blue line is the recurrent hitchhiking equation line from Figure 8.13. Code here.

As our annotations of functional regions of the genome have improved, so have our methods to infer background selection. A more rigorous version of this analysis today would incorporate variation in coding density among windows into the parameter  $\mu_{BP}$ . With detailed genomic annotations showing coding regions and constrained non-coding regions, we can also move beyond just analyzing broad-scale patterns. For example, MCVICKER *et al.* (2009) fit a model of background selection to putatively neutral pairwise diversity along the human genome, using equation 8.16 to estimate the effect of BGS at each locus, weighing the genetic distance to all of the surrounding coding regions and constrained non-coding sites. This allowed MCVICKER *et al.* (2009) to estimate mutation rates and average selection coefficients acting against deleterious alleles in these regions of the genome. This best fitting model also allowed them to predict

Figure 8.17: Observed (black line) and predicted pairwise diversity across chromosome 1, from a background selection model that assumes a uniform mutation rate (red line) or a mutation rate that varies with local human/dog divergence (blue line). Figure from (MCVICKER *et al.*, 2009), licensed under CC BY 4.0.

diversity levels along the genome, a section of which is shown in figure 8.17. Thus, broad-scale features of polymorphism along the genome are well described by background selection (or by linked selection more generally).

The deleterious mutation rates estimated by MC VICKER *et al.* (2009) from fitting a model of BGS were again too high, as in the *Drosophila* example above, suggesting the BGS alone is not sufficient to explain all of the effect of linked selection. But how then do we go about distinguishing the impact of BGS from hitchhiking?

*Distinguishing the impact of hitchhiking from background selection in genome-wide data* A variety of approaches have been taken to start to separate the effects of hitchhiking from background selection. Much of the strongest evidence showing the effects of both comes from *Drosophila melanogaster* and we review some of that evidence here. Hitchhiking is expected to have systematic effects on the neutral site frequency spectrum, distorting it towards rare minor alleles, (reflecting the slow recovery of diversity following a sweep). Therefore, we should expect a distortion of summary statistics such as Tajima's D in regions of low recombination if hitchhiking is contributing to the reduction in diversity in these regions (BRAVERMAN *et al.*, 1995; PRZEWORSKI, 2002; KIM, 2006). In *D. melanogaster*, there is a greater skew towards rare alleles at putatively neutral sites in regions of low recombination (ANDOLFATTO and PRZEWORSKI, 2001; SHAPIRO *et al.*, 2007), see left panel of Figure 8.18. However, while this skew isn't expected under simple models of strong background selection, other models of background selection can lead to such patterns.

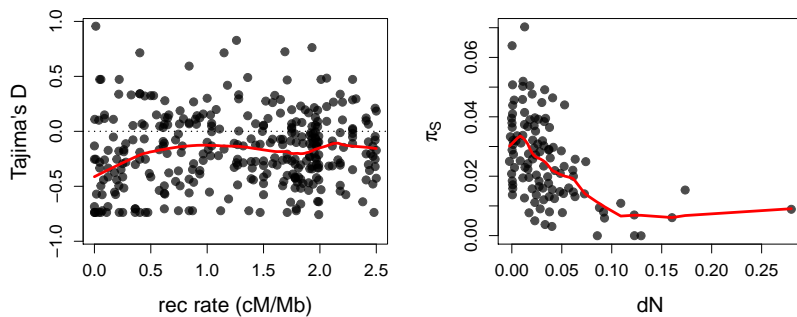


Figure 8.18: **Left)** Average Tajima's D in genomic windows plotted against their recombination rate in *D. melanogaster*. Data from SHAPIRO *et al.* (2007). **Right)** Synonymous pairwise diversity in genomic windows as a function of the density of non-synonymous substitutions in the window. Data from ANDOLFATTO (2007). Code here.

Another prediction of the hitchhiking model, where an allele sweeps to fixation, is that there should be a functional substitution associated with each sweep. Or, to flip that around, we might expect to see a greater impact of hitchhiking where there are more functional

substitutions. For example, regions surrounding non-synonymous substitutions should have lower levels of diversity, if a high fraction of non-synonymous substitutions are adaptive. Again, this pattern is seen in *D. melanogaster* (ANDOLFATTO, 2007; MACPHERSON *et al.*, 2007; SATTATH *et al.*, 2011b), right side of Figure 8.18.

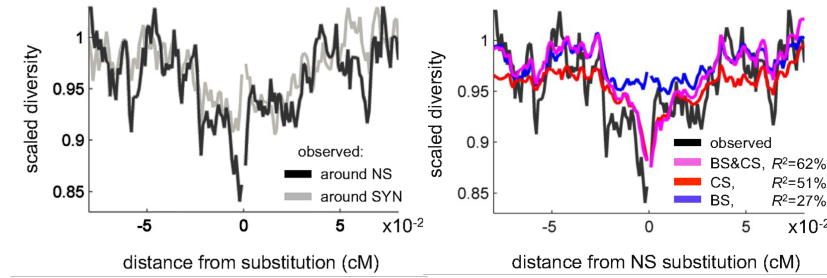


Figure 8.19: **Left)** Scaled synonymous pairwise diversity levels around non-synonymous (NS) and synonymous (SYN) substitutions in *D. melanogaster*. **Right)** Predicted scaled diversity levels around non-synonymous substitutions based on models including background selection (BS), classic sweeps (CS) and both (BS & CS). Figure from ELYASHIV *et al.* (2016), licensed under CC BY 4.0.

Pushing this idea further, we can look at the dip in diversity surrounding a non-synonymous substitution averaged across all the substitutions in the genome. ELYASHIV *et al.* (2016) found a stronger dip in diversity around non-synonymous substitutions than synonymous substitutions (see also SATTATH *et al.*, 2011a). Extending the model of MCVICKER *et al.* (2009) to fit a model of background selection and hitchhiking to putative neutral diversity along the genome, they found that the dip in diversity around synonymous substitutions comes mostly from BGS. But to fully explain the dip in diversity around non-synonymous substitutions, a reasonable proportion of these non-synonymous substitutions have to have been accompanied by a classic (hard) sweep. The majority of these sweeps are estimated to be due to very weak selection, with selection coefficients  $< 10^{-4}$ . Furthermore, ELYASHIV *et al.* (2016) estimated a 77 - 89% reduction in neutral diversity due to selection on linked sites, and concluded that no genomic window was entirely free of the effects of selection. Thus linked selection has a profound effect in some species such as *Drosophila melanogaster*.

## Bibliography

- AGUADÉ, M., N. MIYASHITA, and C. H. LANGLEY, 1989 Reduced variation in the yellow-achaete-scute region in natural populations of *Drosophila melanogaster*. *Genetics* **122**: 607–615.
- AGUILLO, S. M., J. W. FITZPATRICK, R. BOWMAN, S. J. SCHOECH, A. G. CLARK, G. COOP, and N. CHEN, 2017, 08) Deconstructing isolation-by-distance: The genomic consequences of limited dispersal. *PLOS Genetics* **13**(8): 1–27.
- AKÇAY, E. and J. VAN CLEVE, 2016 There is no fitness but fitness, and the lineage is its bearer. *Phil. Trans. R. Soc. B* **371**(1687): 20150085.
- ALCAIDE, M., E. S. SCORDATO, T. D. PRICE, and D. E. IRWIN, 2014 Genomic divergence in a ring species complex. *Nature* **511**(7507): 83.
- ALEXANDER, D. H., J. NOVEMBRE, and K. LANGE, 2009 Fast model-based estimation of ancestry in unrelated individuals. *Genome research* **19**(9): 1655–1664.
- ALGEE-HEWITT, B. F., M. D. EDGE, J. KIM, J. Z. LI, and N. A. ROSENBERG, 2016 Individual identifiability predicts population identifiability in forensic microsatellite markers. *Current Biology* **26**(7): 935–942.
- ALLENDORF, F. W. and J. J. HARD, 2009 Human-induced evolution caused by unnatural selection through harvest of wild animals. *Proceedings of the National Academy of Sciences* **106**(Supplement 1): 9987–9994.
- ALVAREZ, G., F. C. CEBALLOS, and C. QUINTEIRO, 2009 The role of inbreeding in the extinction of a European royal dynasty. *PLoS One* **4**(4): e5174.

ANDOLFATTO, P., 2007 Hitchhiking effects of recurrent beneficial amino acid substitutions in the *Drosophila melanogaster* genome. *Genome Res.* **17**: 1755–1762.

ANDOLFATTO, P. and M. PRZEWORSKI, 2001 Regions of lower crossing over harbor more rare variants in African populations of *Drosophila melanogaster*. *Genetics* **158**: 657–665.

AYLLON, F., E. KJÆRNER-SEMB, T. FURMANEK, V. WENNEVIK, M. F. SOLBERG, G. DAHLE, G. L. TARANGER, K. A. GLOVER, M. S. ALMÉN, C. J. RUBIN, and OTHERS, 2015 The vgl3 locus controls age at maturity in wild and domesticated Atlantic salmon (*Salmo salar* L.) males. *PLoS genetics* **11**(11): e1005628.

BARRETT, R. D. H., S. M. ROGERS, and D. SCHLUTER, 2008 Natural Selection on a Major Armor Gene in Threespine Stickleback. *Science* **322**(5899): 255–257.

BARSON, N. J., T. AYKANAT, K. HINDAR, M. BARANSKI, G. H. BOLSTAD, P. FISKE, C. JACQ, A. J. JENSEN, S. E. JOHNSTON, S. KARLSSON, and OTHERS, 2015 Sex-dependent dominance at a single locus maintains variation in age at maturity in salmon. *Nature* **528**(7582): 405.

BARTON, N. H., 2000 Genetic hitchhiking. *Philos. Trans. R. Soc. Lond., B, Biol. Sci.* **355**: 1553–1562.

BECQUET, C., N. PATTERSON, A. C. STONE, M. PRZEWORSKI, and D. REICH, 2007 Genetic structure of chimpanzee populations. *PLoS genetics* **3**(4): e66.

BEGUN, D. J. and C. F. AQUADRO, 1992 Levels of naturally occurring DNA polymorphism correlate with recombination rates in *D. melanogaster*. *Nature* **356**: 519–520.

BEISSINGER, T. M., L. WANG, K. CROSBY, A. DURVASULA, M. B. HUFFORD, and J. ROSS-IBARRA, 2016 Recent demography drives changes in linked selection across the maize genome. *Nature plants* **2**(7): 16084.

BOX, G. E., 1979 Robustness in the strategy of scientific model building. In *Robustness in statistics*, pp. 201–236. Elsevier.

BRADBURY, G. S., P. L. RALPH, and G. M. COOP, 2016 A spatial framework for understanding population structure and admixture. *PLoS genetics* **12**(1): e1005703.

BRANDVAIN, Y., A. M. KENNEY, L. FLAGEL, G. COOP, and A. L. SWEIGART, 2014 Speciation and introgression between *Mimulus nasutus* and *Mimulus guttatus*. *PLoS Genetics* **10**(6): e1004410.

BRAVERMAN, J. M., R. R. HUDSON, N. L. KAPLAN, C. H. LANGLEY, and W. STEPHAN, 1995 The hitchhiking effect on the site frequency spectrum of DNA polymorphisms. *Genetics* **140**: 783–796.

CAI, J. J., J. M. MACPHERSON, G. SELLA, and D. A. PETROV, 2009 Pervasive hitchhiking at coding and regulatory sites in humans. *PLoS Genet.* **5**: e1000336.

CASSA, C. A., D. WEGHORN, D. J. BALICK, D. M. JORDAN, D. NUSINOW, K. E. SAMOCHA, A. O'DONNELL-LURIA, D. G. MACARTHUR, M. J. DALY, D. R. BEIER, and OTHERS, 2017 Estimating the selective effects of heterozygous protein-truncating variants from human exome data. *Nature genetics* **49**(5): 806.

CHARLESWORTH, B., 2009 Effective population size and patterns of molecular evolution and variation. *Nature Reviews Genetics* **10**(3): 195.

CHARLESWORTH, D., B. CHARLESWORTH, and M. T. MORGAN, 1995 The pattern of neutral molecular variation under the background selection model. *Genetics* **141**: 1619–1632.

CHEN, N., E. J. COSGROVE, R. BOWMAN, J. W. FITZPATRICK, and A. G. CLARK, 2016 Genomic Consequences of Population Decline in the Endangered Florida Scrub-Jay. *Current Biology* **26**(21): 2974 – 2979.

COOK, L. M., B. S. GRANT, I. J. SACCHERI, and J. MALLETT, 2012 Selective bird predation on the peppered moth: the last experiment of Michael Majerus. *Biology Letters* **8**(4): 609–612.

COTTERMAN, C. W., 1940 A calculus for statistico-genetics. Ph. D. thesis, The Ohio State University.

COUSMINER, D. L., D. J. BERRY, N. J. TIMPSON, W. ANG, E. THIERING, E. M. BYRNE, H. R. TAAL, V. HUIKARI, J. P. BRADFIELD, M. KERKHOF, and OTHERS, 2013 Genome-wide association and longitudinal analyses reveal genetic loci linking pubertal height growth, pubertal timing and childhood adiposity. *Human molecular genetics* **22**(13): 2735–2747.

- CUTTER, A. D. and J. Y. CHOI, 2010 Natural selection shapes nucleotide polymorphism across the genome of the nematode *Caenorhabditis briggsae*. *Genome Res.* **20**: 1103–1111.
- DARWIN, C., 1859 *On the Origin of Species by Means of Natural Selection*. London: Murray. or the Preservation of Favored Races in the Struggle for Life.
- DARWIN, C., 1876 The effect of cross and self fertilization in the vegetable kingdom: Murray. London, UK.
- DARWIN, C., 1888 *The descent of man and selection in relation to sex*, Volume 1. Murray.
- DEMPSTER, E., 1955 Maintenance of genetic heterogeneity. *Cold Spring Harb Symp Quant Biol* **20**: 25–32.
- DICKERSON, R. E., 1971 The structure of cytochrome c and the rates of molecular evolution. *Journal of Molecular Evolution* **1**(1): 26–45.
- DOBZHANSKY, T., 1943 Genetics of natural populations IX. Temporal changes in the composition of populations of *Drosophila pseudobscura*. *Genetics* **28**(2): 162.
- DOBZHANSKY, T., 1951 *Genetics and the Origin of Species* (3rd Ed. ed.), pp. 16.
- ELTON, C., 1942 *Voles, mice and lemmings. Problems in population dynamics*. Oxford: Clarendon Press.
- ELYASHIV, E., S. SATTATH, T. T. HU, A. STRUTSOVSKY, G. MCVICKER, P. ANDOLFATTO, G. COOP, and G. SELLA, 2016 A genomic map of the effects of linked selection in *Drosophila*. *PLoS genetics* **12**(8): e1006130.
- EWENS, W. J., 2016 Motoo Kimura and James Crow on the Infinitely Many Alleles Model. *Genetics* **202**(4): 1243–1245.
- FAY, J. C. and C. I. WU, 2000 Hitchhiking under positive Darwinian selection. *Genetics* **155**: 1405–1413.
- FEDER, A. F., C. KLINE, P. POLACINO, M. COTTRELL, A. D. KASHUBA, B. F. KEELE, S.-L. HU, D. A. PETROV, P. S. PENNINGS, and Z. AMBROSE, 2017 A spatio-temporal assessment of simian/human immunodeficiency virus (SHIV) evolution reveals a highly dynamic process within the host. *PLoS pathogens* **13**(5): e1006358.

- FISHER, R. A., 1915 The evolution of sexual preference. *The Eugenics Review* **7**(3): 184.
- FISHER, R. A., 1923 XXI.—on the dominance ratio. *Proceedings of the royal society of Edinburgh* **42**: 321–341.
- FRANCIOLI, L. C., A. MENELAOU, S. L. PULIT, F. VAN DIJK, P. F. PALAMARA, C. C. ELBERS, P. B. NEERINCX, K. YE, V. GURYEV, W. P. KLOOSTERMAN, and OTHERS, 2014 Whole-genome sequence variation, population structure and demographic history of the Dutch population. *Nature genetics* **46**(8): 818.
- FRENTIU, F. D., G. D. BERNARD, C. I. CUEVAS, M. P. SISON-MANGUS, K. L. PRUDIC, and A. D. BRISCOE, 2007 Adaptive evolution of color vision as seen through the eyes of butterflies. *Proceedings of the National Academy of Sciences* **104**(suppl 1): 8634–8640.
- GALEN, C., 1996 Rates of floral evolution: adaptation to bumblebee pollination in an alpine wildflower, *Polemonium viscosum*. *Evolution* **50**(1): 120–125.
- GALTIER, N., 2016 Adaptive protein evolution in animals and the effective population size hypothesis. *PLoS genetics* **12**(1): e1005774.
- GIGORD, L. D., M. R. MACNAIR, and A. SMITHSON, 2001 Negative frequency-dependent selection maintains a dramatic flower color polymorphism in the rewardless orchid *Dactylorhiza sambucina* (L.) Soo. *Proceedings of the National Academy of Sciences* **98**(11): 6253–6255.
- GILLESPIE, J. H., 2000 Genetic drift in an infinite population. The pseudohitchhiking model. *Genetics* **155**: 909–919.
- HALDANE, J., 1942 The selective elimination of silver foxes in eastern Canada. *Journal of Genetics* **44**(2-3): 296–304.
- HALDANE, J. and S. JAYAKAR, 1963 Polymorphism due to selection of varying direction. *Journal of Genetics* **58**(2): 237–242.
- HALDANE, J. B. S., 1927 A mathematical theory of natural and artificial selection, part V: selection and mutation. In *Mathematical Proceedings of the Cambridge Philosophical Society*, Volume 23, pp. 838–844. Cambridge University Press.
- HALDANE, J. B. S., 1937 The Effect of Variation of Fitness. *The American Naturalist* **71**(735): 337–349.

- HAMILTON, W. D., 1964a The genetical evolution of social behaviour. II. Journal of theoretical biology 7(1): 17–52.
- HAMILTON, W. D., 1964b The genetical evolution of social behaviour. II. Journal of theoretical biology 7(1): 17–52.
- HERMISSON, J. and P. S. PENNINGS, 2017 Soft sweeps and beyond: understanding the patterns and probabilities of selection footprints under rapid adaptation. Methods in Ecology and Evolution 8(6): 700–716.
- HEY, J. and R. M. KLIMAN, 2002 Interactions between natural selection, recombination and gene density in the genes of *Drosophila*. Genetics 160(2): 595–608.
- HOEKSTRA, H. E., K. E. DRUMM, and M. W. NACHMAN, 2004 Ecological genetics of adaptive color polymorphism in pocket mice: geographic variation in selected and neutral genes. Evolution 58(6): 1329–1341.
- HOHENLOHE, P. A., S. BASSHAM, P. D. ETTER, N. STIFFLER, E. A. JOHNSON, and W. A. CRESKO, 2010 Population genomics of parallel adaptation in threespine stickleback using sequenced RAD tags. PLoS genetics 6(2): e1000862.
- HOPKINS, J., G. BAUDRY, U. CANDOLIN, and A. KAITALA, 2015 I'm sexy and I glow it: female ornamentation in a nocturnal capital breeder. Biology letters 11(10): 20150599.
- HOUDE, A. E., 1994 Effect of artificial selection on male colour patterns on mating preference of female guppies. Proc. R. Soc. Lond. B 256(1346): 125–130.
- HOWES, R. E., M. DEWI, F. B. PIEL, W. M. MONTEIRO, K. E. BATTLE, J. P. MESSINA, A. SAKUNTABHAI, A. W. SATYAGRAHA, T. N. WILLIAMS, J. K. BAIRD, and S. I. HAY, 2013 Spatial distribution of G6PD deficiency variants across malaria-endemic regions. Malar. J. 12: 418.
- HOWES, R. E., F. B. PIEL, A. P. PATIL, O. A. NYANGIRI, P. W. GETHING, M. DEWI, M. M. HOGG, K. E. BATTLE, C. D. PADILLA, J. K. BAIRD, and S. I. HAY, 2012 G6PD deficiency prevalence and estimates of affected populations in malaria endemic countries: a geostatistical model-based map. PLoS Medicine 9(11): e1001339.
- HUDSON, R. R., 2015, 07)A New Proof of the Expected Frequency Spectrum under the Standard Neutral Model. PLOS ONE 10(7): 1–5.

- HUDSON, R. R. and N. L. KAPLAN, 1995a Deleterious background selection with recombination. *Genetics* **141**: 1605–1617.
- HUDSON, R. R. and N. L. KAPLAN, 1995b The coalescent process and background selection. *Philos. Trans. R. Soc. Lond., B, Biol. Sci.* **349**: 19–23.
- HUDSON, R. R., M. KREITMAN, and M. AGUADÉ, 1987 A test of neutral molecular evolution based on nucleotide data. *Genetics* **116**(1): 153–159.
- JAIN, S. and A. D. BRADSHAW, 1966 Evolutionary divergence among adjacent plant populations I. The evidence and its theoretical analysis. *Heredity* **21**(3): 407.
- JANICKE, T., I. K. HÄDERER, M. J. LAJEUNESSE, and N. ANTHES, 2016 Darwinian sex roles confirmed across the animal kingdom. *Science advances* **2**(2): e1500983.
- JENNINGS, W. B. and S. V. EDWARDS, 2005 Speciation history of Australian grass finches (*Poephila*) inferred from thirty gene trees. *Evolution* **59**(9): 2033–2047.
- JOHANNSEN, W., 1911 The Genotype Conception of Heredity. *The American Naturalist* **45**(531): 129–159.
- JOHNSTON, S. E., J. GRATTON, C. BERENOS, J. G. PILKINGTON, T. H. CLUTTON-BROCK, J. M. PEMBERTON, and J. SLATE, 2013 Life history trade-offs at a single locus maintain sexually selected genetic variation. *Nature* **502**(7469): 93.
- JUKEMA, J. and T. PIERSMA, 2006 Permanent female mimics in a lekking shorebird. *Biology letters* **2**(2): 161–164.
- KAPLAN, N. L., R. R. HUDSON, and C. H. LANGLEY, 1989 The hitchhiking effect revisited. *Genetics* **123**: 887–899.
- KETTLEWELL, H. B. D., 1955 Selection experiments on industrial melanism in the Lepidoptera. *Heredity* **9**(3): 323.
- KIM, Y., 2006 Allele frequency distribution under recurrent selective sweeps. *Genetics* **172**: 1967–1978.
- KIMURA, M., 1968 Evolutionary rate at the molecular level. *Nature* **217**(5129): 624–626.
- KIMURA, M., 1983 *The neutral theory of molecular evolution*. Cambridge University Press.
- KIMURA, M. and J. F. CROW, 1964 The number of alleles that can be maintained in a finite population. *Genetics* **49**(4): 725.

- KIMURA, M. and T. OHTA, 1974 On some principles governing molecular evolution. *Proceedings of the National Academy of Sciences* *71*(7): 2848–2852.
- KING, J. L. and T. H. JUKES, 1969 Non-darwinian evolution. *Science* *164*(3881): 788–798.
- KORNEGAY, J. R., J. W. SCHILLING, and A. C. WILSON, 1994 Molecular adaptation of a leaf-eating bird: stomach lysozyme of the hoatzin. *Molecular Biology and Evolution* *11*(6): 921–928.
- KRAKAUER, A. H., 2005 Kin selection and cooperative courtship in wild turkeys. *Nature* *434*(7029): 69.
- KRUUK, L. E., J. SLATE, J. M. PEMBERTON, S. BROTH-ERSTONE, F. GUINNESS, and T. CLUTTON-BROCK, 2002 Antler size in red deer: heritability and selection but no evolution. *Evolution* *56*(8): 1683–1695.
- KÜPPER, C., M. STOCKS, J. E. RISSE, N. DOS REMEDIOS, L. L. FARRELL, S. B. MCRAE, T. C. MORGAN, N. KARLIONOVA, P. PINCHUK, Y. I. VERKUIL, and OTHERS, 2016 A supergene determines highly divergent male reproductive morphs in the ruff. *Nature Genetics* *48*(1): 79.
- KWIATKOWSKI, D. P., 2005, August)How malaria has affected the human genome and what human genetics can teach us about malaria. *Am. J. Hum. Genet.* *77*(2): 171–192.
- LAMICHHANEY, S., G. FAN, F. WIDEMO, U. GUNNARSSON, D. S. THALMANN, M. P. HOEPPNER, S. KERJE, U. GUSTAFSON, C. SHI, H. ZHANG, and OTHERS, 2016 Structural genomic changes underlie alternative reproductive strategies in the ruff (*Philomachus pugnax*). *Nature Genetics* *48*(1): 84.
- LANDE, R., 1979 Quantitative genetic analysis of multivariate evolution, applied to brain: body size allometry. *Evolution* *33*(1Part2): 402–416.
- LAURIE, C. C., D. A. NICKERSON, A. D. ANDERSON, B. S. WEIR, R. J. LIVINGSTON, M. D. DEAN, K. L. SMITH, E. E. SCHADT, and M. W. NACHMAN, 2007, 08)Linkage Disequilibrium in Wild Mice. *PLOS Genetics* *3*(8): 1–9.
- LAWSON, D. J., L. VAN DORP, and D. FALUSH, 2018 A tutorial on how not to over-interpret STRUCTURE and ADMIXTURE bar plots. *Nature communications* *9*(1): 3258.

LEFÉBURE, T., C. MORVAN, F. MALARD, C. FRANÇOIS,  
L. KONECNY-DUPRÉ, L. GUÉGUEN, M. WEISS-GAYET,  
A. SEGUIN-ORLANDO, L. ERMINI, C. DER SARKISSIAN,  
and OTHERS, 2017 Less effective selection leads to larger genomes.  
Genome research: gr-212589.

LEFFLER, E. M., K. BULLAUGHEY, D. R. MATUTE, W. K.  
MEYER, L. SEGUREL, A. VENKAT, P. ANDOLFATTO, and  
M. PRZEWORSKI, 2012 Revisiting an old riddle: what deter-  
mines genetic diversity levels within species? PLoS biology 10(9):  
e1001388.

LEK, M., K. J. KARCZEWSKI, E. V. MINIKEL, K. E.  
SAMOCHA, E. BANKS, T. FENNELL, A. H. O'DONNELL-  
LURIA, J. S. WARE, A. J. HILL, B. B. CUMMINGS, and  
OTHERS, 2016 Analysis of protein-coding genetic variation in  
60,706 humans. Nature 536(7616): 285.

LENORMAND, T., D. BOURGUET, T. GUILLEMAUD, and  
M. RAYMOND, 1999 Tracking the evolution of insecticide resis-  
tance in the mosquito *Culex pipiens*. Nature 400(6747): 861.

LEWONTIN, R. C., 1970 The units of selection. Annual review of  
ecology and systematics 1(1): 1–18.

LEWONTIN, R. C., 1974 *The Genetic Basis of Evolutionary  
Change*. Columbia University Press, New York.

LEWONTIN, R. C., 1994, 05)[DNA Fingerprinting: A Review of  
the Controversy]: Comment: The Use of DNA Profiles in Forensic  
Contexts. Statist. Sci. 9(2): 259–262.

LEWONTIN, R. C., 2001 *Thinking about evolution: historical, philo-  
sophical, and political perspectives*, Chapter Natural History and  
Formalism in Evolutionary Genetics, pp. 7–20. Cambridge Univer-  
sity Press.

LI, J. Z., D. M. ABSHER, H. TANG, A. M. SOUTHWICK,  
A. M. CASTO, S. RAMACHANDRAN, H. M. CANN, G. S.  
BARSH, M. FELDMAN, L. L. CAVALLI-SFORZA, and OTH-  
ERS, 2008 Worldwide human relationships inferred from genome-  
wide patterns of variation. science 319(5866): 1100–1104.

LISTER, A., 1989 Rapid dwarfing of red deer on Jersey in the last  
interglacial. Nature 342(6249): 539.

LOCKE, D. P., L. W. HILLIER, W. C. WARREN, K. C.  
WORLEY, L. V. NAZARETH, D. M. MUZNY, S.-P. YANG,

- Z. WANG, A. T. CHINWALLA, P. MINX, and OTHERS, 2011 Comparative and demographic analysis of orang-utan genomes. *Nature* **469**(7331): 529.
- LOUICHAROEN, C., E. PATIN, R. PAUL, I. NUCHPRAY-OON, B. WITOONPANICH, C. PEERAPITTAYAMONGKOL, I. CASADEMONT, T. SURA, N. M. LAIRD, P. SINGHASIVANON, L. QUINTANA-MURCI, and A. SAKUNTABHAI, 2009, December)Positively selected G6PD-Mahidol mutation reduces *Plasmodium vivax* density in Southeast Asians. *Science* **326**(5959): 1546–1549.
- MACARTHUR, D. G., S. BALASUBRAMANIAN, A. FRANKISH, N. HUANG, J. MORRIS, K. WALTER, L. JOSTINS, L. HABEGGER, J. K. PICKRELL, S. B. MONTGOMERY, and OTHERS, 2012 A systematic survey of loss-of-function variants in human protein-coding genes. *Science* **335**(6070): 823–828.
- MACPHERSON, J. M., G. SELLA, J. C. DAVIS, and D. A. PETROV, 2007 Genomewide spatial correspondence between non-synonymous divergence and neutral polymorphism reveals extensive adaptation in *Drosophila*. *Genetics* **177**: 2083–2099.
- MAJERUS, M. E., 2009 Industrial melanism in the peppered moth, *Biston betularia*: an excellent teaching example of Darwinian evolution in action. *Evolution: Education and Outreach* **2**(1): 63.
- MALÉCOT, G., 1948 Les mathématiques de l'hérédité.
- MALÉCOT, G., 1969 The Mathematics of Heredity (Revised, edited and translated by Yermanos, DM).
- MARCINIAK, S. and G. H. PERRY, 2017 Harnessing ancient genomes to study the history of human adaptation. *Nature Reviews Genetics* **18**(11): 659.
- MAYNARD SMITH, J., 1964 Group selection and kin selection. *Nature* **201**(4924): 1145.
- MAYNARD SMITH, J. and J. HAIGH, 1974 The hitch-hiking effect of a favourable gene. *Genet. Res.* **23**: 23–35.
- MCDONALD, J. H. and M. KREITMAN, 1991 Adaptive protein evolution at the Adh locus in *Drosophila*. *Nature* **351**(6328): 652.
- MCVICKER, G., D. GORDON, C. DAVIS, and P. GREEN, 2009 Widespread genomic signatures of natural selection in hominid evolution. *PLoS Genet.* **5**: e1000471.

- MENOZZI, P., A. PIAZZA, and L. CAVALLI-SFORZA, 1978 Synthetic maps of human gene frequencies in Europeans. *Science* 201(4358): 786–792.
- MEREDITH, R. W., J. GATESY, W. J. MURPHY, O. A. RYDER, and M. S. SPRINGER, 2009, 09) Molecular Decay of the Tooth Gene Enamelin (ENAM) Mirrors the Loss of Enamel in the Fossil Record of Placental Mammals. *PLOS Genetics* 5(9): 1–12.
- MESSIER, W. and C.-B. STEWART, 1997 Episodic adaptive evolution of primate lysozymes. *Nature* 385(6612): 151.
- NACHMAN, M. W., H. E. HOEKSTRA, and S. L. D'AGOSTINO, 2003 The genetic basis of adaptive melanism in pocket mice. *Proceedings of the National Academy of Sciences* 100(9): 5268–5273.
- NASH, D., S. NAIR, M. MAYXAY, P. N. NEWTON, J.-P. GUTHMANN, F. NOSTEN, and T. J. ANDERSON, 2005 Selection strength and hitchhiking around two anti-malarial resistance genes. *Proceedings of the Royal Society of London B: Biological Sciences* 272(1568): 1153–1161.
- NELSON, M. R., D. WEGMANN, M. G. EHM, D. KESSNER, P. S. JEAN, C. VERZILLI, J. SHEN, Z. TANG, S.-A. BACANU, D. FRASER, and OTHERS, 2012 An abundance of rare functional variants in 202 drug target genes sequenced in 14,002 people. *Science*: 1217876.
- NORDBORG, M., B. CHARLESWORTH, and D. CHARLESWORTH, 1996 The effect of recombination on background selection. *Genet. Res.* 67: 159–174.
- NOVEMBRE, J. and M. STEPHENS, 2008 Interpreting principal component analyses of spatial population genetic variation. *Nature genetics* 40(5): 646.
- OHTA, T., 1972 Population size and rate of evolution. *Journal of Molecular Evolution* 1(4): 305–314.
- OHTA, T., 1973 Slightly deleterious mutant substitutions in evolution. *Nature* 246(5428): 96.
- OHTA, T., 1987 Very slightly deleterious mutations and the molecular clock. *Journal of Molecular Evolution* 26(1-2): 1–6.
- OHTA, T. and J. H. GILLESPIE, 1996 Development of neutral and nearly neutral theories. *Theoretical population biology* 49(2): 128–142.

- OWEN, D. and D. CHANTER, 1972 Polymorphic mimicry in a population of the African butterfly, *Pseudacraea eurytus* (L.) (Lep. Nymphalidae). *Insect Systematics & Evolution* **3**(4): 258–266.
- PAABY, A. B., A. O. BERGLAND, E. L. BEHRMAN, and P. S. SCHMIDT, 2014 A highly pleiotropic amino acid polymorphism in the *Drosophila* insulin receptor contributes to life-history adaptation. *Evolution* **68**(12): 3395–3409.
- PATTERSON, N., A. L. PRICE, and D. REICH, 2006 Population structure and eigenanalysis. *PLoS genetics* **2**(12): e190.
- PICKRELL, J. K., T. BERISA, J. Z. LIU, L. SÉGUREL, J. Y. TUNG, and D. A. HINDS, 2016 Detection and interpretation of shared genetic influences on 42 human traits. *Nature genetics* **48**(7): 709.
- POTTI, J. and D. CANAL, 2011 Heritability and genetic correlation between the sexes in a songbird sexual ornament. *Heredity* **106**(6): 945.
- PRITCHARD, J. K., M. STEPHENS, and P. DONNELLY, 2000 Inference of population structure using multilocus genotype data. *Genetics* **155**(2): 945–959.
- PROVINE, W. B., 2001 *The origins of theoretical population genetics: with a new afterword*. University of Chicago Press.
- PRZEWORSKI, M., 2002 The signature of positive selection at randomly chosen loci. *Genetics* **160**: 1179–1189.
- PTAK, S. E., A. D. ROEDER, M. STEPHENS, Y. GILAD, S. PÄÄBO, and M. PRZEWORSKI, 2004 Absence of the TAP2 human recombination hotspot in chimpanzees. *PLoS biology* **2**(6): e155.
- QUELLER, D. C., 1992 Quantitative genetics, inclusive fitness, and group selection. *The American Naturalist* **139**(3): 540–558.
- R, 2018 R: A Language and Environment for Statistical Computing.
- RALPH, P. L. and G. COOP, 2015 The role of standing variation in geographic convergent adaptation. *The American Naturalist* **186**(S1): S5–S23.
- RANDS, C. M., S. MEADER, C. P. PONTING, and G. LUNTER, 2014 8.2% of the human genome is constrained: variation in rates of turnover across functional element classes in the human lineage. *PLoS genetics* **10**(7): e1004525.

- RICHARDS, C. M., 2000 Inbreeding depression and genetic rescue in a plant metapopulation. *The American Naturalist* **155**(3): 383–394.
- RITLAND, K., C. NEWTON, and H. MARSHALL, 2001 Inheritance and population structure of the white-phased “Kermode” black bear. *Current Biology* **11**(18): 1468 – 1472.
- ROBERTSON, A., 1961 Inbreeding in artificial selection programmes. *Genet. Res.* **2**: 189—194.
- ROBINSON, J. A., D. ORTEGA-DEL VECCHYO, Z. FAN, B. Y. KIM, C. D. MARSDEN, K. E. LOHMUELLER, R. K. WAYNE, and OTHERS, 2016 Genomic flatlining in the endangered island fox. *Current Biology* **26**(9): 1183–1189.
- ROBINSON, L. M., J. R. BOLAND, and J. M. BRAVERMAN, 2016 Revisiting a Classic Study of the Molecular Clock. *Journal of molecular evolution* **82**(2-3): 110–116.
- ROSENBERG, N. A., J. K. PRITCHARD, J. L. WEBER, H. M. CANN, K. K. KIDD, L. A. ZHIVOTOVSKY, and M. W. FELDMAN, 2002 Genetic structure of human populations. *science* **298**(5602): 2381–2385.
- RUWENDE, C., S. C. KHOO, R. W. SNOW, S. N. YATES, D. KWIATKOWSKI, S. GUPTA, P. WARN, C. E. ALLSOPP, S. C. GILBERT, and N. PESCHU, 1995, July)Natural selection of hemi- and heterozygotes for G6PD deficiency in Africa by resistance to severe malaria. *Nature* **376**(6537): 246–249.
- SAMS, A. J. and A. R. BOYKO, 2018a Fine-scale resolution and analysis of runs of homozygosity in domestic dogs. *bioRxiv*.
- SAMS, A. J. and A. R. BOYKO, 2018b Fine-Scale Resolution of Runs of Homozygosity Reveal Patterns of Inbreeding and Substantial Overlap with Recessive Disease Genotypes in Domestic Dogs. *G3: Genes, Genomes, Genetics*: g3–200836.
- SANKARARAMAN, S., N. PATTERSON, H. LI, S. PÄÄBO, and D. REICH, 2012, 10)The Date of Interbreeding between Neandertals and Modern Humans. *PLOS Genetics* **8**(10): 1–9.
- SANTIAGO, E. and A. CABALLERO, 1995 Effective size of populations under selection. *Genetics* **139**: 1013–1030.
- SANTIAGO, E. and A. CABALLERO, 1998 Effective size and polymorphism of linked neutral loci in populations under directional selection. *Genetics* **149**: 2105–2117.

- SATTATH, S., E. ELYASHIV, O. KOLODNY, Y. RINOTT, and G. SELLA, 2011a Pervasive adaptive protein evolution apparent in diversity patterns around amino acid substitutions in *Drosophila simulans*. PLoS genetics 7(2): e1001302.
- SATTATH, S., E. ELYASHIV, O. KOLODNY, Y. RINOTT, and G. SELLA, 2011b Pervasive adaptive protein evolution apparent in diversity patterns around amino acid substitutions in *Drosophila simulans*. PLoS Genet. 7: e1001302.
- SCHEMSKE, D. W. and P. BIERZYCHUDEK, 2001 Perspective: evolution of flower color in the desert annual Linanthus parryae: Wright revisited. Evolution 55(7): 1269–1282.
- SELLA, G., D. A. PETROV, M. PRZEWORSKI, and P. ANDOLFATTO, 2009 Pervasive natural selection in the *Drosophila* genome? PLoS genetics 5(6): e1000495.
- SHAPIRO, J. A., W. HUANG, C. ZHANG, M. J. HUBISZ, J. LU, D. A. TURISSINI, S. FANG, H. Y. WANG, R. R. HUDSON, R. NIELSEN, Z. CHEN, and C. I. WU, 2007 Adaptive genic evolution in the *Drosophila* genomes. Proc. Natl. Acad. Sci. U.S.A. 104: 2271–2276.
- SMITHSON, A. and M. R. MACNAIR, 1997 Negative frequency-dependent selection by pollinators on artificial flowers without rewards. Evolution 51(3): 715–723.
- STURTEVANT, A. H., 1915 The behavior of the chromosomes as studied through linkage. Zeitschrift für induktive Abstammungs-und Vererbungslehre 13(1): 234–287.
- TAJIMA, F., 1989 Statistical method for testing the neutral mutation hypothesis by DNA polymorphism. Genetics 123(3): 585–595.
- TISHKOFF, S. A., R. VARKONYI, N. CAHINHINAN, S. ABBES, G. ARGYROPOULOS, G. DESTRO-BISOL, A. DROUSIOTOU, B. DANGERFIELD, G. LEFRANC, J. LOISELET, A. PIRO, M. STONEKING, A. TAGARELLI, G. TAGARELLI, E. H. TOUMA, S. M. WILLIAMS, and A. G. CLARK, 2001 Haplotype Diversity and Linkage Disequilibrium at Human G6PD: Recent Origin of Alleles That Confer Malarial Resistance. Science 293(5529): 455–462.
- TOEWS, D. P., S. A. TAYLOR, R. VALLENDER, A. BRELFORD, B. G. BUTCHER, P. W. MESSEY, and I. J. LOVETTE, 2016 Plumage Genes and Little Else Distinguish the Genomes of Hybridizing Warblers. Current Biology 26(17): 2313 – 2318.

- TURELLI, M., D. W. SCHEMSKE, and P. BIERZYCHUDEK, 2001 Stable two-allele polymorphisms maintained by fluctuating fitnesses and seed banks: protecting the blues in *Linanthus parryae*. *Evolution* 55(7): 1283–1298.
- VAN'T HOF, A. E., N. EDMONDS, M. DALÍKOVÁ, F. MAREC, and I. J. SACCHERI, 2011 Industrial melanism in British peppered moths has a singular and recent mutational origin. *Science* 332(6032): 958–960.
- VOIGHT, B. F., A. M. ADAMS, L. A. FRISSE, Y. QIAN, R. R. HUDSON, and A. DI RIENZO, 2005 Interrogating multiple aspects of variation in a full resequencing data set to infer human population size changes. *Proceedings of the National Academy of Sciences* 102(51): 18508–18513.
- VONHOLDT, B. M., J. P. POLLINGER, D. A. EARL, J. C. KNOWLES, A. R. BOYKO, H. PARKER, E. GEFEN, M. PILOT, W. JEDRZEJEWSKI, B. JEDRZEJEWSKA, V. SIDOROVICH, C. GRECO, E. RANDI, M. MUSIANI, R. KAYS, C. D. BUSTAMANTE, E. A. OSTRANDER, J. NOVEMBRE, and R. K. WAYNE, 2011 A genome-wide perspective on the evolutionary history of enigmatic wolf-like canids. *Genome Research*.
- WANG, J., J. DING, B. TAN, K. M. ROBINSON, I. H. MICHELSON, A. JOHANSSON, B. NYSTEDT, D. G. SCOFIELD, O. NILSSON, S. JANSSON, and OTHERS, 2018 A major locus controls local adaptation and adaptive life history variation in a perennial plant. *Genome biology* 19(1): 72.
- WATTERSON, G., 1975 On the number of segregating sites in genetical models without recombination. *Theoretical population biology* 7(2): 256–276.
- WHEELER, W. M., 1907 Pink Insect Mutants. *The American Naturalist* 41(492): 773–780.
- WIDEMO, F., 1998 Alternative reproductive strategies in the ruff, *Philomachus pugnax*: a mixed ESS? *Animal Behaviour* 56(2): 329–336.
- WIEHE, T. and W. STEPHAN, 1993a Analysis of a genetic hitchhiking model, and its application to DNA polymorphism data from *Drosophila melanogaster*. *Molecular Biology and Evolution* 10(4): 842–854.

- WIEHE, T. H. and W. STEPHAN, 1993b Analysis of a genetic hitchhiking model, and its application to DNA polymorphism data from *Drosophila melanogaster*. *Mol. Biol. Evol.* **10**: 842–854.
- WILKINSON, G. S., 1993 Artificial sexual selection alters allometry in the stalk-eyed fly *Cyrtodiopsis dalmanni* (Diptera: Diopsidae). *Genetics Research* **62**(3): 213–222.
- WILLIAMS, G. C., 1966 *Adaptation and Natural Selection*. Princeton.
- WILLIAMS, K.-A. and P. S. PENNINGS, 2019 Drug resistance evolution in HIV in the late 1990s: hard sweeps, soft sweeps, clonal interference and the accumulation of drug resistance mutations. *bioRxiv*.
- WISELY, S. M., S. W. BUSKIRK, M. A. FLEMING, D. B. McDONALD, and E. A. OSTRANDER, 2002 Genetic Diversity and Fitness in Black-Footed Ferrets Before and During a Bottleneck. *Journal of Heredity* **93**(4): 231–237.
- WRIGHT, K. M., U. HELLSTEN, C. XU, A. L. JEONG, A. SREEDASYAM, J. A. CHAPMAN, J. SCHMUTZ, G. COOP, D. S. ROKHSAR, and J. H. WILLIS, 2015 Adaptation to heavy-metal contaminated environments proceeds via selection on pre-existing genetic variation. *bioRxiv*: 029900.
- WRIGHT, S., 1943 Isolation by Distance. *Genetics* **28**(2): 114–138.
- WRIGHT, S., 1949 The Genetical Structure of Populations. *Annals of Eugenics* **15**(1): 323–354.
- WRIGHT, S. and T. DOBZHANSKY, 1946 Genetics of natural populations. XII. Experimental reproduction of some of the changes caused by natural selection in certain populations of *Drosophila pseudoobscura*. *Genetics* **31**(2): 125.
- WRIGHT, S. I., I. V. BI, S. G. SCHROEDER, M. YAMASAKI, J. F. DOEBLEY, M. D. McMULLEN, and B. S. GAUT, 2005 The Effects of Artificial Selection on the Maize Genome. *Science* **308**(5726): 1310–1314.
- YANG, Z., 1998 Likelihood ratio tests for detecting positive selection and application to primate lysozyme evolution. *Molecular Biology and Evolution* **15**(5): 568–573.
- ZUCKERKANDL, E. and L. PAULING, 1965 Evolutionary divergence and convergence in proteins. In *Evolving genes and proteins*, pp. 97–166. Elsevier.